DEVELOPMENT OF BRICK BUILDING SYSTEMS FOR IMPROVED EARTHQUAKE PERFORMANCE

A THESIS

Submitted in fulfilment

of the requirements for the award of the degree

of

DOCTOR OF PHILOSOPHY

in

EARTHQUAKE ENGINEERING

By

M. QAMARUDDIN

DEPARTMENT OF EARTHQUAKE ENGINEERING
UNIVERSITY OF ROORKEE
ROORKEE (INDIA)

September 1978

C E R T I F I C A T E

Certified that the Thesis entitled "Development of Brick Building Systems for Improved Earthquake Performance" which is being submitted by Shri M. Qamaruddin in fulfilment of the requirements for the award of the Degree of Doctor of Philosophy in Earthquake Engineering of the University of Roorkee, is a record of the student's own work carried out by him under our supervision and guidance. The matter embodied in this Thesis has not been submitted for the award of any other degree.

This is to further certify that he has worked for a period of 39 months from July 1975 to September 1978 for preparing this thesis.

(BRIJESH CHANDRA)
PROFESSOR
DEPARTMENT OF
EARTHQUAKE ENGINEERING
UNIVERSITY OF ROORKEE
ROORKEE

(ANAND S. ARYA)
PROFESSOR AND HEAD
DEPARTMENT OF
EARTHQUAKE ENGINEERING
UNIVERSITY OF ROORKEE
ROORKEE

University of Roorkee, Roorkee
Certified that the attached Thesis/ Dissertation has been accepted for the award of Degree of Doctor of Philosophy / ~~Master of Engineering~~ Earthquake Engg. vide notification No. Ex/39/1965 (Degree) dated 25/4/79

Assistant Registrar (Exam.)

A B S T R A C T

Studies of seismic performance of brick buildings have revealed their inadequacy to resist earthquake shocks due to their heavy weight, poor tensile strength, low shearing resistance, lack of proper bonding between the shear walls and the cross-walls and poor workmanship. Systematic dynamic studies do not appear to have been carried out for investigating their realistic seismic capabilities. The strengthening methods as recommended in some of the earthquake regulations of the countries are meant for conventional brick buildings to improve their performance with little increase in the overall cost. But a dynamic evaluation of the specification is still wanting. The aim of this thesis is to fill this gap to some extent as well as to examine a new possibility of saving such buildings from the damaging influence of earthquake on the principle of vibration isolation. The following studies are made:

1. Seismic Response Analysis of Conventional Buildings

A typical multistoreyed brick building is chosen here for seismic response analysis. A number of variables representing the physical properties of the structural system, namely, number of storeys from one to four, wall thickness in various storeys from 1

to $1\frac{1}{2}$ brick thick and damping from 5 to 15% of critical value are considered. Shear beam type multi-degrees freedom system is taken to represent these buildings mathematically in which the masses of the floors and walls are assumed as lumped at the floor levels, the floors are assumed as rigid diaphragms and the 'Pier Method' is to use to derive the storey stiffness. The restoring force versus lateral deflection characteristics are assumed to be linear in each storey. Both shearing and bending deformations are considered to take place in the piers. Two accelerograms are used for computing dynamic response of the buildings : (a) Longitudinal component of Koyna earthquake of December 11, 1967 recorded close to the epicentre of the shock and having high acceleration pulses and high frequency contents and (b) North-South component of El Centro shock of May 18, 1940 recorded at about 50 km from the epicentre and having relatively lower acceleration peaks and frequency contents. Runge-Kutta fourth order method is used for computing the seismic response. Overturning and torsional effects have been included in the determination of timewise net stresses in the piers and their capabilities have been examined for resisting earthquake shock. From this study the critical sections for providing reinforcing have been identified and the minimum amount of necessary steel has been estimated.

2. Brick Buildings with Sliding Joint at Plinth Level

To investigate the ground motion isolation feasibility, a new system is considered in which a clear smoothened surface is created at plinth level just above the damp-proof course and the superstructure simply rests at this level and is free to slide except for the frictional resistance. Pilot tests carried out on 1/4 scale models showed very large reduction in the roof acceleration as compared with conventional fixed base case under given shake table motion indicating a definite possibility of earthquake isolation. The seismic response of one storey sliding type buildings is worked out through a two-mass mathematical model treating the frictional resistance as rigid plastic. The various parameters involved in the analysis are: time period, roof-base mass ratio, viscous damping and coefficient of friction. The seismic response of the system is computed using the same acceleograms and the same numerical techniques as for the conventional system. This study leads us to a concept of 'frictional response spectra' in which the spectral quantities of a sliding mass-spring-dashpot system are plotted against the undamped natural period for various coefficients of friction and mass ratios. These spectra clearly show the reduction of response of sliding system as compared with the conventional buildings.

3. Large Model Shake Table Tests on Conventional and Sliding Buildings

Eight half scale single storeyed brick building models are tested under base shocks so as to study their behaviour upto ultimate failure when constructed with different strengthening arrangements or sliding base arrangement. Their relative competence to withstand severe shocks is throughly examined. The outside dimensions of these models are 2.17 m x 1.75 m in plan and 1.60 m high above the plinth level with a 7.5 cm reinforced concrete slab roof. The tests were performed on a specially made railway wagon shake table facility in group of four models at a time. The eight models were of the following types:

(a) Conventional Fixed Base Types - One each, unstrengthened, in mud and cement mortars; one unstrengthened in cement mortar but with lintel band; One strengthened in cement mortar with lintel band and vertical steel at corners and jambs; and another similarly strengthened in cement mortar but with plinth band in addition.

(b) Sliding Types - One each in mud and cement mortars having lintel band. These tests show that unstrengthened brick buildings of conventional construction are not only weak but inadequate in energy absorption and that models with horizontal ring beam at lintel level and vertical reinforcement at critical

sections achieve strength and toughness both. The models with sliding permitted at base, again show a significant reduction in response and adequate behaviour upto very high base accelerations. As such, sliding arrangement shows great promise for adoption in actual building construction as a measure of earthquake safety.

The following main conclusions are drawn:

Once a brick building cracks, its stiffness, strength as well as damage threshold acceleration go on reducing and at a faster rate as the extent of damage increases. Reinforcing the brickwork at critical sections both in vertical and horizontal directions is a must for achieving adequate plateau of strength and ductility. The critical sections are identified and an estimate of required steel given for moderate and severe seismic zones. A sliding joint created at plinth level between foundation and superstructure could be used as an effective means of isolating the base motion.

ACKNOWLEDGEMENT

The author expresses, with deep sense of gratitude, his sincere thanks to his supervisors, Dr. Anand S. Arya, Professor and Head, and Dr. Brijesh Chandra, Professor, Department of Earthquake Engineering, Roorkee University for their expert guidance and constant encouragement throughout the course of this study.

The author is grateful to Dr. Jai Krishna, Professor Emeritus, and Dr. A.R. Chandrasekaran, Professor, Department of Earthquake Engineering for the technical discussions he had with them. The author wishes to thank Dr. W.O. Keightley, Professor, Department of Civil Engineering and Engineering Mechanics, Montana,State University, Bozeman, U.S.A. for the technical discussions with him, encouragement in the work and development of railway wagon shake table test facility while he was at the University of Roorkee as a Visiting Professor.

The author thanks Shri Krishen Kumar, Reader in the Department of Civil Engineering, Roorkee for his valuable help in the initial stages of this study and exchange of ideas and technical discussions with him throughout the course of work which proved fruitful.

Thanks are due to Shri H.C. Dhiman and other staff of the Workshops and laboratories of the Department of Earthquake Engineering for their assistance and help in the experimental phase of the study.

Thanks are also due to Sarva Shri S.C. Sharma, Deen Dayal and Kundan Lal for their help in bringing out the thesis in the present form.

The computational work was done on IBM 1620 at the Structural Engineering Research Centre, Roorkee, on IBM 1130 at the Aligarh Muslim University, Aligarh, on IBM 360 at the University of Delhi and on IBM 370 at the Institute of Petroleum Expoloration, Dehradun. The author takes this opportunity to thank these organizations for the computer facilities made available to him.

The author expresses his grateful thanks to the Aligarh Muslim University, Aligarh, for sponsoring him under Quality Improvement Programme to pursue research work at the University of Roorkee.

The author is very much grateful to his parents for their constant encouragement and help in many ways during the course of the study. Finally, the author wishes to express his sincerest appreciation to his wife Ayesha for her patience and continued encouragement to him during the period of work.

C O N T E N T S

Page No.

LIST OF TABLES

LIST OF FIGURES

LIST OF PHOTOGRAPHS

N O T A T I O N

Symbol	Description
A	Cross-Sectional Area of Pier
A_1, A_2, A_3	Cross-Sectional Area of Piers 1, 2 and 3
ΣA	Sum of Cross-Sectional Areas of all Piers and Walls at a Section
a	Actual Peak Ground Acceleration of Prototype Earthquake Motion
a_1	Distance between G_1 and G_2
a_2	Distance between G_2 and G_3
a_f	Acceleration Coefficient of Accelerating Force
a_g	Acceleration Coefficient of Ground Motion
a_p	Scaled Peak Ground Acceleration of Prototype Earthquake Accelerogram Corresponding to Threshold Damage of Prototype
a_{th}	Base Acceleration for Threshold Damage
b	Thickness of Pier
b_e	Total number of Piers in a Wall
$[C]$	Viscous Damping Matrix
CG	Combined Centroid of Piers
$C_1, C_2, C_3 \ldots$	Interfloor Viscous Damping Coefficient for Storeys 1, 2, 3, ...
C_m	Seismic Coefficient for Model

Symbol	Description
C_p	Seismic Coefficient for Prototype
C_s	Coefficient of Viscous Damping of Sliding System
d	Width of the Pier in the Plane of Bending
E	Modulus of Elasticity of Brickwork
E_{th}	Cumulative Input Energy for Damage Threshold
F	Horizontal Shear in a Pier
F_1, F_2, F_3	Horizontal Shear in Piers 1, 2 and 3
F_L	Shear Resulting from Lateral Loads without Torsion
F_T	Shear Produced by Torsional Moment
G	Modulus of Rigidity of Brickwork
G_1, G_2, G_3	Centroid of the Piers 1, 2 and 3
g	Acceleration due to Gravity
h	Height of a Pier
h_1, h_2, h_3	Height of the Piers 1,2 and 3
I	Moment of Inertia of a Pier about the Axis of Bending
$[K]$	Tridiagonal Stiffness Matrix
$K_1, K_2, K_3, \ldots$	Stiffness for the Storeys 1,2,3,...
K_p	Coefficient of Proportionality
K_s	Spring Constant of Sliding System

Symbol	Description
K_{st}	Storey Stiffness
k	Shear Stiffness of a Pier or a Solid Wall
k^{s}_{ij}	Shear Stiffness of jth Pier in ith Shear Wall of sth Storey of a Multistoreyed Brick Building
$[M]$	Diagonal Mass Matrix
$M_1, M_2, M_3, \ldots$	Lumped Mass at the Storey Levels 1,2,3,...
M_F	Moment of the Horizontal Forces about G_1
M_T	Sum of the Masses Lumped at the Roof and Plinth Levels
M_b	Mass Lumped at the Plinth Level
M_t	Mass Lumped at the Roof Level
m_t	Total Mass of Table including Models
N	Number of Modes considered in the analysis
n	Number of Degrees of Freedom
P	Total Shear in a Building Element
p	Natural Circular Frequency of Sliding System
p_b	Maximum Bending Stress in a Pier
p_d	Uniform Direct Stress due to Vertical Loads in a Pier
p_o	Overturning Stress in a Pier
p_r	Natural Circular Frequency in rth Mode of Vibration

Symbol	Description
p_{ct}	Resultant Stress in a Pier
p_{bm}	Bending Stress in the Pier of the Model due to Earthquake Force
p_{bp}	Bending Stress in the Prototype Pier due to Earthquake Load
p_{dm}	Uniform Stress in the Pier of the Model due to Dead and Live Loads
p_{dp}	Uniform Dead and Live Loads Stress in the Prototype Pier
p_{dr}	Damped Natural Frequency in rth Mode of Vibration
p_{om}	Overturning Stress in the Pier of the Model due to Earthquake Force
p_{op}	Overturning Stress in the Prototype Pier due to Earthquake Load
p_{tm}	Net tensile Stress in the Pier of the Model
p_{tp}	Net tensile Stress in the Pier of the Prototype
Q_r	Modal Participation Factor in rth Mode
q	Maximum Shear Stress in a Pier
r	rth Mode of Vibration
S_F	Force to Cause Sliding
S_v	Velocity Spectrum
SI	Spectral Intensity
S_{am}	Spectral Acceleration of the Model for the Table Motion

Symbol	Description
S_{ap}	Spectral Acceleration of the Prototype for the Prototype Earthquake
S'_a	Spectral Acceleration of the prototype for the Table Input
s_w	Total Number of Shear Walls in a Storey
T	Fundamental Period of Structure
U	Total Energy per Unit Mass
U_t	Total Energy Input in the Shock
$v,\dot{v}$	Relative Velocity and Acceleration of Rigid Mass
V_t	Velocity of Table Attained at the End of the Shock
v_f	Maximum Velocity of the Accelerating Force
W	Total vertical Load above the Horizontal Section of the Building through the Piers
$x,\dot{x},\ddot{x}$	Absolute Displacement, Velocity and Acceleration of Rigid Mass
x'	Distance of Centroid of Pier from Centroid of Pier Areas
$x_1,x_2,x_3,\ldots$	Absolute Displacement of the Mass $M_1,M_2,M_3,..$
x'_1,x'_2,x'_3	Distance between CG and G_1, G_2 and G_3
$\ddot{x}_b$, $\ddot{x}_t$	Absolute Acceleration of the Bottom and Top Mass of the Sliding System
$y,\dot{y},\ddot{y}$	Ground Displacement, Velocity and Acceleration

Symbol	Description
$\{Z\}, \{\dot{Z}\}, \{\ddot{Z}\}$	Relative values of Displacement, Velocity and Acceleration Vector with respect to Ground Motion
$Z_b, \dot{Z}_b, \ddot{Z}_b$	Relative values of Displacement, Velocity and Acceleration of the Bottom Mass of the Sliding System with respect to Ground Motion
Z_m	Maximum Relative Displacement of a Friction Mounted Rigid Mass
$Z_t, \dot{Z}_t, \ddot{Z}_t$	Relative values of Displacement, Velocity and Acceleration of the Top Mass of the Sliding System with respect to Ground Motion
α_B	Base Acceleration
$\{\beta\}$	Normal Coordinates
δ	Lateral Deflection at the Top of a Shear Wall
ξ	Fraction of Critical Damping
ξ_r	Fraction of Critical Damping in rth Mode of Vibration
θ	Mass Ratio
λ	Scale Ratio
μ	Coefficient of Friction
τ	Time Variable for Integration
$[\phi]$	Square Matrix having Modal Vectors as its Column
$[\phi_r]$	rth Modal Column Vector

C H A P T E R 1

INTRODUCTION

1.1 GENERAL

Earthquakes are known to cause the worst forms of natural calamity. Many types of relatively safe building constructions have been intuitively developed in the past by people around the world based on local availability of materials, weather requirements and economic conditions of the people and all this perhaps without knowing earthquake damage phenomena scientifically. A study of earthquake affected areas would show that the loss of human lives is primarily on account of collapse of dwellings, and that most of the lives could have been saved if the buildings were earthquake resistant. It is, however, recognized that complete protection may not be economically feasible in all probable earthquakes. But loss of life and damage to property could be minimized by developing a building system so as to have improved and safer performance during earthquakes.

Load bearing masonry construction is the most popular and suitable for housing purposes in almost all the developing countries due to its economy, ease of construction, ability to insulate the variations in temperature and other weather conditions. Structurally the basic advantage of this type of construction is the use of same element to perform a variety of functions. Such

construction varies from sundried brick walls with thatch roof on bamboo frames to burnt brick or stone walls or hollow concrete blocks wall with jack arch roofs or reinforced brick or reinforced concrete slab roofs. Sometimes, the roofs are sloping on wooden or steel trusses or in the form of domes.

The design of stfuctures subjected to earthquake forces requires a consideration of both the characteristics of the ground motion and the dynamic properties and behaviour of structures. Ground motions are random and have been fairly well studied for certain well known past earthquakes. The designer is, therefore, mainly interested in the dynamic properties and behaviour of the structure while designing for earthquake forces. Earthquake resistant structures are usually designed on the principle of inelastic deformation. According to this philosophy, the structure is made strong enough so that it withstands the maximum probable earthquake with limited and non-collapse damage but remains within elastic limit for frequent shocks.

1.2 PROBLEMS ASSOCIATED WITH BRICK BUILDINGS

Strong motion earthquakes provide prototype testing of structure and offer an opportunity to study the validity of code provisions, methods of analysis and inadequacies in design and construction practices. A study of the seismic performance of the brick buildings

has revealed their vulnerability to resit earthquakes due to their heavy weight, poor tensile strength, low shearing resistance, lack of proper bonding between the shear walls and the cross-walls, and poor workmanship. So, earthquake resistance of building construction is a serious problem in areas where steel, reinforced concrete or timber cannot be used extensively for want of material and finance.

The basic properties of brickwork for dynamic loads, which play an important part in the dynamic response of brick structures, have not been fully studied so far. This type of construction can rightly be termed as non-engineered since there is no well established method as yet to evaluate the stiffness and strength of a wall element as used in brick buildings. Apart from this, even the true distribution of vertical stress on the building elements is not well understood. In case of brick buildings with load bearing walls, the load carried by the building is transferred to the foundation sequentially through the roof and/or floor system and the walls and piers. The roof and floor system are usually assumed as rigid diaphragms which may not be true for some of the forms now being employed. Therefore, this assumption has to be verified experimentally. Apart from these, systematic dynamic studies for such structures have not been carried out for investigating their

capabilities to resist the earthquake forces. In effect, a rational method of design for such structures to earthquake shock is wanting.

Some strengthening methods for brick buildings have been suggested by earlier investigators (Krishna and Chandra, 1965; Arya, 1967; Arya, 1969 and Krishna and Chandra, 1969) for improving their lateral strength with a small increase in the overall cost of their construction, and these have been incorporated in IS: 4326-1976 'Recommendations for Earthquake Resistant Building Construction'. But these have not been tested experimentally for actual or simulated ground motion inputs. Though, effectiveness of only R.C. bands in brick building (Photo 1.1) has been proved in keeping the building

Photo 1.1 BRICK BUILDING WITH R.C. BANDS SHOWING EFFECTIVENESS OF THE BAND IN KEEPING THE BUILDING SAFE IN AREA OF MOST SEVERE SHAKING IN EARTHQUAKE OF MAY 1971 (TURKEY)

safe from collapse in area of most severe shaking in Burdur (Turkey) earthquake of May 1971 (Arya, Chandra and Thakkar, 1977), worth of overall strengthened brick buildings has yet to be seen in future earthquakes and still awaits the test of time. Therefore, more extensive investigations are required for evolving suitable aseismic brick building system, rational methods of seismic analysis and design and construction practices for such structure.

Two types of construction of brick buildings are defined for further reference in the present thesis. The first type consists of buildings of normal constructions with all horizontal courses laid in mortar. This is termed here as 'conventional'.

The second type involves a new concept, namely, a clear smoothened surface is created just above the damp-proof course at plinth level without any mortar and the superstructure simply rests at this level and is free to slide except for frictional resistance. This construction is called here as 'sliding type'.

1.3 PROBLEMS IDENTIFIED

The strengthening methods as recommended in IS:4326 are meant for conventional buildings. A thorough study does not seem to have been made as yet of real brick buildings of several storeys under

realistic earthquake motions so as to arrive at the critical sections requiring the reinforcing through steel bars and the amount of steel needed for different seismicity levels. The recommendations seem to be based on a combination of simplified analyses and engineering judgement. For checking the above a real building plan with varying number of storeyes is considered here and analysed assuming it to remain uncracked so that the tensile stresses as developing at the various points could be relatively worked out.

The other aspects of the conventional building is to test them under dynamic loads to see their relative strength and evaluate the efficacy of any of the strengthening methods.

So far as the sliding type building is concerned, it is based on the concept of vibration isolation and no work has yet been done on sliding building system. The feasibility of the concept has to be seen and analytical as well as experimental results are to be obtained.

1.4 OBJECTS OF STUDY

The objectives of this thesis are chosen to investigate the above problems and are more specifically stated below:

(a) To carry out dynamic response analysis of conventional single and multistoreyed brick buildings

when subjected to real earthquake motions at the base, work out the maximum dynamic and static vertical stresses, identify the critical sections, estimate the requirements of reinforcing steel, and thereby evaluate the reinforcing provisions in the Indian Standard Code.

(b) To perform pilot tests on sliding building models to see the feasibility of isolating base motion or reducing its influence on the structure.

(c) To carry out a theoretical study of the sliding type single-storeyed brick buildings subjected to earthquake excitations, consisting of

(i) computation of seismic response of the building, and

(ii) comparison of this response with the seismic response of conventional type building having same dimensions.

(d) To perform dynamic shock tests on single storeyed half scale models constructed in clay mud and cement-sand mortar having various types of reinforcing arrangement as well as sliding at base so as

(i) to study experimental behaviour of conventional type and sliding type buildings from small shocks upto ultimate condition,

(ii) to compare experimentally observed dynamic response with that obtained by analytical method, and

(iii) to examine the relative competence of brick building systems.

1.5 SCOPE OF STUDY

The investigations made in the present work are briefly summarized in the following paragraphs.

1.5.1 Brick Buildings Studied

Earthquake responses of single and multistoreyed conventional type brick structures are studied. Typical floor plans of one- , two- , three - and four - storeyed buildings have been chosen for analysis using the 'Pier Method' (PCA, 1955). Since the conventional load - bearing unreinforced wall construction is usually limited to 3 to 4 storeys, the analysis of buildings only upto four storeys has been carried out. Taller masonry building using reinforced masonry or sandwitch type constructions are not included here. For parametric studies of such structures, a number of variables representing the physical properties of the structural system are chosen as follows:

(i) Number of storeys - The number of storeys varies from one to four.

(ii) Wall Thickness -

(a) Uniform thickness of main walls in all the storeys (one brick thick, 229 mm).

(b) Non-uniform thickness of main walls in the storeyes ($1\frac{1}{2}$ to 1 brick thick, that is, 343 to 229 mm).

(iii) Damping - Three values of viscous damping, viz., 5%, 10% and 15% of critical are used.

The seismic response of one storey sliding type buildings is calculated through a mathematical two mass model treating the frictional resistance as rigid plastic. The various parameters involved in the analysis and their values chosen are given below:

(i) Time Period - The natural periods chosen are : 0.04, 0.05, 0.06, 0.08 and 0.10 s.

(ii) Mass - Ratio - The ratio of top to bottom mass selected for the systems are: 1.6, 1.8, 2.0, 3.0, 4.0 and 5.0.

(iii) Viscous-Damping - 5%, 10% and 15% of critical damping are considered.

(iv) Cofficient of friction - The values chosen are: 0.15, 0.20, 0.25, 0.30 and 0.40.

Experimental investigations are carried out to study the behaviour of brick buildings constructed with different strengthening arrangements and examine their relative competence to stand shocks. For this purpose, model tests are conducted on eight differently constructed single-storeyed brick structures, in two sets of four models each. The outside dimensions of these structures are 2.17 m x 1.75 m x 1.60 m high above the plinth level with a 7.5 cm reinforced concrete roof

slab. The models in the first set are constructed using (i) clay mud mortar, (ii) 1:6 cement - sand mortar, (iii) clay mud mortar together with vertical reinforcement at the corners and jambs as also a reinforced concrete lintel band (ring beam) and (iv) similar to (iii) but in 1:6 cement sand mortar. For the second set, the structures are constructed in (v) mud mortar with superstructure free to slide at the plinth level, (vi) cement sand 1:6 mortar with reinforced concrete lintel band, (vii) 1:6 cement sand mortar with sliding possible at plinth level and (viii) cement sand 1:6 mortar with plinth and lintel bands together with vertical steel at corners and jambs.

The tests were performed on a railway wagon shake table facility described in Chapter 5.

1.5.2 Methods of Analysis and the Results Derived

(a) Conventional Buildings: The mathematical model chosen to represent conventional type multistoreyed-brick buildings is a shear beam type multi-degree of freedom system in which the mass of the floors and walls is assumed as lumped at the floor levels and the floors are assumed as rigid diaphragms. The restoring force vs. lateral deflection characteristics in each storey are assumed to be linear. The coupled equations of motion for such a model are uncoupled into modal equations and are then solved numerically by using Runge-Kutta fourth

order solution, whence, time-wise earthquake response is computed employing modal superposition method. Overturning and torsional effects due to earthquake forces are worked out and superimposed.

The time-wise net stresses in the building elements are then computed and their capabilities examined for resisting earthquake shock. From this study the critical sections for providing reinforcing could be identified and minimum necessary steel reinforcement estimated.

(b) Sliding Type Buildings: Here the analysis is made of single-storeyed buildings regarding their sliding movements. The building was represented by a mathematical model consisting of two masses (lumped at the roof and plinth levels) connected through a spring and a viscous damping system. The lower mass is assumed to rest on a plane with dry frictional resistance to permit required motion of the system. The earthquake response of the system is computed using the same numerical techniques as for conventional system.

(c) Dynamic Analysis of Models: To predict the dynamic behaviour and to compute the dynamic response of the brick building models, the table motion is used as the ground motion and the models treated as small size prototype structures subjected to this ground motion.

1.5.3 Ground Motion Data Used in the Analysis

Two accelerograms are used here for dynamic analysis of the buildings: (a) Longitudinal component of Koyna earthquake of December 11, 1967 and (b) North-South component of El Centro shock of May 18, 1940. Koyna accelerogram was recorded close to the epicentre of the shock and had high acceleration pulses and high frequency contents while El Centro accelerogram was recorded at about 50 km from epicentre of the shock and relatively lower peak acceleration and frequency contents. Response analysis of the structures is made for one horizontal component of the shock at a time as usual.

1.5.4 Experimental Studies-Dynamic Behaviour and Response of Building Models:

Qualitative and quantitative analyses are made to study the dynamic behaviour of models under shock loads. Also their relative competence to withstand the shock has been examined. A comprehensive study of damage was undertaken for all the test structures after every shock.

1.5.5 Concept of Frictional Response Spectra:

The earthquake response study of sliding type structure, carried out above, led to a concept of frictional response spectra in which the spectral quantities - 'maximum absolute acceleration, maximum relative velocity and maximum relative displacement' of a sliding mass-spring-dashpot system are worked out for a particular earthquake motion,

and plotted against the undamped natural period of vibration for various frictional coefficients and mass ratios. These spectra are worked out here for a variety of the parameters representing the physical properties of the structural system.

1.5.6 Computer Programmes

Two main computer programmes are developed for the present work to compute

(a) timewise earthquake response of conventional type multistoreyed brick buildings- timewise stress analysis of the building elements is also incorporated; and

(b) earthquake response of single-storeyed sliding type brick structure and frictional response spectra.

1.6 OUTLINE OF THESIS

A review of earlier investigations on performance of brick buildings under past earthquakes, seismic behaviour of rigid objects and aseismic strongthening measures adopted for brick buildings are presented in Chapter 2.

Chapter 3 describes the details of analysis and earthquake response computations of conventional type single and multistoreyed brick buildings.

Chapter 4 presents the preliminary tests on sliding type small scale models on shake table as well as the

seismic response study of sliding type brick buildings. Also a new concept of frictional response spectra is presented in this chapter.

Experimental behaviour of half-scale brick buildings is reported in Chapter 5 and their relative competence to resist base shocks is analysed with reference to strength as well as toughness. This dynamic response to shock loading is included in this chapter.

The results of the whole study are summarized in Chapter 6. Also the conclusions of the present work and suggestions for future studies are advanced in this chapter.

C H A P T E R 2

REVIEW OF EARLIER INVESTIGATIONS

2.1 GENERAL

Different modes and mechanisms of failures of damaged brick buildings during past earthquakes are briefly presented in this chapter. The remedial measures as suggested by the various investigators for aseismic strengthening of such buildings are also briefly reviewed. Sliding behaviour of rigid objects subjected to ground shaking as investigated in the past is discussed to examine the possibility of a sliding type brick building system for its improved seismic performance. Finally, the experimental investigations carried out on brick structure models for dynamic and/or lateral loads are briefly reported.

2.2 PERFORMANCE OF BRICK BUILDINGS DURING PAST EARTHQUAKES

Buildings constructed in brick adobe, mud, timber or a combination thereof have been damaged much more than reinforced concrete ones during the past earthquakes (Arya, Chandra and Gupta, 1977) in various parts of world. A comparative study of the performance of different types of construction in 1960 Chilean earthquake (Steinbrugge and Flores, 1963) showed that adobe and unreinforced brick buildings were the most severely damaged.

Monge (1969) has presented a statistics of about 20,000 small buildings (of adobe, unreinforced, reinforced brickwork, wooden framed buildings and reinforced masonry block buildings) in Chile during six destructive earthquakes.

The study exposes the poor seismic resistance of such construction and recommends that adobe and unreinforced brick buildings should not be used in earthquake prone areas.

Adobe, random rubble masonry and composite constructions of unburnt and burnt bricks are frequently used in India. Seismic behaviour of such buildings has been observed (Chandra and Kumar, 1974) to be similar to that pointed out in Monge's study referred above. Some of the typical cases of damage to such construction during some of the past earthquakes are shown in Photos 2.1 to 2.3. During ground shaking, structures are subjected to alternating stresses due to horizontal forces acting alternately from opposite sides in quick succession. Shear forces and overturning moments are caused which lead to combined shear, direct and bending stresses. Damage occur mostly due to cracking of building elements weak in tension and shear. Cracking occurs in several ways: vertical cracks at the corners and junctions of the walls, separation of walls, horizontal and diagonal cracks starting at corners of window

and door openings, and their propagation in all sorts of ways. The extent of damage is a function of the intensity and duration of ground shaking, the openings in the structure, type of mortar used, strength of bricks, the quality of construction and the nature of soil-foundation system supporting the building, etc. Due to too many factors involved, it is not easy to predict damage to such buildings in precise terms.

The different modes of typical failures (Arya, Chandra and Thakkar, 1977) commonly observed during earthquakes may be attributed to one or more of these factors: lack of tensile and shearing strength in the material of construction, lack of lateral and torsional strengths in the structure, failure of joints, excessive deformation of the structure and excessive settlement of the foundation soil. The collapse mechanism of whole or portion of a wall is caused when enough cracks occur so as to separate blocks of masonry which could move freely except for frictional resistance. The cracks usually originate from the sections around openings (Agnihotri, 1962; Krishna and Arya, 1965). Due to direct or bending tension, cracks begin horizontally and then propagate horizontally or change direction diagonally. The horizontal cracks also occur due to shear failure at other planes where rigidity changes suddenly (Krishna and Chandra, 1969). The

piers on both sides of openings are subjected to diagonal tension and crack diagonally. As the seismic force is reversible, the cracks may occur along both diagonals of the piers showing X or star shaped pattern.

Torsional moments are caused in a building due to non-coincidence of the centroid of lateral stiffnesses of various building elements with the centre of gravity of the masses. Thus, increased shears are imposed in the elements by these moments resulting in their cracking and failure. These cracks are invariably diagonal and show a helical pattern around the elements as well as the building as a whole.

Innumerable masonry buildings have collapsed due to lack of proper bonding walls at right angles at their junctions. Due to such cracks the integral box action of the enclosure is lost and each wall tends to act as a vertical cantilever which has little stability and tends to overturn. Also on account of excessive cracking, big chunks of brickwork get loosened, move out under the action of further shocks and finally the wall collapses. Excessive settlement of foundation due to partial or complete liquefaction occurs due to ground motion in water bearing loose cohesionless soils. This invariably involves unequal settlements too under different parts of the building and results in extensive cracking of walls as well as floors. Even complete

collapse may occur. The pattern of cracking is different than that seen under the action of lateral forces. In most cases these cracks are fine near footing and become wider towards top. Tilting and overturning of buildings also occurs due to liquefaction of soil as in the Niigata earthquake in Japan (Arya, Chandra and Gupta, 1977).

2.3 INVESTIGATIONS ON BRICK SHEAR WALLS

2.3.1 Basic Properties of Brickwork

Results of basic tests for determining different properties of the non-homogeneous brick masonry elements are briefly reviewed here. These include the compressive, tensile and bond tests results on small test specimens.

Extensive studies were done by Benjamin and Williams (1958) to determine the physical properties of bricks and bond strength through cross-brick couplets. It was found that compressive strength and modulus of rupture vary by as much as 100 per cent. The suction and absorption properties were found to be important in defining the strength of brickwork. The couplet tests showed that the shear strength of the mortar joints is greatly affected by the normal stress on the joint. Further tests on couplets were conducted by Agnihotri (1962) to determine the bond strength and tensile

strength of brickwork for various mortars. The results indicated that the failure of brick masonry was due to tensile failure of brick-mortar bond.

Tests were also performed by Sinha and Hendry (1966) to study bond strength in brickwork. The results showed that the moisture contents of the bricks at the time of laying influenced it appreciably. An analytical procedure was presented by Hilsdorf (1969) to arrive at the compressive strength of brickwork which was found to increase with the tensile and compressive strengths of brick and mortar. A decrease in the ratio of joint thickness to height of bricks also increased the compressive strength of brickwork. Workmanship factor was not considered in the analysis, which could certainly affect the compressive strength significantly.

The tensile and compressive strengths, and also modulus of elasticity of brickwork for different mortars were found by conducting tests on brickwork test specimens (Krishna and Chandra, 1965). The test results are listed in Table 2.1. Damping values as determined by Mallick (1961) for brickwork in various mortar mixes are shown in Table 2.2. It was further found (Krishna and Chandra, 1965) that damping values increase with the increase in strain. This is indicated in Table 2.3. All these damping values are for uncracked bending specimens. Cracking increases

damping considerably.

It is seen from Table 2.2 that brickwork in clay mud has 10% of critical damping. This value may further increase to about 15% of critical damping in wet or cracked condition.

A very comprehensive literature survey on compressive, tensile, bond and shear strength of masonry was carried out by Mayes and Clough (1975). Here, only a few of the investigations on the properties of brickwork are briefly introduced above.

2.3.2 Strength of Unreinforced Brick Shear Walls

Effectiveness of unreinforced brick masonry shear walls to resist lateral loads was first investigated through experimental studies (Benjamin and Williams,1958).A series of walls verying from 0.34 scale to full size were tested without bounding frames. Thickness of wall was also varied. From this investigation, it turned out that the behaviour of brick masonry could be studied by means of models. Errors caused by scaling of model were not significant compared to variations resulting from workmanship. In the case of unbounded shear walls, failure occurred due to the tension at the joint of the wall and the foundation.

In an analytical investigation (Agnihotri, 1962) generalized expressions were derived for

computing the strength of shear walls with single opening in terms of earthquake force expressed as proportion of gravity. Tests carried out by him clearly brought out the importance of workmanship. The walls with greater cubic content of masonry in which high standard of workmanship could not be maintained indicated lower strength than the tensile bond strength found from smaller size column tests.

The lateral loads to cause first crack and the ultimate failure for unreinforced shear walls were determined by Lal (1968) through experimental and theoretical studies. It was shown that the first crack load could be predicted with a reasonable accuracy by treating the wall as a free standing cantilever. The cracks invariably originated at wall openings and the weak joints. Haller (1969) also tested two different sizes of specimens of masonry walls to study their shear strength and employed two different types of bricks and mortar in the masonry walls. From the results, it was observed that the shear strength was composed of the adhesion of mortar to the brick, the shear resistance of the mortar plugs (i.e. the mortar that penetrates into the perforations of bricks) and the frictional forces which increase with compressive stress. Murthy and Hendry (1965) compared the compressive strengths of 1/3 and 1/6 scale model piers and walls with that of full size specimens. The parameters were, the mortar

strength, joint thickness and the slenderness of the walls. It was found that the strength of full scale brickwork for given strengths of brick and mortar could be reproduced by means of model tests. Also, if the same mortar was used to construct the model and full scale walls, the model walls would take higher stresses than the equivalent full-scale one[+].

Five identical specimens of one-sixth scale single-storey shear wall test structure were built by Sinha and Hendry (1969). Each model structure was subjected to different compressive load and tested to failure under a lateral load. All the models failed with cracks passing through horizontal and vertical joints. It was found that brickwork subjected to combined compression and shear exhibited two distinct types of failure: shear failure at the brick-mortar interface and diagonal tensile cracking through bricks and mortar. From this study, it was further inferred that presence of compressive stress increased the shear strength of the brickwork upto a certain limit which depended on the compressive strength of the brickwork. The rigidity and shear modulus of brickwork decreased non-linearly with an increase in lateral

---

[+] The order of difference in the model and prototype unit strengths is not established. It would depend on the scale ratio. It may be conservative to assume the strength of 1/3 model to be 20% higher and that of 1/2 scale model to be 10% higher than the full scale walls.

load and a decrease in compressive load.

Further experimental and analytical studies were made (Sinha et al, 1970) to investigate the overall deflections using five-storeyed 1/6 scale and full scale test structures subjected to lateral loads. The model structure was analysed treating it as an individual cantilever, a continuum, and as a wide column. The full-scale structure was analysed by the same methods as the model and, in addition, by the finite element method. It was found from this study that existing analytical methods do not give reliable results for stress and deflection in brick structures. The above mentioned investigation was further extended (Kalita and Hendry, 1970) to clarify the applicability of the shear wall theory to brick structures and also to determine the contribution of cross-wall and floor slabs to the rigidity of the shear walls. The investigation was done through a simplified one-sixth scale five storey model test structure. In the analytical study, a simplified approach (Benjamin, 1959) and the finite element method were used. A comparison of the analytical and experimental results indicated that the finite element method was slightly more accurate than the simplified approach and gave about 10 per cent lower deflections than the experimental results for a lateral load equal to one-third of the ultimate load. But considering the variation due to workmanship

the simplified approach should be adequate for use in the design office for the analysis and design of brick structures.

The investigators also studied analytically (using finite element method) and experimentally the effect of flange width, and analytically the effect of slab width on the rigidity of shear walls. The model structures investigated were single storeyed consisting of one shear wall, two cross walls as flanges and a slab. The wall had one central opening. It was concluded that the 'effective' flange width was 0.35 of the storey height (there was a uniform 20 per cent discrepancy in the experimental and analytical results) and the 'effective' slab width was 0.5 of the bay width. In an actual brick enclosure the effectiveness of cross walls to act as flange of the shear walls will depend whether the walls at right angles are built integrally or connected rather loosely. Also, if horizontal bending of walls during an earthquake would cause a vertical crack at the junction of walls, the effectiveness of the flange would be reduced drastically.

2.3.3 Behaviour of Reinforced Brick Shear Walls

Building failures during past earthquakes have shown cracking of mortar joints along section through jambs of openings sometimes diagonally and sometimes horizontally along the lintels. In view

of this, an investigation was undertaken (Krishna, Chandra and Kamungo, 1966) to study the behaviour of shear wall particularly with the introduction of steel at various locations of the walls experimentally and theoretically. Static and dynamic tests were performed on 16 wall models. It was inferred from this study that the behaviour of wall in the elastic limit could be predicted by the pier analysis (PCA, 1955) which was supported by static and dynamic test results. Also, contribution of steel in improving the lateral resistance of the wall can also be calculated on these lines. In the post-elastic range, however, since the cracks complicate the situation to a large extent, it was not possible to formulate a general criterion to predict the behaviour.

Another series of tests was carried out to study the behaviour of reinforced brick walls subjected to a quasi-static cyclic load (Scrivener and Williams, 1971) and also a simusoidally varying load (Williams and Scrivener, 1972). The parameters varied were the magnitude of superimposed compressive loads, wall aspect ratios and reinforcing percentages and distribution. The modes of failure of walls observed in the tests were: flexural or yield failure and shear failure.

In flexural behaviour of walls, the initial cracking occurred mainly in the horizontal joints near

the base of the wall. It was naturally produced by the vertical movements necessary in the brickwork to achieve compatibility with the yield deformation of the steel. After yielding, same load was required to maintain the yield stress while the deformation increased until failure occurred by crushing, usually accompanied by diagonal cracking at the toe of the walls. On the other hand, shear behaviour was characterised by initial diagonal cracking resulting in reduced stiffness. In this case the load could not be maintained for keeping the yield level but a tendency of sharp reduction in load from its maximum values with increasing deformation was observed. Extensive and sudden damage to the masonry was observed causing loss of strength and eventually wall failure occurred by disintegration of masonry at the toe of the wall. It was found that the ultimate strength increased and the ductility decreased with an increase in the superimposed compressive load. An increase of vertical reinforcing increased the horizontal load to cause yielding of the steel without altering the shear strength appreciably. In this test series, the aspect ratio of the walls (height to length ratio) ranged between 0.5 to 2. The study showed that walls of very high aspect ratio could be regarded as vertical cantilever with a characteristic flexural behaviour. On the other hand very low aspect ratio walls essentially had shear type of deformation and could be considered

as predominantly shear resisting elements with non-ductile behaviour like deep beams. The walls with intermediate aspect ratio would have a mixed behaviour not so clearly defined.

Further investigation was conducted (Priestly and Bridgeman, 1974) through testing of reinforced brick masonry walls of unit aspect ratio on the effect of horizontal and vertical reinforcement on the shear strength of cantilever piers. The main parameter in the test was the amount of reinforcing. The lateral loads were cyclically applied to the walls which were tested by the cantilever method. Contrary to earlier researchers, from this investigation it was found that horizontal steel was effective in improving the ultimate shear capacity of masonry where sufficient vertical steel was provided to carry the full ultimate flexural load. It was inferred further from this study that horizontal steel was approximately three times as efficient as vertical steel in carrying a shear force across a diagonal crack.

From the above presentation, it is clearly seen that lateral load strength as well as deformability of a brick shear wall is improved a great deal by reinforcing it vertically and horizontally. But provision of steel reinforcing in brick shear walls would create many constructional problems. Therefore the

quantity of steel must be small and placed at a few locations only. In view of this, other strengthening schemes have been suggested by other investigators. These are discussed in the following section.

2.4 SEISMIC STRENGTHENING OF BRICK BUILDINGS

The main requirements of structural safety of brick buildings (Arya, 1967), as emerged out from the studies of mode and mechanism of failures in Section 2.2, are outlined as follows:

(a) The roof and/or floor elements must be effectively tied together and capable of exhibiting diaphragm action.

(b) Horizontal reinforcement in cross-walls is required for transferring their own out-of-plane inertia load horizontally to the shear walls.

(c) The shear walls are required along both the axes of the building and must be capable of resisting all horizontal inertia forces due to their own mass and those transmitted to them from cross-walls and floors and roofs.

(d) All the walls must be properly tied together to avoid separation at vertical joints so as to form box section for greater bending and overturning resistance.

To meet these requirements, the strengthening measures have been suggested by various investigators (e.g. see Krishna and Chandra, 1965) and adopted by the Codes of practice such as the Indian Standards Code of Practice for Earthquake Resistant Construction of Buildings (IS: 4326-1976). These provisions are briefly reviewed here. For this purpose, seismic zones are identified based on expected maximum MM intensities (Arya, 1968; Arya, Chandra and Thakkar, 1977) and are defined as follows:

Zone A - Probable maximum MM Intensity IX or more

Zone B - Probable maximum MM Intensity VIII

Zone C - Probable maximum MM Intensity VII

Zone D - Probable maximum MM Intensity VI or less

As stated earlier the softness of soil has generally adverse effect on the earthquake resistance of buildings. Therefore for determining strengthening requirements, a combination of seismic intensity zone as well as soil condition is considered. Such a combination is shown in four categories in Table 2.4.

No strengthening measures are considered necessary for Zone D in view of low seismicity except emphasis on good quality of construction according to usual standard norms. The recommendations being presented are for Zones A, B and C.

2.4.1 Materials

Use of mud or very lean mortars is not suitable for seismic resistance of brick walls due to their poor tensile and shear strength. Appropriate mortar mixes for various categories of construction are detailed in Table 2.5 based on their strength characteristics. Use of a richer mortar mix in narrow piers between openings is desirable.

Well burnt bricks of crushing strength (Chandra, 1963) not less than 35 kg/cm^2 should be used for brickwork.

2.4.2 Load Bearing Brick Walls

From experience on observations of earthquake damage to unreinforced brick building in Iran, it has been reported (Moinfar, 1972) that for ordinary workmanship and quality of building materials, the height of a dwelling should not be more than three storeys, preferably two, and under no circumstances should its total height exceed 11 m including the height of the parapet. In view of the strengthening measures of the brick buildings, the load bearing walls should not be more than 15 m total height or four storeys in India.

One brick (20 cm) thick walls upto two storeys or for the upper two storeys of three or four storey buildings has been suggested (Arya, 1968). For

bottom storey of three storey buildings, $1\frac{1}{2}$ bricks thick (30 cm) walls are suggested. Also $1\frac{1}{2}$ to 2 bricks thick (30 or 40 cm) walls may be used for bottom storey of four storey buildings. These thicknesses may be used in the case of walls properly connected to cross-walls not more than about 6 m apart. The wall thickness should be increased for larger spacing.

The effect of different wall thickness in various storeys of multistoreyed brick buildings subjected to ground shaking may be studied theoretically to investigate the pattern of seismic force distribution in the building elements. As such, a suitable thickness of walls in different storys may be suggested. Also,the contribution of cross-wall on the seismic resistance of the shear walls may be investigated. As far as possible, the walls in both directions of the building should be straight and symmetrical in plan to minimize torsional effects.

Investigations carried out on the effect of openings on the strength of walls show that their strength is reduced by openings. For high resistance, the openings should be small in size and as centrally located (Arya, 1967; Indian Standard Code,IS: 4326-1976; Moinfar, 1972) as functionally possible. Also the following would be desirable.

(i) The total width of openings should not be more than half the length of the wall between the consecutive cross-walls.

(ii) Openings in any storey should preferably have their top at the same level.

(iii) Openings should be located away from the corner by a clear distance equal to at-least 1/4 of the height of openings.

(iv) The horizontal distance (pier width) between two openings should not be less than 1/2 of the height of the shorter opening (Fig. 2.1).

(v) The vertical distance from an opening to an opening directly above it should not be less than 60 cm nor less than 1/2 of the width of the smaller opening (Fig. 2.1).

(vi) Openings should either be boxed in reinforced concrete alround or reinforcing bars should be provided at the jambs through the brick-work (Fig. 2.2) if they do not comply with the requirements (i) to (v).

The above guidelines for providing openings in the walls are mainly based on the theoretical analysis of the isolated walls under lateral loads. There is however a need to carry out investigations on brick building

models subjected to dynamic loads to study the various aspects as enumerated above. A theoretical study may also be done on the same line. The investigation may thus provide better guidelines on location of openings in the walls so as to have maximum seismic resistance.

2.4.3 Bond in Brickwork

The usual bonds specified for brickwork are aimed at breaking the vertical joints from course to course for achieving full strength in the brickwork. Here, a special mention may be made regarding vertical joint between walls constructed at right angles to each other. Bricklayers prefer to make a vertical toothed joint between them, for convenience of construction. Though theoretically, the joints are to be properly filled with mortar, more often than not these are left hollow and thus become weak and tend to open out at the first instance of ground shaking. To obtain full bonding between the walls, it is necessary to make a stepped joint. Alternatively, the toothed joints should be staggered in both the walls, making it alternately in lifts of about 60 cm. Proper bonding between cross walls will ensure the flange or box action of the shear walls in both directions. Alternative to bonding of bricks, mechanical jointing through steel dowels or bond beams in the form of reinforced concrete ring runners or bands is to be used. These are explained later.

2.4.4 Horizontal Reinforcement in Walls

For imparting horizontal bending strength against plate-action for out-of-plane inertia load and for tying the perpendicular walls together, horizontal reinforcing of the walls is required. For this, the following reinforcing arrangements have been suggested.

(a) Horizontal Band: Reinforced concrete bands, are provided continuously through all the walls. Such a band consists of two or four longitudinal steel bars with links or stirrups embedded in concrete of medium grade such as M150 (having a 15 cm cube crushing strength of 150 kg/cm^2 after 28 days of curing). The concrete thickness may be kept equal to one or two brick courses. In reinforced brickwork, the steel may be provided in two consecutive courses with two bars near each face of the wall so that the total area of steel is the same as in a reinforced concrete band (Fig. 2.3). The minimum size of band and amount of reinforcing depend upon the unsupported length of wall between cross-walls, the seismic zone, importance of building, type of soil and storey of the building. The appropriate steel and size of band for different cases are detailed in Table 2.6.

Depending on the level where such a band is provided it is called a plinth, lintel or a roof band.

(i) Plinth Band: This band is not too critical and so should be provided only in those cases where the soil is soft or uneven in their properties.

(ii) Lintel Band: This embraces all door and window lintels in itself. It must be provided in all storeys as per Table 2.6. This is the most important of all the bands.

(iii) Roof Band : This band will be required in those cases where the floor or roof is other than reinforced concrete or reinforced brick slab which has a binding effect on the walls automatically. For instance if a floor consists of precast concrete or timber joists with covering elements, the joists must be properly integrated at the ends and anchored into the roof band laid on walls just underneath.

(b) Dowels at Corners and Junctions: Steel dowel bars may be used at corners and junctions to integrate the box action of walls as an alternative to the horizontal band. However, the dowels do not provide horizontal bending strength to the walls except near the corners and junctions. These are placed (Fig. 2.4) in every fourth course or at about 30 cm intervals.

2.3.5 Vertical Reinforcement in Walls

Brick buildings upto four storeys can be strengthened sufficiently at a small additional cost to avoid collapse under severe ground shaking by providing vertical steel at corners and junctions of walls and the jambs of openings. The amount of vertical steel depends upon the number of storeys, storey heights, importance of building, effective seismic coefficient based on seismic zone and foundation soil. The values of reinforcement (Arya, Chandra and Thakkar 1977; Indian Standard Code 4326-1976) are given in Table 2.7. Typical details of placing the vertical steel in brickwork at corners and junctions are shown in Fig. 2.5.

The overall arrangement of providing reinforcement in brick building construction is schematically shown in Fig. 2.6.

2.4.6 Problems for Study

The strengthening measures as discussed here above are based on theoretical and experimental investigations carried on brick structures subjected to static lateral loads. For evaluation of the efficacy of strengthening, it would be necessary and realistic to theoretically analyse strengthened brick buildings subjected to ground shaking. The inelastic behaviour of such brick building system has yet to be studied. Experimental investigations of such buildings subjected to dynamic

loads is still wanting so as to observe their dynamic behaviour and to compute dynamic response.

The provisions for strengthening brick buildings on the basis of such investigations would be more rational.

2.5 BEHAVIOUR OF RIGID OBJECTS DURING EARTHQUAKES

2.5.1 Introduction

In Dubri earthquake of 1930, it was observed (Joshi, 1960) that in the structures consisting of wooden framework with wooden posts fixed in the masonry stub columns, random vibrations were set up tending to tear away different parts of the structures resulting in their heavy damage. However in similar structures where the wooden posts were not fixed to the masonry stub columns, and merely rested on them, no damage occurred in the superstructure since it was free to slide with respect to the foundation. Similar observations were also reported in the earthquakes of 1934 Bihar and 1950 Assam in India.

Taking a cue from these observations, the feasibility of developing a building system could be studied in which the superstructure is allowed to slide at the plinth level so that the separation acts as an isolation system as well as some of the input energy due to ground motion may be dissipated in sliding.

Already the sliding and overturning of the objects not tied to the ground have been the subject of study by some investigators and the same has been briefly reviewed here.

2.5.2 Theoretical Studies

A simple relation was developed (Newmark, 1965) to estimate maximum relative displacement, Z_m, of a friction mounted rigid mass subjected to dynamic force due to an earthquake pulse as follows:

$$Z_m = \frac{1}{2} \frac{v_f^2}{g\, a_g} \left(1 - \frac{a_g}{a_f}\right) \qquad \ldots (2.1)$$

in which

a_f = acceleration coefficient of the accelerating force

v_f = maximum velocity of the accelerating force

a_g = acceleration coefficient of ground motion

g = acceleration due to gravity

The results given by this equation generally overestimate the relative displacement for an earthquake as it does not take into account the acceleration pulses in opposite direction.

The effect of alternating pulses as in an earthquake motion has been incorporated in another seismic response study (Chandrasekaran, 1970) of

friction mounted rigid objects. Two cases were considered in this study. First, a dashpot with viscous damping connecting the object with the ground was considered in which the damping force was assumed as a linear function of velocity. Secondly, a dashpot with coulomb damping was assumed in the analysis where damping force was kept independent of the magnitude of velocity but depended upon its phase. It was concluded that the relative displacement of the object always occurred irrespective of the coefficient of friction. This appears to be quite illogical as the sliding must stop when the acceleration coefficient of the object becomes less than the coefficient of friction.

2.5.3 Theoretical and Experimental Studies

The problem has been studied rationally by observing the response of small rigid object allowed to slide or overturn on shake table under dynamic loads (Mittal, 1971). The response was computed theoretically also for the table motion. This analytical formulation included the frictional resistance as such, the object moving only when the acceleration coefficient exceeded the coefficient of friction and the direction of frictional force determined by the direction of velocity of the object. The order of computed displacements for sliding of these objects was found in good agreement with those obtained experimentally, though in some cases the correlation

was seen to be not so good. Theoretical response of rigid objects for the longitudinal component of Koyna earthquake of Dec. 11, 1967 (Krishna, Arya and Kumar, 1973) was also calculated for various values of coefficient of friction which showed that the total sliding of the objects would be rather small and was sensitive to coefficient of friction. From this study, it was concluded that the train of alternating acceleration peaks in succession had significant contribution in sliding motion. Obviously a single peak pulse cannot simulate this effect. A comprehensive studyb (Krishna, Arya and Kumar, 1973) of sliding and overturning behaviour of thousands of small objects during an earthquake has been made in an attempt to solve the problem of estimating peak ground acceleration near the epicentre and its attenuation with distance in the absence of strong motion instruments.

Such studies have been made (Krishna, Arya and Kumar, 1969; Krishna, Arya and Kumar, 1971) after Koyna earthquake of Dec. 11, 1967 and Broach earthquake of March 23, 1970 in India. The investigators have also made a dynamic analysis to obtain theoretical seismic response of the objects. This concept of sliding behaviour of objects may also be applied to the structures. The equation of motion for the rigid object subjected to one horizontal component of ground

acceleration has been written (Krishna, Arya and Kumar, 1973) as follows (for which, the mathematical model is shown in Fig. 2.7).

$$\dot{V} + f(V) = -\ddot{y} \qquad \ldots(2.2)$$

where $f(V) = \mu g \ \text{sign}(V)$ when $V \neq 0$ $\qquad \ldots(2.3)$

or, $f(V) = -\ddot{y}$ when $V = 0$

and $V = \dot{x} - \dot{y}$; $\dot{V} = \ddot{x} - \ddot{y}$ $\qquad \ldots(2.4)$

in which

μ = coefficient of friction between the surfaces of contact

$x, \dot{x}, \ddot{x}$ = absolute displacement, velocity and acceleration of rigid mass

V = relative velocity of rigid mass

$\dot{V}$ = relative acceleration of rigid mass

$y, \dot{y}, \ddot{y}$ = ground displacement, velocity and acceleration respectively

The results obtained using Equation (2.2) for sliding movement of objects with various frictional coefficient for Koyna and El Centro earthquakes (peak ground acceleration 0.63 g and 0.34 g respectively) are given in Table 2.8. It is seen that as μ approaches the peak ground acceleration, the extent of sliding becomes zero (Figs. 2.8 and 2.9). The relative movement of the object increases as μ decreases and the difference between μ and the peak ground acceleration coefficient increases. Rasidual displacement of the object also generally inceases as μ decreases but the

trend is not regular (Figs. 2.8 and 2.9). Under such condition, the seismic force attracted by the object would be less.

2.5.4 Problem for Study

The observations during past earthquakes indicate good behaviour of wooden huts which were not fixed into footings. Theoretical and experimental studies on sliding of rigid objects indicate only a limited extent of movement even in severe earthquakes for moderate values of coefficients of friction. The observations suggest that it may indeed be profitable to study the feasibility of brick-buildings having a sliding joint at ground floor or plinth level and to investigate the seismic behaviour through analysis as well as testing. Unlike the small rigid objects studied so far, the superstructure of even single storey building will have finite stiffness. In such a study, the coefficient of friction between the sliding surfaces and the earthquake parameters would play very significant role. The structural properties of the superstructure should also be considered in the dynamic analysis.

2.6 MULTISTOREYED BRICK BUILDING MODELS TESTED UNDER LATERAL LOADS

Three-storeyed single room (122 x 122 x 122 cm high) building models (one-third scale) were tested (Arya and Swaminathan, 1969) under lateral loads for

determining their dynamic behaviour. The experimental results were compared with theoretical results obtained by considering the structural behaviour in different ways. The following four types of models were tested each constructed in 1:6 cement sand mortar

(i) Unstrengthened model

(ii) Strengthened model with vertical steel at the corners

(iii) Model with corner reinforcement and lintel band

(iv) Vertical steel at the corners and jambs with lintel band in the model.

Under lateral load testing, the unstrengthened model developed initial cracks at very early stage revealing its brittleness and unsuitability for resisting lateral loads. A small percentage of 0.05% steel at the corners totally transformed the behaviour of the building making it resilient and ductile. This behaviour improved further in the other two more strengthened models. Experimentally observed deflections in the models were compared with those theoretically computed. This showed that 'Pier-method' of analysis may be employed with sufficient accuracy for computing the deflection and stiffness in the brick building.

Such study of multistoreyed brick buildings having at least two rooms would have been better from structural viewpoint as the ratio of height to width of the building may completely change the behaviour. Testing of multistoreyed building models for dynamic loads would certainly be a step towards understanding and predicting their behaviour under ground shaking. For a realistic study of such buildings, however, the soil-structure interaction should also be considered. Larger scale models will be preferable for dynamic testing so that the results thus obtained may permit more realistic prediction of prototype performance under seismic conditions.

2.7 SUMMARY

The state of understanding achieved through the work of earlier investigators on various aspects of seismic resistance of brick buildings is summarised below:

(i) Materials of Construction. The compressive strength of brickwork is seen to depend on the compressive strength of bricks, strength of mortar used and quality of construction including wetting of bricks before laying, etc. The tensile strength is mainly a function of the adhesion between the mortar and the brick. The shearing strength depends on the compressive stress present besides the bond in the brick-mortar

composite. A good amount of data on the strengths as well as modulus of elasticity and damping values in brickwork has already become available.

(ii) Behaviour of Shear Walls. The weakness of unreinforced brick shear walls to resist lateral loads has been studied well. Tests on single-storey shear walls show that failure occurred by cracks passing through mainly horizontal joints due to vertical bending tension. Analysis carried out by different existing methods, indicates that these methods do not give reliable results for stress and deflection. Considering the variation due to workmanship, the simplified approach given by Benjamin (1959) appears to be adequate for the analysis and design of brick structures.

Not much work has yet been done on the dynamic behaviour and response analysis of brick shear walls.

Studies on the behaviour of reinforced brick shear walls subjected to static lateral load and quasi-static cyclic load have been made by many investigators. From such studies, it is clearly seen that lateral load strength as well as deformability of a brick shear wall is greatly improved by reinforcing it vertically and horizontally. But such provision of reinforcing in the walls would create many constructional problems. In view of this, other strengthening schemes have been suggested by other investigators as discussed

herein at a later stage.

(iii) Behaviour of Cross-Walls. Horizontal bending of cross-wall under lateral load should affect the behaviour of shear walls considerably. Behaviour of cross-walls for the seismic resistance of the brick building has not yet been investigated and both analytical and experimental studies are required.

(iv) Openings in Brick Walls. Investigations carried out on the effect of openings on the strength of walls show that their strength is considerably reduced by openings. Also openings in the walls complicate their behaviour. For high seismic resistance, the openings should be as small in size and as centrally located as functionally possible. The prevailing guidelines for providing openings in the walls are mainly based on the theoretical analysis of the isolated walls under inplane lateral loads. There is still a need to carry out investigations on brick building models subjected to dynamic loads to study the influence of size and position of openings in the walls. Analytical dynamic study is also needed for understanding the effects of openings on the stiffness as well as strength.

(v) Integral Action of Walls. Though some work has been done regarding contribution of cross-wall as flanges on the seismic resistance of the shear walls, but to a limited applicability only. In a

brick building, the effectiveness of cross-wall to act as flange of the shear walls will depend upon whether the walls at right angles are built integrally or connected rather loosely. All the walls must be properly tied together to avoid separation at vertical joints so as to form box section for greater seismic resistance. There is a need to investigate the dynamic behaviour and seismic resistance of brick building to establish how far the box action is achieved in realistic constructions and to arrive at the proper minimum mechanical connection so as to achieve the full integral action.

(vi) Reinforcing of Brick Building. Horizontal reinforcing of the walls is required for tying the perpendicular walls together and for imparting horizontal bending strength against plate action of the cross-walls. Vertical steel at corners and junctions of walls and the jambs of openings is required due to poor tensile strength of brickwork. Seismic behaviour and response of brick buildings strengthened with horizontal and vertical reinforcements at the critical locations needs to be studied through experimental investigation. For evaluation of the efficacy of strengthening, it would also be necessary to theoretically analyse strengthened brick buildings subjected to ground shaking.

(vii) Static and Dynamic Testing. From the earlier work, it is seen that models of isolated shear walls and a few brick structures have been tested either under static lateral load or quasi-static cyclic load. For investigating their seismic behaviour and response it would be rational to test models of brick structures subjected to base motion for simulating the ground shaking.

(viii) Model versus Prototype Behaviour. The compressive strength tests of 1/3 and 1/6 scale model and full size piers and walls show that the strength of full size specimen for given strengths of brick and mortar could be reproduced by means of model tests. Also, if the same mortar was used to construct the model and full scale walls, the model walls would take higher stresses than the equivalent full-scale one.

Three-storeyed single room 1/3 scale brick building models built with different strengthening arrangements have been tested under lateral loads. Testing of models of such buildings through base motions would certainly be a step towards real understanding and predicting their behaviour under ground shaking. Large scale models will be better for more realistic prediction of prototype seismic performance of brick structures.

(ix) New System of Brick Building. Studies on sliding of rigid objects indicate only a limited extent of movement even in severe earthquakes for moderate values of coefficient of friction. The observations suggest that it may indeed be profitable to investigate the feasibility of brick buildings having a sliding joint at plinth level so that the superstructure is allowed to slide at that level. Seismic behaviour of such a system needs to be investigated through theoretical and experimental studies.

It is thus seen that there are a number of unsolved problems in regard to understanding the seismic behaviour of brick building fully. Only a few of these could indeed be tackled in this thesis as described in the succeeding chapters.

TABLE 2.1

STRENGTHS AND MODULUS OF ELASTICITY FOR DIFFERENT MORTARS

Sl. No.	Mortar Mix	Compressive Strength kg/cm^2	Tensile Strength kg/cm^2	Shear Strength + kg/cm^2	Modulus of Elasticity E kg/cm^2
1	1:3 Cement-Sand	94.3	7.1	10.4	16,900
2	1:6 Cement-Sand	61.2	2.5	3.9	14,100
3	1:12 Cement-Sand	53.8	0.4	2.2	7,700
4	1:2 Lime-Surkhi++	58.7	0.9	2.5	9,900
5	Clay Mud	47.5	0.3	0.8	4,200

+ Arya, Chandra and Thakkar, 1977

++ Crushed red-brick powder

TABLE 2.2

DAMPING VALUES FOR DIFFERENT MORTARS

S. No.	Mortar Mix	Damping as % of critical damping increasing with strain level
1.	1:6 Cement Sand	2.5% to 4.0%
2.	1:2 Lime- Surkhi	4.0% to 6.5%
3.	Clay Mud	7.5% to 10.0%

TABLE 2.3

DAMPING VALUES FOR DIFFERENT CEMENT SAND MORTAR MIX

S. No.	Mortar Mix	Damping as % of Critical damping rising with the increase in strain
1.	1:3 Cement-Sand	1.8% to 5.5%
2.	1:6 Cement-Sand	2.2% to 6.2%
3.	1:12 Cement-Sand	3.8% to 7.5%

TABLE 2.4

CATEGORIES OF CONSTRUCTION FOR STRENGTHENING

Category	Conditions for the Category	
	Seismic Zone	Soil
I	A	Soft
II	A	Firm, Soft
	B	Soft
III	A	Firm
	B	Firm, Soft
	C	Soft
IV	B	Firm
	C	Firm, Soft

Notes:

i) Firm soil refers to those having bearing capacity $> 11\ t/m^2$

ii) Soft soil refers to those having bearing capacity $\leq 11\ t/m^2$

iii) Weak soil liable to compaction and liquefaction under earthquake are excluded.

TABLE 2.5

MORTAR MIXES

(Arya, Chandra and Thakkar,1977)

S. No.	Cement	Lime	Sand	Categories of Construction (See Table 2.4)
1	1	1	6	I
2	1	2	9	I
3	1	-	6	I, II, III
4	-	1	3	II, III, IV

TABLE 2.6

REINFORCEMENT IN R.C. BAND

(Arya, Chandra and Thakkar, 1977)

S. No.	Span (m)	Longitudinal Steel in R.C. Band							
		Category I		Category II		Category III		Category IV	
		No.of Bars	Dia.of Bars (mm)	No.of Bars	Dia.of Bars (mm)	No.of Bars	Dia.of Bars (mm)	No.of Bars	Dia.of Bars (mm)
1	5	2	12	2	10	2	10	2	10
2	6	2	16	2	12	2	10	2	10
3	7	2	16	2	16	2	12	2	10
4	8	4	12	2	16	2	16	2	12
5	9	4	16	4	12	2	16	2	12

Notes: (i) Width of the R.C. band is assumed to be the same as the thickness of wall.

(ii) Thickness of R.C. band may be kept minimum as 7.5 cm where two bars are specified and 15 cm where four bars are specified.

(iii) Concrete mix 1:2:4 by volume or having 150 kg/cm^2 cube crushing strength at 28 days is to be used.

(iv) The longitudinal bars should be held in position by steel links or stirrups 6 mm dia. spaced at 15 cm apart.

TABLE 2.7

VERTICAL STEEL AT CRITICAL SECTIONS

(Arya, Chandra and Thakkar, 1977)

No.of Storeys	Storey	Diameter of Single Bar in mm at each critical section for Categories			
		Category I	Category II	Category III	Category IV
One	-	16	12	12	Nil
Two	Top	16	12	12	Nil
	Bottom	20	16	12	Nil
Three	Top	16	12	12	Nil
	Middle	20	16	12	Nil
	Bottom	20	16	16	Nil

TABLE 2.8

SLIDING DISPLACEMENTS OF RIGID MASS UNDER KOYNA AND EL CENTRO EARTHQUAKES

S.No.	μ	Maximum Relative Displacement (mm)		Residual Relative Displacement (mm)	
		Koyna EQ.	El Centro EQ.	Koyna EQ.	El Centro EQ.
1	0.05	56.4	67.2	22.3	67.2
2	0.10	23.6	26.3	5.4	19.7
3	0.15	16.3	16.9	15.1	7.8
4	0.20	7.6	11.7	7.1	8.2
5	0.25	2.9	3.4	1.9	2.4
6	0.30	1.3	0.08	1.2	0.08
7	0.40	0.34	0.0	0.34	0.0
8	0.50	0.06	0.0	0.06	0.0

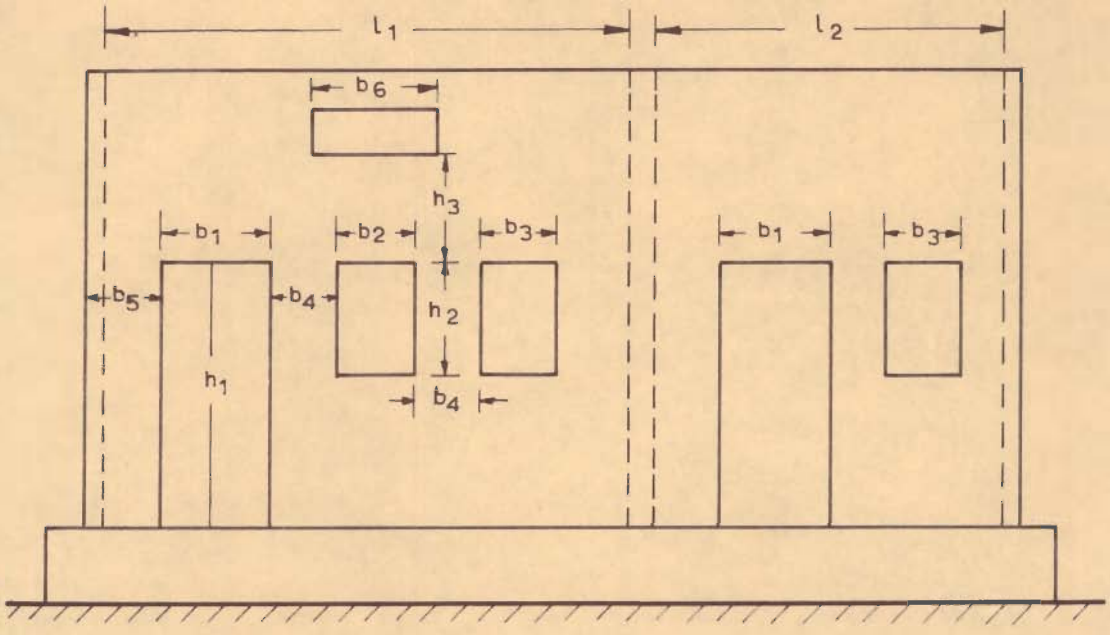

NOTES: $b_1 + b_2 + b_3 \leq 0.5\, l_1$

$b_4 > 0.5 h_2$

$b_5 \geq 0.25 h_1$

$h_3 >$ 60cm or $0.5(b_2$ or 0.5 WHICHEVER IS LESS)

FIG. 2.1 – OPENINGS IN BEARING WALLS

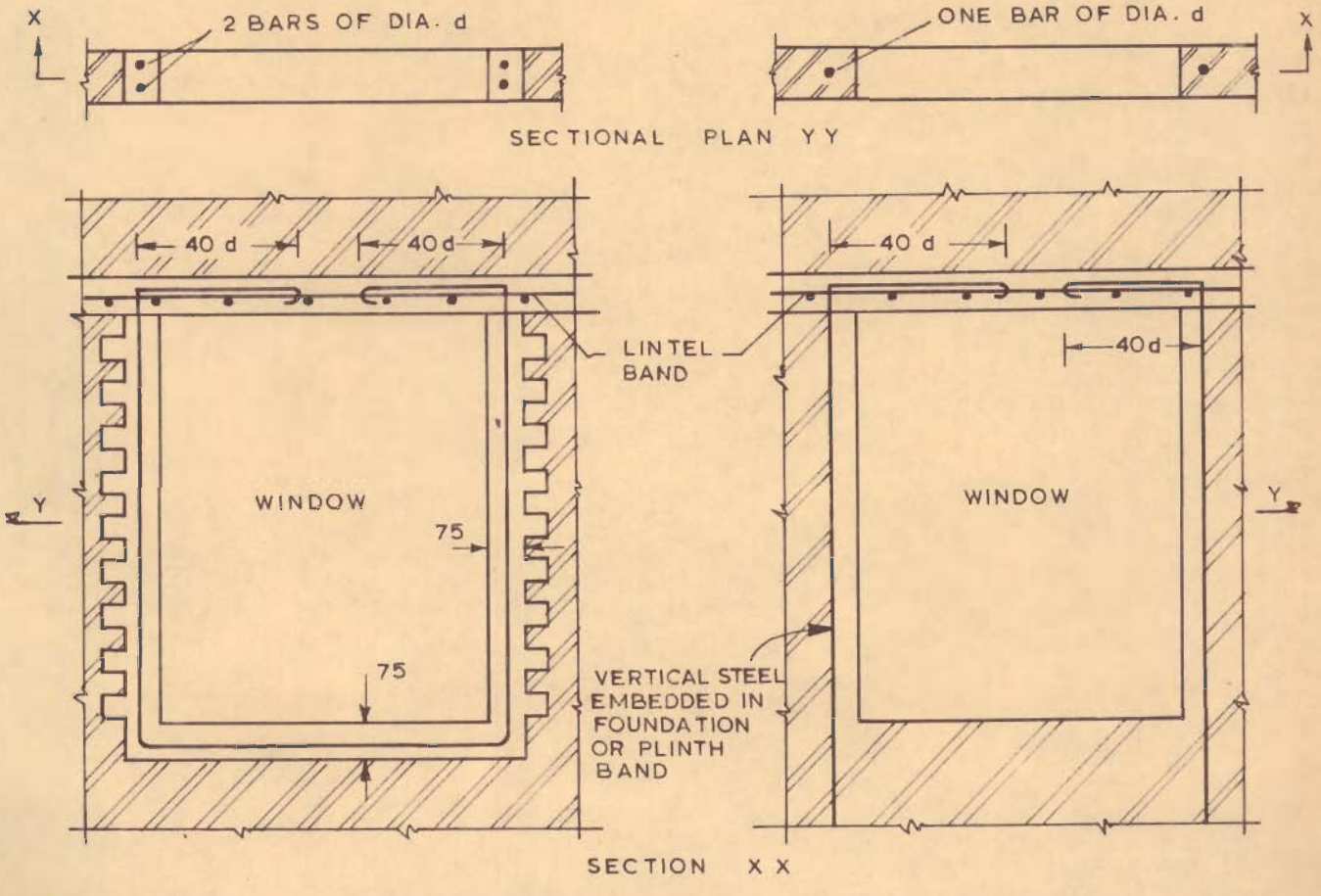

FIG. 2.2 – STRENGTHENING OF MASONRY AROUND OPENINGS

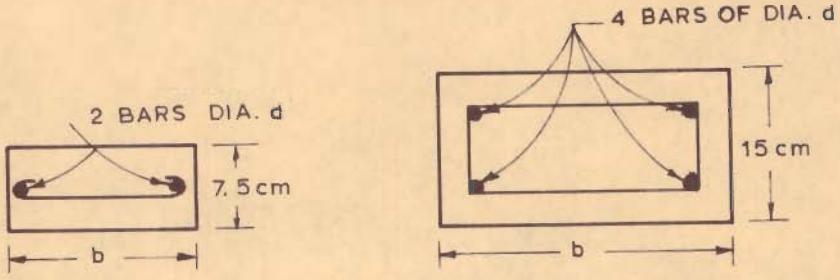

a - CROSS SECTION OF R.C. BAND FOR TWO BARS AND FOUR BARS

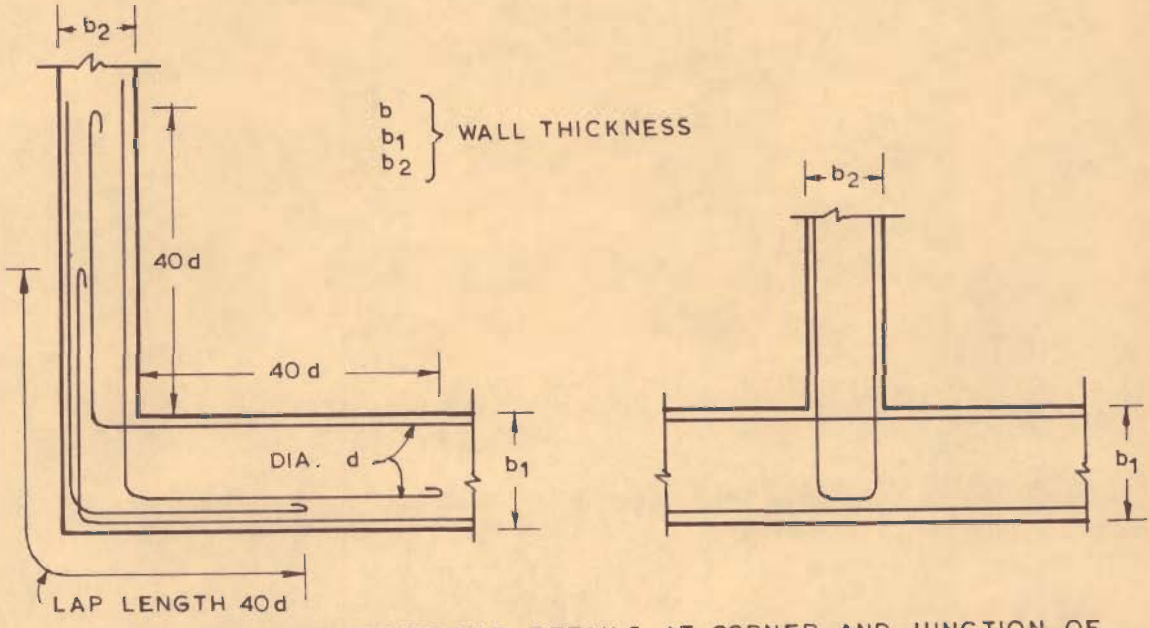

b - RC BAND REINFORCEMENT DETAILS AT CORNER AND JUNCTION OF TWO WALLS

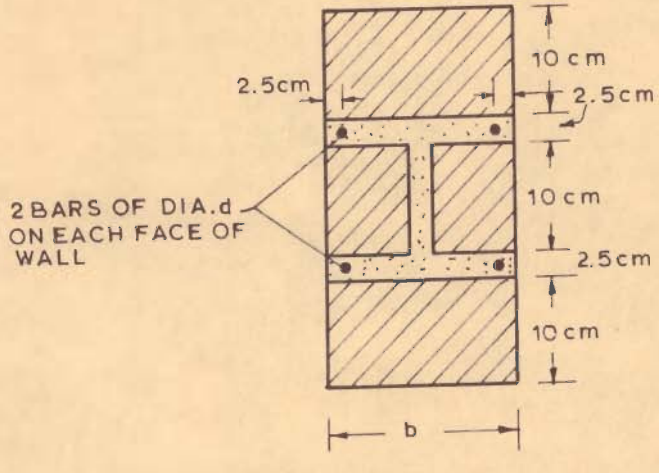

c - REINFORCED BRICKWORK BAND

FIG. 2.3 - REINFORCEMENT IN BAND (Arya, Chandra and Thakkar, 1977)

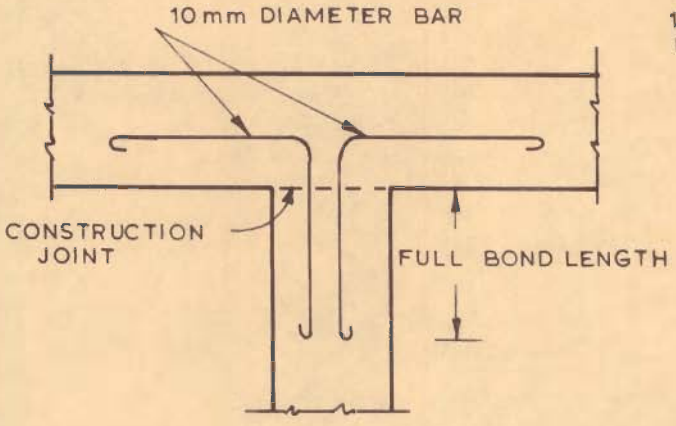

DOWEL BARS AT T-JUNCTION

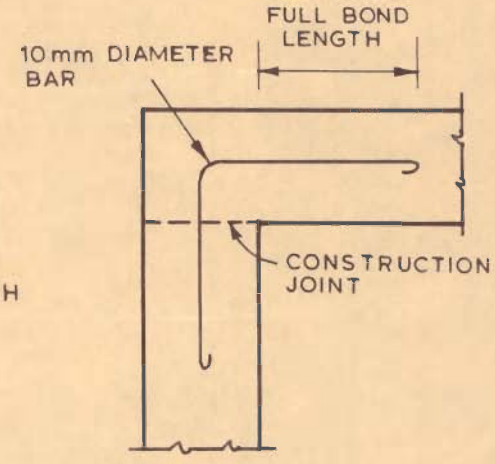

DOWEL BAR AT CORNER

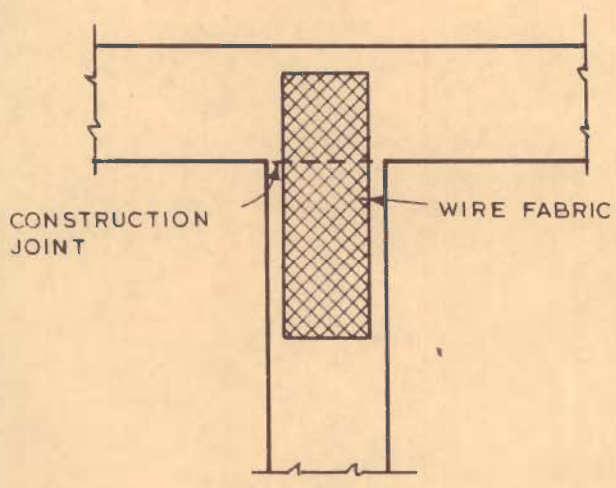

WIRE FABRIC AT T-JUNCTION

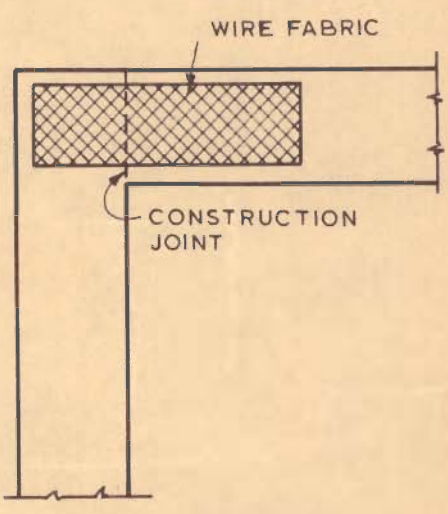

WIRE FABRIC AT CORNER

FIG. 2.4 _ DOWEL BARS AND WIRE FABRIC AT JUNCTION AND CORNER (Arya, Chandra and Thakkar 1977)

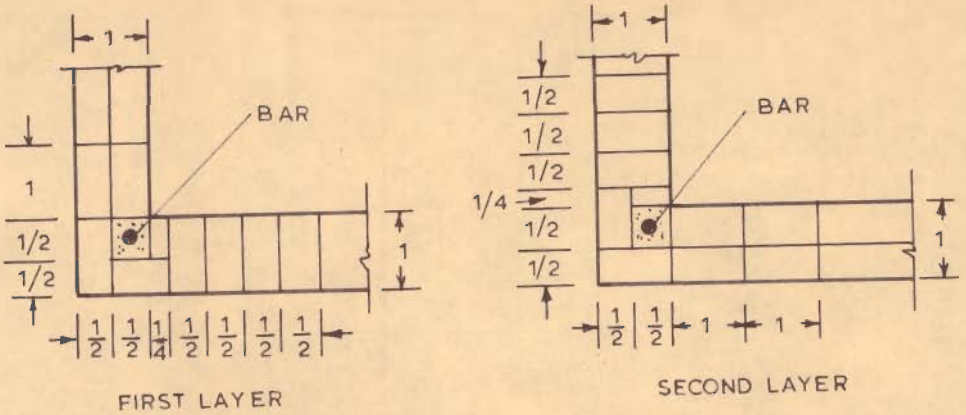

Corner junction details for one brick wall for providing vertical steel

1/4, 1/2 AND 1 INDICATE THE THICKNESS OF BRICK
- 1/4 BRICK THICK
- 1/2 BRICK THICK
- 1 BRICK THICK ETC.

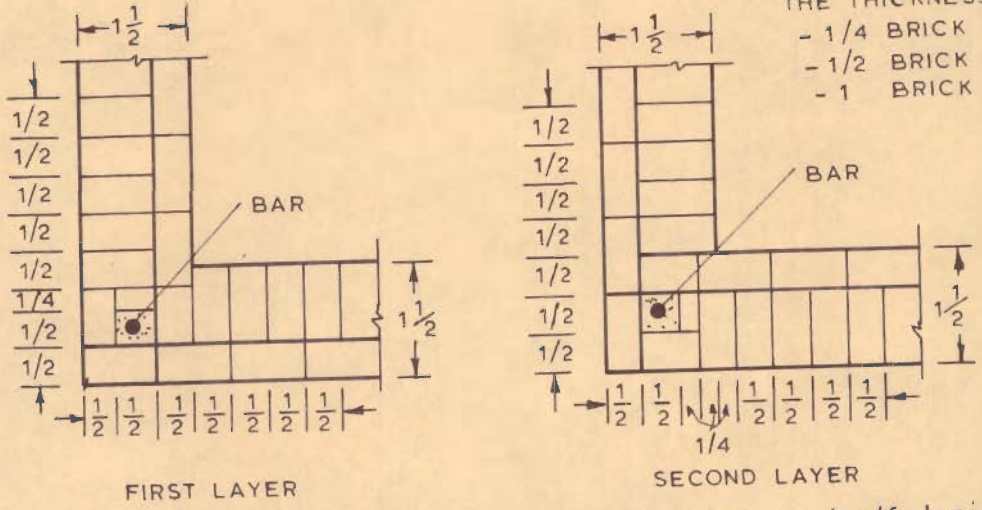

Corner junction details for one and a half brick wall for providing steel

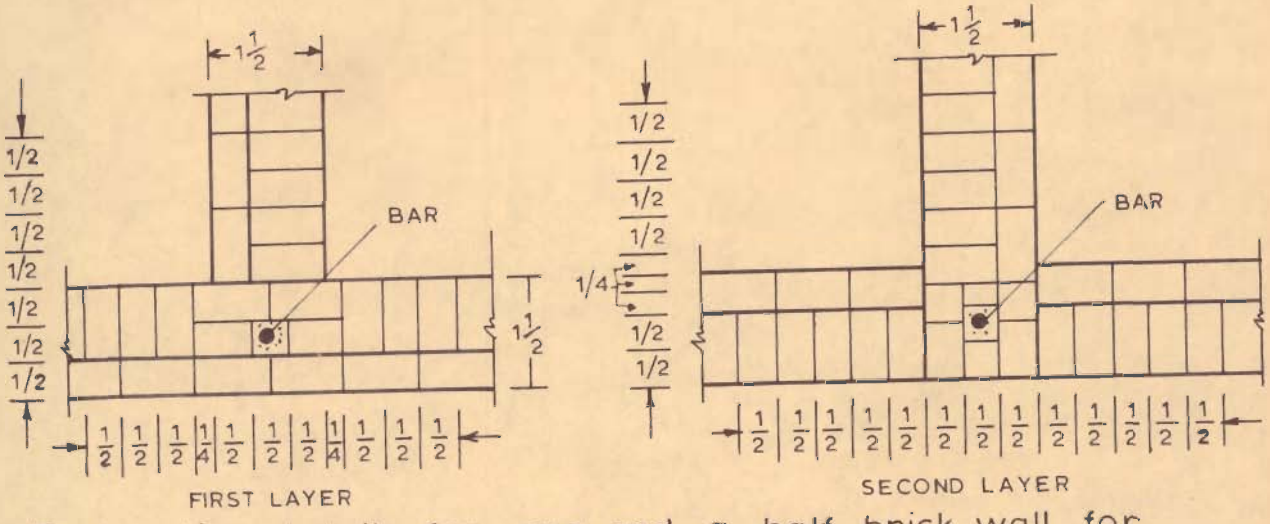

T- Junction details for one and a half brick wall for providing vertical steel

FIG.2.5 _ VERTICAL REINFORCEMENT IN WALLS
(Arya, Chandra and Thakkar, 1977)

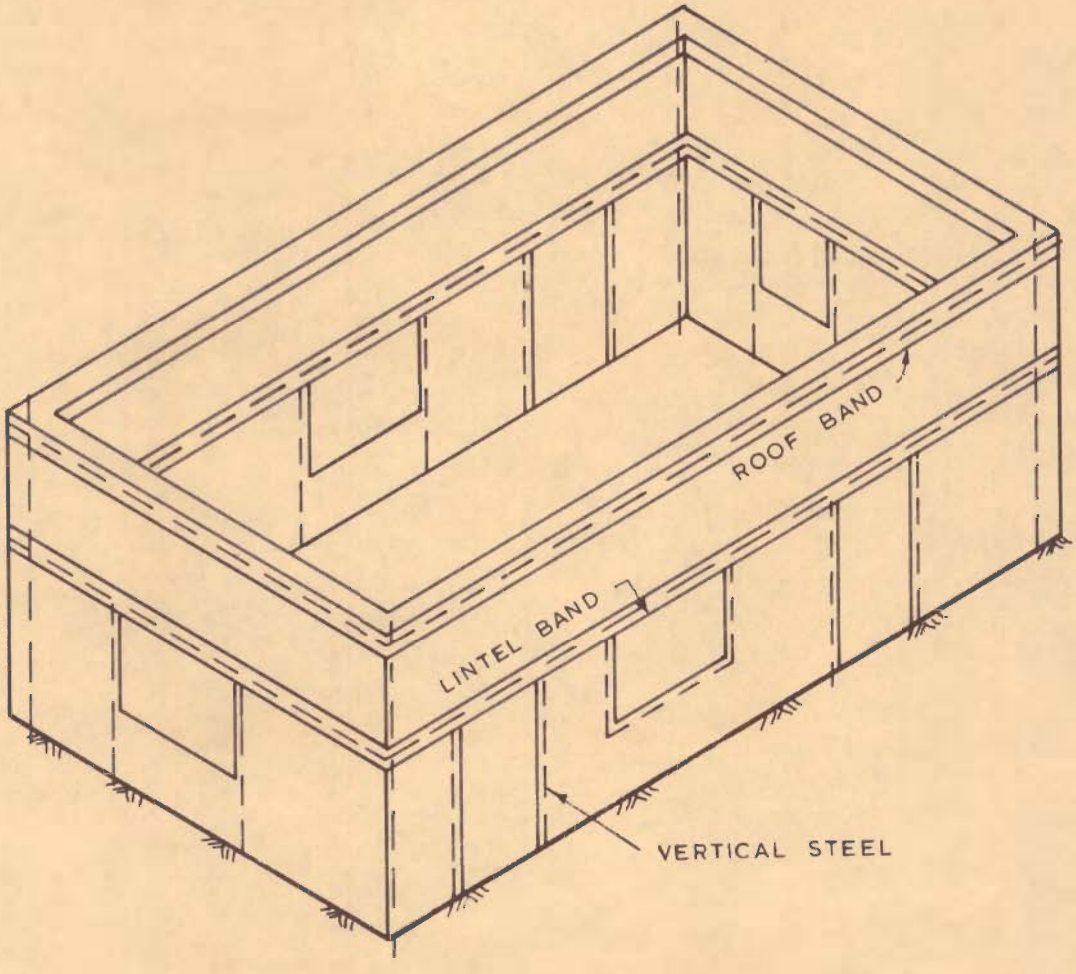

FIG. 2.6 _ OVERALL ARRANGEMENT OF STRENGTHENING
(Arya, Chandra and Thakkar, 1977)

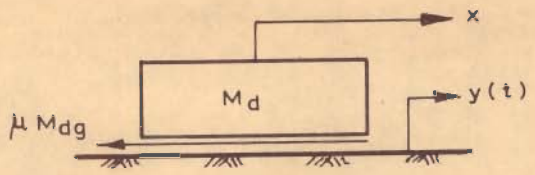

FIG. 2.7_MATHEMATICAL MODEL OF FRICTION MOUNTED SYSTEM

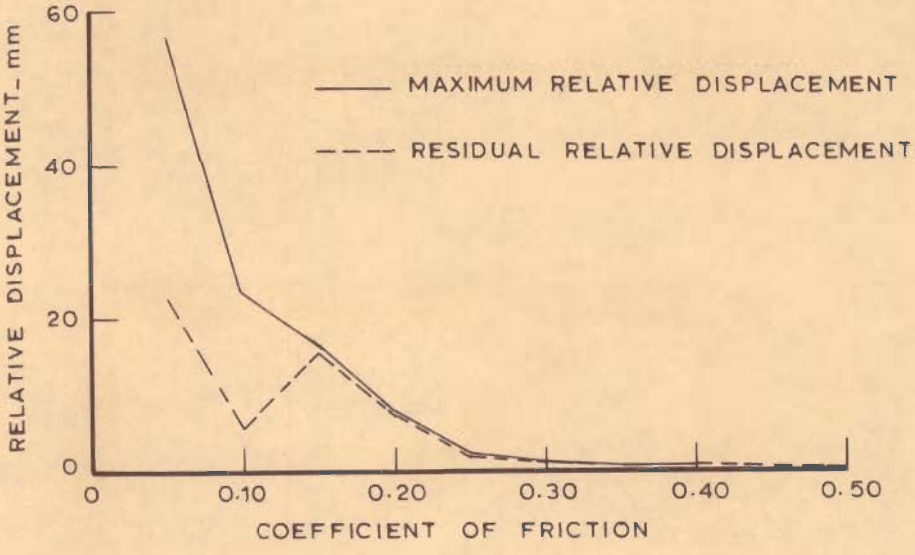

FIG. 2.8_VARIATION OF RELATIVE DISPLACEMENT OF RIGID OBJECTS WITH COEFFICIENT OF FRICTION UNDER KOYNA EARTHQUAKE

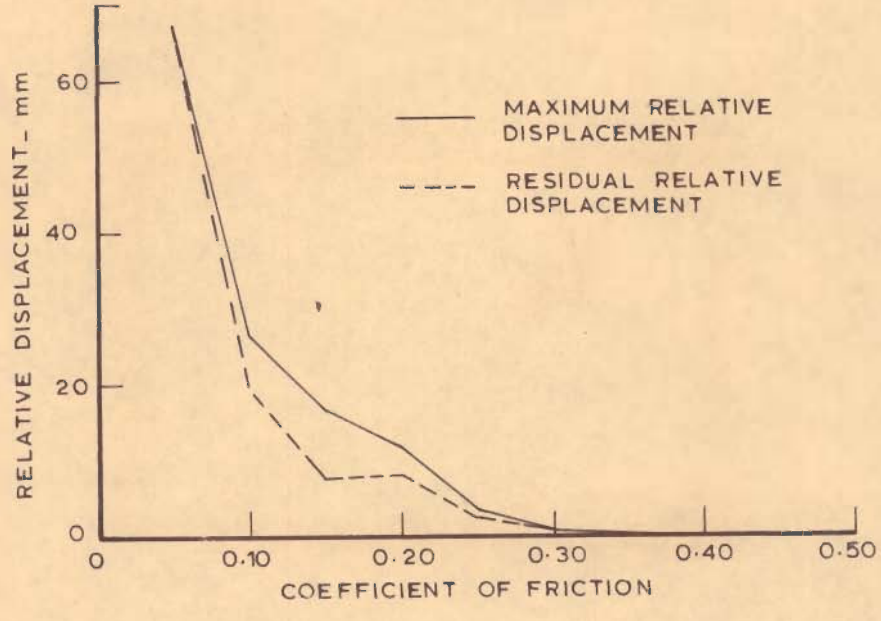

FIG. 2.9_VARIATION OF RELATIVE DISPLACEMENT OF RIGID OBJECTS WITH COEFFICIENT OF FRICTION UNDER EL CENTRO SHOCK

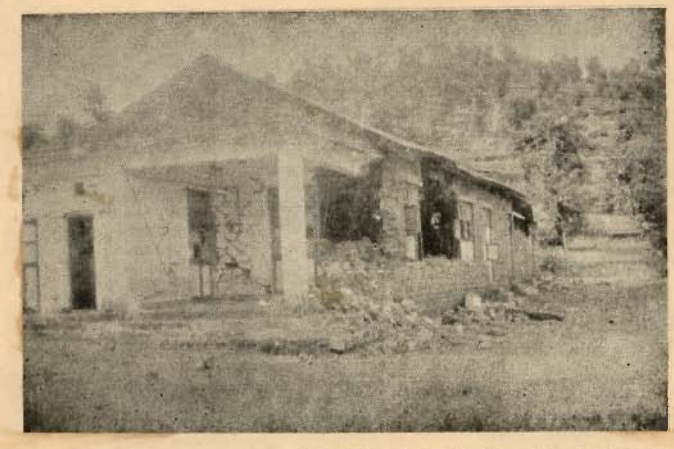

PHOTO 2.1 - DAMAGE TO SCHOOL IN KOYNA EARTHQUAKE, INDIA (STAR CRACK PATTERN IN BRICK WALL)

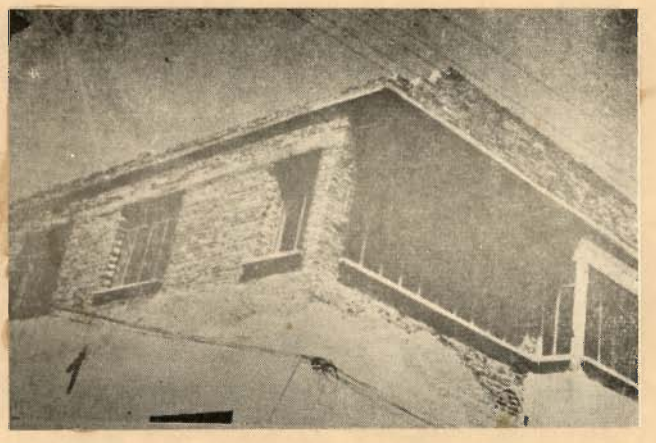

PHOTO 2.2 - EARTHQUAKE DAMAGE TO UNREINFORCED BRICK PARAPET

PHOTO 2.3 - DIAGONAL CRACKING OF WALLS NEAR WINDOW OPENING (GEDIZ EARTHQUAKE OF 1970 TURKEY)

C H A P T E R 3

EARTHQUAKE ANALYSIS OF CONVENTIONAL BRICK BUILDINGS

3.1 GENERAL

As stated in Chapter 2, it is now well established that the failure of brick buildings during earthquakes occurs mainly due to a combination of horizontal flexural and diagonal (shear) cracking. The cracking starts at certain critical points and spreads quickly in the absence of reinforcing steel. The aim of the present chapter is to analyse typical brick buildings of one to four storeys for identifying the critical sections, magnitudes of tensile or shearing stresses, requirements of steel, etc. under realistic earthquake motions in moderate to severe seismic zones. For this purpose a building plan as actually put up at Delhi has been chosen and two recorded earthquake accelerograms used for response calculation. The steel requirements as calculated have been compared with those specified in the Indian Standard.

As is well known, seismic response of a structure depends upon its own characteristics and those of ground motion. Two methods are normally employed for computing elastic response of a structure : (a) time-wise superposition of modal responses and (b) direct integration of differential equations of motion. The

former is adopted here because the first few modes always have dominant contribution to the response in this type of structures and therefore only as many modal equations are required to be integrated. In the second method, all simultaneous equations are essentially required to be integrated involving considerable additional computational effort.

3.2 STRUCTURAL BEHAVIOUR OF BRICK BUILDINGS

Before discussing the method of seismic analysis of conventional brick buildings, it would be worthwhile to consider their structural behaviour. The behaviour of single-storeyed brick building is discussed here, yet it applies equally to the multistoreyed buildings also since shear beam model has been assumed for the later. In fact, it is basically the horizontal and vertical resisting elements which are present in the structural system to carry gravity and lateral loads. Their combined action under earthquake force is explained in the following paragraphs.

An inertia force acts on the mass of a building due to ground shaking on account of which the building tends to remain stationary while the ground moves. If the building is assumed rigidly fixed into the ground, inertia force would cause horizontal shears in the building. The magnitude of the horizontal shear is function of the ground shaking and the stiffness and

damping characteristics of the building. The roof system transfers the seismic force to the shear walls through diaphragm action. For diaphragm action, a roof and/or floor system should be able to transmit the lateral forces to the shear walls without excessive deflection of its own.

The stiffness of a horizontal diaphragm affects the distribution of the lateral forces to the shear wall. For the purpose of analysis, diaphragms may be classified (Yorkdale, 1970) as : (a) rigid, (b) semi-rigid and (c) flexible. Each type of diaphragm is bound to disttibute the lateral forces in a different way. A rigid diaphragm is assumed to transfer lateral forces to the shear walls in proportion to their stiffnesses. Semirigid diaphragms have significant deflection under load but also have sufficient stiffness to distribute a portion of the load to the shear walls in proportion to stiffnesses of the shear walls. A flexible diaphragm is considered to distribute the forces to all the walls on a tributary area basis.

For discussing the structural action of the walls under ground shaking (Arya, 1967), consider a single-storeyed building as shown in Fig. 3.1. When the ground motion is along x-axis, the walls SW would act as shear walls whereas CW as cross-walls. If the roof slab is rigid to act as a horizontal diaphragm

and is securely held to the four walls, it would be reasonable to assume that the horizontal displacement of walls will be uniform at the slab level. Since the shear walls are several times stiffer than the cross-walls, the inertia force of the roof slab would almost be wholly taken by them. The plate-action of walls CW would be restrained by the roof slab at the top thereby reducing the horizontal bending of the wall CW. On the other hand, if the roof is flexible, then its inertia force would be transferred to the wall on which it is supported and the support peovided to plate-action of walls CW would also be little. In either case if the walls CW and SW are securely connected to each other at the corenrs, a substantial part of the inertia force of CW will also be supported by SW.

3.3 ANALYSIS OF SHEAR WALL

From the discussion in the preceding sections, it turns out that the shear walls are the main structural element for transferring the seismic forces to the foundation. Factors determining their strength are too many and too varied as indicated by their tests (Agnihotri, 1962; Chandra, 1963; Lal and Chandra, 1970). The main source of error and uncertainty is the workmanship which is a very difficult parameter to control. During building construction, generally toothed joints are left at corner and/or junction of a wall which are

supposed to be filled with mortar when the construction of the transverse wall starts. Very often such vertical joints remain unfilled or poorly filled (Photo 3.1) and there remains a plane of weakness at the junctions of shear and cross-walls. Such joints open out very easily when earthquake motion shakes the building. In the analysis of conventional buildings it is conservatively assumed that the shear walls act separately in resisting lateral forces and the flange effect of the cross-walls is ignored. Besides such uncertainties, door and window openings in the shear walls lead to discontinuities and stress concentrations, the analysis of which is made uncertain due to the hetrogenous nature of all types of masonry. Various exact and semi-exact mathematical methods (Arya and Pal, 1969) have been suggested for the analysis of shear walls treating them as two dimensional plane stress problem. Such methods are too refined and complicated to be applied to brick shear walls having so many uncertainties as discussed above. Therefore, the simplest available approach is adopted here (PAC, 1955; Krishna and Arya, 1965). The method of analysis is briefly explained below.

A brick shear wall, assumed as rigidly fixed at the base, is shown in Fig. 3.2 wherein the three 'piers' 1, 2 and 3 which are relatively more flexible

than other portions are specifically indicated. The horizontal inertia forces due to the weight of roof and walls are marked in figure 3.2. If F is the horizontal shear in a building element, then the deflection, δ, at its top is given by

$$\delta = \frac{F h^3}{12EI} + \frac{1.2\ Fh}{GA} \qquad \ldots(3.1)$$

where

h = height of the pier

I = moment of inertia about the axis of bending

A = cross-sectional area of the pier

E,G = modulii of elasticity and rigidity of the brickwork respectively.

Shape factor for shear deflection computation of the pier having a rectangular cross-section has been taken as 1.2. The shear stiffness, k, of the pier or a solid wall, assuming its top and bottom ends are fully restrained against rotation, is obtained as.

$$k = \frac{12EI}{h^3} \cdot \frac{1}{1+ 2.4\ (d/h)^2} \qquad \ldots(3.2)$$

in which d is width of the pier in the plane of bending. In working out the above relationship Poisson's ratio of brickwork is assumed as zero giving $G = E/2$.

In the case of a multistoreyed bcick building, the shear stiffness of any building element is represented by k^s_{ij} which is defined as:

k^s_{ij} = shear stiffness of jth pier in the ith shear wall of sth storey.

Thus, knowing the shear stiffness of all the piers in a storey, the total horizontal shear in that storey is shared by the building elements in the ratio of their shear stiffnesses. For the shear wall shown in Fig. 3.2 let the share of the horizontal shear by the piers 1, 2 and 3 be F_1, F_2 and F_3 respectively as shown in Fig. 3.3. Then, each such pier carries a shear force, F, which would cause bending moment, Fh/2, at its top as well as bottom. The resulting values of maximum shear stress, q, and bending stress, p_b, are given by

$$q = 1.5\ F/\ bd \qquad \ldots (3.3)$$

$$p_b = 3\ Fh/bd^2 \qquad \ldots (3.4)$$

Distribution of direct vertical stress due to vertical loads on roof and floor is also subject to much variation in different buildings depending on the longitudinal stiffness of wall elements, locations and width of openings in walls, presence of wall plates, rigidity of floors and roof in vertical direction, rigidity of lintels and construction sequence. For simplicity the

direct stress p_d due to vertical loads, assumed to be uniform is given by

$$p_d = W/\Sigma A \qquad \ldots(3.5)$$

where

W = the total vertical load above the horizontal section of the building through the piers and

ΣA = the sum of the cross-sectional area of the piers and walls at that section.

The vertical stress p_o caused by the overturning moments, applied by the horizontal inertia forces, in any of the piers 1, 2 and 3,etc. is assumed to be proportional to the distance of the point from the centroid of the pier areas. Thus the average stress in a pier will be

$$p_o = K_p x' \qquad \ldots(3.6)$$

where

$$K_P = \frac{M_F + F_3 (h_2-h_1)/2}{A_3 x_3'(a_1 + a_2) - A_2 x_2' a_1} \qquad \ldots(3.7)$$

x' = distance of centroid of pier from centroid of pier areas

A_1, A_2 and A_3 = cross-sectional areas of the piers

K_P = coefficient of proportionality

x_1', x_2' and x_3' = distances of G_1, G_2 and G_3 from C.G. (as shown in Fig. 3.5)

a_1 = distance between G_1 and G_2

a_2 = distance between G_2 and G_3

M_F = moment of the horizontal forces about G_1

G_1, G_2 and G_3 = centroid of the piers 1, 2 and 3

The resultant stress, p_{ct}, in any pier may be compressive or tensile and is given by

$$p_{ct} = p_b + p_d + p_o \qquad \ldots (3.8)$$

Such stress analyses are to be made for every shear wall and along two axes of the building and for reversible earthquake force. In case of multistoreyed buildings, the structural idealization and the mathematical modelling of the actual building are presented in the following sections.

3.4 STRUCTURAL IDEALIZATION OF MULTISTOREYED BRICK BUILDING

Figure 3.5 shows schematic view of a typical single-roomed three-storeyed idealized brick building. Non-structural elements as may be present in actual buildings are not shown in the figure as they are assumed to have no contribution in resisting seismic forces. Only first storey walls A-1 and B-1 are shown in Fig. 3.6 for illustration. For the ground shaking parallel to x-axis, walls A-1 and B-1 would behave as shear walls whereas walls C-1 and D-1 as cross walls. But when the ground motion is along y-axis, the

situation would be reversed. Therefore, each wall has to be analysed as shear wall for the relevant direction of earthquake shock.

3.5 MATHEMATICAL MODEL OF THE BUILDING

The earthquake analysis of multistoreyed brick buildings subjected to earthquake shock consists of determining forces in their structural elements from dynamic displacements, velocities or accelerations. For computing these response parameters, it is necessary to convert the building into a mathematical model. The choice of this model is to be made suitably so that the structural properties are appropriately taken into account. Here the following assumptions are made for arriving at the mathematical model:

(1) The building material is elastic and lies within limit of proportionality. The limitation of this assumption is that the tension in the building material should develop upto such a stage that cracking does not occur. If cracking occurs, redistribution of stresses in different building elements would take place and this assumption will not be valid for unreinforced walls. However, if reinforcement is placed to take the tension in its elastic range, the elastic analysis could still be used as for reinforced concrete sections.

(2) The building is subjected to only one horizontal component of ground motion at a time and that the building vibrates only in the direction of ground motion.

(3) The building behaves as shear structure while vibrating laterally. Since the top and bottom spandrels of the wall are relatively much stiffer than the piers (see Fig. 3.6) and also axial deformation of the piers due to the overturning moment are likely to be small compared to their bending and shearing deformation, the lateral displacements at top of the piers in a given storey of the building, are assumed to be equal. This is further strengthened by observation of the actual behaviour of a three-storeyed brick building after Gediz (Arya, Chandra and Thakkar, 1977) earthquake of 1970 (Turkey) as shown in Photo 3.2

(4) The shear walls resist the earthquake force without any aid from the cross walls, that is, the 'flange effect' of cross-walls is neglected. It has been stated earlier that due to usual toothed joints adopted between walls at right angles, there remains a plane of weakness at the junction of the shear and cross-walls. As such, the joints may open out very easily during ground shaking, leaving the shear walls to act separately in resisting seismic forces. This is an assumption in the conservative side so far as

stresses in the walls are concerned.

(5) Interfloor damping is represented in the form of viscous damping. The material damping values assumed in the study (Mallick, 1961; Krishna and Chandra, 1965) depend on the ratio of mortar mix and the rate of straining as well. The values of damping for different mortars are given in Section 2.3 of Chapter 2.

(6) The building configuration is symmetrical about its principal axes. Although, this assumption has been made to achieve a simple mathematical model for the building, yet a building having unsymmetrical configuration could also be analysed by computing the additional shears on account of torsional effect (see Section 3.9).

A multistoreyed brick building is thus represented by a multiple degree freedom shear-beam system. The piers, which are located parallel to the direction of earthquake shaking are assumed to provide spring action. The mass of the walls and slabs are assumed lumped at the storey levels. The lumped masses are assumed to be connected to each other through massless spring and viscous dampers. The degree of freedom of each mass in horizontal translation is one neglecting the vertical translational and rotational degrees of freedom.

Thus, the system leads to a simplified mathematical model as shown in Fig. 3.7.

3.6 EQUATIONS OF MOTION OF LUMPED MASS BUILDING SYSTEM SUBJECTED TO GROUND MOTION

The equations of motion for a multiple degree of freedom system when subjected to ground motion can be written in the matrix notation as follows:

$$[M]\{\ddot{Z}\} + [C]\{\dot{Z}\} + [K]\{Z\} = -[M]\{\ddot{y}\} \quad \ldots(3.9)$$

where $[M]$ is a diagonal mass matrix, $[C]$ is a viscous damping matrix, $[K]$ is a tridiagonal stiffness matrix, $\{Z\}$ is the vector of the relative displacement of masses with respect to ground and y is the horizontal component of ground displacement. Superscript dots represent differentiation with respect to time. The storey stiffness, K_{st}, in a building is evaluated as follows:

$$K_{st} = \sum_{i=1}^{s_w} \sum_{j=1}^{b_e} k_{ij} \quad \ldots(3.10)$$

where,

b_e = total number of building elements, that is, piers in a wall

s_w = total number of shear walls in a storey

k_{ij} = lateral stiffness of a pier considering its bending as well as shearing deformations

Equation (3.9) represents simultaneous linear differential equations of second order. To compute dynamic response of the system, these equations are to be solved numerically.

It is well known that only first few modes of vibration have significant contribution whereas share of higher modes is small in the dynamic response of the system. Therefore, the mode superposition method will be good enough for evaluating the response of the system.

3.7 SOLUTION OF EQUATIONS OF MOTION

The equations of motion for the idealized multi-storeyed brick building model subjected to ground shaking are given by Eq. (3.9). As pointed out in the preceding section, the mode superposition method will be used for response computation. For this, Eq. (3.9) are converted into a set of N uncoupled equations in normal coordinates, $\{\beta\}$. The rth mode equation is written as

$$\ddot{\beta}_r + 2p_r \zeta_r \dot{\beta}_r + p_r^2 \beta_r = - Q_r \ddot{y}(t) \quad \ldots(3.11)$$

the solution of which is given by

$$\beta_r = \frac{Q_r}{p_{dr}} \int_0^t \ddot{y}(\tau) \exp\left\{-p_r \zeta_r (t-\tau)\right\} \sin p_{dr}(t-\tau) d\tau \quad \ldots(3.12)$$

where p_r and ζ_r are natural circular frequency and fraction of critical damping respectively in this mode of vibration, Q_r is rth mode participation factor,

p_{dr} is damped natural frequency in rth mode and τ is time variable for integration. Using the principle of superposition, the relative displacement can be computed as

$$\{Z\} = \sum_{r=1}^{N} \{\phi_r\} \beta_r \qquad \ldots(3.13)$$

where $\{\phi_r\}$ is a rth modal column vector of a square matrix $[\phi]$ and N is the number of modes considered in the analysis.

3.8 METHOD OF NUMERICAL INTEGRATION

Runge-Kutta fourth order method (Benett et al,1956) is employed in the present study for numerical integration of Eq. (3.12) since this method is self starting and the solutions are stable and accurate to a definite precision.

3.9 SEISMIC STRESS ANALYSIS OF THE BUILDING ELEMENTS

Knowing the absolute accelerations at various storey levels of the building subjected to ground motion in any mode, the storey shears are easily found by multiplying the absolute acceleration by the mass lumped at the corresponding storey level. The storey shears at any instant of time is then obtained by superimposing the modal shears at that instant of time. Here, the storey shears are obtained by superimposing the shears of all the modes. The shear force in each shear wall of the storey is then determined by distributing the

storey shear force among the shear walls in proportion to their stiffnesses. The timewise stresses in each pier are then worked out as explained in Section 3.3. Maximum of the timewise stress in the pier thus gives the maximum stress in the pier for the ground motion.

Computation of Torsional Shear: Torsion of whole building normally occurs when the centre of rigidity, of the building elements in a storey, does not coincide with the centre of gravity of the structure. This condition is automatically satisfied in a building with symmetrical plan about both its main directions. In others, such a condition can be achieved by proper planning and design of the building elements. Where the condition of no-torsion is not satisfied, the distance between the centre of mass and rigidity gives the eccentricity of the earthquake force in plan. The torsional moment is then equal to the seismic force times the eccentricity. Often the design eccentricity is taken as 50% higher than the actual (IS: 1893-1975). Knowing the torsional moment, the resulting shears in the building elements can be computed using the usual simplified procedure (Blume et al, 1961).

The total shear, P, in a building element is then given by

$$P = F_L + F_T \qquad \ldots(3.13)$$

where F_L is the shear resulting from lateral loads without torsion and F_T the shear produced by torsional moment. This analysis is also done mode-wise as described above.

3.10 COMPUTATIONAL SCHEME FOR SEISMIC STRESS ANALYSIS OF MULTISTOREYED BRICK BUILDING

A computer programme has been developed for time-wise seismic response computation of conventional type multistoreyed brick building. Provisions are also made in the computer code to perform time-wise seismic stress analysis of the building elements. The complete computational scheme for this purpose has been given through a flow diagram (Appendix-A).

3.11 DATA FOR STUDY OF CONVENTIONAL BUILDINGS

3.11.1 Buildings Studied

A typical plan of a residential building (Figs. 3.8 and 3.9), having twin blocks, has been chosen for the study. The following two main variables are considered for the buildings:

(a) Number of Storeys - The number of storeys varies from one to four. The same plan has been adopted for different storeys.

(b) Wall Thickness - The thickness of main walls in different storeys is kept in two ways:

(i) Uniform thickness of main walls in all the storeys. This applies to all buildings from one to four storeyed.

(ii) First storey main walls thicker than the top two in the three storeyed buildings and first and second storeys main walls thicker than the top two in four storeyed buildings.

The buildings studies are referred to in the later descriptions as follows:

(a) B1 - single - storeyed building having thickness of main walls as 229 mm (Fig. 3.8).

(b) B2 - two-storeyed building with 229 mm thick main walls in both the storeys (Fig. 3.8).

(c) B3A - three-storeyed building with 229 mm thick main walls in all the storeys (Fig.3.8).

(d) B3B - three-storeyed building having 343 mm thick main walls in the first storey (Fig. 3.9) and 229 mm thick main walls in the upper storeys (Fig. 3.8).

(e) B4A - four-storeyed building with 229mm main walls in all the storeys (Fig. 3.8).

(f) B4B - four-storeyed building having 343 mm main walls in the first and second storeys (Fig.3.9) and 229 mm main walls in upper two storeys (Fig. 3.8).

3.11.2 Damping

The most common way of considering damping in the dynamic analysis of a structure is to assume it to be of viscous type. For the present study of the multistoreyed brick building, three values of viscous damping have been taken in the fundamental mode. These are: 5%, 10% and 15% of critical. The damping values as determined for brickwork in various mortar mixes have been discussed in Section 2.3 of Chapter 2. The fraction of critical damping in higher modes has been assumed in proportion to their respective model frequencies (Mital, 1969). The damping in the fundamental mode, is therefore the only data to be prescribed for seismic response computations.

3.11.3 Ground Motion Characteristics

The influence of the characteristics of ground motion upon the structural response is an important aspect in the study. It is now recognized that in an accelerogram, peak acceleration as well as the frequencies associated with acceleration pulses are equally important. This is significant since the accelerograms recorded at different distances from the epicentre contain different predominant frequencies. The damaging potential of a shock is represented more realistically by its spectral intensity SI, (Housner, 1959; Chandra, 1971) which gives a quantitative idea

of structural response over a range of structural periods. Mathematically,

$$SI = \int_{T_1}^{T_2} S_v \quad (T, \zeta) \, dT \qquad \ldots(3.14)$$

where T is the fundamental period of structure and S_v is the velocity spectrum. The following two accelerograms have been examined on the basis of their spectral values for the present investigation:

(a) Longitudinal component of Koyna earthquake of December 11, 1967 with peak ground acceleration of 0.63 g and predominant frequency approximately equal to 11 Hz, (Fig. 3.10) and

(b) North-South component of El Centro shock of May 18, 1940 with peak ground acceleration 0.34 g and predominant frequency approximately equal to 3 Hz (Fig. 3.11).

Koyna accelerogram was recorded close to the epicentre of the shock and had high acceleration pulses and high frequency content while El Centro accelerogram was recorded at about 50 km from epicentre of shock and had relatively lower acceleration ordinates as well as frequency content. Thus the influence of pattern of accelerogram on the structural response has been studied with these two different earthquakes selected in the present study.

Although Housner (1959) had defined the spectral intensity (SI) as the area under velocity spectrum curves between the period 0.1 and 2.5 sec, yet, for the present study, SI values of the two chosen earthquakes have been computed between the periods 0.04 and 0.30 sec for 5% of critical damping. This was done to cover the range of periods of interest in the buildings under study. It is found that the spectral intensity thus computed for the Koyna shock is almost two times that of El Centro shock.

Incidentally, the above two earthquakes could be considered appropriate for MM Intensity IX and VIII Zones (seismic Zones V and IV of IS: 1893-1975) respectively so far as short period structures are concerned since Intensity IX Zone generally consists of epicentral tracts whereas Intensity VIII Zones lie at moderate distance from epicentres of severe earthquake shocks. Considered in this light, the Indian Standard specifications for strengthening brick buildings (IS: 4326-1976) could be checked with the strengthening requirements based on dynamic response calculations.

3.11.4 Material Elasticity and Strength

The material properties of the brickwork have been investigated earlier (Agnihotri, 1962; Chandra, 1963) for different types of specimens as

discussed in Section 2.3 of Chapter 2. For brickwork in various mortars, the values of compressive, tensile and shear strengths and modulus of elasticity were listed in Table 2.1. The cement mortar of 1:6 proportion is assumed for the present analysis for which 5% damping will be representative value in the uncracked condition and 10% damping for cracked condition with reinforcing bars. The higher value of 15% of critical will indeed represent the cracked state of mud mortar construction and has been included just for comparison.

3.12 PRESENTATION AND DISCUSSION OF RESULTS

The mass, stiffness and free vibration characteristics of conventional unstrengthened brick buildings B1 to B4B as defined earlier are given in Tables 3.1 to 3.8. The results of seismic analysis of these buildings when subjected to Koyna and El Centro shocks are presented in Tables 3.10 to 3.15. Each table gives the magnitude of maximum bending, direct and overturning stresses in the various storeys occurring any where in the storey. The net tensile and shearing stresses are also shown. The values are given for both the earthquakes and the three damping values chosen in the fundamental mode. The variations of the stress along the height are plotted in Figs. 3.12 and 3.13. The influence of different parameters of the buildings on the stresses is discussed in the

following paragraphs.

3.12.1 Number of Storeys

The effect of number of storeys on the maximum stresses is best seen in Figs. 3.12 and 3.13 for three and four storeyed buildings.

(i) As would be expected, in all the buildings analysed, maximum stresses - bending, overturning, net and shear - go on reducing in higher storeys as compared to that in lower storeys but the rate of decrease and its pattern is different with the type of stress. For instance, referring to Fig. 3.13 (b), the shape of stress curve for bending stress which is based on storey shears and the overturning stress which depends on cantilever bending of the whole building are different. The significant point to note is the overturning stresses increase towards base almost linearly but the bending stresses in a broken line fashion more slowly. This is also seen from the following ratios of overturning to bending stress in the first storeys of the buildings.

Building Types	B1	B2	B3A	B3B	B4A	B4B
Number of Storeys	1	2	3	3	4	4
Ratio of Overturning to Bending Stress in Pier	0.115	0.209	0.254	0.256	0.278	0.281

Thus with buildings of larger number of storeys the proportion of the two stresses in the net tensile stress would go on changing and whole piers may come in tension rather than each pier having a change of sign.

(ii) The single storey building is similar in all respects to the top storeys of multistoreyed buildings in cases B2, B3B and B4B. Similarly the second storey from top in B2, B3B and B4B and the third storey from top in B3B and B4B are similar in all respects. Comparing the bending and shearing stresses we see the results for Koyna earthquake and 5% damping as given in Table 3.9. From the results shown in Table 3.9 we find the interesting result that the earthquake stresses in upper two storeys of multi-storey buildings are higher but the maximum margin is about 28% only. Consequently if the reinforcing scheme is worked out for a 4 storeyed building, the same scheme could be applied to shorter buildings of similar plan by a slight extra margin of safety.

The higher stresses in upper storeys are occurring inspite of the fact that the taller buildings have longer time period and less spectral acceleration but the mode shape transfers the higher shears towards the upper storeys.

(iii) From Figs. 3.12 and 3.13, it is clear that the tensile and shearing stress are larger in the lower storeys which will need higher strength, greater amount of vertical reinforcing and greater ductility consideration due to larger compressive stresses. Since the shearing stresses also exceed the shearing strength, horizontal reinforcement also is called for at certain critical points.

3.12.2 Thickness of Main Walls

Thickness of main walls in the first storey of the building type B3B (three-storeyed) is more than that in the upper storeys. Similarly, in case of the building type B4B (four-storeyed), the first two storeys are thicker than the upper two storeys. The stresses developed in these buildings under earthquake shock are compared with that of the corresponding building types B3A and B4A (uniform thickness of main walls). The following points are noted from this study:

(i) Dissimilar patterns of stress distribution are obtained in the two cases (Figs. 3.12 and 3.13). This observation is true for various damping values and both the ground motions. This should be expected since there is a change of stiffness suddenly at a level in the non-uniform thickness case.

(ii) It is significantly observed from Figs. 3.12 and 3.13 and Tables 3.12 to 3.15 for the above cases that the stresses in non-uniform buildings are reduced in the lower thick wall storeys but increased in the upper thinner wall. As compared with the uniform case, the reduction is of the order of 20% in the bottom storey. This trend is seen for all damping values and both the earthquakes. The reason for reduction of stress in the bottom storeys is the reduction of inertia force due to reduction of weight in the upper storeys. In the upper storeys the stresses are increased due to larger reduction in the pier cross-section than the decrease in the inertia force.

3.12.3 Damping

The seismic stress analysis for the building types has been done for 5%, 10% and 15% of critical damping in the fundamental mode as described in Section 3.11.2. As expected and seen from Tables 3.10 through 3.15 and Figs. 3.12 and 3.13 that the stresses in all buildings decrease with an increase of the damping. Generally, the stresses reduce faster when the damping is increased from 5% to 10% than from 10% to 15%.

3.12.4 Type of Earthquake

Two types of earthquakes (Koyna and El Centro), as discussed in section 3.11.3, were chosen for the stress computation in all the buildings studied here. In Figs. 3.12 and 3.13, full and broken lines represent the stresses in the buildings subjected to Koyna and El Centro shocks respectively. It turns out that the pattern of the stresses in different building types is similar in the two cases for all the parameters in the analysis.

It is very significantly observed from Tables 3.10 to 3.15 that values of the stresses computed for all the building types under Koyna shock are about double in comparison with the corresponding values for El Centro shock. This observation corroborates well with ratios of the spectral intensities of the two earthquakes as discussed earlier in Section 3.11.3.

3.13 STRENGTH REQUIREMENTS

From the present seismic stresses, as presented in Tables 3.10 to 3.15, developing in the unstrengthened conventional multistoreyd brick buildings it is clearly seen that the demands on tensile and shearing strengths of material in both the Koyna and El Centro earthquakes are very severe and, in all cases except the single storeyed building,

these cannot be met with the strengths of brickwork in 1:6 or even 1:3 cement-sand mortar. Even in single storeyed buildings subjected to Koyna shock, the stresses exceed the strength values given in Section 2.3 of Chapter 2. The tensile stress developed in the four-storeyed brick building subjected to Koyna shock shoots up to 44.7 kg/cm^2 for 5% of critical damping. Thus provision of vertical steel reinforcement at the sections developing more than cracking tension and horizontal steel reinforcement at the sections developing higher shearing stresses is essential to check the development of cracks and sliding in the joints. The critical sections developing tensile stresses which are more than cracking tension are identified in the building plans as shown in Figs. 3.8 and 3.9.

As regards evaluation of their compressive strength, it is observed that the maximum stress of 51.04 kg/cm^2 for 5% of critical damping developed in the four-storeyed building under Koyna shock is less than the ultimate compressive strength, 61.22 kg/cm^2 for 1:6 cement mortar brickwork, some margin of safety is still available. Hence compression does not appear to be a critical factor in these buildings.

3.14 REQUIREMENTS OF REINFORCING STEEL

The critical sections developing tensile stresses are identified in unstrengthened brick

building plans as shown in Figs 3.8 and 3.9. In Section 3.13 it has been seen that these critical sections must be reinforced with steel bars to resist tensile stresses developed in them during the severe earthquake shocks. In estimating the vertical steel section, it is assumed that the total tension developing on any pier section will be resisted by the steel. In view of the earthquakes were being very severe, the stress in steel is allowed to reach the yield stress at the most severely stressed sections the stresses for which were given in Tables 3.10 to 3.15. Naturally if the same steel bars are provided at other sections, as is customary to adopt in beick buildings, the steel will be stressed to smaller extent. In the case of more severe shocks, steel at some sections may go into inelastic yielding range and save the building from collapse by absorption of energy. Thus the assumption of yield stress of steel at the most severely stressed section seems reasonable. Also for calculation of steel, assumption of 10% of critical damping will be justified since the fine cracking in brickwork associated with the development of tensile stresses in steel will naturally raise the damping value to about 10%. The steel bars calculated on this basis, using yield stress equal to 2500 kg/cm^2, are shown in Tables 3.16 and 3.17.

The vertical reinforcements as estimated above is compared with that specified in IS: 4326 on the basis of design seismic coefficients equal to 0.08 or more (that is whole of Zone V and important cases in Zone IV) and between 0.06 and 0.08 (that is most of Zone IV and important structures in Zone III) in the above tables. By this comparison (Tables 3.16 and 3.17), it is seen that the diameters of the vertical bars required herein and that provided in IS: 4326 are remarkably close. There is difference, that too slight, in few cases only. It is to be seen from Table 3.17 that, for the same number of storeys, the requirement of vertical steel is only slightly changed if the thickness of the main walls in all the storeys are kept uniform or otherwise varied.

Horizontal steel at the sections developing higher shearing stresses is estimated here for the most critical section in longitudinal and transverse walls and for both the earthquakes. The spacings of 6 mm diameter 2-legged stirrup, calculated using yield stress in steel and 10% damping, are shown in Table 3.18. It is seen from this table that horizontal reinforcement is definitely required in all the storeys of all the buildings considered when subjected to Koyna shock. But in the case of El Centro shock horizontal steel is not required in some of the top

storeys. The requirement of steel is naturally less in the latter case. The Indian Standard Code however does not recommend such provision of horizontal steel for taking care of the high shear stresses. Thus building designed according to IS:4326 will be liable to damage by diagonal tension. Therefore, recommendations for such horizontal steel are called for in the Code so as to safeguard the brick building from failure due to higher shearing stresses.

TABLE 3.1

FREE VIBRATION CHARACTERISTICS OF SINGLE-STOREYED BRICK BUILDING (TYPE-B1)

Mass kg-sec^2/cm	Stiffness t/m		Time Period for Vibration in(sec)	
	Longitudinal Direction	Transverse Direction	Longitudinal Direction	Transverse Direction
82.1	15.9	25.4	0.045	0.036

TABLE 3.2

FREE VIBRATION CHARACTERISTICS OF TWO-STOREYED BRICK BUILDING (TYPE-B2)

Storey or Floor	Mass kg-sec^2/cm	Stiffness t/m		Mode No.	Time Period for Vibration in(sec)		Modal Participation Factors	Eigen Vectors (ϕ_{ir} values)	
		Longitudinal Direction	Transverse Direction		Longitudinal Direction	Transverse Direction		ϕ_{1r}	ϕ_{2r}
2	82.1	15.9	25.4	1	0.079	0.062	0.808	1.00	1.49
1	128.1	15.9	25.4	2	0.032	0.026	0.192	1.00	-1.05

TABLE 3.3

FREE VIBRATION CHARACTERISTICS OF THREE-STOREYED BRICK BUILDING OF UNIFORM THICKNESS OF MAIN WALLS (TYPE-B3A)

Storey or Floor	Mass kg-sec^2/cm	Stiffness t/m		Mode No.	Time Period for Vibration in (sec)		Modal Participation Factors	Eigen Vectors (ϕ_{ir} Values)		
		Longitudinal Direction	Transverse Direction		Longitudinal Direction	Transverse Direction		ϕ_{1r}	ϕ_{2r}	ϕ_{3r}
3	82.1	15.9	25.4	1	0.114	0.090	0.596	1.00	1.76	2.08
2	128.1	15.9	25.4	2	0.042	0.033	0.334	1.00	0.17	-0.97
1	128.1	15.9	25.4	3	0.030	0.024	0.069	1.00	-1.48	1.20

TABLE 3.4

FREE VIBRATION CHARACTERISTICS (FOR LONGITUDINAL DIRECTION) OF THREE-STOREYED BRICK BUILDING OF NON-UNIFORM THICKNESS OF MAIN WALLS (TYPE-B3B)

Storey of Floor	Mass kg-sec^2/cm	Stiffness t/m	Mode No.	Time Period sec	Modal Participation Factor	Eigen Vectors (ϕ_{ir} Values)		
						ϕ_{1r}	ϕ_{2r}	ϕ_{3r}
3	82.1	15.9	1	0.106	0.521	1.00	2.10	2.46
2	128.1	15.9	2	0.041	0.394	1.00	0.21	-0.98
1	143.1	21.1	3	0.030	0.084	1.00	-1.55	0.11

TABLE 3.5

FREE VIBRATION CHARACTERISTICS (FOR TRANSVERSE DIRECTION) OF THREE-STOREYED BRICK BUILDING OF NON-UNIFORM THICKNESS OF MAIN WALLS (TYPE-B3B)

Storey or Floor	Mass kg-sec^2/cm	Stiffness t/m	Mode No.	Time Period sec	Modal Participation Factor	Eigen Vectors (ϕ_{ir} Values)		
						ϕ_{1r}	ϕ_{2r}	ϕ_{3r}
3	82.1	25.4	1	0.082	0.497	1.00	2.10	2.58
2	128.1	25.4	2	0.032	0,405	1.00	0.25	-0.99
1	143.1	36.2	3	0.024	0.097	1.00	-1.47	0.12

TABLE 3.6

FREE VIBRATION CHARACTERISTICS OF FOUR-STOREYED BRICK BUILDING OF UNIFORM THICKNESS OF MAIN WALLS (TYPE-B4A)

Storey or Floor	Mass kg-sec^2/cm	Stiffness t/m		Mode No.	Time Period for Vibration in (sec)		Modal Participation Factor	Eigen Vectors (ϕ_{ir} Values			
		Longitudinal Direction	Transverse Direction		Longitudinal Direction	Transverse Direction		ϕ_{1r}	ϕ_{2r}	ϕ_{3r}	ϕ_{4r}
4	82.1	15.9	25.4	1	0.153	0.118	0.465	1.00	1.86	2.45	2.70
3	128.1	15.9	25.4	1	0.053	0.042	0.340	1.00	0.85	-0.28	-1.09
2	128.1	15.9	25.4	3	0.035	0.028	0.162	1.00	-0.59	-0.65	0.98
1	128.1	15.9	25.4	4	0.029	0.023	0.033	1.00	-1.67	1.79	-1.33

TABLE 3.7

FREE VIBRATION CHARACTERISTICS (FOR LONGITUDINAL DIRECTION) OF FOUR-STOREYED BRICK BUILDING OF NON-UNIFORM THICKNESS OF MAIN WALLS (TYPE-B4B)

Storey or Floor	Mass kg-sec^2/cm	Stiffness t/m	Mode No.	Time Period sec	Modal Participation Factor	Eigen Vectors (ϕ_{ir} Values)			
						ϕ_{1r}	ϕ_{2r}	ϕ_{3r}	ϕ_{4r}
4	82.1	15.9	1	0.137	0.449	1.00	1.84	2.61	2.93
3	128.1	15.9	2	0.053	0.353	1.00	0.94	-0.33	-1.23
2	143.1	21.1	3	0.034	0.143	1.00	-0.55	-0.93	1.23
1	158.1	21.1	4	0.029	0.055	1.00	-1.49	1.44	-1.03

TABLE 3.8

FREE VIBRATION CHARACTERISTICS (FOR TRANSVERSE DIRECTION) OF FOUR-STOREYED BRICK BUILDING OF NON-UNIFORM THICKNESS OF MAIN WALLS (TYPE-B4B)

Storey or Floor	Mass kg-sec^2/cm	Stiffness t/m	Mode No.	Time Period sec	Modal Participation Factor	Eigen Vectors (ϕ_{ir} Values)			
						ϕ_{1r}	ϕ_{2r}	ϕ_{3r}	ϕ_{4r}
4	82.1	25.4	1	0.105	0.438	1.00	1.84	2.66	3.02
3	128.1	25.4	2	0.041	0.356	1.00	0.99	-0.32	-1.25
2	143.1	36.2	3	0.027	0.131	1.00	-0.45	-1.10	1.35
1	158.2	36.2	4	0.023	0.075	1.00	-1.35	1.13	-0.77

TABLE 3.9

COMPARISON OF STRESSES IN DIFFERENT STOREYS OF THE BUILDINGS

Storey	Building Type	Bending Stress kg/cm^2	Shearing Stress kg/cm^2	Net Tensile Stress kg/cm^2	Ratio to Base value
Top	B4B	9.95	5.91	10.64	1.21
	B3B	10.56	6.27	11.31	1.28
	B2	8.99	5.34	9.57	1.09
	B1	8.21	4.88	8.69	1.00
Second from Top	B4B	22.92	13.62	26.22	1.20
	B3B	24.12	14.33	27.68	1.27
	B2	19.02	11.30	21.69	1.00
Third from Top	B4B	25.47	15.13	30.08	1.04
	B3B	24.43	14.51	28.96	1.00

TABLE 3.10

MAXIMUM STRESSES IN SINGLE-STOREY BRICK BUILDING (TYPE-B1)

Stresses	Damping %	Maximum Stresses in Various Storeys kg/cm^2	
		Koyna EQ.	El Centro EQ.
Bending	5	8.21	2.55
	10	6.85	2.44
	15	5.85	2.42
Over-turning	5	0.94	0.29
	10	0.78	0.28
	15	0.69	0.27
Compressive (Net)	5	9.95	3.65
	10	8.45	3.53
	15	7.33	3.50
Tensile (Net)	5	8.69	2.39
	10	7.18	2.26
	15	6.06	2.24
Shear	5	4.88	1.52
	10	4.07	1.45
	15	3.48	1.44

TABLE 3.11

MAXIMUM STRESSES IN TWO-STOREYED BRICK BUILDING (TYPE- B2)

Stresses	Damping %	Maximum Stresses in Various Storeys kg/cm^2			
		Storey I		Storey II	
		Koyna EQ.	El Centro EQ.	Koyna EQ.	El Centro EQ.
Bending	5	19.02	9.37	8.99	4.32
	10	16.15	8.05	7.54	3.69
	15	14.11	7.35	6.50	3.32
Over-turning	5	3.97	1.93	1.03	0.49
	10	3.35	1.66	0.86	0.42
	15	2.91	1.50	0.74	0.38
Compressive (Net)	5	24.64	12.96	10.83	5.63
	10	21.16	11.37	9.21	4.92
	15	18.67	10.51	8.05	4.51
Tensile (Net)	5	21.69	10.00	9.57	4.37
	10	18.20	8.41	7.95	3.66
	15	15.72	7.56	6.79	3.25
Shear	5	11.30	5.57	5.34	2.57
	10	9.60	4.79	4.48	2.19
	15	8.38	4.37	3.86	1.97

TABLE 3.12

MAXIMUM STRESSES IN THREE-STOREYED BRICK BUILDING OF UNIFORM THICKNESS OF MAIN WALLS (TYPE-B3A)

Stresses	Damping %	Maximum Stresses in Various Storeys kg/cm^2					
		Storey I		Storey II		Storey III	
		Koyna EQ.	El Centro EQ.	Koyna EQ.	El Centro EQ.	Koyna EQ.	El Centro EQ.
Bending	5	30.63	15.74	21.52	11.57	8.98	5.04
	10	24.91	13.13	17.13	9.48	7.06	4.07
	15	20.99	12.28	14.28	8.65	5.91	3.63
Over-turning	5	7.79	4.10	4.25	2.33	1.03	0.58
	10	6.26	3.39	3.37	1.90	0.81	0.47
	15	5.23	3.13	2.81	1.71	0.68	0.41
Compressive (Net)	5	40.91	22.35	27.42	15.55	10.82	6.42
	10	33.67	19.02	22.15	13.03	8.68	5.35
	15	28.72	17.91	18.74	12.02	7.39	4.85
Tensile (Net)	5	36.27	17.70	24.47	12.59	9.55	5.16
	10	29.02	14.38	19.19	10.08	7.42	4.08
	15	24.07	13.26	15.79	9.07	6.13	3.59
Shear	5	18.20	9.35	12.79	6.87	5.34	2.99
	10	14.80	7.80	10.18	5.63	4.20	2.42
	15	12.48	7.30	8.48	5.14	3.51	2.16

TABLE 3.13

MAXIMUM STRESSES IN THREE-STOREYED BRICK BUILDING OF NON-UNIFORM THICKNESS OF MAIN WALLS (TYPE-B3B)

Stresses	Damping %	Maximum Stresses in Various Storeys kg/cm^2					
		Storey I		Storey II		Storey III	
		Koyna EQ.	El Centro EQ.	Koyna EQ.	El Centro EQ.	Koyna EQ.	El Centro EQ.
Bending	5	24.43	11.28	24.12	10.73	10.56	4.59
	10	19.08	10.05	17.30	9.39	7.53	3.99
	15	16.18	9.38	14.36	8.63	6.04	3.65
Over-turning	5	6.21	2.96	4.86	2.14	1.21	0.53
	10	4.87	2.50	3.46	1.87	0.86	0.46
	15	4.08	2.42	2.84	1.71	0.69	0.42
Compressive (Net)	5	32.78	16.08	30.64	14.53	12.58	5.93
	10	25.91	14.51	22.40	12.92	9.20	5.26
	15	22.22	13.66	18.86	12.00	7.54	4.87
Tensile (Net)	5	28.96	12.64	27.68	11.57	11.31	4.67
	10	22.15	11.06	19.44	9.96	7.94	3.99
	15	18.49	10.19	15.90	9.05	6.27	3.61
Shear	5	14.51	6.70	14.33	6.38	6.27	2.37
	10	11.34	5.97	10.28	5.58	4.48	2.37
	15	9.61	5.57	8.53	5.13	3.59	2.17

TABLE 3.14

MAXIMUM STRESSES IN FOUR-STOREYED BRICK BUILDING OF UNIFORM THICKNESS OF MAIN WALLS (TYPE-B4A)

Stresses	Damping %	Maximum Stresses in Various Storeys kg/cm²							
		Storey I		Storey II		Storey III		Storey IV	
		Koyna EQ.	El Centro EQ.	Koyna EQ.	El Centro EQ.	Koyna EQ.	El Centro EQ.	Koyna EQ.	El Centro EQ.
Bending	5	37.34	20.43	30.55	17.13	20.82	11.71	8.56	4.81
	10	33.83	17.96	27.64	14.56	18.73	9.83	7.68	4.04
	15	30.07	17.24	24.36	13.94	16.41	9.39	6.70	3.84
Overturning	5	10.36	5.75	7.64	4.29	4.09	2.30	0.98	0.55
	10	9.37	4.95	6.89	3.62	3.67	1.92	0.88	0.46
	15	8.29	4.75	6.06	3.46	3.21	1.84	0.77	0.44
Compressive (Net)	5	51.04	29.53	40.69	23.92	26.56	15.66	10.35	6.17
	10	46.55	26.26	37.03	20.68	24.05	13.42	9.36	5.31
	15	41.71	25.34	32.92	19.91	21.28	12.88	8.28	5.09
Tensile (Net)	5	44.70	23.19	36.05	19.28	23.60	12.70	9.09	4.91
	10	40.21	19.92	32.38	16.04	21.10	10.46	8.10	4.04
	15	35.37	19.00	28.27	15.26	18.33	9.92	7.01	3.83
Shear	5	22.19	12.14	18.16	10.18	12.37	6.96	5.09	2.86
	10	20.10	10.67	16.42	8.65	11.13	5.84	4.56	2.40
	15	17.87	10.25	14.48	8.26	9.75	5.58	4.45	2.28

TABLE 3.15

MAXIMUM STRESSES IN FOUR-STOREYED BRICK BUILDING OF NON-UNIFORM THICKNESS OF MAIN WALLS (TYPE - B4B)

Stresses	Damping %	Maximum Stresses in Various Storeys kg/cm^2							
		Storey I		Storey II		Storey III		Storey IV	
		Koyna EQ.	El Centro EQ.	Koyna EQ.	El Centro EQ.	Koyna EQ.	El Centro EQ.	Koyna EQ.	El Centro EQ.
Bending	5	31.45	21.55	25.47	17.33	22.92	15.35	9.95	6.33
	10	26.71	15.36	20.92	12.21	18.36	10.94	7.55	4.55
	15	24.61	13.94	19.05	11.02	16.54	9.76	6.77	4.04
Overturning	5	8.86	6.05	6.48	4.37	4.60	3.02	1.14	0.72
	10	7.38	4.28	5.25	3.10	3.60	2.16	0.86	0.52
	15	6.76	3.87	4.75	2.78	3.24	1.92	0.77	0.46
Compressive (Net)	5	43.03	30.06	33.90	23.48	29.18	20.02	11.90	7.86
	10	36.51	22.18	27.92	17.14	23.61	14.76	9.23	5.88
	15	33.80	20.38	25.56	15.64	21.44	13.34	8.35	5.31
Tensile (Net)	5	37.59	25.23	30.08	20.09	26.22	17.06	10.64	6.60
	10	31.73	17.28	24.57	13.71	20.66	11.80	7.96	4.62
	15	29.00	15.46	22.20	12.19	18.48	10.38	7.09	4.04
Shear	5	18.69	12.80	15.13	10.29	13.62	9.12	5.91	3.76
	10	15.87	9.12	12.43	7.26	10.91	6.50	4.49	2.71
	15	14.62	8.28	11.32	6.55	9.83	5.80	4.02	2.40

TABLE 3.16

VERTICAL REINFORCEMENT AT THE MOST CRITICAL SECTION OF LONGITUDINAL WALLS FOR ρ = 0.10%

S.No.	Type	Number of Storeys	Storey	Diameter for Single Bar, mm				Thickness of Main Wall in the Storey mm
				Required for Koyna Earthquake	IS: 4326 for Severe+ Case	Required for El Centro Earthquake	IS: 4326 for Moderate+ Case	
1	B1	One	-	10	12	nil	nil	223
2	B2	Two	Top	10	12	8	nil	223
			Bottom	16	16	10	nil	
3	B3A Uniform Wall Thickness Case	Three	Top	10	12	8	12	223
			Middle	16	16	12	12	
			Bottom	20	16	16	16	
4	B3B Non-Uniform Wall Thickness Case	Three	Top	10	12	8	12	223
			Middle	16	16	12	12	223
			Bottom	20	16	12	16	343
5	B4A Uniform Wall Thickness Case	Four	Top	10	12	8	12	223
			Third	16	16	12	12	
			Second	20	20	16	16	
			Bottom	22	25	16	16	
6	B4B Non-Uniform Wall Thickness Case	Four	Top	10	12	8	12	223
			Third	16	16	12	12	223
			Second	20	20	16	16	343
			Bottom	22	25	16	16	343

+Severe cases are those in seismic zones where the design seismic coefficient becomes more than 0.08 (Zones V and IV) and moderate cases where the design seismic coefficient can come between 0.06 and 0.08 (Zones IV and III).

TABLE 3.17

VERTICAL REINFORCEMENT AT THE MOST CRITICAL SECTION OF TRANSVERSE WALL FOR ρ = 0.10 %

S.No.	Type	Number of Storeys	Storey	Diameter for Single Bar, mm				Thickness of Main Walls in the Storey mm
				Required for Koyna Earthquake	IS: 4326 for Severe+ Case	Required for El Centro Earthquake	IS: 4326 for Moderate+ Case	
1	B1	One	-	6	12	nil	nil	223
2	B2	Two	Top	8	12	6	nil	223
			Bottom	12	16	8	nil	
3	B3A Uniform Wall Thickness Case	Three	Top	8	12	6	12	223
			Middle	12	16	10	12	
			Bottom	16	16	10	16	
4	B3B Non-Uniform Wall Thickness Case	Three	Top	8	12	6	12	223
			Middle	10	16	10	12	
			Bottom	12	16	10	16	343
5	B4A Uniform Wall Thickness Case	Four	Top	8	12	6	12	223
			Third	16	16	10	12	
			Second	20	20	12	16	
			Bottom	20	25	16	16	
6	B4B Non-Uniform Wall Thickness Case	Four	Top	8	12	6	12	223
			Third	16	16	10	12	
			Second	16	20	10	16	343
			Bottom	16	25	12	16	

+ Severe cases are those in seismic zones where the design seismic coefficient becomes more than 0.08 (Zone V and IV) and moderate cases where the design seismic coefficient comes between 0.06 and 0.08 (Zone IV and III)

TABLE 3.18

HORIZONTAL REINFORCEMENT AT THE MOST CRITICAL SECTION OF LONGITUDINAL AND TRANSVERSE WALLS FOR p = 0.10%

S.No.	Type	Number of Storeys	Storey	Vertical Spacing of a 6 mm Diameter 2-legged Horizontal Stirrup in Terms of 7.6 cm Thick Brick Courses				Thickness of Main Wall in the Storey
				Required for Koyna Shock		Required for El Centro Shock		
				Longitudinal Wall	Transverse Wall	Longitudinal Wall	Transverse Wall	mm
1	B1	One	-	5	nil	nil	nil	223
2	B2	Two	Top	4	nil	nil	nil	223
			Bottom	2	3	4	nil	
3	B3A Uniform Wall Thickness Case	Three	Top	5	nil	nil	nil	223
			Middle	2	3	3	nil	
			Bottom	1	2	2	4	
4	B3B Non-Uniform Wall Thickness Case	Three	Top	4	nil	nil	nil	223
			Middle	2	4	3	nil	
			Bottom	1	3	3	nil	343
5	B4A Uniform Wall Thickness Case	Four	Top	4	nil	nil	nil	223
			Third	1	3	3	nil	
			Second	1	2	2	4	
			Bottom	1	1	1	3	
6	B4B Non-Uniform Wall Thickness Case	Four	Top	2	nil	nil	nil	223
			Third	1	3	3	nil	
			Second	1	3	3	nil	
			Bottom	1	2	2	4	343

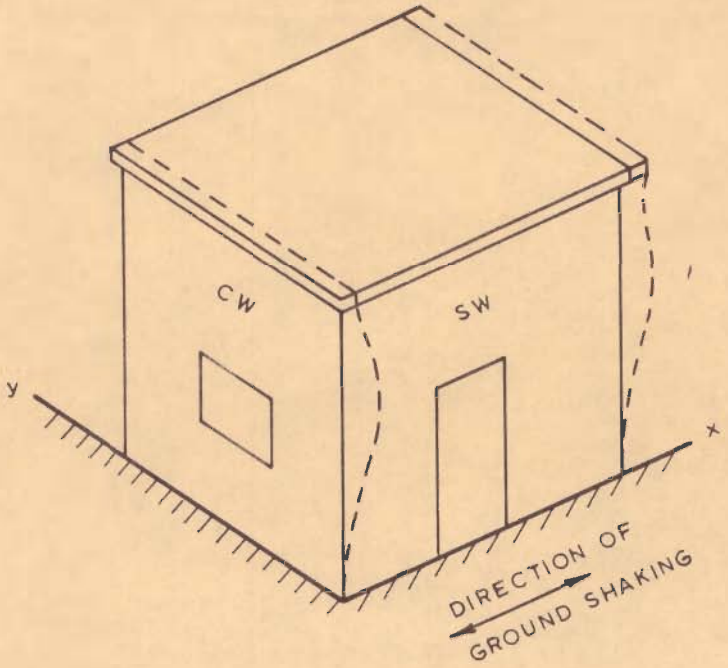

FIG. 3.1 _ SCHEMATIC VIEW OF A SINGLE-STOREYED BUILDING

PHOTO 3.1 _ BRICK BUILDING SHOWING USUAL TOOTHED JOINT AS SOURCE OF WEAKNESS DURING EARTHQUAKE (PHOTO BY A.S. ARYA)

PHOTO 3.2 _ SHEAR STRUCTURE BEHAVIOUR OF A THREE STOREYED BRICK BUILDING SUBJECTED TO GEDIZ EARTHQUAKE OF 1970 (TURKEY)

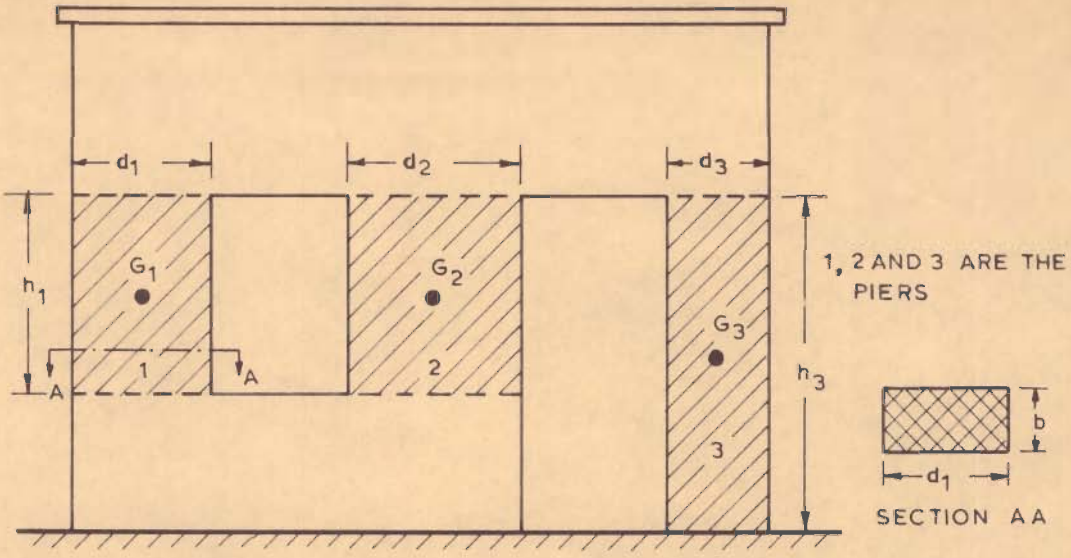

FIG. 3.2 _BRICK SHEAR WALL WITH OPENINGS

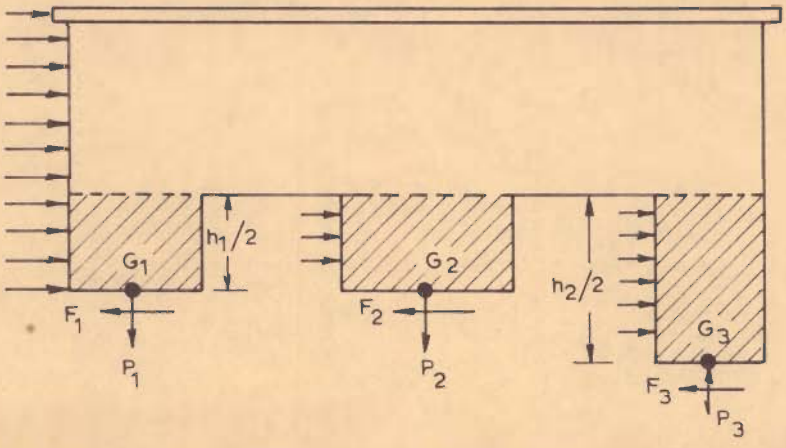

FIG. 3.3 _FREE BODY DIAGRAM OF THE SHEAR WALL

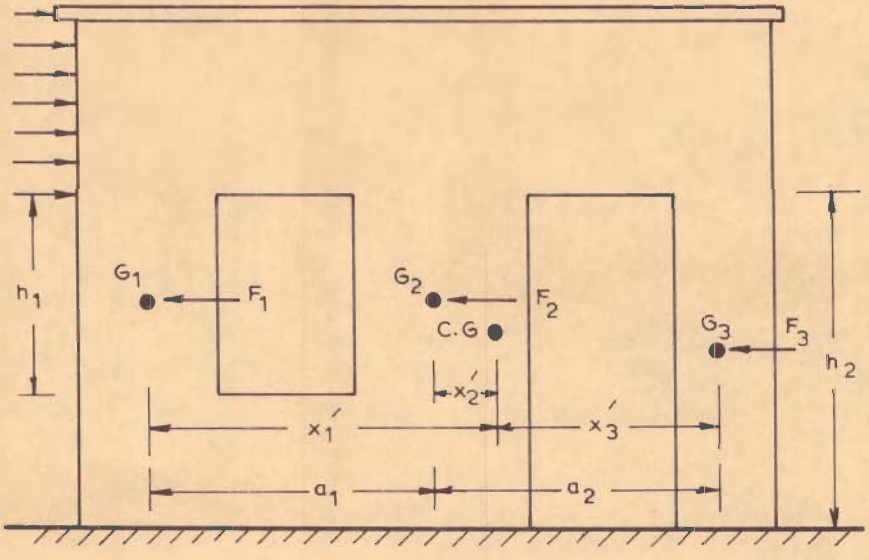

FIG. 3.4 _DIAGRAM FOR COMPUTING OVERTURNING FORCES IN PIERS

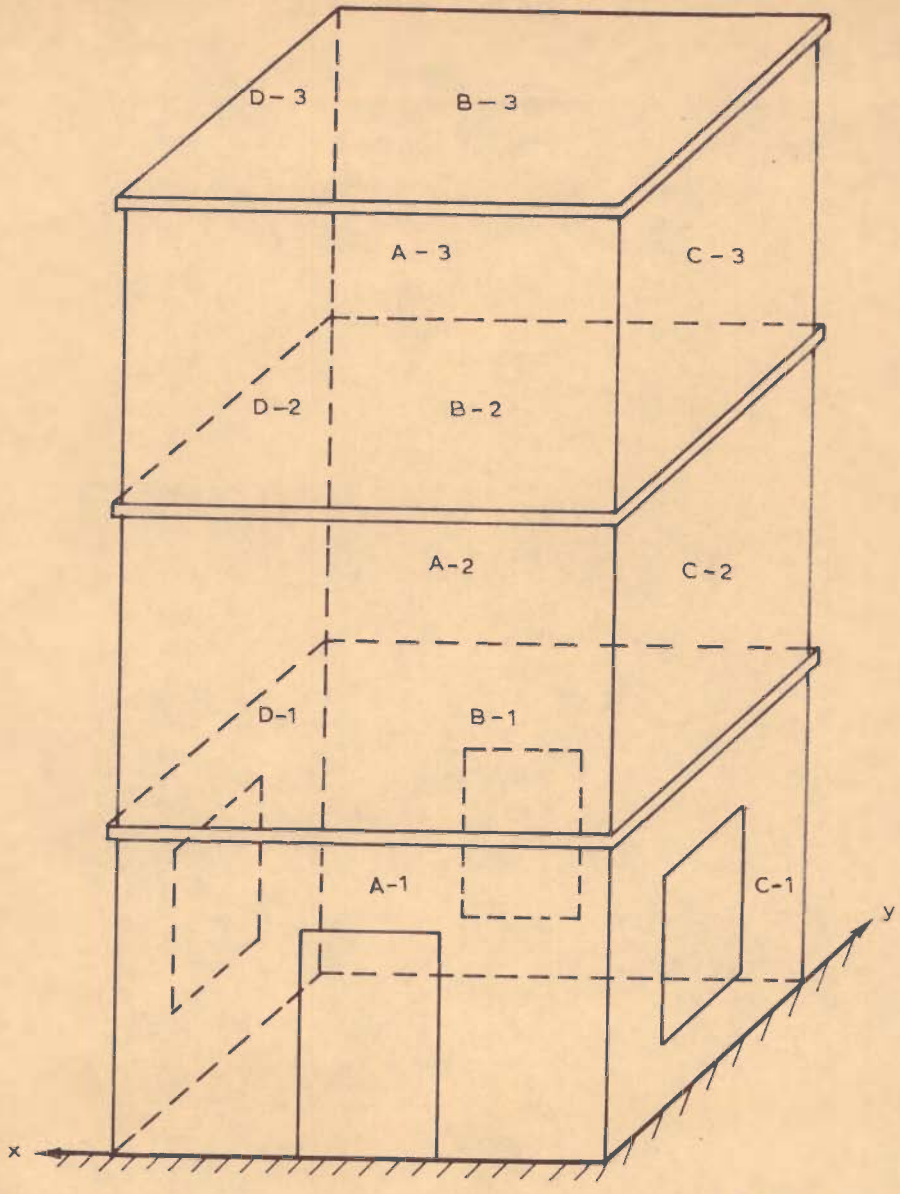

NOTE - DOOR AND WINDOW OPENING IN UPPER STOREYES NOT SHOWN FOR CLARITY OF THE FIGURE

FIG. 3.5 - SCHEMATIC VIEW OF A TYPICAL REPRESENTATIVE MULTISTOREYED BRICK BUILDING

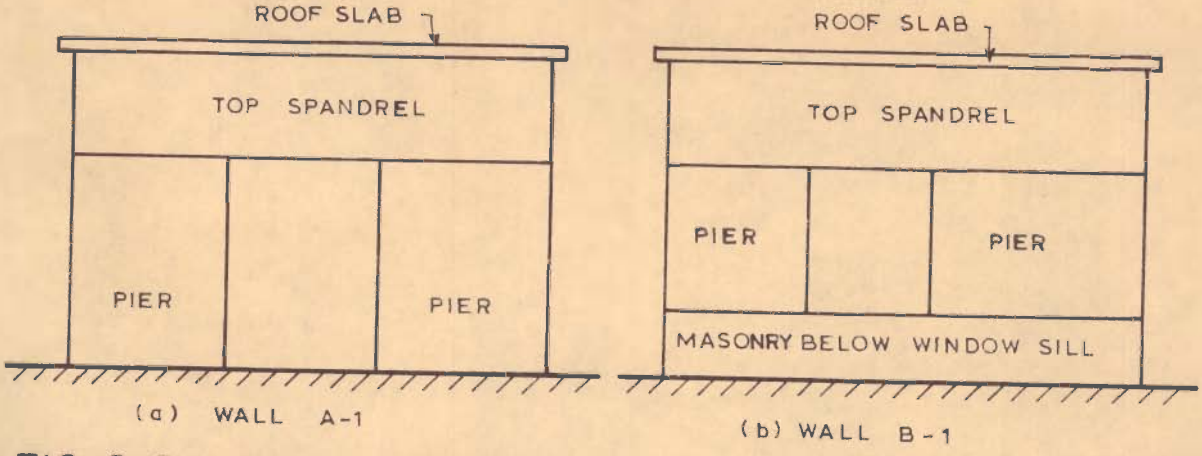

FIG. 3.6 - FIRST STOREY SHEAR WALLS FOR GROUND SHAKING PARALLEL TO X- AXIS

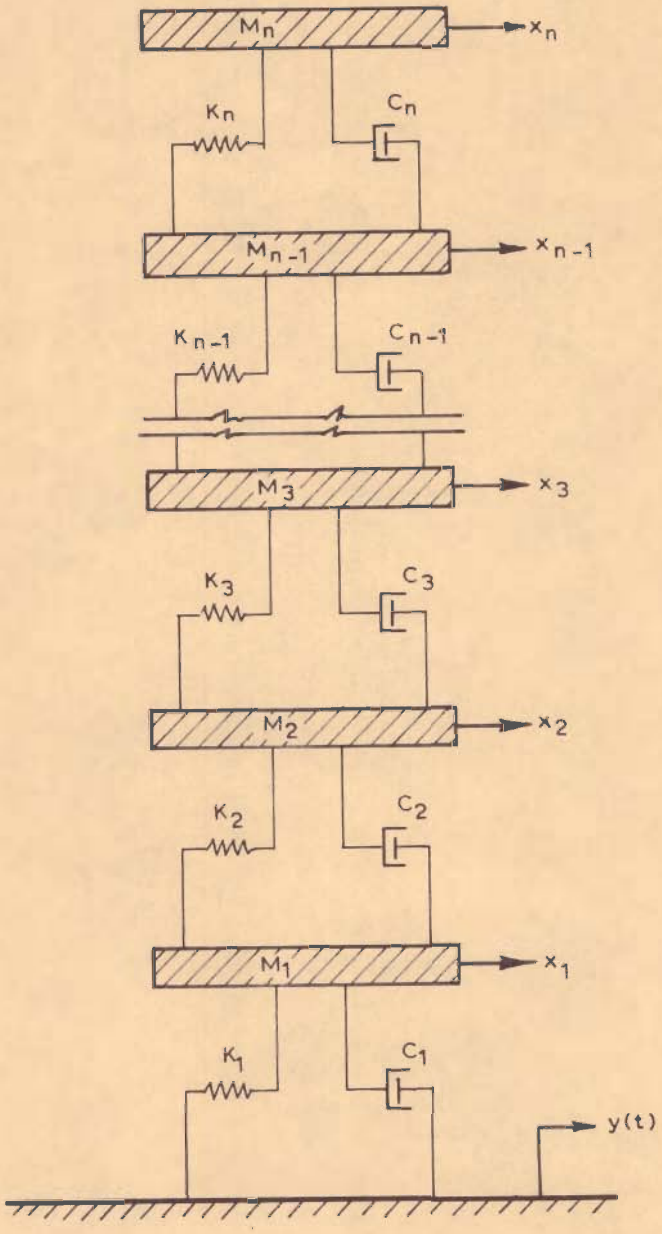

FIG. 3.7 _ MATHEMATICAL MODEL OF A MULTISTOREYED BRICK BUILDING

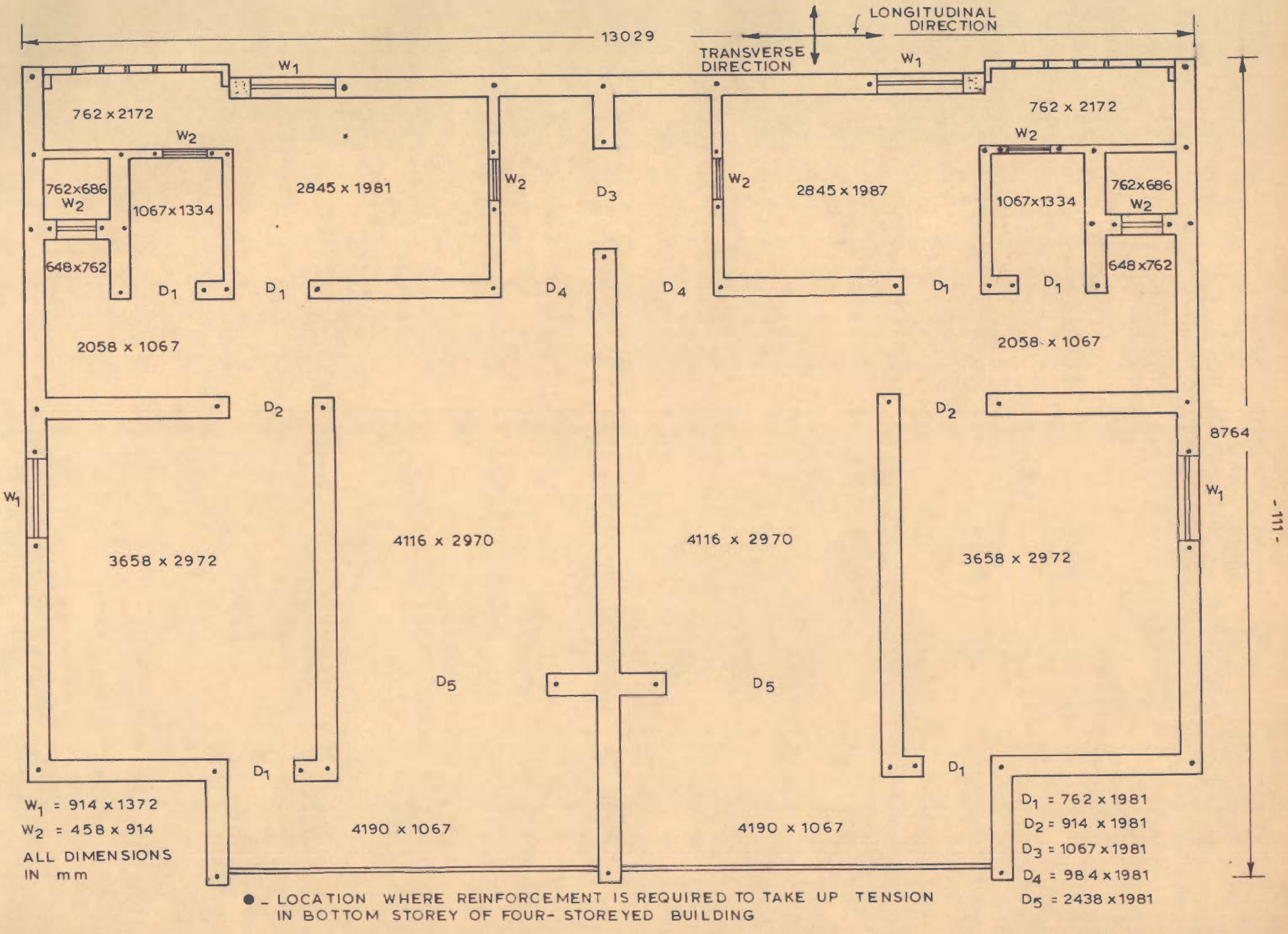

FIG. 3.8 - TYPICAL PLAN AT GROUND AND OTHER FLOORS OF A MULTISTOREYED BRICK BUILDING (Main walls 1-brick thick)

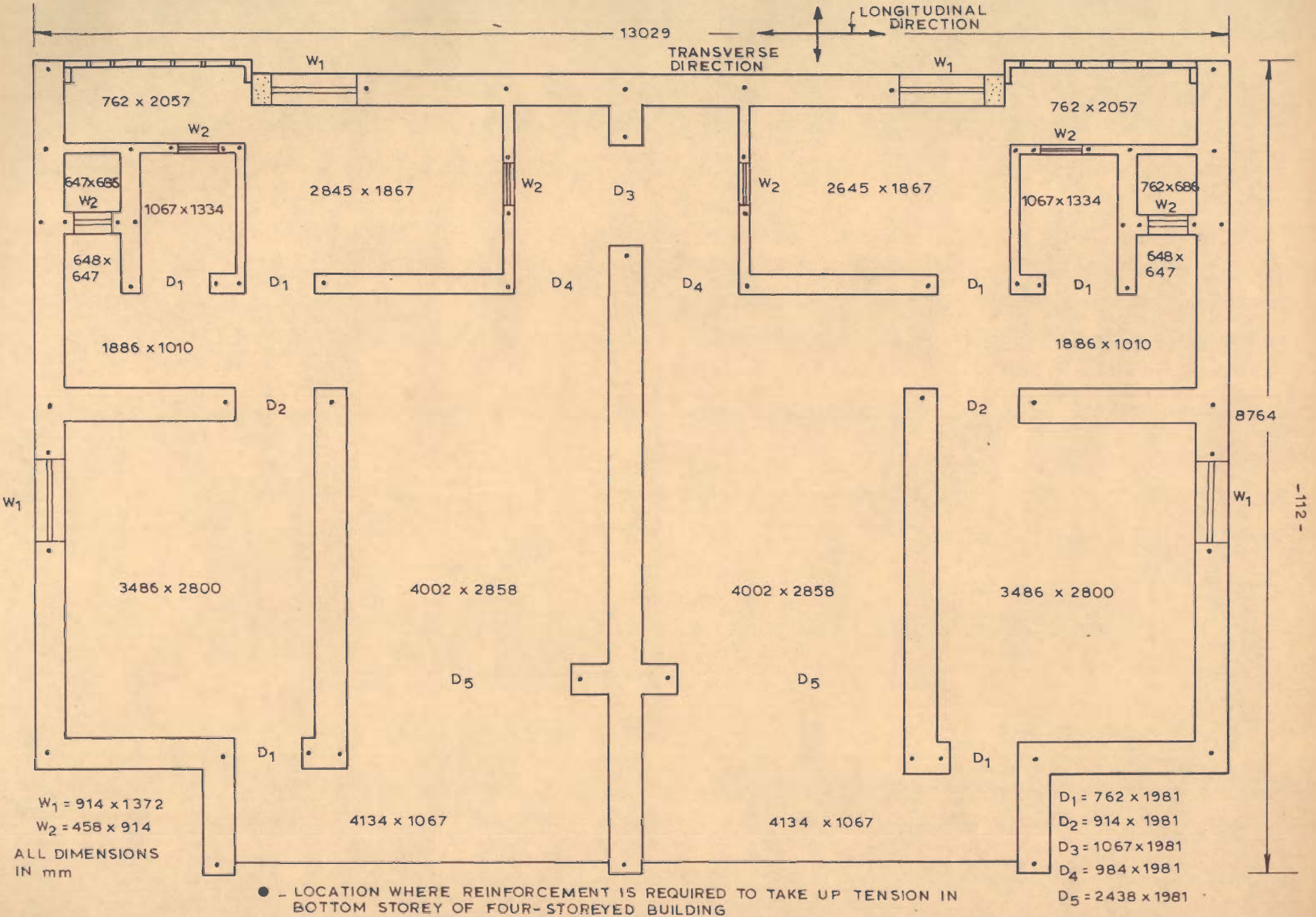

FIG. 3.9_TYPICAL PLAN AT GROUND FLOOR OF A MULTISTOREYED BRICK BUILDING
(Main walls 1½- bricks thick)

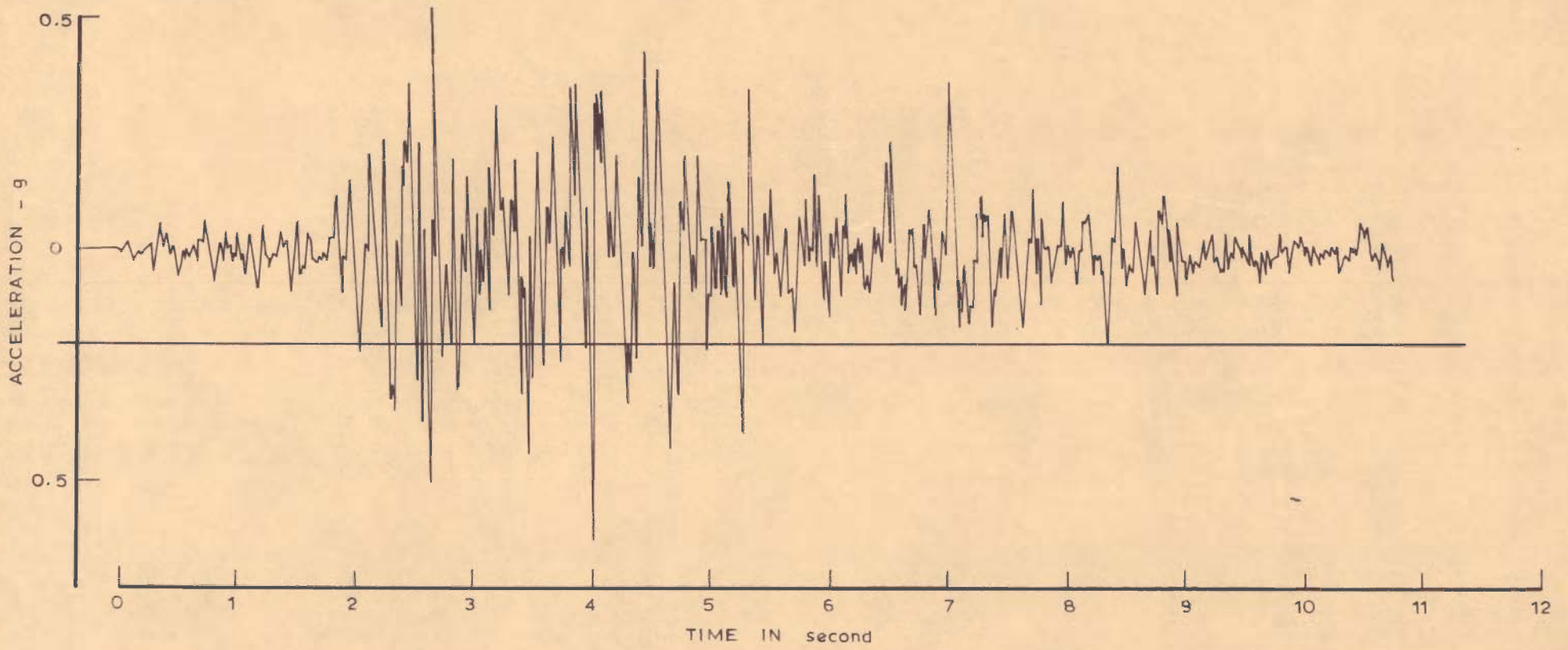

FIG. 3.10 - ACCELEROGRAM OF KOYNA EARTHQUAKE OF DEC. 11, 1967
(LONGITUDINAL COMPONENT)

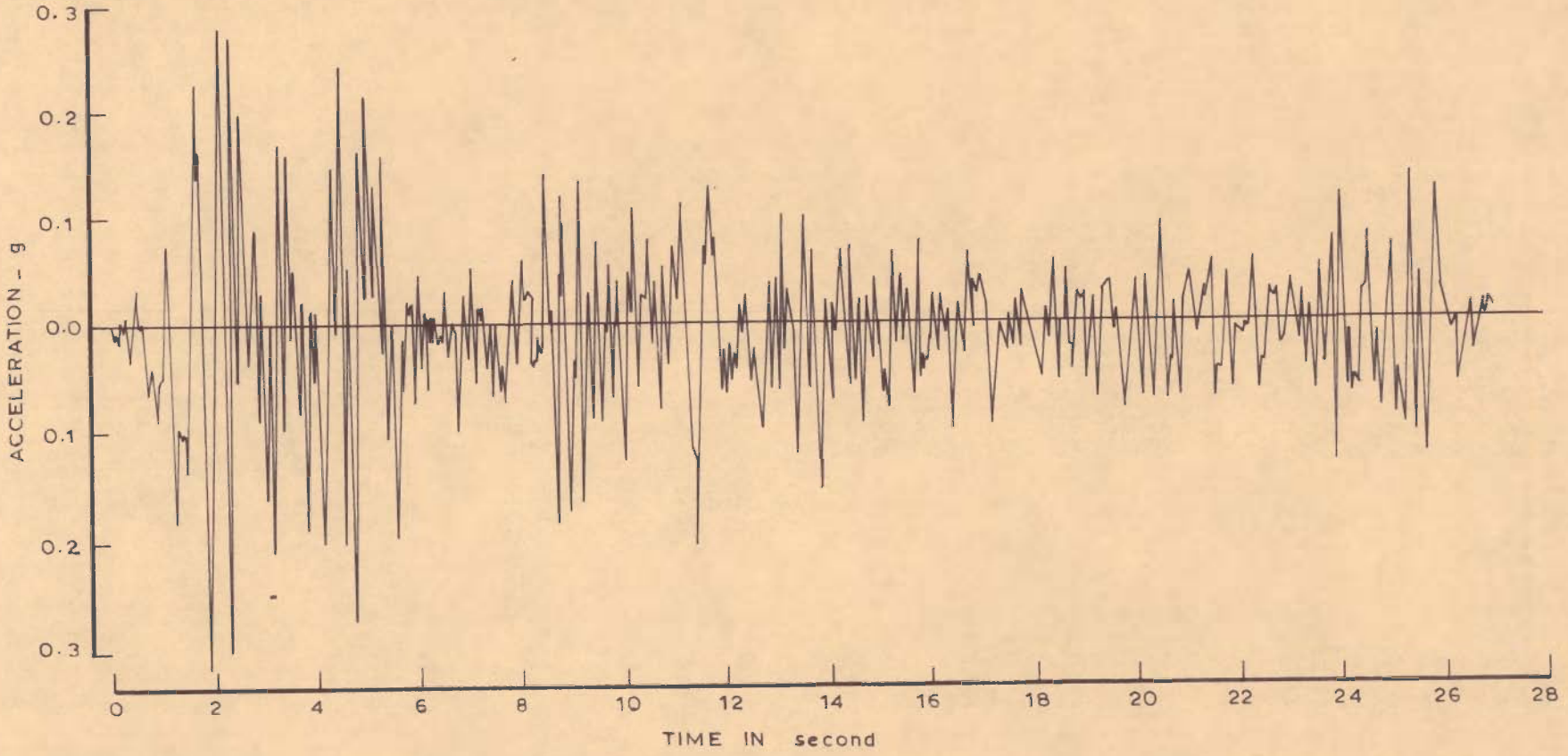

FIG. 3.11 _ ACCELEROGRAM OF EL CENTRO SHOCK OF MAY 18, 1940
(N-S COMPONENT)

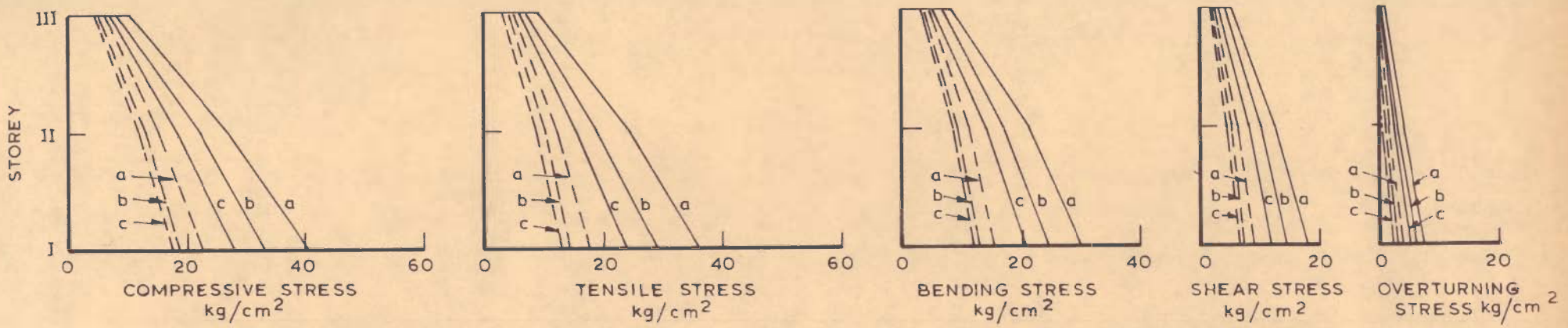

a - FOR UNIFORM THICKNESS OF MAIN WALLS IN ALL THE STOREYS

——— FOR KOYNA SHOCK

– – – – FOR EL CENTRO SHOCK

a - DAMPING 5 %

b - DAMPING 10 %

c - DAMPING 15 %

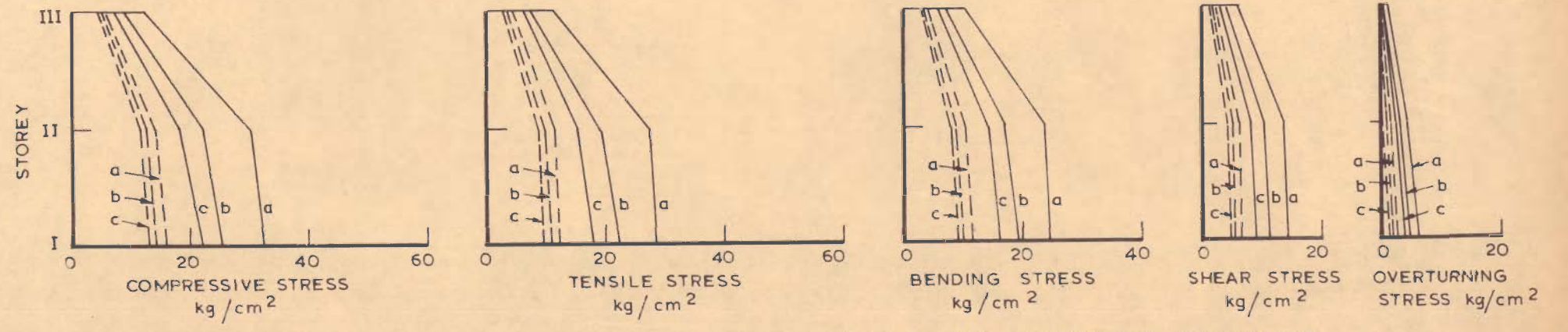

b_FOR NON-UNIFORM THICKNESS OF MAIN WALLS IN VARIOUS STOREYS

FIG. 3.12 _MAXIMUM STRESSES IN DIFFERENT STOREYS OF THREE- STOREYED CONVENTIONAL BRICK BUILDING

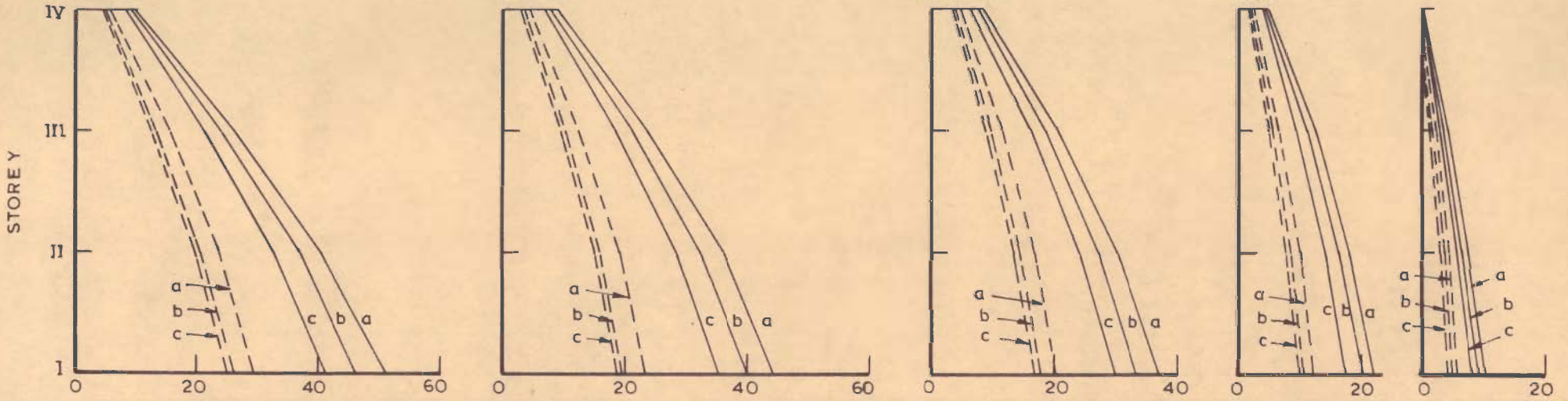

a _ FOR UNIFORM THICKNESS OF MAIN WALLS IN ALL THE STOREYS

——— FOR KOYNA SHOCK

– – – FOR ELCENTRO SHOCK

a _ DAMPING 5 %
b _ DAMPING 10 %
c _ DAMPING 15 %

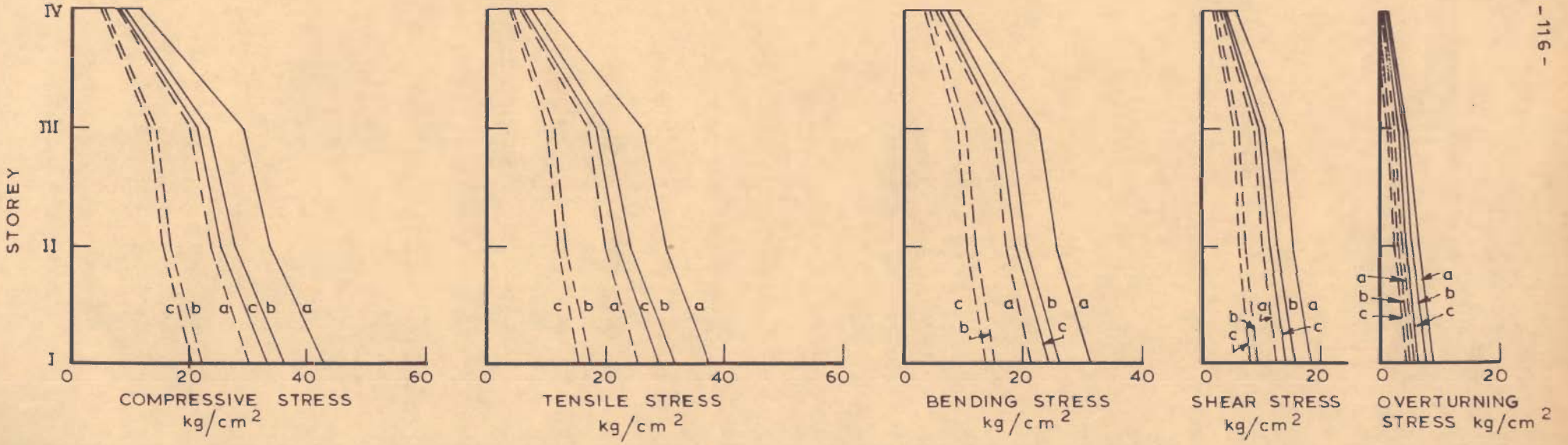

b _ FOR NON-UNIFORM THICKNESS OF MAIN WALLS IN VARIOUS STOREYS

FIG.3.13 _ MAXIMUM STRESSES IN DIFFERENT STOREYS OF FOUR STOREYED CONVENTIONAL BRICK BUILDING

C H A P T E R 4

EARTHQUAKE RESPONSE OF SLIDING TYPE BRICK BUILDING

4.1 GENERAL

In the preceding chapter, a study of unstrengthened conventional brick buildings was presented to highlight the problems associated with them under earthquake conditions. It was found that due to their short periods such structures attract very large seismic forces thereby developing high tensile stresses in the wall elements resulting in heavy cracking. Therefore for adequate earthquake resistance such buildings have either to be suitably reinforced or some vibration isolation or energy dissipation measures have to be adopted. Here it is proposed to introduce a sliding joint at plinth level of the building with the idea that as soon as the coefficient of friction is overcome, almost an infinite flexibility will be introduced which should limit the seismic force on the structure above the joint and therefore be advantageous from earthquake view point. Besides the 'flexibility' as stated above the dissipation of seismic energy through coulomb friction at the sliding joint could also lead to some reduction of seismic force in the structure when compared with conventional system.

As a first step, an attempt has been made to study the feasibility of the concept through small scale models as well as computation of earthquake response of sliding type single-storeyed buildings. This work is

presented in this chapter. As a second step, large size models have been tested whose details and results are given in the next chapter.

4.2 TESTS ON SLIDING TYPE MODELS

4.2.1 Details of Models and Testing Arrangement

Two single-storeyed one roomed models, 914 mm x 762 mm in plan and 572 mm high with an opening in each wall were constructed in 1:6 cement-sand mortar using 114 mm x 57 mm x 38 mm bricks (Fig. 4.1). A steel channel frame with flanges vertical and web flat, served as base for the superstructure (Photo 4.1 and 4.2). The bottom of the channel, that is, the web was machine finished so as to have less coefficient of friction between the contact surfaces. One course of brickwork in 1:3 cement sand mortar was placed between the flanges of the channel developing good bond, thus forming base for the superstructure.

For trials with different coefficients of friction at the sliding surface, the following materials were inserted between the shake table top and the channel bottom:

(a) Graphite powder

(b) Dry sand

(c) Wet sand

By carrying out sliding tests separately, the coefficient of friction between steel and steel using the above material layers in between, the coefficients of friction were found as follows:

Graphite powder	0.25
Dry sand	0.34
Wet sand	0.41

Portions of the steel channel at the four corners were projected beyond the outside edge of the building model in which threaded holes were made for inserting bolts (Fig. 4.1 and Photos 4.1 and 4.2). The whole model could be lifted up, for inserting layers of different frictional materials, with the help of four bolts inserted in the threaded holes.

Acceleration pick ups were mounted at the (i) base of the model, (ii) top of the roof slab and (iii) table base. One displacement pick up (LVDT), as shown in Photo 4.2, was connected with the model at the base level to measure the amount of its sliding, that is, the relative displacement between the model base and the shake table. Two guides each with ball-bearing arrangement were fixed to the table near the base of the two walls (Photo 4.3) which were parallel to the direction of table motion so as to prevent twisting and allow sliding of the model in one direction only.

The model was first tested with base free to slide for steady-state horizontal table motion between the frequencies 8 Hz to 26 Hz. The accelerations and the amount of sliding were recorded. The testing of the model was continued for different dynamic forces as well as using different sliding materials. After completing the tests on the model with base free to slide, the model base was fixed to the table top (Photos 4.4 through 4.7). Then similar steady-state tests were performed on the same model with fixed base. The tests were repeated for the second model in the same manner as the first one.

4.2.2. Observations

All the acceleration records could not be taken in case of model 1 as preliminary tests were performed on this model. Therefore this model has been studied qualitatively. The results of dynamic tests performed on model 2 are listed in Table 4.1. It is observed from this table that for free base of the model, in all cases the roof acceleration is less than the corresponding table acceleration. Also, as the coefficient of friction increases from 0.25 to 0.41, the ratio of roof to base acceleration increases from 0.625 to 0.90 and in the case of fixed base this becomes 2.34. These observations indicate that the 'isolation' due to the sliding had appreciable influence and also that the input energy at base was dissipated to some extent in

sliding of the model. This reduction in roof acceleration varies with the type of materials used to permit sliding.

In the case of model with fixed base, roof acceleration is much more than the table acceleration which clearly indicates amplification of the motion due to the stiffness of the model.

For a given dynamic force, no damage was observed to the models in the case of free base (Photos 4.2 and 4.3) while contrary to this happened in the case of model with fixed base (Photos 4.4 through 4.7). Therefore, it may be inferred that by providing sliding base, the input energy to the model gets dissipated in sliding and hence the model attracts less dynamic force whereas this does not happen in the case of models with fixed base. Thus, these preliminary tests on sliding type models strengthen the idea that by introducing sliding joint at the plinth level, the effective seismic force can be reduced as compared with fixed base structures.

4.3 MATHEMATICAL IDEALIZATION OF SLIDING TYPE BUILDING

A representative single-storeyed sliding type brick building as shown in Fig. 4.2 is chosen to compute its earthquake response. It is assumed that a layer of suitable material with a known coefficient of friction is laid between the contact surfaces of bond beam of the superstructure and plinth band in the substructure. The

building elements of one of the shear walls are shown shaded in the figure for the marked direction of shaking. Non-structural elements, as present in actual buildings, are not shown in the figure.

For computing earthquake response of this type of buildings, it is proposed here to idealize the building as a two degrees of freedom discrete mass model. The spring action in the system is assumed to be provided by the building elements resisting shear parallel to the direction of earthquake shock. The mass of the roof slab and that of half the height of walls is assumed as lumped at the roof level and half the mass of walls at the plinth level. In this way a two masses model is obtained.

Thus, the mathematical model (Fig. 4.3) of the superstructure of the sliding type building consists of two masses mutually connected through a spring and a viscous damper. The lower mass is assumed to rest on a plane with dry frictional damping to permit motion of the system.

4.4 EQUATIONS OF MOTION

The following assumptions are made for writing the equations of motion for the system shown in Fig. 4.3:

(1) The coefficient of friction between the sliding surfaces remains constant throughout the motion

of the system right from the start to the stop, that is, a rigid plastic idealization is assumed.

(2) The building material is assumed to be elastic and remaining within the limit of proportionality. Thus the idealized spring is linearly elastic. Its stiffness is worked out by considering bending as well as shear deformations.

(3) The building is subjected to only one horizontal component of ground shaking at a time.

(4) In the analysis, it is assumed that unlimited sliding displacement can occur at the contact surface without overturning or tilting. In real structure it will not really be so but this assumption is made so as to arrive at the maximum sliding displacements during some of the actual earthquakes and examine the feasibility of providing for them in practice.

The equations of motion for different phases of the motion of the sliding system subjected to ground shaking are written as follows.

(a) Initially so long as the acceleration of the moving system does not overcome the frictional resistance, mass M_b will move with the base since there will be no sliding and the system would behave as a single degree of freedom system. Therefore the equation could be wrriten as:

$$M_t \ddot{x}_t + C_s(\dot{Z}_t - \dot{Z}_b) + K_s(Z_t - Z_b) = 0 \qquad \ldots(4.1)$$

in which

M_t = top mass lumped at the roof level;

$\ddot{x}_t, \ddot{Z}_t$ = absolute and relative accelerations of the top mass M_t;

Z_b, Z_t = lateral relative displacements of masses M_b and M_t;

$\dot{Z}_b, \dot{Z}_t$ = relative velocities of masses M_b and M_t;

C_s = coefficient of the viscous damper and

K_s = spring constant

Equation (4.1) can also be expressed as follows

$$\ddot{Z}_t + 2p\zeta(\dot{Z}_t - \dot{Z}_b) + p^2(Z_t - Z_b) = -\ddot{y}(t) \qquad \ldots(4.2)$$

in which

p = natural circular frequency of the system equal to $\sqrt{K_s/M_t}$

ζ = fraction of critical damping and equal to $C_s/2pM_t$ and

$\ddot{y}(t)$ = ground acceleration at any instant of time t.

(b) The sliding of the bottom mass would begin if the frictional resistance at the plinth level is overcome by the force which causes sliding. The force to cause sliding (S_F) is given by

$$S_F = C_s(\dot{Z}_t - \dot{Z}_b) + K_s(Z_t - Z_b) - M_b \ddot{x}_b \qquad \ldots(4.3a)$$

where $\ddot{x}_b$ is the absolute acceleration of the bottom mass. Therefore, sliding of bottom mass will occur if

$$|S_F| > \mu M_T g \qquad \ldots(4.3b)$$

in which

M_T = $M_b + M_t$;

μ = coefficient of friction, and

g = acceleration due to gravity

The system would now act as two degrees of freedom system for which the equations of motion can be written in a simplified form as follows:

$$\ddot{Z}_b - 2p\zeta\theta(\dot{Z}_t - \dot{Z}_b) - p^2\theta(Z_t - Z_b) + F = -\ddot{y}(t) \qquad \ldots(4.4)$$

and

$$\ddot{Z}_t + 2p\zeta(\dot{Z}_t - \dot{Z}_b) + p^2(Z_t - Z_b) = -\ddot{y}(t) \qquad \ldots(4.5)$$

where

$\ddot{Z}_b$ = relative acceleration of the bottom mass M_b;

θ = mass ratio = M_t/M_b, and

$$F = \mu g (1 + \theta) \operatorname{sgn}(Z_b) \qquad \ldots(4.6)$$

where

$\operatorname{sgn}(\dot{Z}_b) = +1$ if $\dot{Z}_b$ is positive

$\operatorname{sgn}(\dot{Z}_b) = -1$ if $\dot{Z}_b$ is negative.

(c) At any instant of time during motion of the system if $|S_F| < \mu M_T g$, then the sliding of the bottom

mass would stop whereas the top mass would continue to vibrate. Therefore, again the system becomes single degree of freedom system and hence its motion would be expressed by Eq. (4.2).

Throughout the time history of the ground shaking, the bottom mass of the system would either stop or continue to slide according to the conditions enumerated in the preceding paragraphs. The equations of motion for the different phases in sliding of the system have to be solved for obtaining its seismic response.

4.5 SOLUTION OF EQUATIONS OF MOTION

Equations (4.2), (4.4) and (4.5) are the ordinary differential equations of second order with constant coefficients. The dynamic response of the system will be obtained by integrating these equations. For this, the same numerical technique, viz. Runge-Kutta Fourth Order (Benett, 1956) as discussed in section 3.8 of Chapter 3, has been used.

A computer programme has been developed to compute timewise earthquake response of sliding type system. Its flow diagram is described in Appendix-B.

4.6 PARAMETRIC STUDY OF SLIDING TYPE BUILDINGS

The earthquake response of sliding type building has been computed for the same two earthquake accelerograms as done for conventional buildings in Chapter 3.

A range of parameteric values representing the physical properties of the single storey building have been used to arrive at generalised results. The results of this study are then compared with those of associated conventional non-sliding buildings subjected to same ground shaking. The various parameters of the sliding system are described below:

As seen in Equations (4.2), (4.4) and (4.5), there are three dimensionless parameters p (or inversely time period T), ζ and θ which would determine the dynamic response of the system to a given ground motion. The parameters respectively take care of the spring-mass-damping characteristics of the superstructure of the building idealized as a single degree system and the ratio of masses lumped at the top and base of the super-structure. In actual buildings, these values will naturally vary depending on the conditions of planning, materials and quality of construction. It is estimated that the following range of values of these parameters should cover a wide variety of single storeyed masonry structures.

Time period T=0.04, 0.05, 0.06, 0.08, 0.10 second

Damping value ζ = 0.05, 0.10, 0.15

Mass ratio θ = 1.6, 1.8, 2.0, 3.0, 4.0, 5.0

The coefficient of friction will naturally be a very important parameter which should affect the

response of the sliding system considerably. For the present theoretical study, the value of this coefficient chosen are the following:

μ = 0.15, 0.20, 0.25, 0.30 and 0.40.

It is imagined that a coefficient of friction less than 0.15 in sliding will be hard to obtain and for a value greater than 0.40, no sliding motion may indeed occur in most real earthquakes and the system may just act like a fixed system.

The earthquake response computation of the sliding type systems have been done for the same two shocks as given in section 3.11.3 of Chapter 3, thus incorporating the effect of ground shaking characteristics.

4.7 DYNAMIC RESPONSE CALCULATION

The quantities of interest in the present theoretical response calculation are the following:

1) absolute acceleration of the top mass M_t which determines the forces acting on the shear walls for given damping value,

2) the maximum relative displacement of the superstructure at the plinth level, that is, the maximum relative displacement of mass M_b at any instant of time, so that the extent of movement to be provided for in design

may be known, and

3) the residual relative displacement after the earthquake is over. This will indicate the position the superstructure may occupy at the end.

As stated earlier, the results have been computed by the Runge-Kutta fourth order method for the various parameter combinations stated in the preceding paragraph. The results are presented finally in the form of response spectra. That is, absolute acceleration of mass M_t, the maximum relative displacement and also the residual or permanent relative displacement of mass M_b are plotted in Fig. 4.4 to 4.21 against undamped natural period of the superstructure of sliding systems, between 0.04 and 0.10 sec., subjected to Koyna and El Centro shocks for different values of viscous damping, coefficient of friction at base and mass ratio M_t/M_b. The spectral acceleration for the similar conventional type single degree of freedom system have also been plotted on the corresponding graphs of the sliding system for comparison. These spectra may be termed as 'frictional response spectra'.

4.8 DISCUSSION OF RESULTS

The frictional response spectra as presented in Figs. 4.4 to 4.21 are studied here to find out the influence of various parameters on maximum response of

the systems when subjected to Koyna and El Centro shocks.

4.8.1 Effect of Time Period

Figures 4.4 through 4.12 show the acceleration spectra for Koyna and El Centro earthquakes for different parameters. Dashed lines in these figures show, for direct comparison, the acceleration spectra for the associated conventional type systems. It is seen that unlike the conventional systems, the friction spectral acceleration curves are flat and the values do not change much as the period of the system changes for any value of mass ratio, critical damping or coefficient of friction for both the shocks. Only slight variation in spectral acceleration is observed in case of Koyna shock for higher range of coefficients of friction more than 0.25 while for El Centro shock, this variation is noticed for friction coefficient of 0.30.

It was seen earlier (Krishna, Arya and Kumar, 1973) that in a friction mounted rigid system, if ground acceleration coefficient at any instant of time exceeded the coefficient of friction, the rigid body would begin to slide, the limiting force remaining equal to mass time this threshold acceleration. In other words, the response of the system is independent of its time period for different values of coefficient of friction. Since here, only short period structures have been studied,

it is logical that the acceleration response of such structures should not much depend on their period and only slight variation could be expected. In brick buildings of several storeys, however, there could be greater influence of the flexibility, a point which is not studied here and is for further research.

Residual as well as maximum relative displacement spectra for the system are shown in Figs. 4.13 to 4.21 for both the earthquakes which show peculiar features unlike acceleration spectra. Naturally spectral values of maximum displacement are more than the residual ones. For a particular value of mass ratio, critical damping and friction coefficient, there is significant variation in the displacement as time period varies. The trend of the dispaacement versus time period curves is observed to be somewhat similar in the following cases: Koyna shock for μ = 0.4 and El Centro shock for μ equal to 0.15, 0.20 and 0.30. But it varies for other cases. This variation in trend of the displacement for some of these cases may be mainly attributed to the complex nature of vibrations for non-linear behaviour of such system. Throughout the time-history of the sliding system, many times the bottom mass of the system stops while the top mass continues to vibrate. This fact might have introduced such peculiar features in the case of displacement spectra.

4.8.2 Influence of Viscous Damping

The variation of spectral acceleration with viscous damping is discussed here with reference to Figs. 4.4 to 4.12. Under both the shocks, the increase in viscous damping decreases the spectral acceleration value for various values of other parameters . This is the usual result as for conventional spectra and indicates the increasing energy dissipation in internal friction of the system as the damping coefficient increases.

It is seen from Figs. 4.13 to 4.21, that the variation of relative displacement with viscous damping is rather inconsistent and does not follow the usual pattern where the response is less as damping becomes larger. Specifically referring to Fig. 4.13 (Koyna shock, $\mu = 0.15$) it is seen that spectral displacement decreases slightly with the increase of damping for period between 0.04 and 0.05s in case of mass ratios 1.6, 1.8, 3.0 and 4.0 but it increases between period 0.06 and 0.10s for mass ratios 1.6, 1.8, 2.0, 3.0 and 4.0. This random trend is difficult to explain and perhaps occurs due to the non-linear rigid plastic behaviour of the bottom mass which many times comes to a stop whereas the top mass continues to vibrate. As the value of μ increases, this random variation of the spectral displacement becomes more regular with respect to β (Figs. 4.14 and 4.15). That is, for most of the time period range and almost all values of θ,

the response decreases by increase of ξ . This trend further improved for μ equal to 0.30 and 0.40 (Figs. 4.16 and 4.17) in which higher damping reduces the response as usual.

Figures 4.18 through 4.21 show the spectral displacement for the system subjected to El Centro shock. It is observed from Fig. 4.18 that for the period range 0.04 to 0.05 sec, change in the response with damping is not significant though lower damping value shows decreased response. But the response decreases as ξ increases for period between 0.05 and 0.10 sec. Fig. 4.19 shows just the reverse trend as observed by Fig. 4.18. This type of mixed trend is also indicated by Fig. 4.20 while Fig. 4.21 shows that response of the system is independent of ξ for period less than 0.06 sec (θ = 1.6 to 3.0) and it decreases as ξ increases (θ = 3.0 to 5.0). So, it turns out from the above that a definite pattern of the spectral displacement with respect to viscous damping of the system subjected to Koyna and El Centro earthquakes is not observed.

4.8.3 Effect of Coefficient of Friction

Influence of frictional coefficient on the spectral acceleration is studied here through Figs.4.4 to 4.12 and Fig. 4.22. It is seen that in every case, the spectral acceleration decreases as friction coefficient decreases in all cases of different parameter

combinations of the system for both the earthquakes with only one exception. In this case which occurs for the El Centro shock, the spectral acceleration for μ equal to 0.25 is more than that for μ equal to 0.30 (see Fig. 4.11 and 4.12) for $T < 0.05$ sec. Why this is occurring is not clear due to the complexity of the frictional behaviour. All other cases are easily reasoned out as follows:

The resistance against sliding of the system decreases as the coefficient of friction between the sliding surfaces decreases. Thus, a build up of larger inertia force in the superstructure gets restricted and the spectral acceleration of such a system decreases. The spectral displacement decreases as μ increases for various values of θ and ξ as seen in Figs 4.13 to 4.21.

4.8.4 Effect of Mass Ratio

Referring to Figs. 4.4 through 4.12 again and Fig. 4.23 it is seen that as the mass ratio increases, the spectral acceleration decreases in all cases of parameter combinations for both the earthquakes. The possible reason for the decrease in the spectral acceleration values due to increase of mass ratio is that for a system as the mass ratio increases for a given period, it means a decrease in the value of bottom mass as well as the total mass. Thus the input dynamic

energy gets a decrease and the spectral acceleration reduces. Though, this is not true of the spectral displacement for all the cases, for most cases it does hold good.

From Figs. 4.13 to 4.15, it appears that as the mass ratio increases, no definite pattern of the spectral displacement is obtained for Koyna shock in which it does increase but not for all values of damping and time period. In these cases, a mixed pattern is observed. The spectral displacement for μ equal to 0.30 and 0.40 (Figs. 4.16 and 4.17) exhibits an increase in its values as mass ratio also increases for 10% and 15% of critical damping.

Figures 4.18 and 4.19 show an increase in the spectral displacement for increased mass ratios of the system when subjected to El Centro shock for μ = 0.15 and 0.20 and various damping ratios. But this trend no longer holds for μ equal to 0.25 and 0.30. For these two cases (Figs. 4.20 and 4.21) the spectral displacement does increase but only for 5% damping.

4.9 COMPARISON OF RESPONSE FOR CONVENTIONAL AND SLIDING SYSTEMS

Dashed lines in Figs. 4.4 to 4.12 show the acceleration spectra for the conventional system having the same period and damping as the sliding system but fixed at the bases. It is observed from these figures that the spectral acceleration of the sliding system

is much less than that of the corresponding conventional system subjected to Koyna shock for all parameter combinations. The same trend is generally seen in case of El Centro shock too. The only exceptions, are the systems having period less than 0.05 sec and coefficient of friction nearer to the peak ground acceleration of the El Centro shock (Figs. 4.10 to 4.12). A plaussible explanation of this case is like this: So long as the bottom mass does not move, the inertia force is contributed by the top mass only. But as the bottom mass moves, two things happen; firstly, the inertia force due to bottom mass is also added to the system and secondly the flexibility of the system increases which tends to reduce the dynamic amplification. Generally the flexibility effect predominates and the response is reduced due to sliding. But when the coefficient of friction approaches the fixity condition with respect to the peak ground acceleration, the inertia force of the bottom mass seems to become more influential and the response increases.

4.10 CONCLUDING REMARKS

It is seen from the study of frictional response spectra that for most of the cases investigated for two accelerograms which are widely different in their frequency-acceleration characteristics, the sliding type structure shows significant reduction

in effective seismic force. The maximum and residual relative displacements at the plinth are also estimated to remain small for the coefficients of friction considered, that is, from 0.15 to 0.30. The maximum computed value is 18 mm only. As such sliding arrangement shows great promise for adoption in actual building construction as a measure of seismic safety.

TABLE 4.1

TEST RESULTS OF MODEL 2

S.No.	Type of Model Base	Materials used to permit sliding	Coeffi-cient of fri-ction	Acceleration Recorded at		Ratio of Roof to Base Accele-ration	Amount of sli-ding at Table Base mm
				Table Base g	Roof Top g		
1	Free	Graphite Powder	0.25	0.32	0.20	0.625	2.0
2	Free	Dry Sand	0.34	0.86	0.60	0.70	0.5
3	Free	Wet Sand	0.41	0.86	0.77	0.90	0.5
4	Fixed	-	-	0.38	0.89	2.34	-

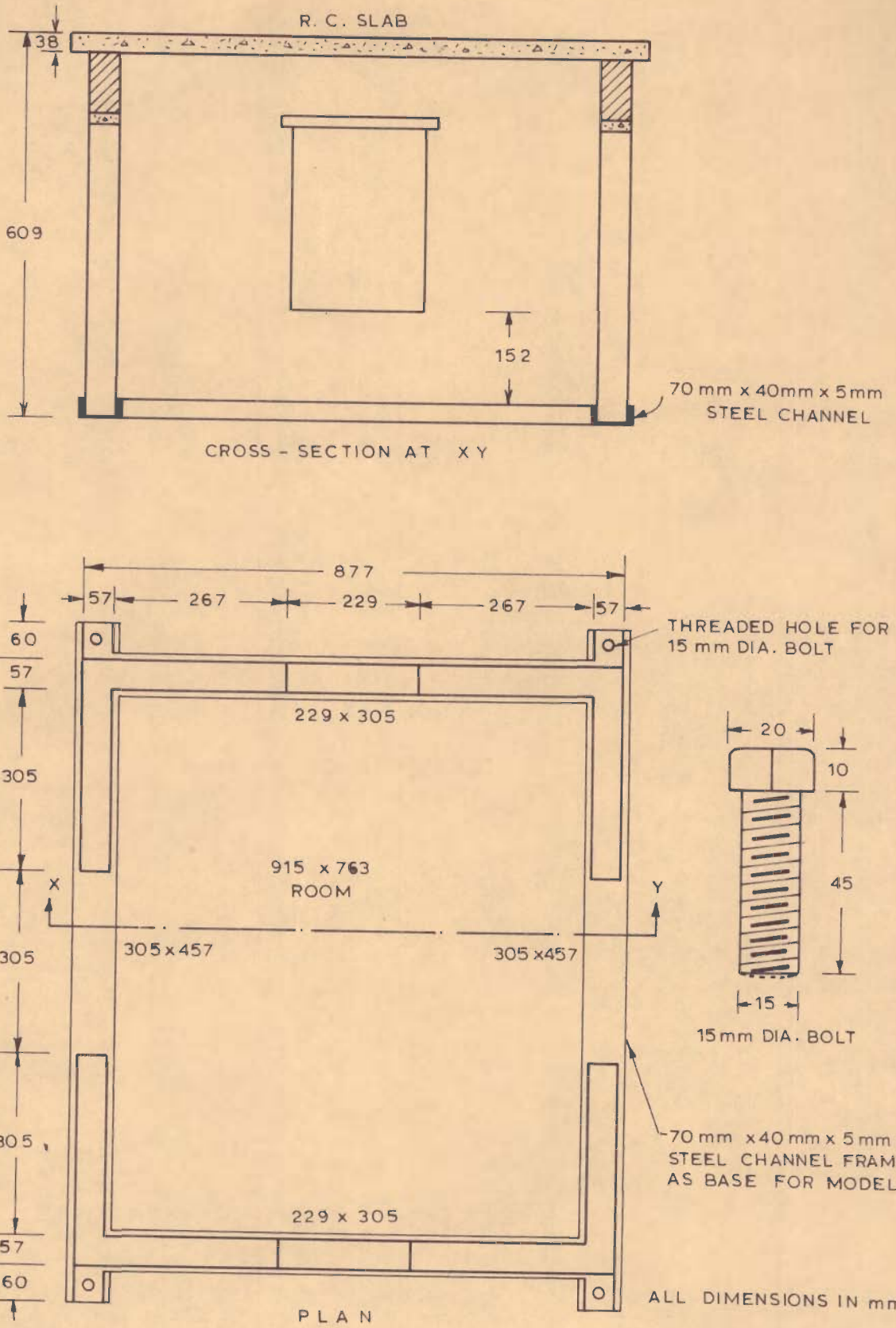

FIG. 4.1_ SLIDING TYPE, 1/4 SCALE, MODEL IN CEMENT MORTAR

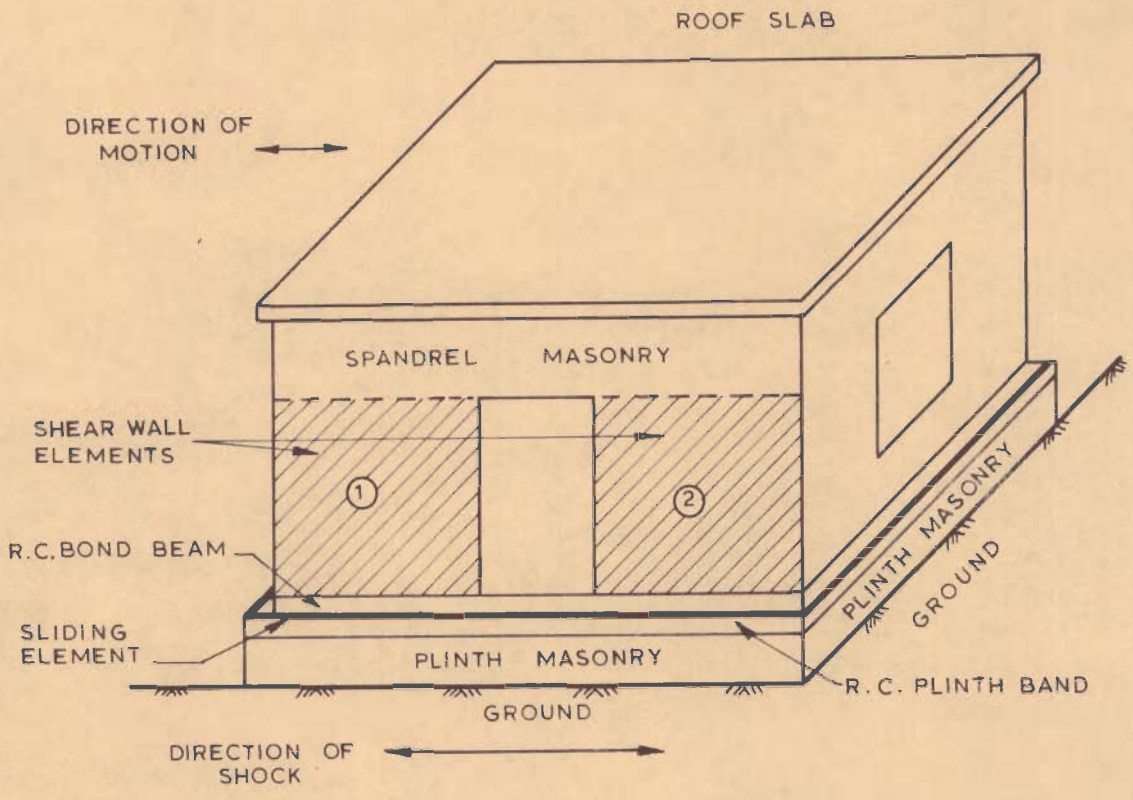

FIG.4.2 _IDEALIZED SLIDING TYPE BRICK BUILDING

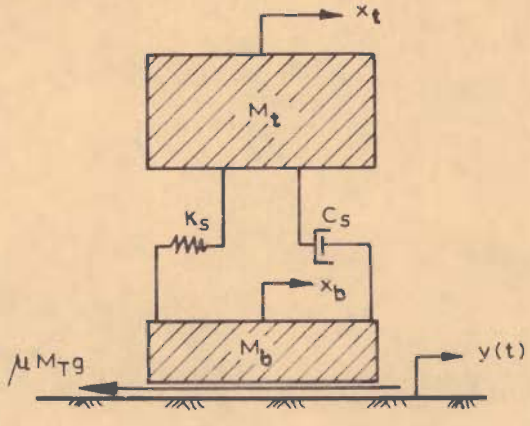

FIG.4.3 _MATHEMATICAL MODEL FOR SLIDING TYPE SYSTEM

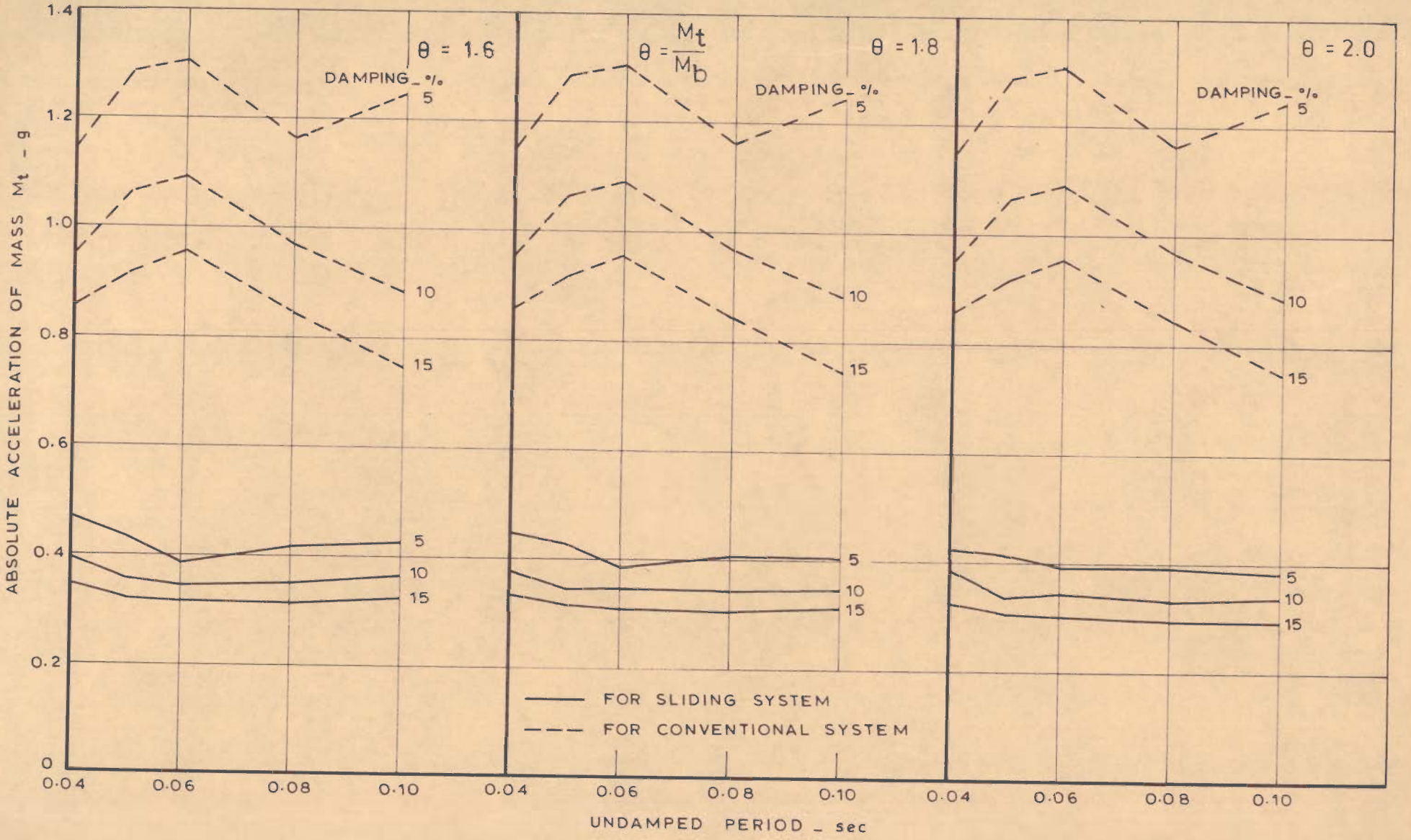

FIG.4.4a - FRICTIONAL RESPONSE ACCELERATION SPECTRA FOR KOYNA SHOCK (μ =0.15)

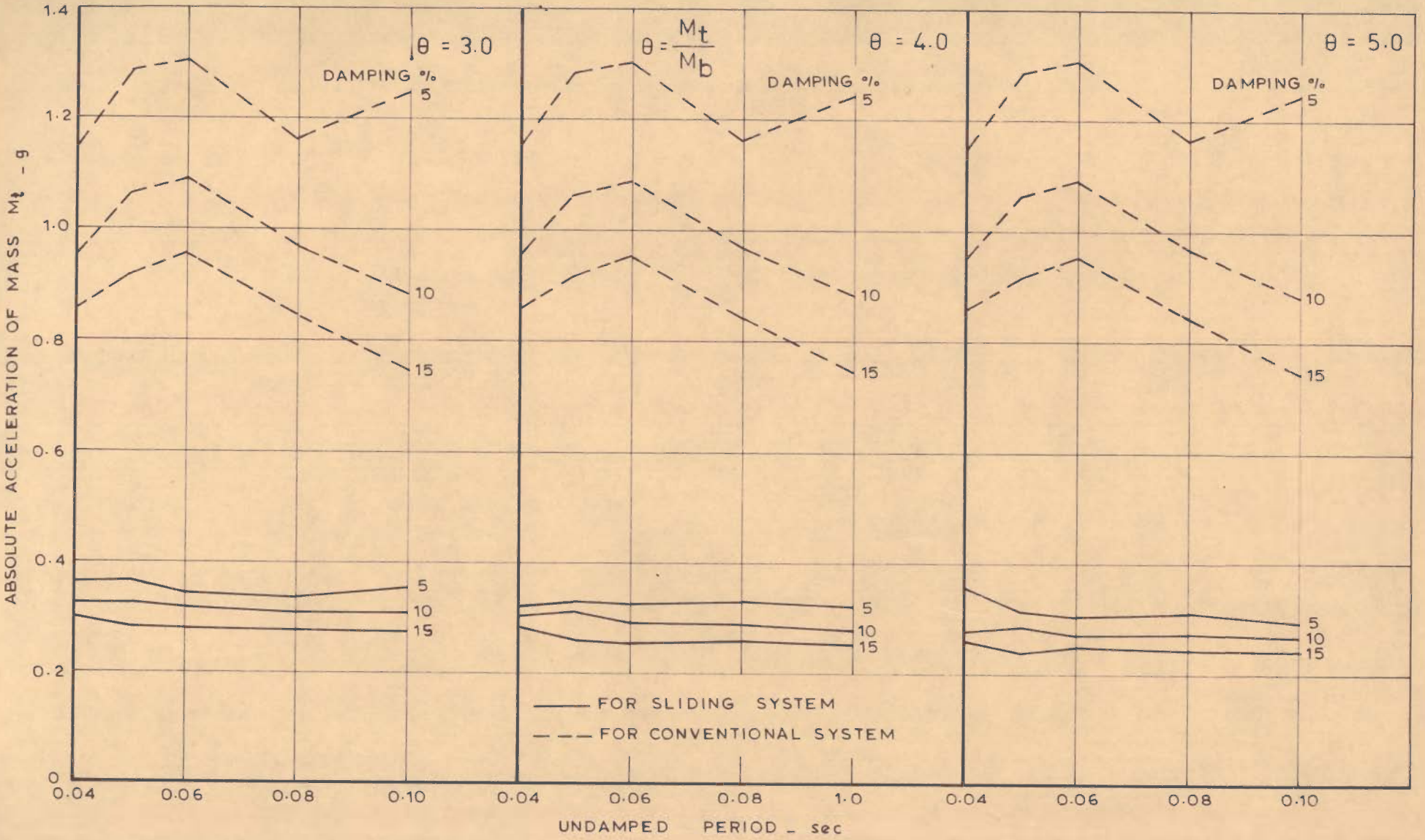

FIG.4.4b_FRICTIONAL RESPONSE ACCELERATION SPECTRA FOR KOYNA SHOCK ($\mu = 0.15$)

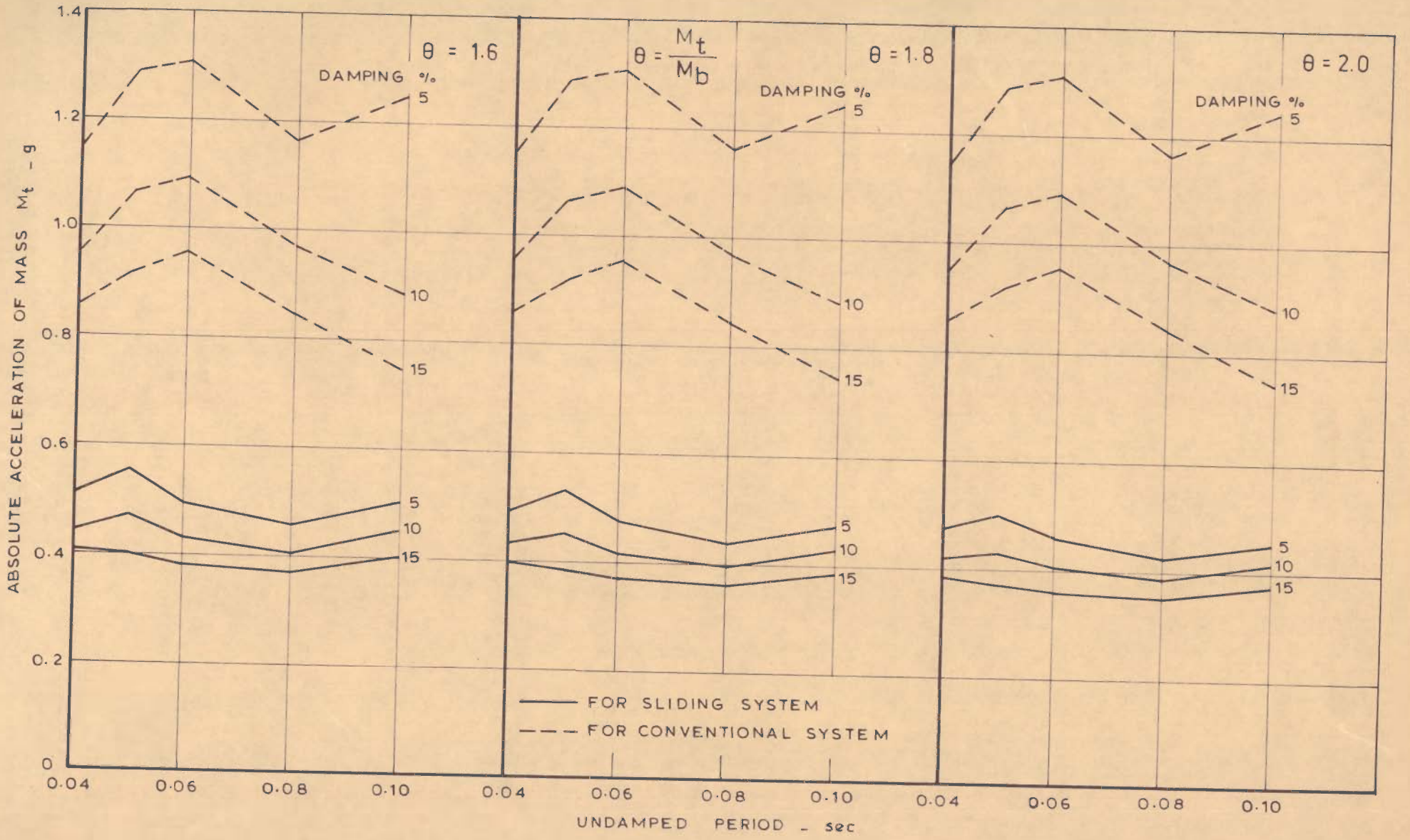

FIG.4.5a_FRICTIONAL RESPONSE ACCELERATION SPECTRA FOR KOYNA SHOCK (μ = 0.20)

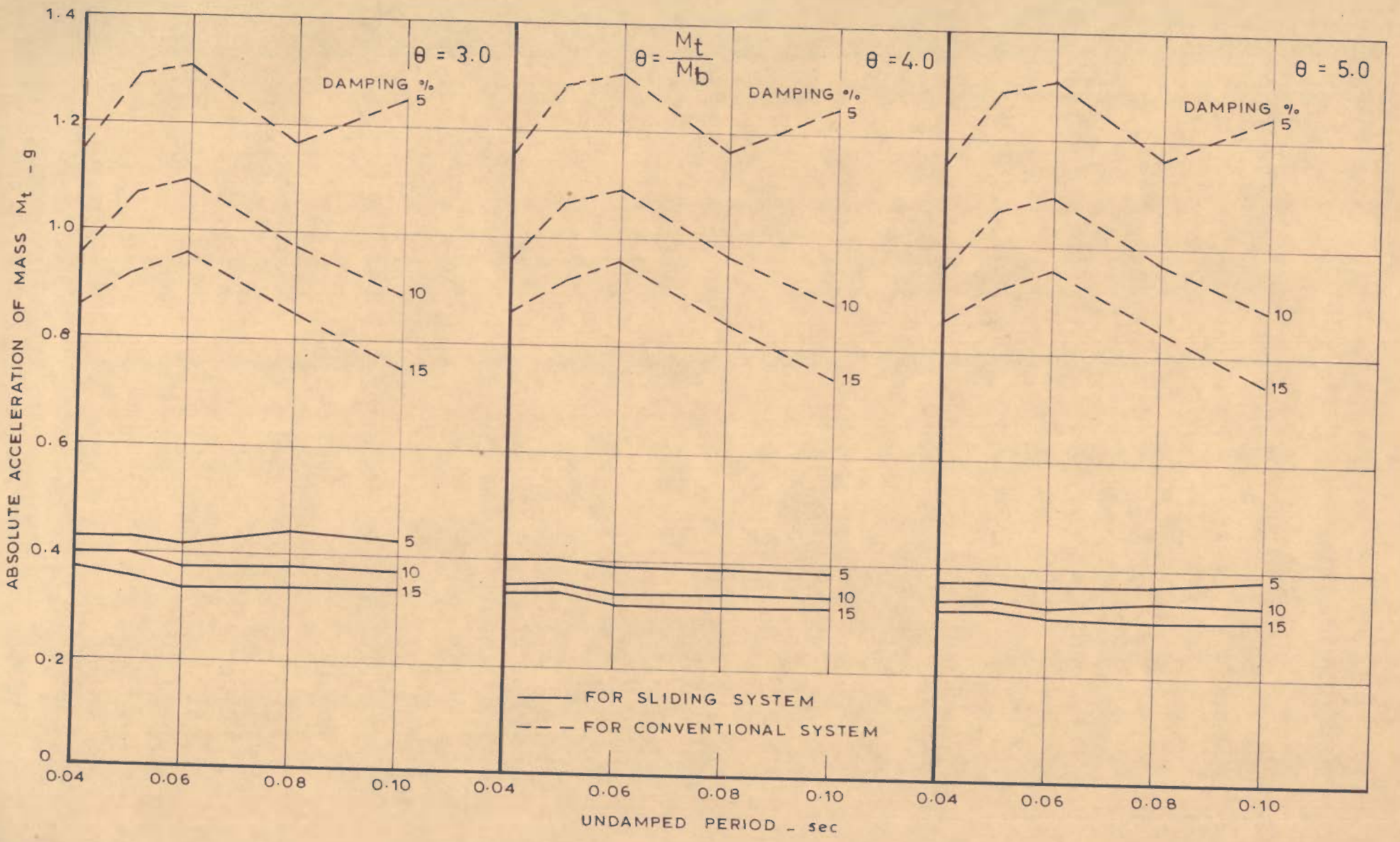

FIG.4.5b_ FRICTIONAL RESPONSE ACCELERATION SPECTRA FOR KOYNA SHOCK ($\mu = 0.20$)

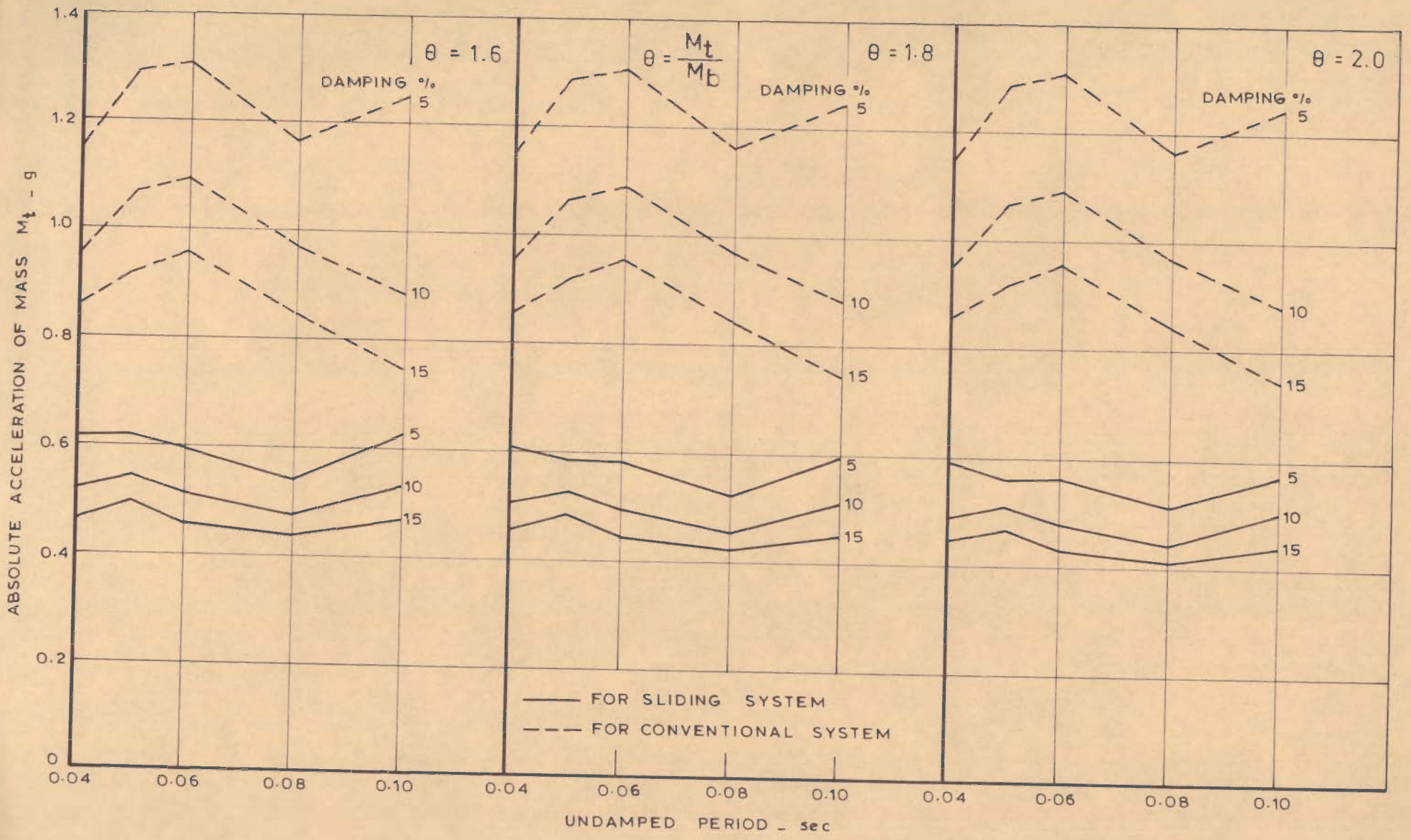

FIG.4.6a-FRICTIONAL RESPONSE ACCELERATION SPECTRA FOR KOYNA SHOCK (μ =0.25)

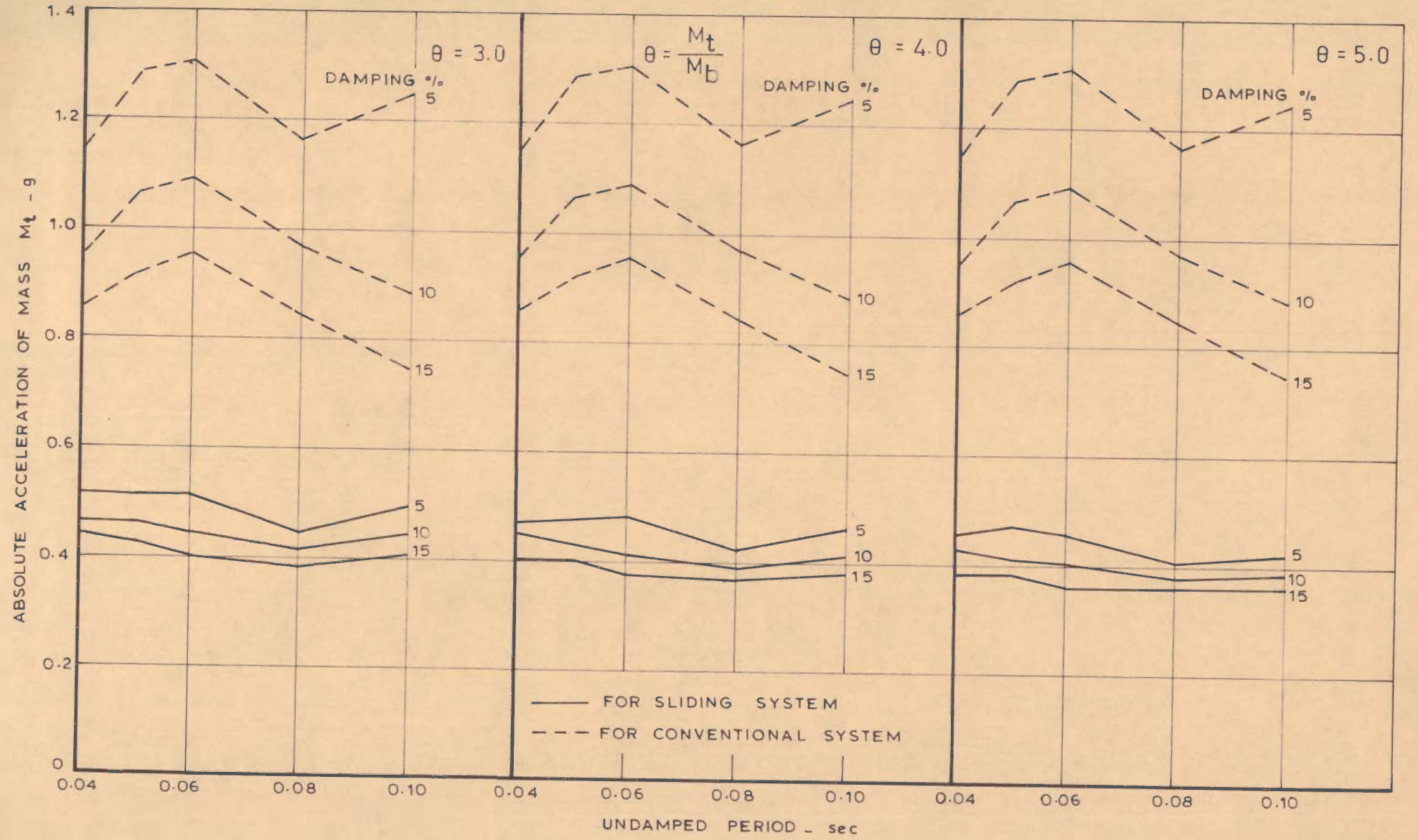

FIG.4.6 b _ FRICTIONAL RESPONSE ACCELERATION SPECTRA FOR KOYNA SHOCK ($\mu = 0.25$)

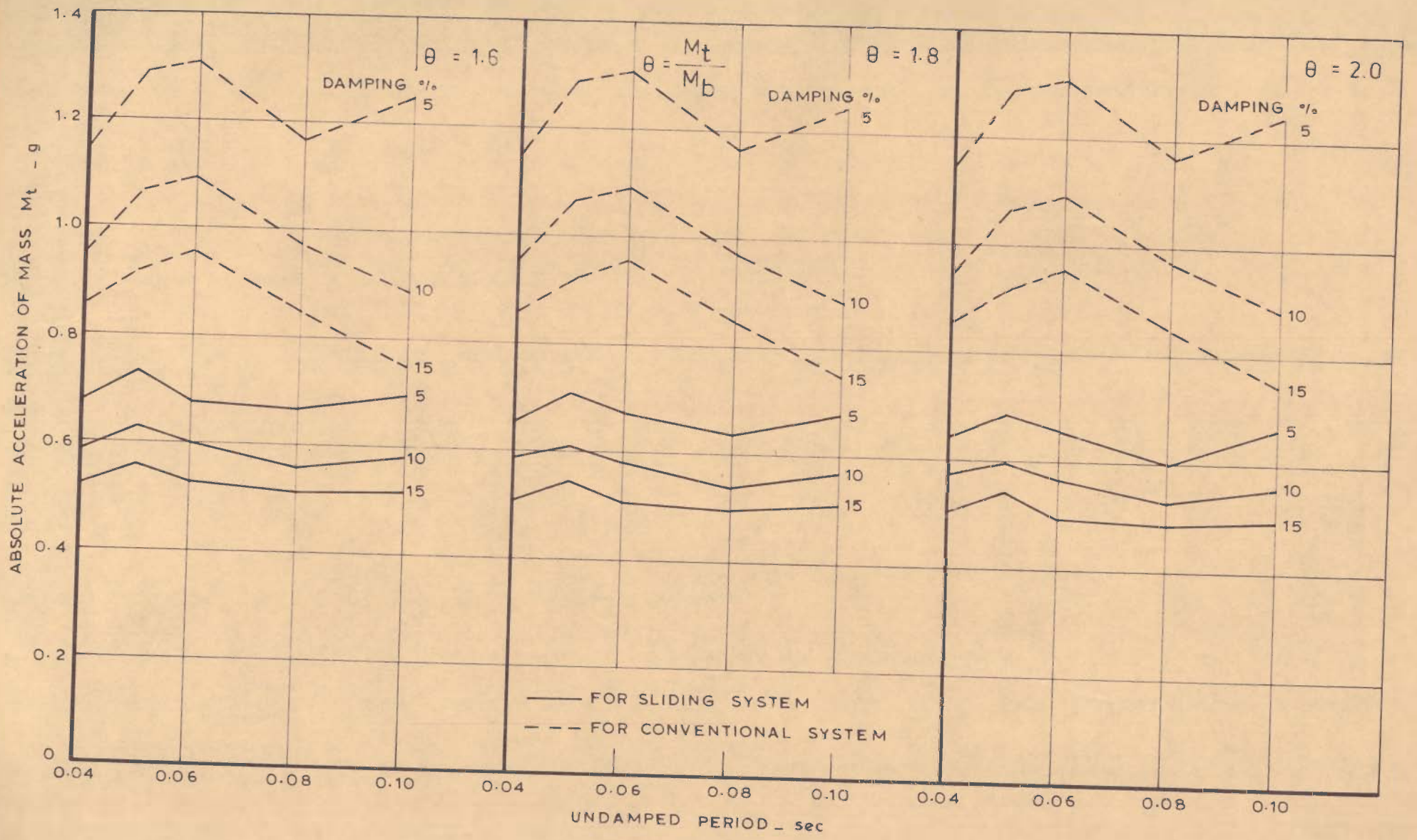

FIG.4.7a - FRICTIONAL RESPONSE ACCELERATION SPECTRA FOR KOYNA SHOCK ($\mu = 0.30$)

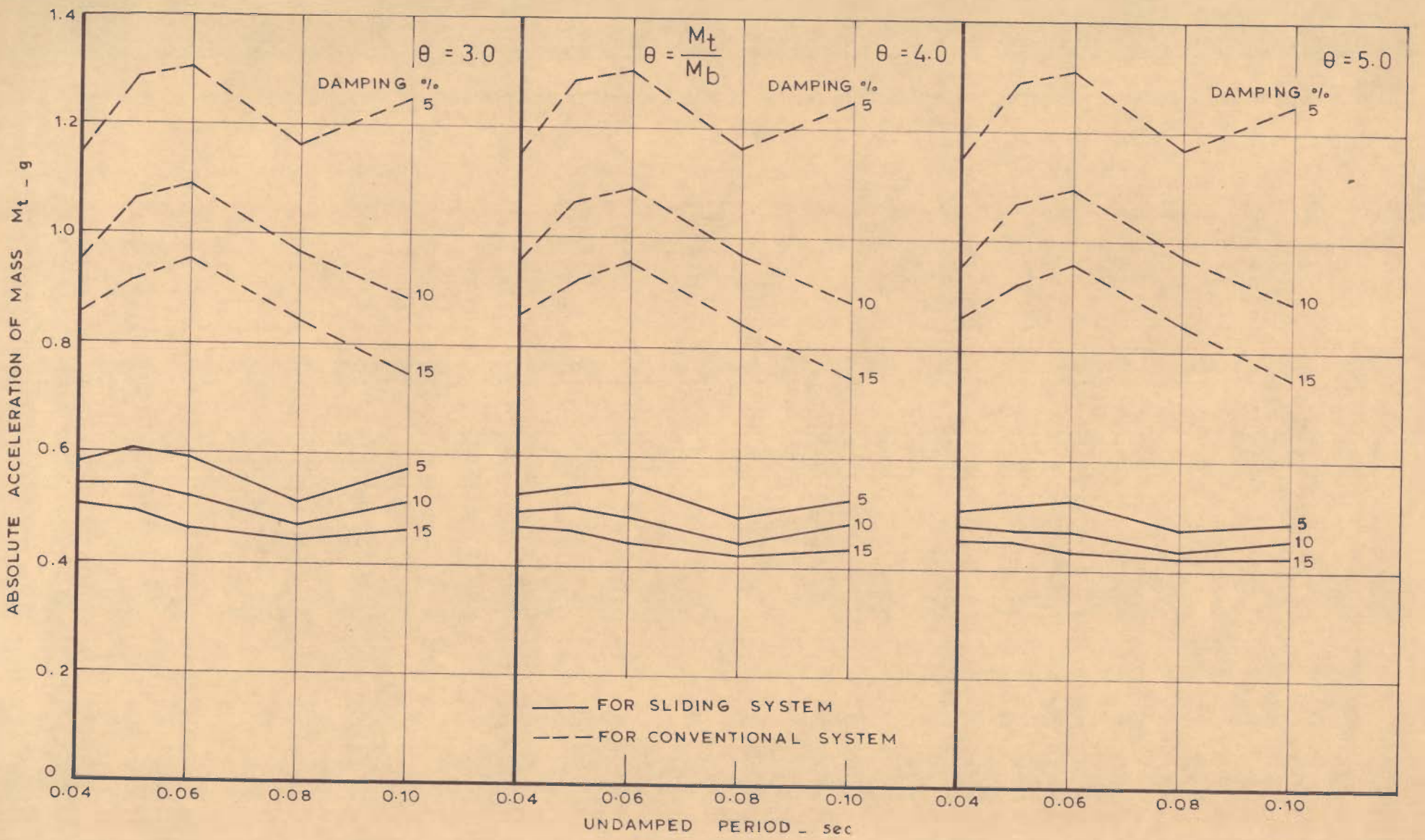

FIG.4.7b_FRICTIONAL RESPONSE ACCELERATION SPECTRA FOR KOYNA SHOCK (μ = 0.30)

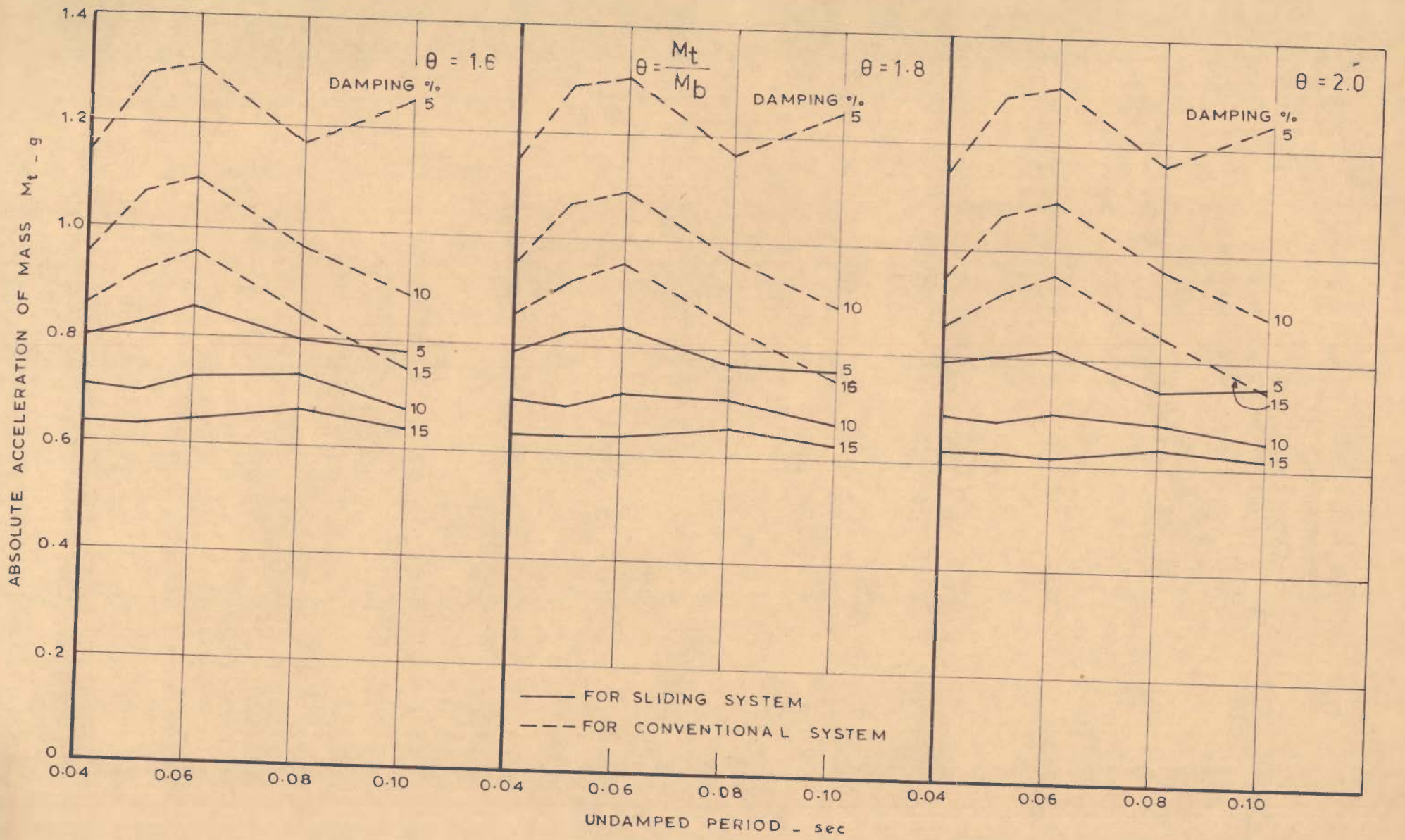

FIG.4.8a_FRICTIONAL RESPONSE ACCELERATION SPECTRA FOR KOYNA SHOCK ($\mu = 0.40$)

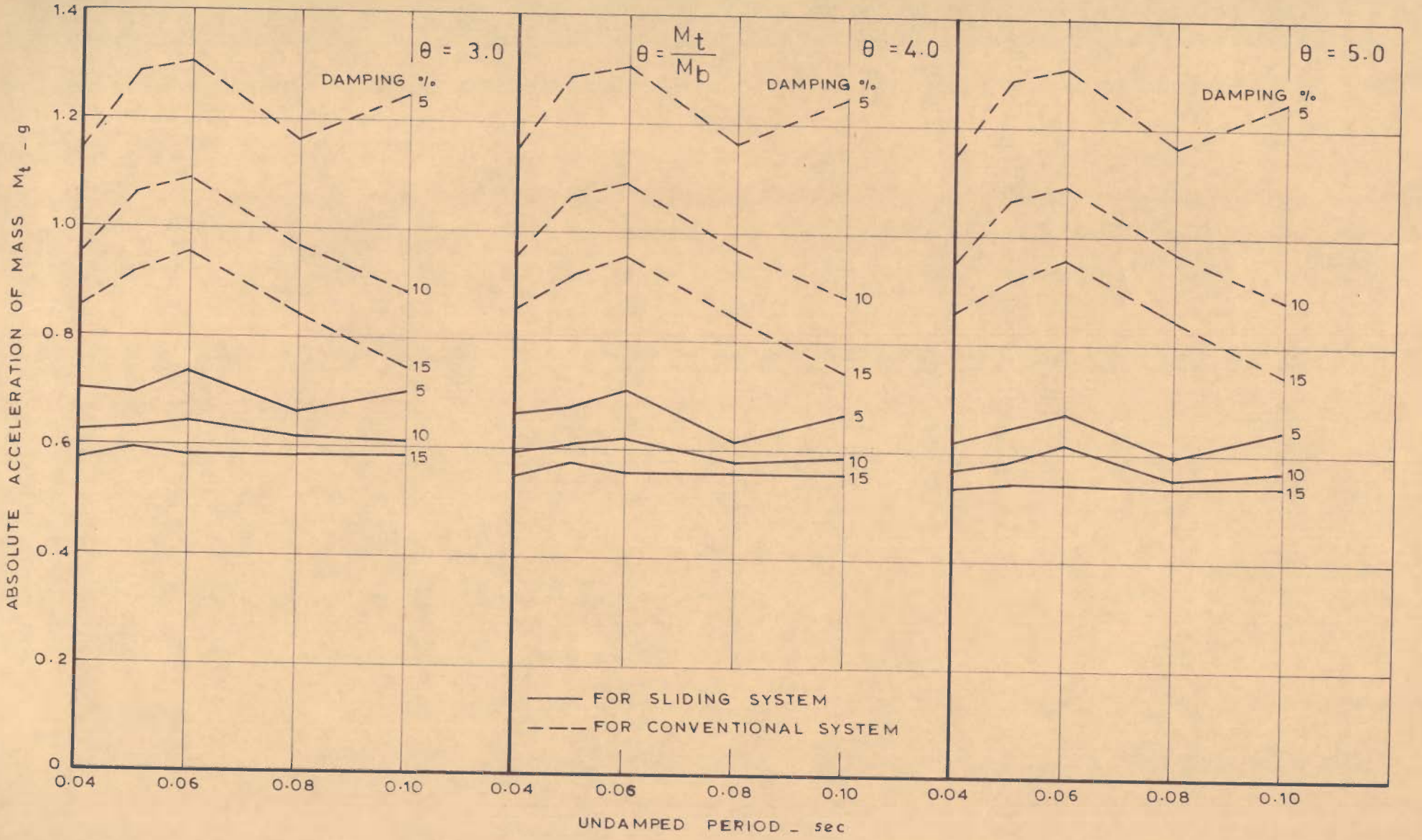

FIG.4.8b_ FRICTIONAL RESPONSE ACCELERATION SPECTRA FOR KOYNA SHOCK ($\mu = 0.40$)

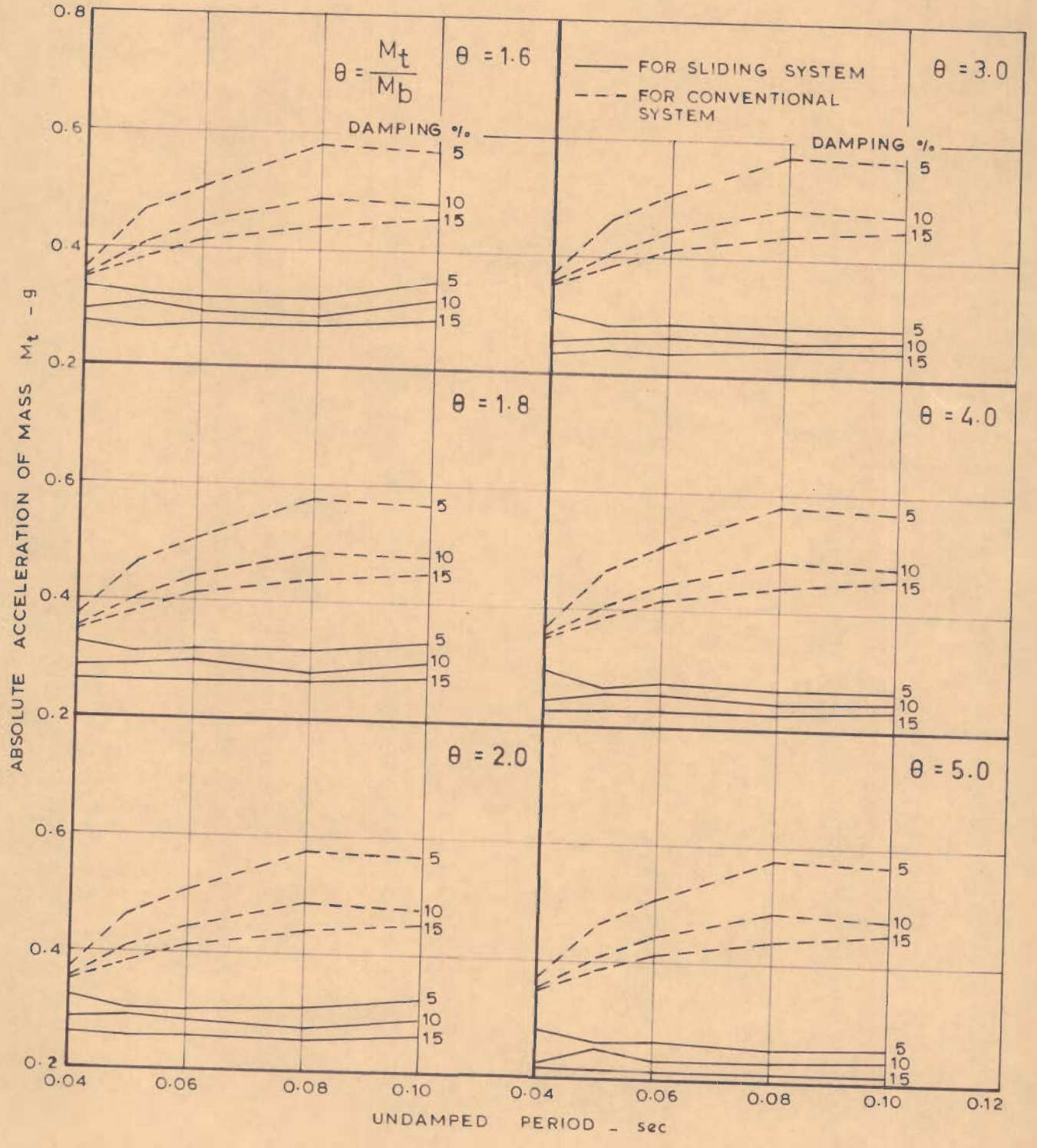

FIG. 4.9 - FRICTIONAL RESPONSE ACCELERATION SPECTRA FOR EL CENTRO SHOCK ($\mu = 0.15$)

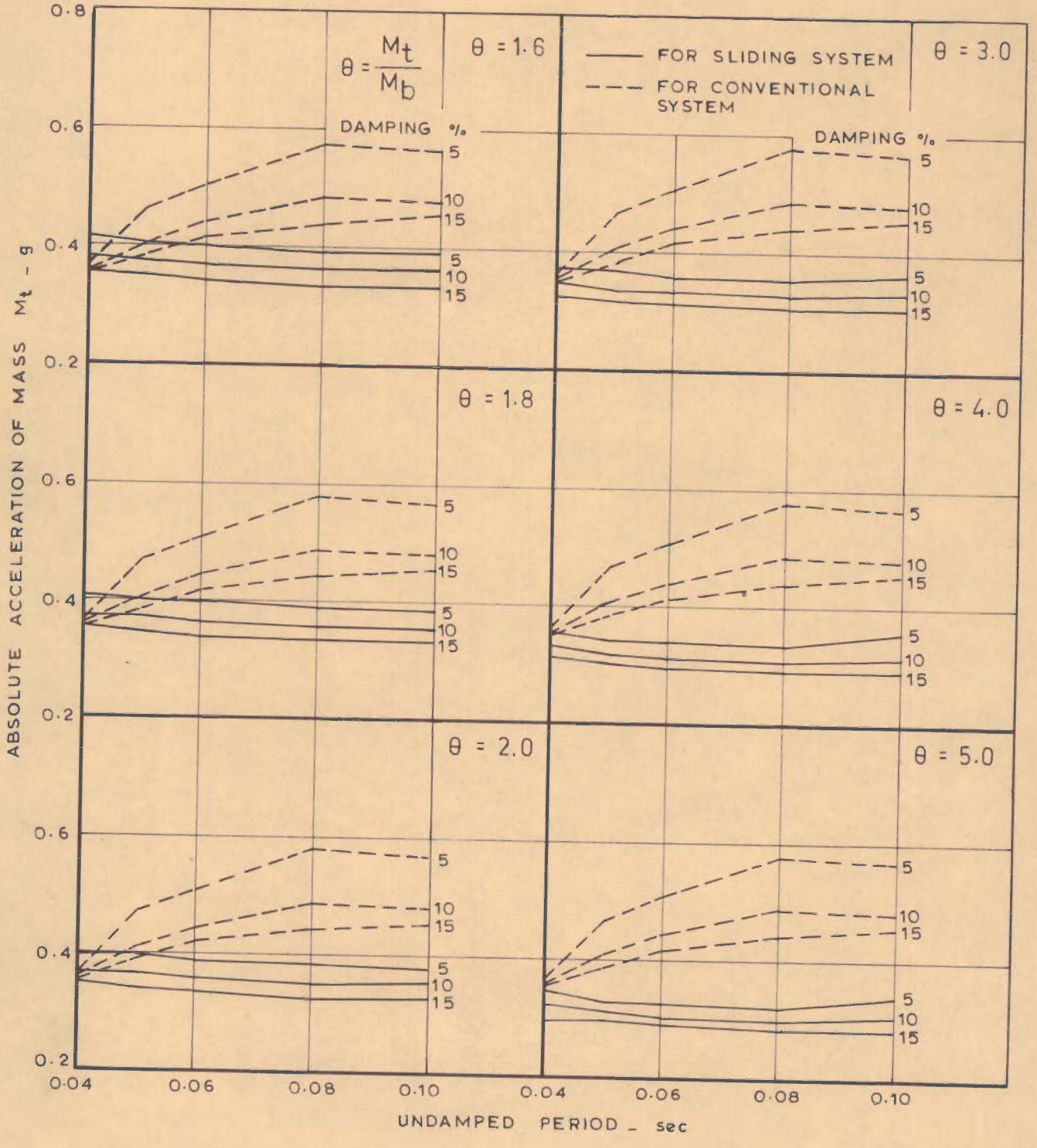

FIG.4.10_FRICTIONAL RESPONSE ACCELERATION SPECTRA FOR EL CENTRO SHOCK (μ = 0.20)

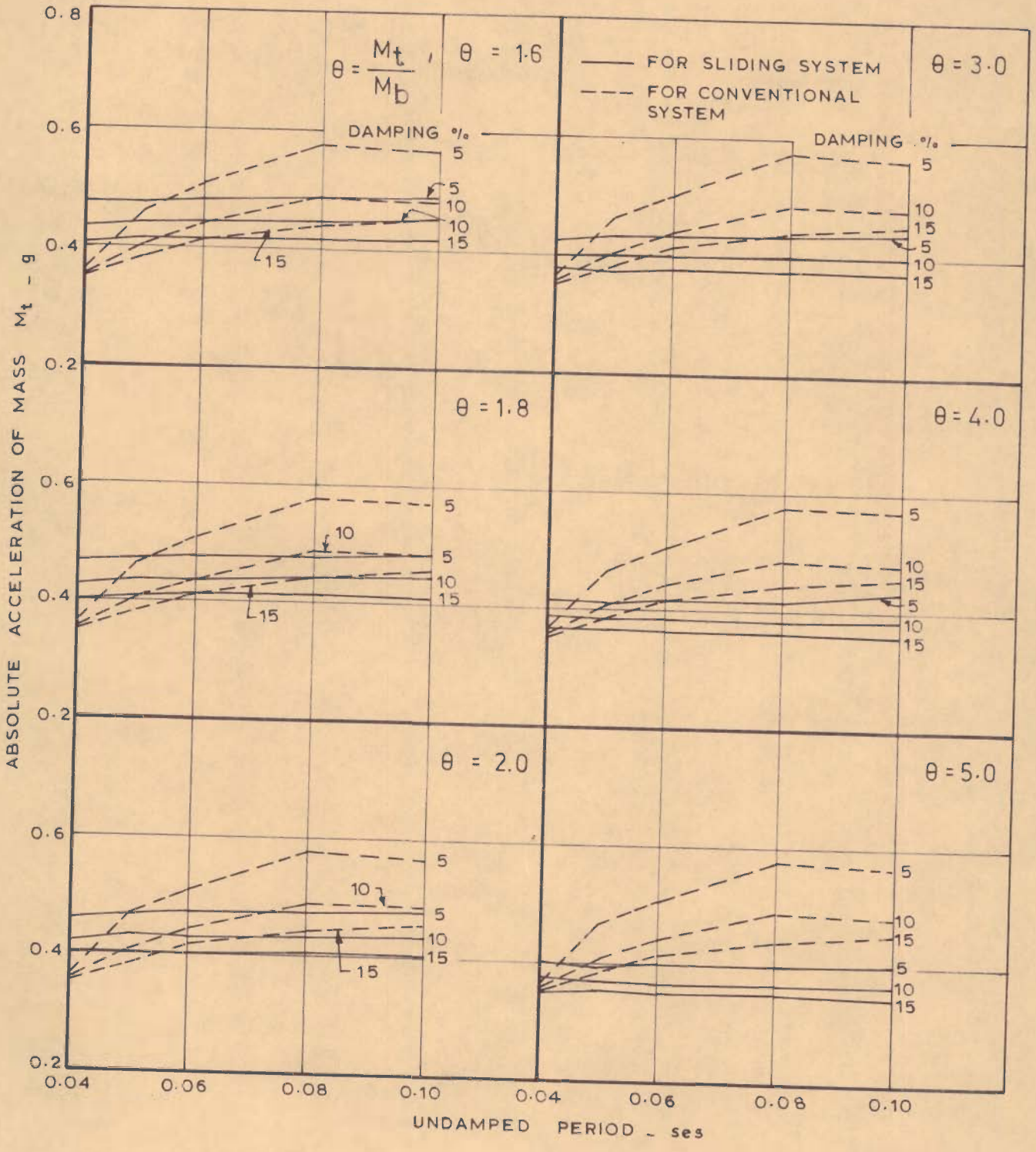

FIG. 4·11 - FRICTIONAL RESPONSE ACCELERATION SPECTRA FOR EL CENTRO SHOCK ($\mu = 0.25$)

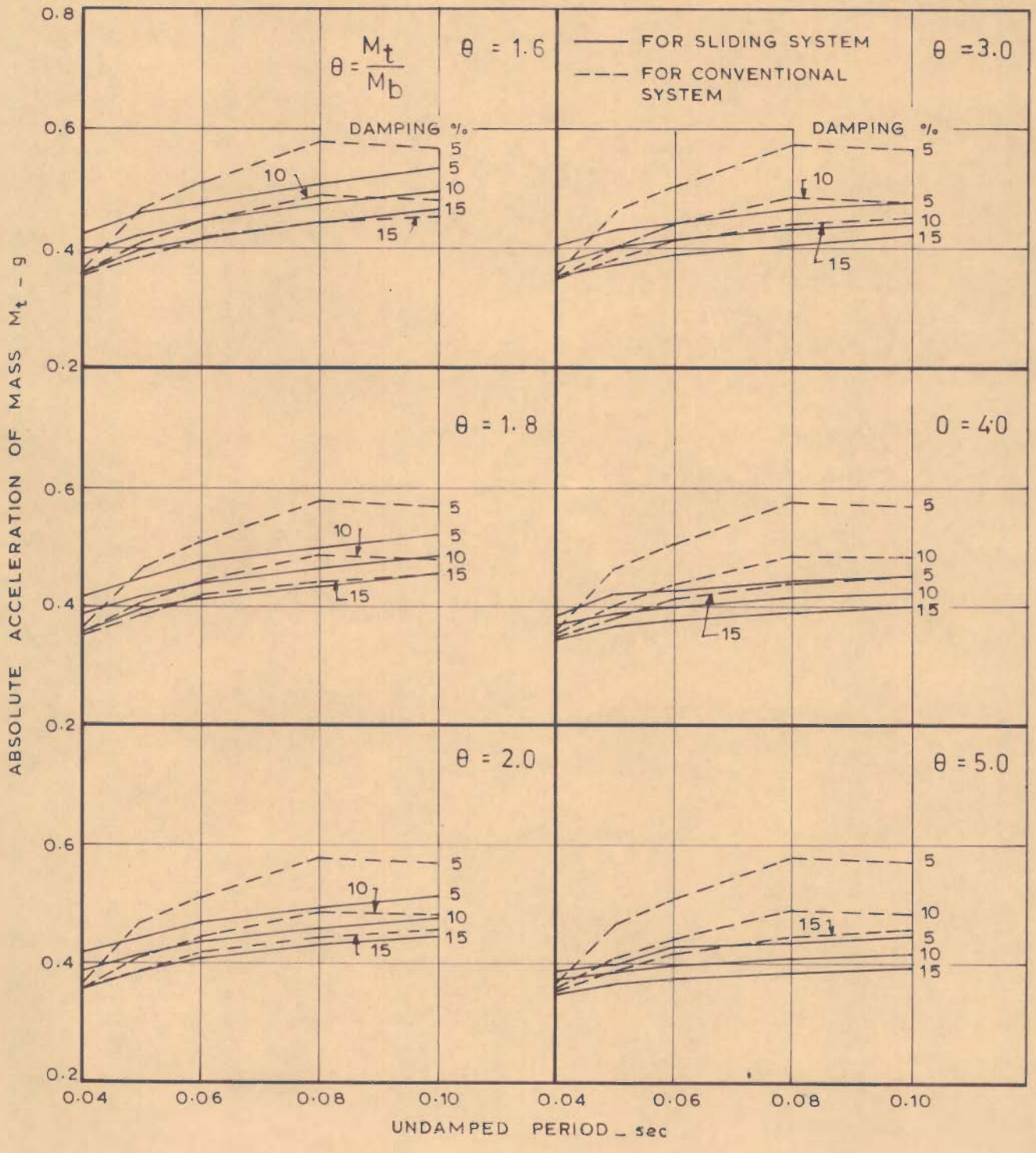

FIG.4.12 - FRICTIONAL RESPONSE ACCELERATION SPECTRA FOR EL CENTRO SHOCK ($\mu = 0.30$)

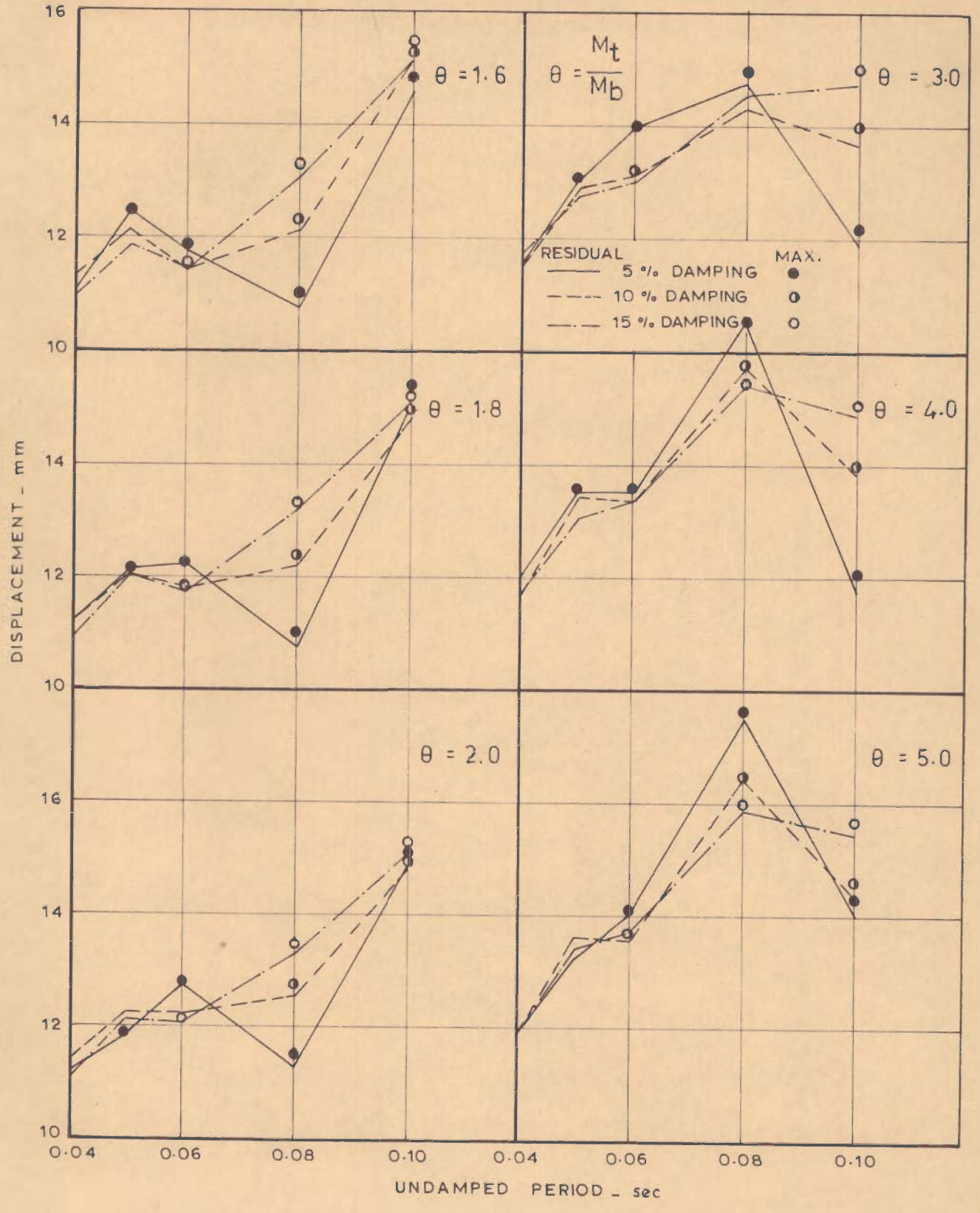

FIG.4.13_FRICTIONAL RESPONSE, RESIDUAL AND MAXIMUM DISPLACEMENT SPECTRA FOR KOYNA SHOCK ($\mu = 0.15$)

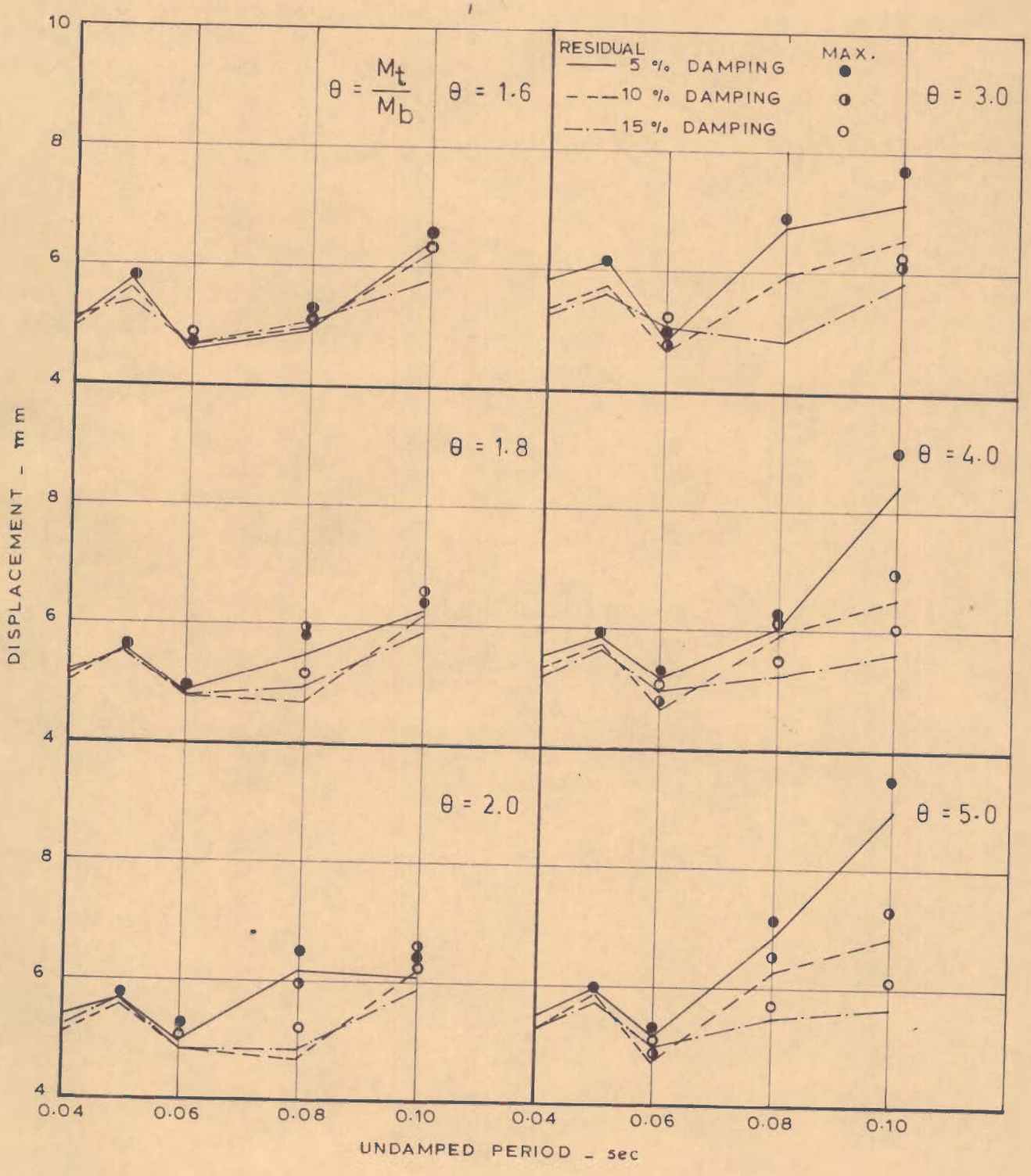

FIG. 4.14 - FRICTIONAL RESPONSE, RESIDUAL AND MAXIMUM DISPLACEMENT SPECTRA FOR KOYNA SHOCK ($\mu = 0.20$)

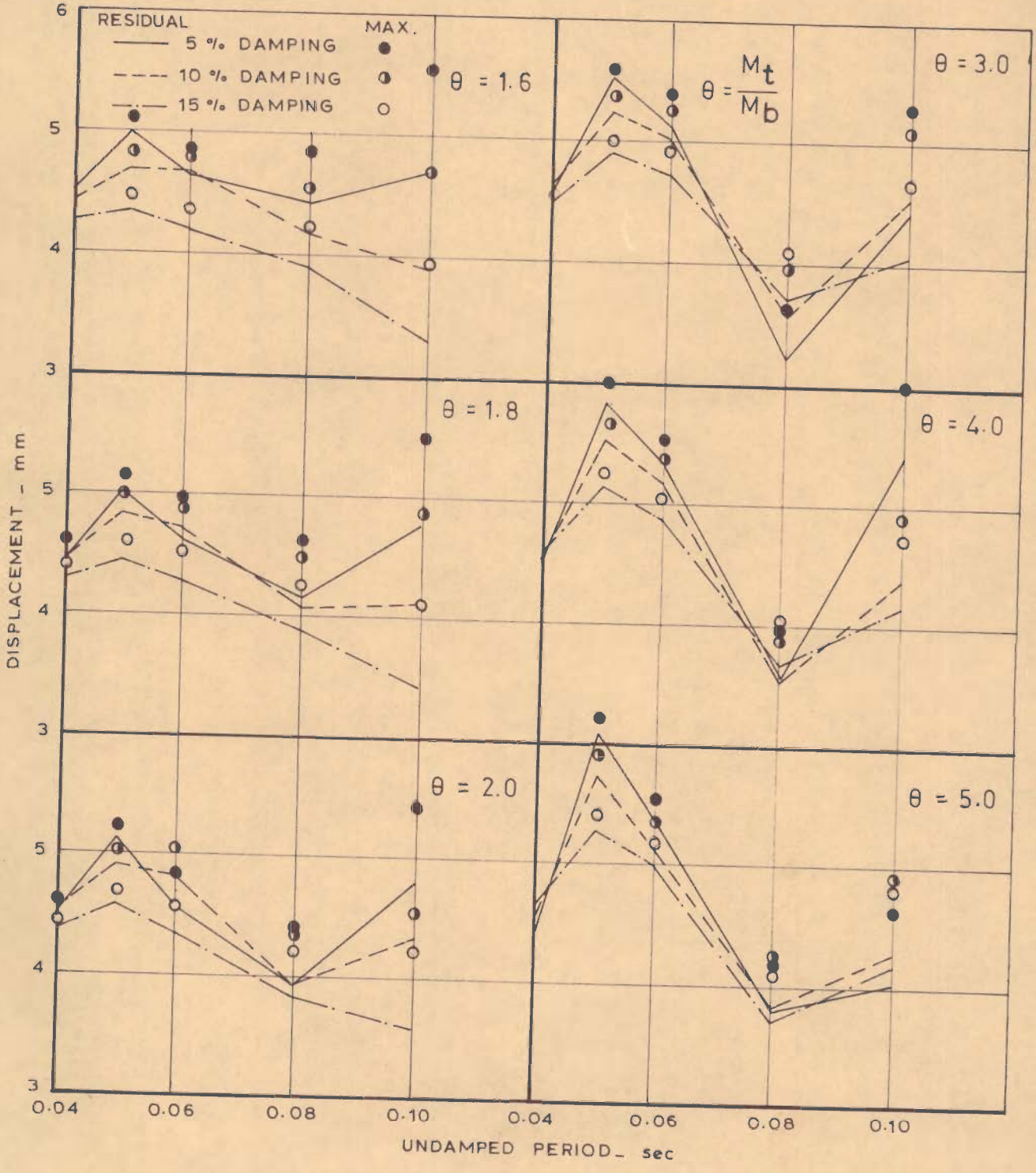

FIG.4.15_FRICTIONAL RESPONSE, RESIDUAL AND MAXIMUM DISPLACEMENT SPECTRA FOR KOYNA SHOCK ($\mu = 0.25$)

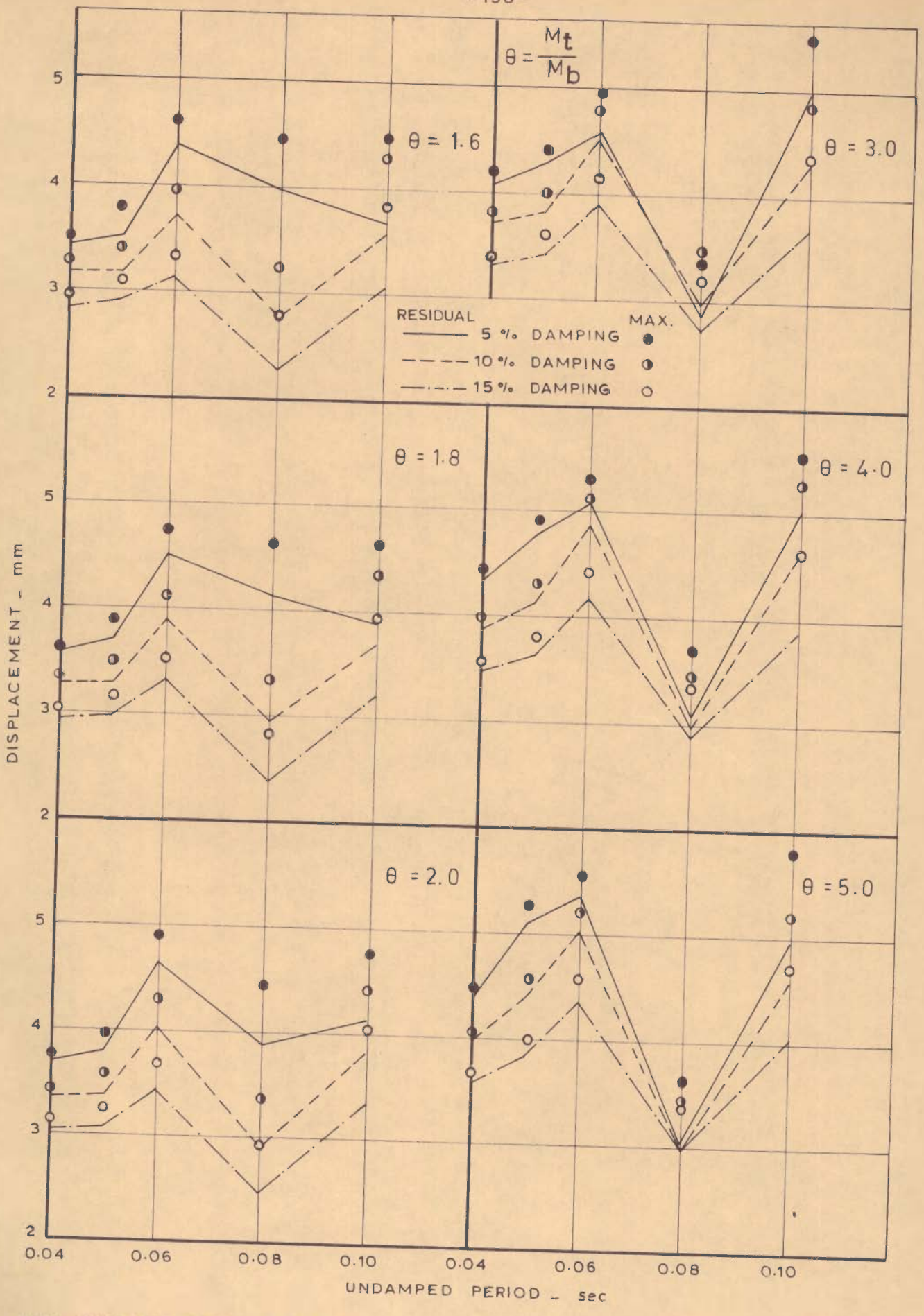

FIG. 4.16_FRICTIONAL RESPONSE, RESIDUAL AND MAXIMUM DISPLACEMENT SPECTRA FOR KOYNA SHOCK ($\mu = 0.30$)

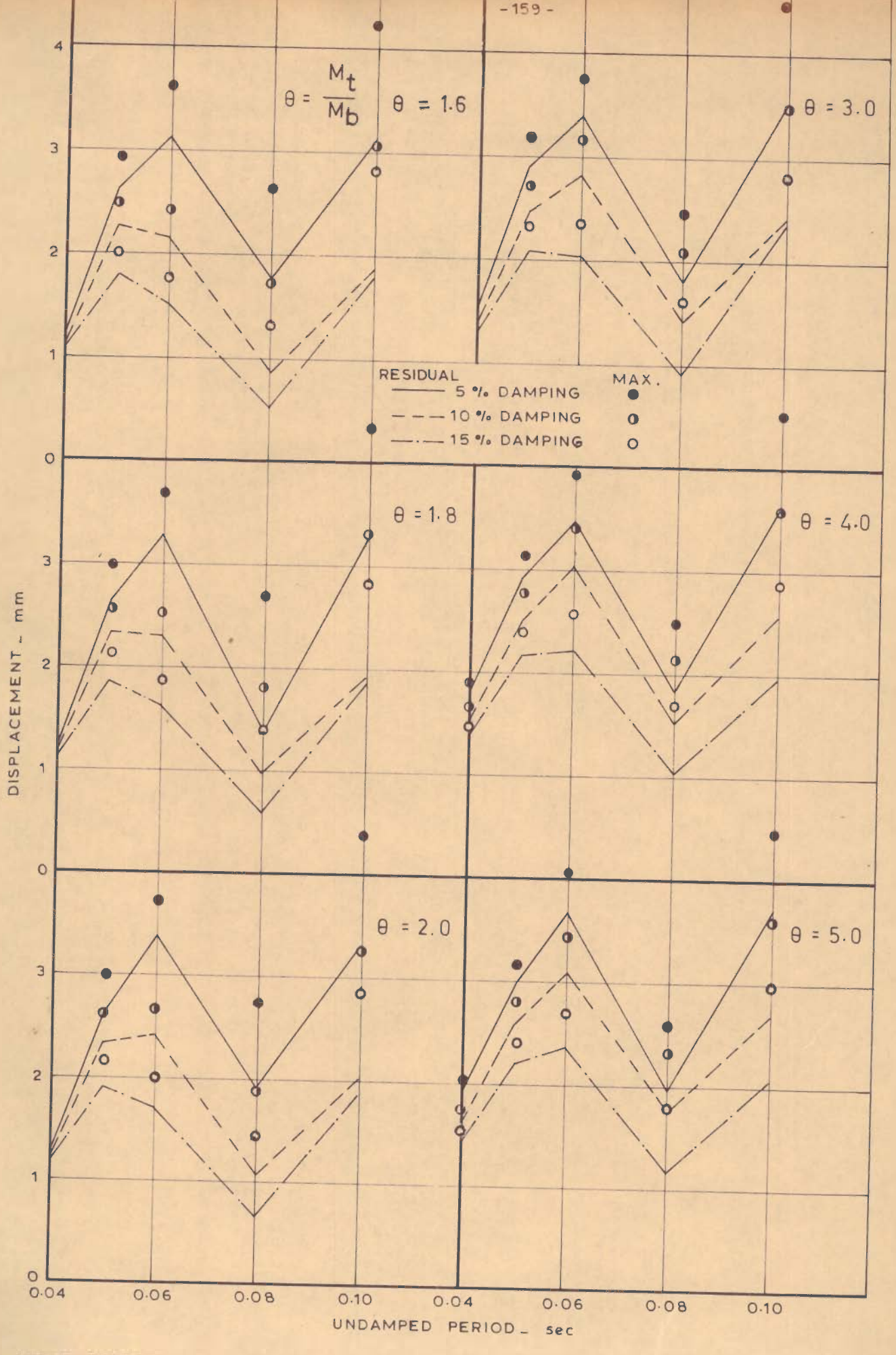

FIG. 4.17_FRICTIONAL RESPONSE, RESIDUAL AND MAXIMUM DISPLACEMENT SPECTRA FOR KOYNA SHOCK (μ =0·40)

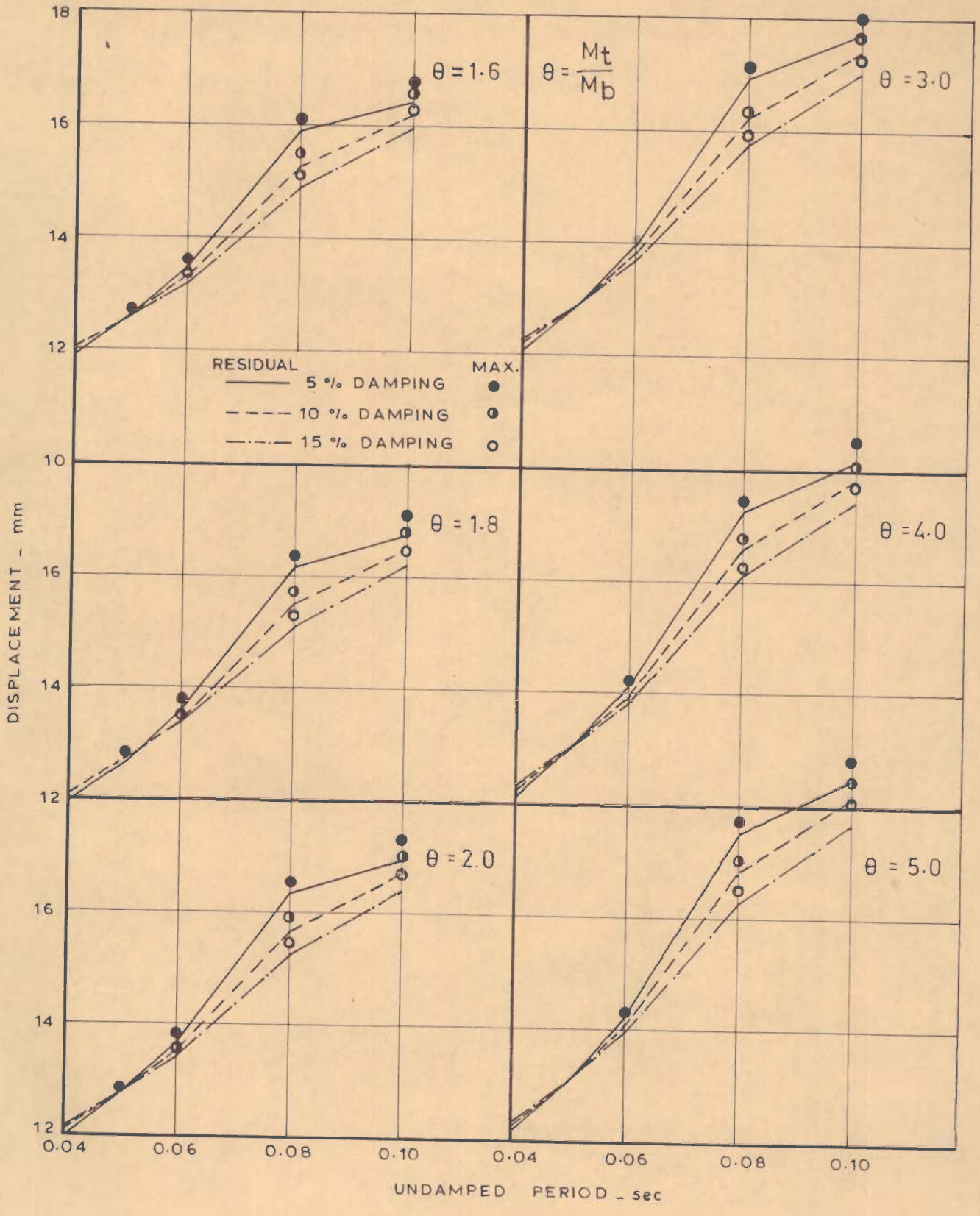

FIG.4.18 - FRICTIONAL RESPONSE, RESIDUAL AND MAXIMUM DISPLACEMENT SPECTRA FOR EL CENTRO SHOCK ($\mu = 0.15$)

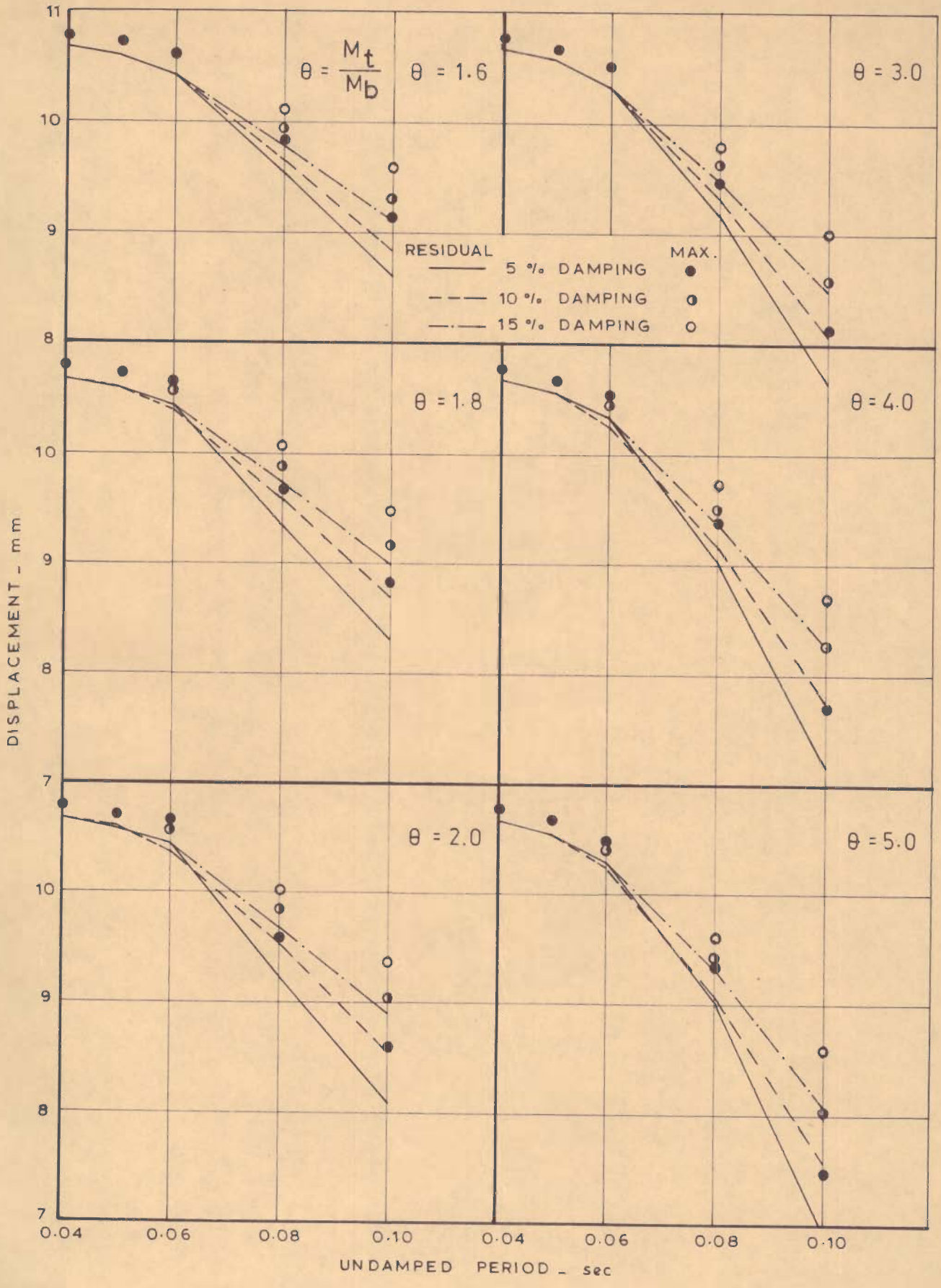

FIG. 4.19_FRICTIONAL RESPONSE, RESIDUAL AND MAXIMUM DISPLACEMENT SPECTRA FOR EL CENTRO SHOCK ($\mu = 0.20$)

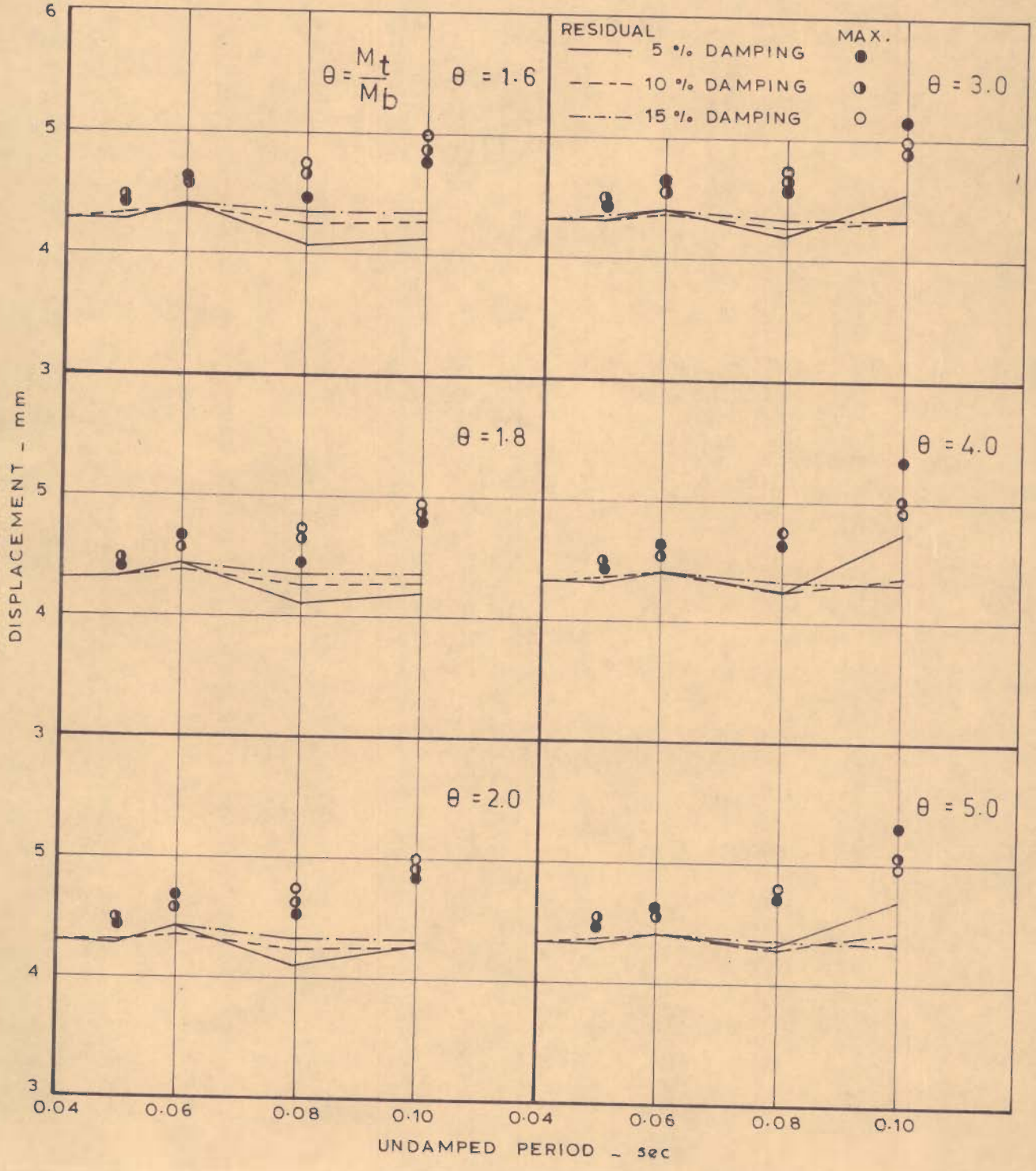

FIG. 4.20_ FRICTIONAL RESPONSE, RESIDUAL AND MAXIMUM DISPLACEMENT SPECTRA FOR EL CENTRO SHOCK (μ = 0.25)

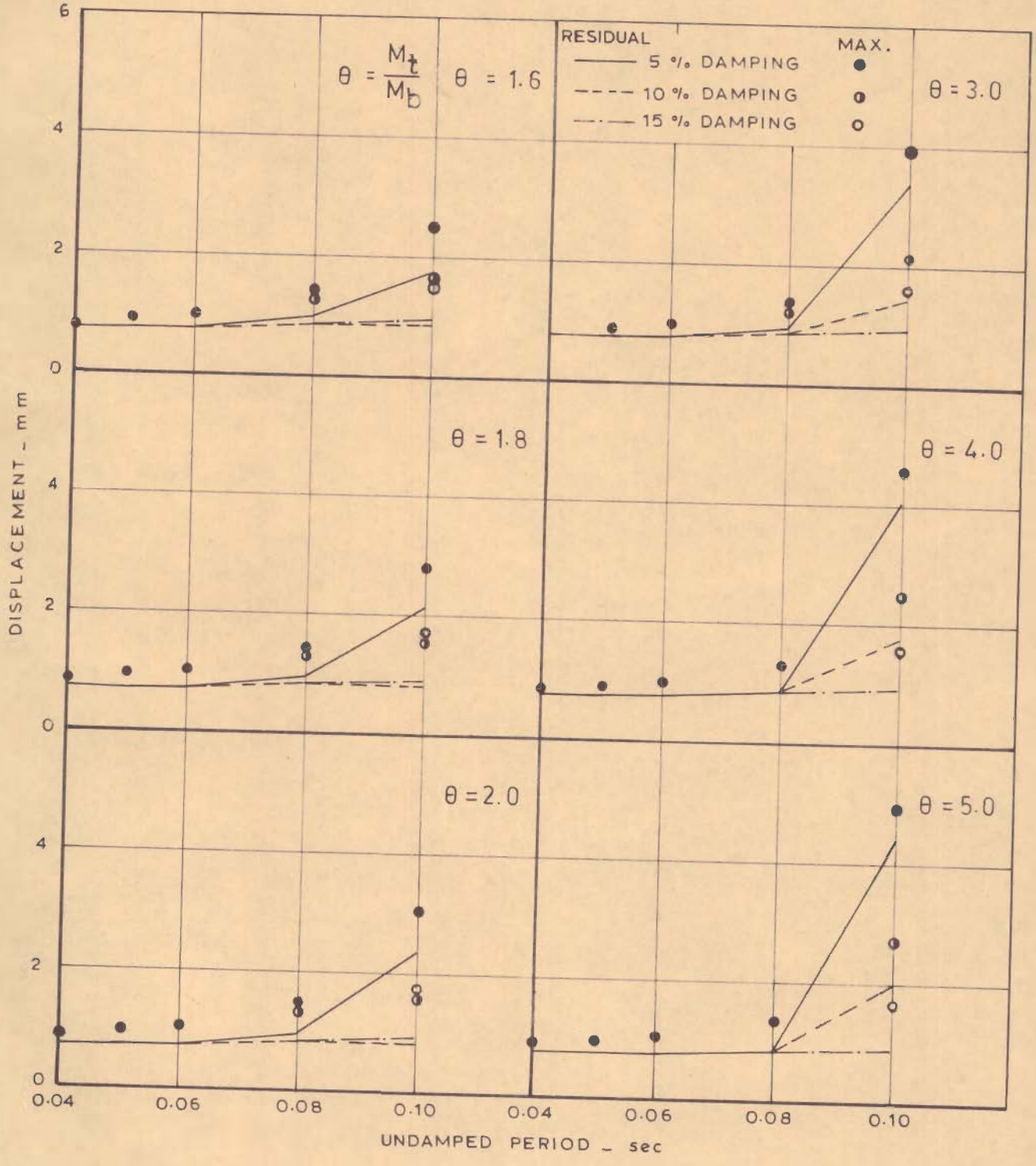

FIG. 4.21 - FRICTIONAL RESPONSE, RESIDUAL AND MAXIMUM DISPLACEMENT SPECTRA FOR EL CENTRO SHOCK ($\mu = 0.30$)

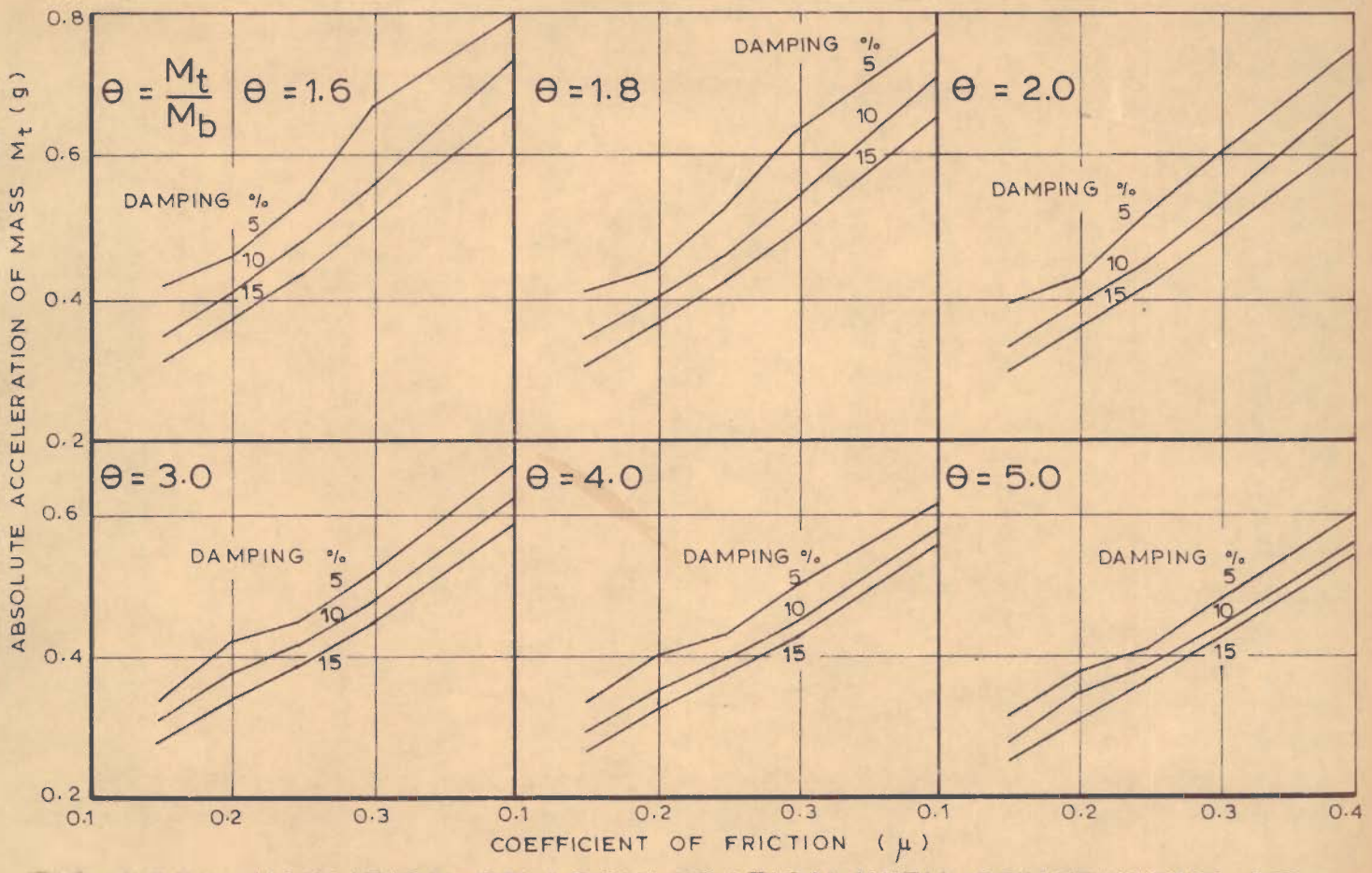

FIG. 4.22 a_VARIATION OF ACCELERATION WITH COEFFICIENT OF FRICTION FOR KOYNA SHOCK (T= 0.08 sec)

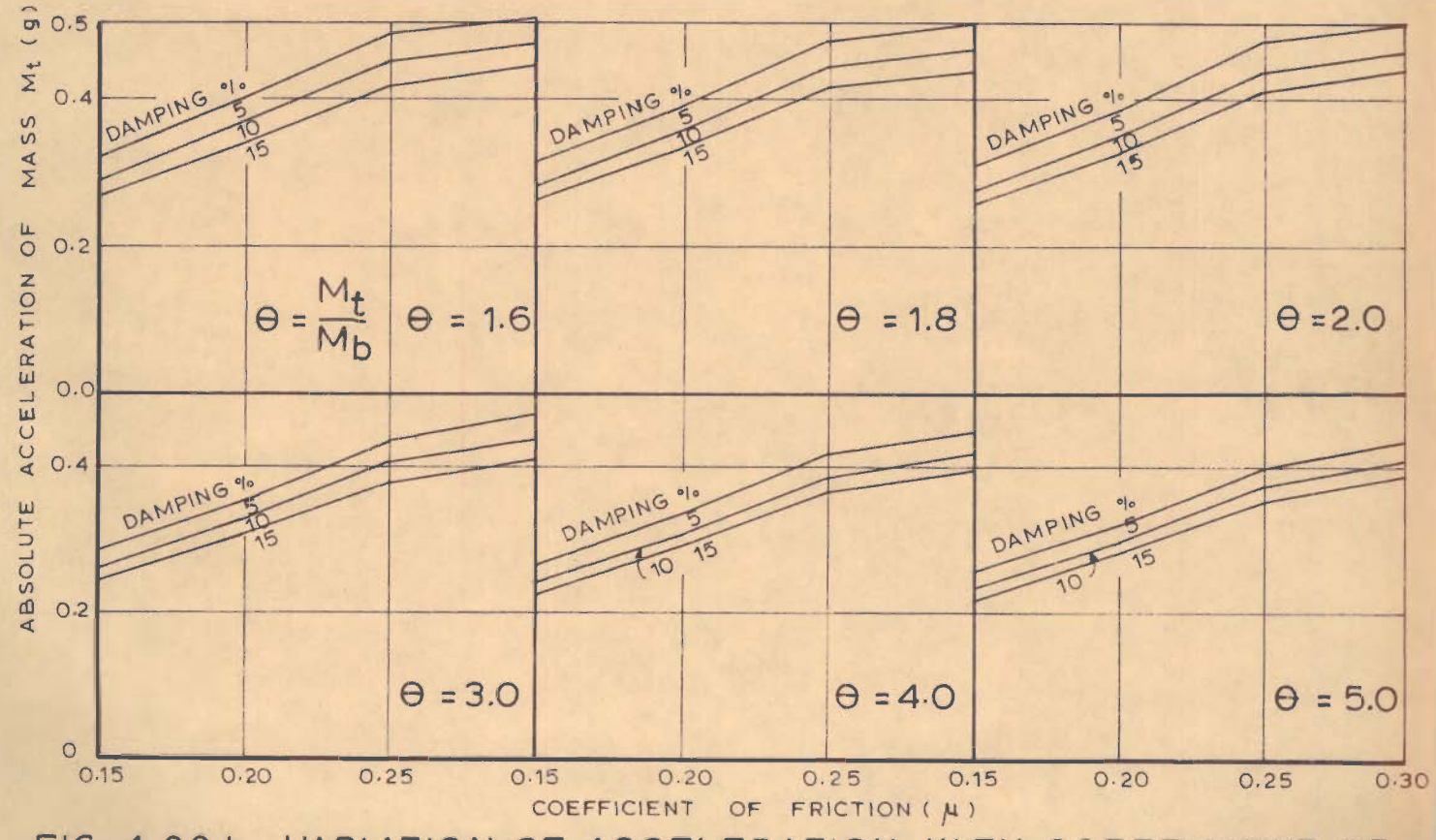

FIG. 4.22 b_VARIATION OF ACCELERATION WITH COEFFICIENT OF FRICTION FOR EL CENTRO SHOCK (T=0.08 sec)

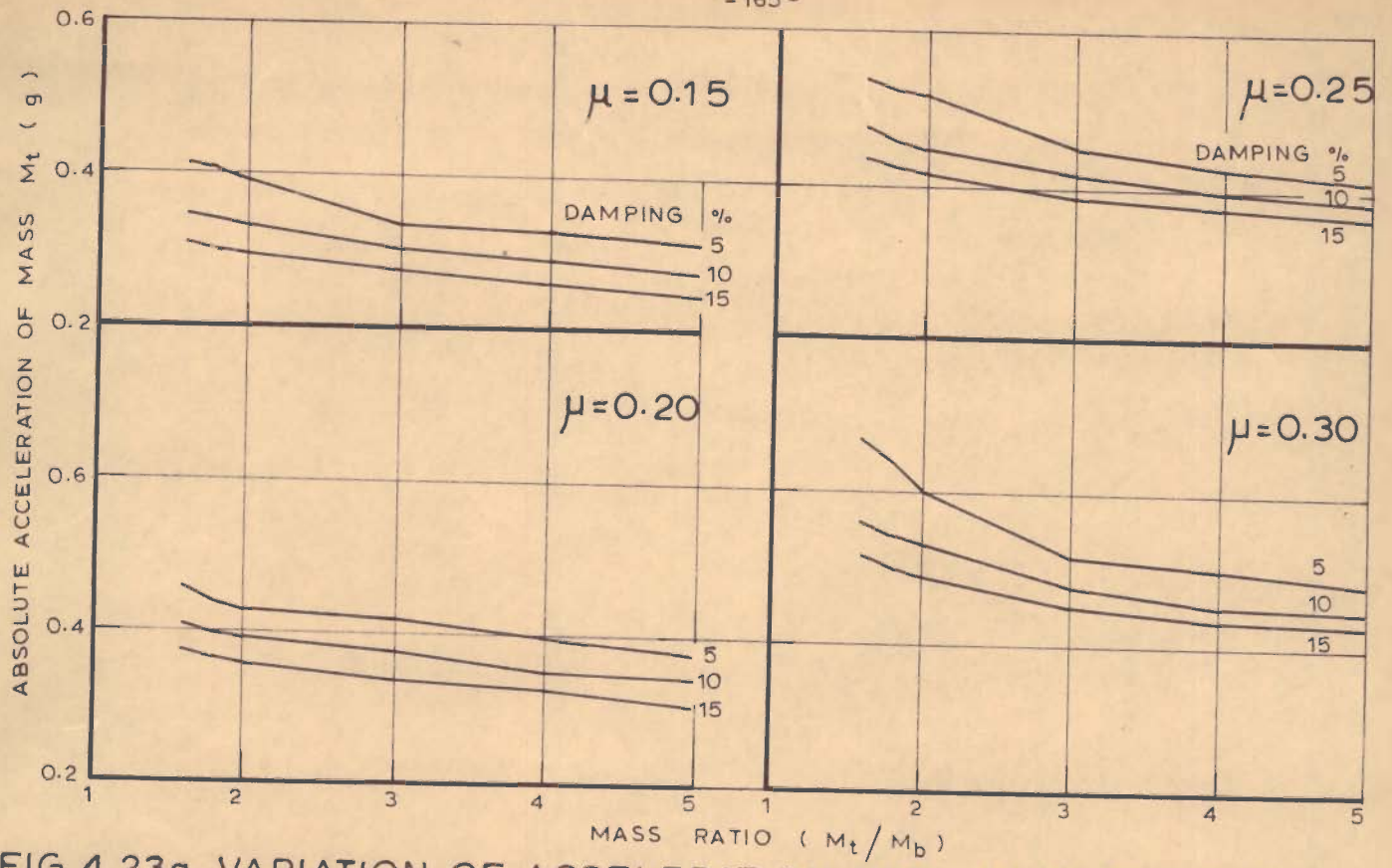

FIG.4.23a_VARIATION OF ACCELERATION WITH MASS RATIO FOR KOYNA SHOCK (T=0·08 sec)

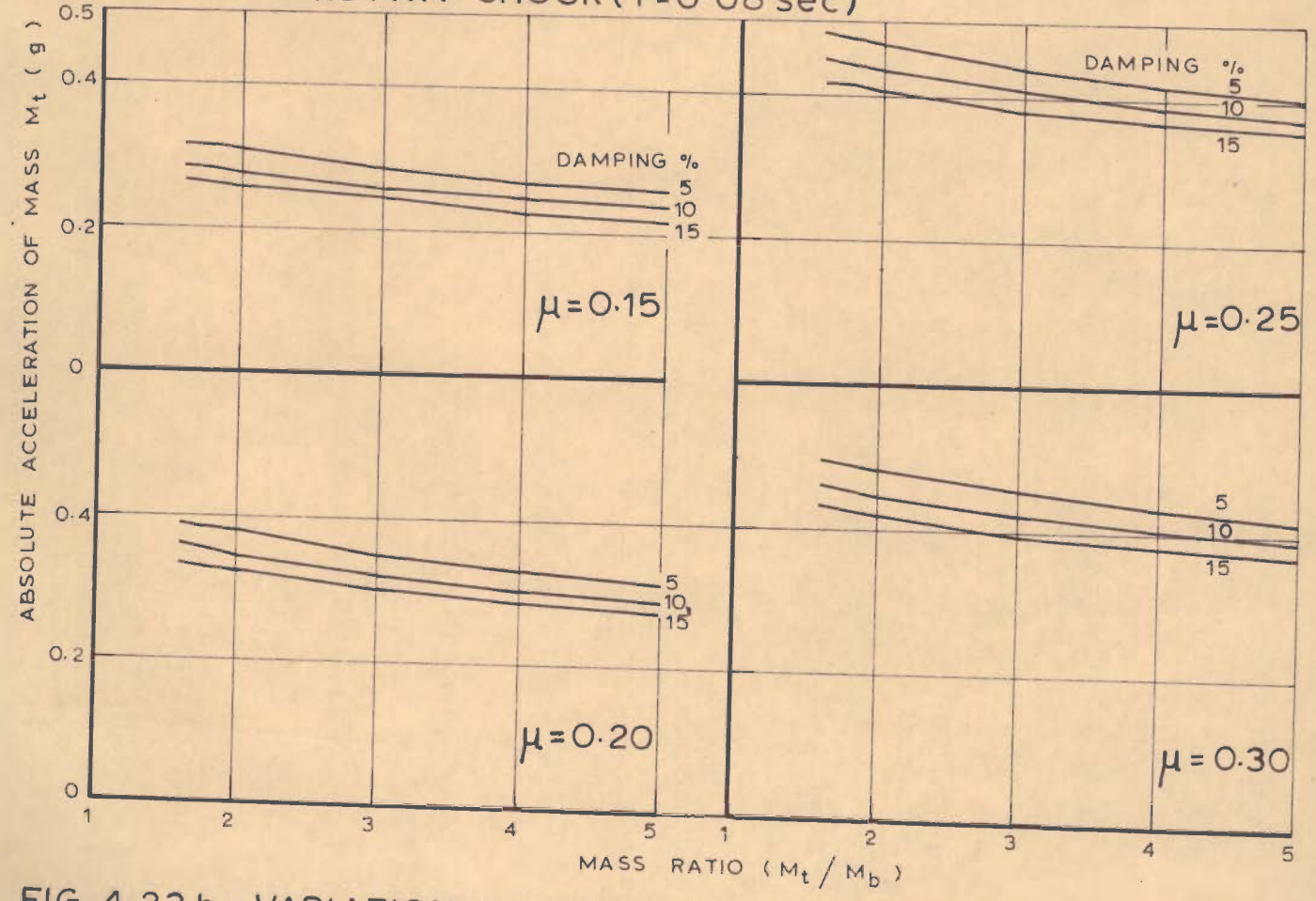

FIG. 4·23 b = VARIATION OF ACCELERATION WITH MASS RATIO FOR EL CENTRO SHOCK (T=0·08 sec)

PHOTO 4.1 – SLIDING TYPE, 1/4 SCALE, MODEL NO.1 WITH BASE FREE TO SLIDE

PHOTO 4.2 – SLIDING TYPE, 1/4 SCALE, MODEL NO. 2 WITH BASE FREE TO SLIDE

PHOTO 4.3 – THE EXPERIMENTAL SET UP

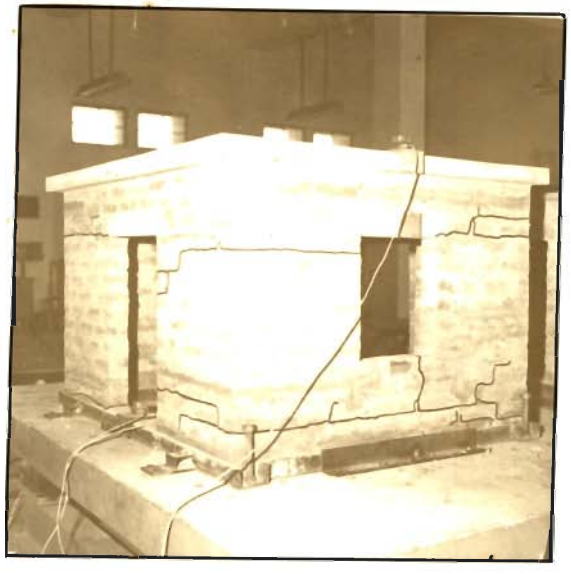

PHOTO 4.4 _ NORTH AND WEST WALLS OF MODEL NO. 1 DAMAGED WITH FIXED BASE

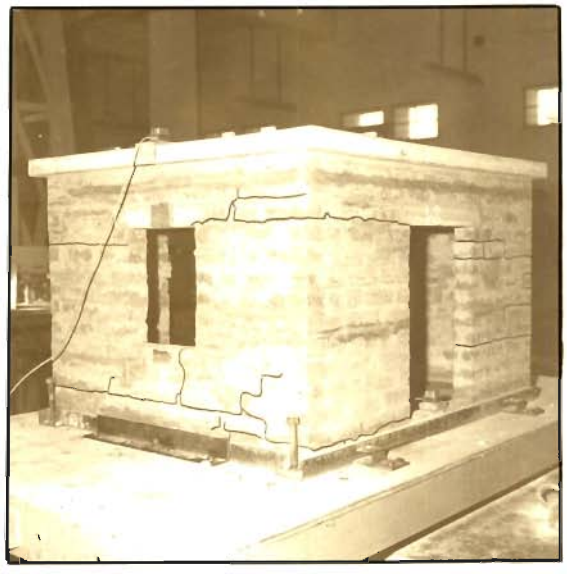

PHOTO 4.5 _ DAMAGE TO SOUTH AND WEST WALLS OF MODEL NO. 1 WITH FIXED BASE

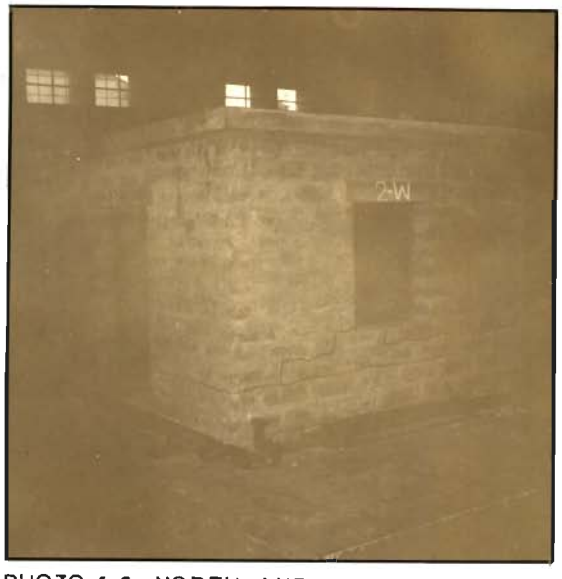

PHOTO 4.6 _ NORTH AND WEST WALLS OF MODEL NO. 2 WITH FIXED BASE CRACKED

PHOTO 4.7 _ SOUTH AND EAST WALLS OF MODEL NO. 2 DAMAGED WITH FIXED BASE

CHAPTER 5

EXPERIMENTAL BEHAVIOUR AND DYNAMIC RESPONSE OF HALF-SCALE BRICK BUILDINGS

5.1 GENERAL

Physical understanding and verification of the actual behaviour of structures subjected to dynamic loading will be best achieved through testing of prototype structures. This should also lead to a realistic formulation of the mathematical model of the system for analytical studies. Such testing, however, involves a number of difficulties due to which it is rarely feasible to adopt it in practice. Therefore, testing of small scale models or small size prototypes is invariably resorted to in order to achieve some of the objectives. Model testing however gives only limited information about prototype behaviour because of the difficulties involved in simulation of various structural and loading parameters. Larger is the size of the models, more realistic are the results expected. In the present investigation also lack of funds as well as testing facilities did not allow testing of full size buildings. But it was possible to adopt half-size models since a large enough shaking platform could be developed. For these tests going upto destruction of the models through large shocks at the base, this facility was built using old railway wagons chassis.

This experimental investigation was undertaken to study the relative competence of conventional as well as sliding type buildings subjected to severe dynamic loads. Qualitative and quantitative analyses have been made to study the experimental behaviour of the models (treated as prototype) under shock loads. Dynamic response of the building models was also computed theoretically for the table motion. Dynamic behaviour of conventional type building has been compared with that of sliding type.

The railway wagon test facility, developed at the Earthquake School, has been briefly described in the following paragraphs.

5.2 RAILWAY WAGON SHAKE TABLE TEST FACILITY

A low cost railway wagon shake table test facility was built for conducting dynamic tests on large size structures upto 20 tonnes weight (Keightley,1977).In the development and fabrication of the facility, the author played an important part. The test facility can be broadly described in the following three parts:

5.2.1 Permanent Way

Figure 5.1 presents a general scheme of the test facility. Firstly, a track was laid before procuring three condemned railway wagon chassis from the Indian Railways. Salwood sleepers were placed at 750 mm spacing

on a well prepared base with about 150 mm thick layer of well graded stone ballast. The track consisting of 40 kg/m rails (three lengths of 12 m each) were spiked to the sleepers at standard Indian broad gauge of 5'-6" (1676 mm) between the inner faces of the rails (Photo 5.1). The rails were cut almost entirely at an interval of four sleepers to form a vertical curve in 8.25 m length of track at both the ends (Fig. 5.1). Marks were painted on one rail at half metre interval as a guide for positioning the wagons before releasing for imparting an impact to the shake table.

5.2.2 Characteristics of the Shake Table

An original wagon chassis (weight about 8.5 tonnes), as received from the Railways is shown in Photo 5.1, which was developed to form a shake table, in plan 7m x 6m (Photo 5.16). Details of the steel added (about 5.7 tonnes) to the wagon chassis so as to fabricate a rigid platform for the shake table is given in Fig. 5.2. Ten helical coil compression springs were mounted around pipe pieces welded on each end of the table to moderate the impact (Photo 5.2). Tests of two springs showed an average stiffness of 137.5 kg/mm each with a maximum capacity of 7.5 tonnes. Maximum acceleration of the table recorded during the testing was 2.45g.

5.2.3 Dead Load Wagons

During testing of a structure built on the shake table, one of the two dead load wagons (loaded with boulders and sand) is allowed to roll down the gentle incline (about 8% grade) giving an impact to the table through the springs, thereby driving it into collision with the second dead load wagon. Thus, the structure constructed on the shake table gets several shocks through the initial impact and then, by subsequent rebounds. The dead load wagons can be drawn up the incline by manually operated portable winch. A wagon release mechanism (Photo 5.3) was fabricated for sudden release of the dead load wagon for rolling down.

A shed 10m long x 13m wide was constructed for the test facility with a 5m headroom above the shake table. On the bottom of one of the roof trusses of the shed, a steel beam was welded to carry a one tonne hoist on a trolley so that the roof slab of a damaged model could be lifted off. The same arrangement was used for placing the slab again on mortar bed on top of another newly constructed model.

5.3 CONSTRUCTION OF BRICK TEST STRUCTURES

Half-scale models of single-storeyed brick structures were constructed using half scale bricks on the shake table for dynamic testing. The outside

dimensions of the structures were 2.17m x 1.75m x 1.60m high above the plinth level with a 7.5 cm reinforced concrete roof slab. Four different types of structures were symmetrically built on the table at a time. The layout plan of such structures is shown in Fig. 5.3 which also shows the position of steel angles, 18 x 18 x 2 mm, welded to the table to act as shear key for the lowest course of foundation bricks laid on a bed of mortar. Experimental investigations were carried out by constructing two sets of four models with different reinforcing arrangements. A brief description of such construction is given in the following paragraphs.

5.3.1 First Set of Brick Structures

Four conventional type brick structure models were constructed with reinforced concrete lintels and cast-in-situ roof slab on the shake table as follows:

Model 1

Built using mud mortar (Fig. 5.4) without any strengthening arrangement.

Model 2

Built in mud mortar and strengthened with a 6mm diameter vertical steel bar set in cement mortar at each corner and at the jambs of the openings (Fig. 5.5). The model was further strengthened by a reinforced concrete lintel band consisting of three steel

bars of 6 mm diameter each. Two brick courses were laid in 1:6 cement-sand mortar at top and bottom of the walls. The reinforced concrete roof slab was cast-in-situ at the top of the walls.

Model 3

Built similar to model 1 but in 1:6 cement-sand mortar (Fig. 5.4).

Model 4

Built using 1:6 cement-sand mortar and strengthened similar to model 2 (Fig. 5.5).

5.3.2 Second Set of Models

Two models each of conventional and sliding type structures were made for the second series of tests as described below:

Model 5

Constructed in mud mortar with superstructure free to slide at the plinth level where a reinforced concrete band was provided. A reinforced concrete bond beam was cast above the plinth band by interposing a thin film of used up mobile oil so that bond may not develop between them (Fig. 5.6). By sliding of the model during its testing, it was confirmed that the contact surfaces were well finished. A lintel band was also provided. In addition, jamb steel consisting of 6 mm diameter bars set in cement mortar was also used on

the sides of the opening.

Model 6

Built similar to model 3 but in addition a reinforced concrete lintel band was also provided (Fig. 5.7).

Model 7

This sliding type structure was made in 1:6 cement-sand mortar. Other provisions in its construction were similar to model 5 (Fig. 5.6).

Model 8

This conventional type model was constructed using 1:6 cement sand mortar with plinth band (Fig. 5.8) in addition to all other strengthening measures as provided in model 4.

Two bricklayers were engaged for the construction of the models. In order to achieve uniform workmanship as far as possible, the same persons were employed and uniform material used throughout the construction programme. Proper curing of the brick structure elements was done by sprinkling water according to the specified norms.

5.4 TESTING PROCEDURE

The method employed for testing the brick models is described in the following paragraphs.

5.4.1 Instrumentation

Acceleration was considered as the most important parameter to be recorded in these studies besides the crack patterns under the action of increasing intensity of base shocks. Acceleration was recorded at important locations of the structures, as shown in Fig. 5.9, with the help of accelerometers and related recording equipment (Photo 5.4). Due to limited number of accelerometers and recording equipment being available the records could not be taken at all the locations at a time. The accelerometer was also fixed to the shake table to record its acceleration. The leads of the accelerometers were connected to the input of the recording equipment (Universal amplifier and pen recorder) to obtain output on recording paper.

5.4.2 Dynamic Loading

As stated earlier, the test structures were subjected to dynamic loads through impact of the dead load wagon with the shake table. Before applying every impact, the shake table was positioned symmetrically in the central region of the track. The first dead load wagon (for example westward wagon as shown in Fig. 5.1) was hauled up the incline by a manually operated winch while the second one (eastward wagon) was placed near the shake table. The wagon release mechanism was then struck by a sledge hammer blow to release the first

wagon instantly. Thus, the released wagon rolled down the slope giving an impact to the table through the springs thereby driving it into collisions with the second wagon which was positioned slightly away from the shake table in a temporarily stationary condition.

Initially, the amplitude of the shock was kept small and was gradually increased in subsequent shocks by further pulling the dead load wagon up the incline. Also, the roles of the two dead load wagons were interchanged so that the main impact occurs from the opposite directions. In this way the structures built on the table got several shock pulses through initial impacts and subsequent rebounds.

5.4.3 Recording of Damage

As stated above the model structures were tested upto ultimate state through gradually increasing shocks imparted to the wagon shake table. After every shock, the damage of the structures, that is, cracking, deformation and displacements were studied and recorded. The cracks developed in the walls were marked by black paint. The shock serial number was also marked along side with cracks so as to differentiate them from subsequent cracks and also to study their progressive widening in the further shocks. The photographs of the damaged structures were also taken for further reference in the study.

The roof slab of any badly damaged test structure was lifted off with the help of the lifting arrangement as described earlier and the walls were demolished. Then, the slab was finally lowered down to rest over the debris so that the same mass distribution on shake table was maintained throughout the testing. The testing of the structures still standing was continued by further increasing the intensity of the shock.

The displacements of the sliding type structures over the plinth band were measured from a reference line marked on the four corners of the plinth band after every shock.

In the first series of testing (models 1 to 4), nineteen main shocks were applied to the test models while in the second one (models 5 to 8) the main shocks were eight.

5.5 OBSERVED BEHAVIOUR OF THE BUILDING MODELS

The behaviour of models and propagation of cracks under increasing intensity of shocks resulting in their progressive failure has been discussed in this section. A criterion is suggested to define "damage level" of the test structure under shock loads. Finally, relative competence of the model structures has been compared and the cost-benifit ratio aspect is also discussed.

Photos 5.5 through 5.8 show the eight building models, constructed on the shake table in two sets of four each. The state as shown is before shock loads were applied to them. For identifying the models and walls, each wall was marked with a number corresponding to the model number and the letter E, W, N or S indicating east, west, north or south. The marking was done at top as well as bottom of each wall. For example, 3-E would refer to the east wall of model 3. In all cases the shocks were applied in the east-west direction. Thus north and south walls acted as shear walls and east and west walls as cross-walls. The cracks, developed in the walls under various shocks, were marked by black paint. The numerals written along side the cracks refer to that particular shock number by which they were caused.

The accelerations recorded at different locations of the models and the shake table are shown in Tables 5.1 and 5.2. The failure of the models that occurred after every shock has been discussed separately for each test structure.

5.5.1 Models of the First Set

Model 1 (Mud mortar, no special strengthening)

(a) No significant cracks were observed in any of the four walls of the model upto shock no. 3 (base acceleration, α_B = 0.40 g). However, some fine invisible cracks might have developed during shock no. 4.

Horizontal cracks developed during shock no. 5 in all the four walls (Photos 5.9 and 5.10) one course below the roof slab. Few vertical and diagonal cracks also developed in the shear walls 1-N and 1-S while vertical cracks were also seen in the cross-walls 1-E and 1-W (Photos 5.9 to 5.11). Overall condition of the shear walls remained satisfactory.

It appears that the vertical cracks near the corners of the walls appeared due to the out-of-plane vibration of the cross-walls behaving as vertical plate in horizontal bending. Also, this may be attributed to the inherent weakness at the corners due to toothed-joint which may finally lead to separation of the adjoining walls.

(b) The previous cracks in the cross-walls got widened considerably during shock no. 6, $\alpha_B = 1.05g$ (Photo 5.12) while in the shear walls, the widening of cracks was to a lesser extent. The cross-wall 1-E deflected inward by as much as 75 mm at top. This wall was badly damaged and deformed as its upper half portion separated from the shear walls and the roof slab due to further opening of the joints at the corners. Fine cracks were also seen at the plinth level of this wall. Though similar behaviour was exhibited by the other cross-wall, yet its damage was less compared to the wall 1-E. The difference in the extent of damage may

be due to the fact that the 1-E cross-wall was exposed to light rains (just before testing) and so the mud mortar in the joints of the wall face lost some of its already low strength thereby prompting the opening of joints.

(c) After shock no. 7, the shear walls were further damaged as width of the old cracks increased and fresh cracks also appeared. The wall 1-N was damaged more than the wall 1-S, as the former would attract larger lateral force due to its greater stiffness. The central portion of the top spandrel of the cross-walls fell down under this shock as shown by Photos 5.13 and 5.14. As explained earlier such behaviour of the cross-walls is attributed to their plate action and lack of shearing strength.

(d) Under shock no. 8, the lower portions of both the piers of the wall 1-S got severe damage and the wall came close to a state of collapse (Photo 5.15). Similar situation was observed for the other shear wall in which the lower spandrel was much damaged. Top spandrel of both the cross-walls had fallen down together with some portions of the piers (Photo 5.16). Thus, the roof slab got freely supported on the top of the two shear walls though their tops had already separated in earlier shocks.

At this stage, it was felt that the next shock might bring down the shear walls and the roof thereby

causing damage to its roof slab and the remaining three models which were in a better condition. Therefore, the roof slab was lifted off using the arrangement meant for this purpose (Photo 5.17) and the remaining portion of the walls were demolished and finally the roof slab was lowered down to rest on the debris. This was essentially required as the weight on the shake table was intended to be kept constant throughout the testing of the models.

Due to absence of horizontal bending strength of this unstrengthened model during its plate-action and lack of bond with the perpendicular walls, the cross-walls were separated from the shear walls. Diagonal tension failure was also observed in the shear walls as discussed above. If this model were strengthened by a lintel band alround, the separation of the cross-walls at the corners could have been checked.

Model 2 (Mud mortar, lintel band, vertical steel at corners and jambs)

(a) No damage was exhibited in any of the walls upto shock no. 5, that is, $\alpha_B = 0.57g$. Since, this structure was strengthened against lateral forces, its performance to resist such forces had considerably improved.

(b) Diagonal cracks developed in the piers of the shear walls (Photos 5.18 and 5.19) while a vertical crack was seen near the left corner of the wall

2-S (Photo 5.19) under shock no. 6 ($\alpha_B = 1.05\,g$). The spandrels of the walls were free from cracks. The cross-walls also remained undamaged after this shock. The cracking of the shear walls was mainly on account of shear failure.

(c) During shock no. 7, the old cracks opened up and few diagonal cracks appeared in wall 2-N (Photo 5.20) while vertical and diagonal cracks were observed in the west pier of wall 2-S as shown in Photo 5.21 but the east pier of this wall was free from any noticeable cracks (Photo 5.22). It is significant to note that top spandrels remained uncracked except in 2-E wall (Photo 5.23). It appears that the lintel band did not allow the cracks in the piers to propagate in the top spandrel. Comparatively, the cross-walls developed less cracks, a definite contribution of the lintel band to the horizontal bending strength of the wall.

In fact, the localized zones of the model in which the reinforcements were provided in cement-sand mortar remained uncracked whereas the cracks appeared mainly in the portion of the walls built in mud mortar where it had almost nil tensile and shear strength. It seems that the provision of lintel band and reinforcements at the critical locations transformed the behaviour of the structure completely as compared to the unstrengthened model 1.

(d) Some new diagonal cracks developed in the shear walls (Photos 5.20 to 5.22) during shock no. 8. Some horizontal cracks were observed in the top spandrel of the shear wall 2-N (Photo 5.20) and 2-S (Photo 5.23) and the cross-wall 2-E (Photo 5.23). The south-east bottom corner cracked in a localized zone (Photo 5.22) as also the south-west bottom corner (Photo 5.21) which had separated one course above the table base and shifted slightly outwards. Diagonal and vertical cracks as developed in the wall 2-W are shown in Photo 5.21. The old cracks widened further. The mechanism of failure has been discussed at a later stage.

(e) Under shock no. 9 (α_B = 1.24g), the earlier cracks got further opened up considerably. The bottom portion of the south-west corner was pushed outwards by about 50 mm (Photo 5.24 and 5.25) by this shock. Also the bottom portion of the south-east corner (Photo 5.25) and that of north-west corner (Photo 5.26) shifted outward. All the walls were significantly damaged under this shock.

(f) The cracks developed in subsequent shocks after shock no. 9 were not marked on all the walls because mostly the old cracks got increasingly widened and a few new cracks also appreared. After these shocks, the south-east and south-west corners were heavily damaged resulting in big gaps (Photo 5.24) between the separated portions

as the corners moved outwards diagonally. The failure in this fashion may be attributed to their parasitic weakness as vertical reinforcement at the corners were initially omitted from models 2 and 4 during their construction due to an oversight. The already set foundation had to be broken at these locations for inserting the vertical steel and then relaid.

One of the reasons for experiencing heavy localized damage at the corners of more rigid shear wall 2-S appears to be that the base shear attracted by it was larger which coupled with overturning tension cracked the corner and led to wide gaps and relative movement. During subsequent shocks, the lower ends of the corners displaced outward diagonally while the reinforced corner remained rigid and uncracked upto the lintel band where the whole corner block of masonry was broken.

(g) During the shock numbers 12 to 14 (α_B = 1.30g), the gaps between the separated portions at the four corners were widened very much (Photos 5.26 through 5.29). All the walls were badly damaged but did not fall down like what happened in model 1. The south-east and south-west corners in the foundation region were so much damaged and separated (about 240 mm) from rest of the walls that they may be considered as separate structural element (Photos 5.28 and 5.29) such as column with hinge at lintel band level which could not share the lateral forces. The top

spandrels of the walls were not much damaged except in the last shock in which the half top spandrel portion fell down and so the vertical corner steel could be seen clearly (Photo 5.30).

After this shock, the shear wall 2-S was so heavily damaged compared to the other shear wall that its mechanism of failure became too complex. It was apparent that due to high rigidity of the wall, it attracted greater lateral force and in turn got damaged heavily.

It was believed that the next shock would collapse the whole structure as the condition of the walls 2-S and 2-W was very bad. Therefore, the roof slab was lifted off as in case of model 1 and then the walls were demolished and finally the roof slab was gently placed over the debris.

Model 3 (Cement mortar, no reinforcing)

It was noted after the construction of this model that all the four walls had developed cracks at different localized locations as shown in Photos 5.31 through 5.34. Some of these initial cracks were marked by white paint. The reasons for the initial cracks may be due to expansion and contraction of the shake table base as the welding work below the table base was also going on simultaneously with construction of models 3 and 4 for its further strengthening.

(a) Upto shock no. 5 (α_B = 0.57g), no damage was observed in this model. After shock no. 6 (α_B= 1.05g) it was observed that a horizontal crack developed alround at the junction of the walls with the foundation. Horizontal and diagonal cracks also developed at different locations of the walls as shown in Photos 5.35 to 5.37. A very slight sliding of the superstructure was also noticed at the plinth level.

It is believed that the walls of this structure were not fully bonded with the foundation at the plinth level due to poor workmanship, though the same bricklayers were employed throughout the construction of the test structures. On account of this fault, the model behaved as if there was a discontinuity at the plinth level alround in effect permitting sliding of the superstructure. In doing so, some of the input energy of the shock might have been dissipated thereby restricting the development of more cracks particularly in the piers of the shear walls.

(b) During shock no. 7, east bottom edge of the structure at the plinth level was observed as lifting up momentarily due to overturning effect of the lateral force as the shock was applied from west direction. Sliding of the superstructure was also observed with the help of marking (not visible in the photographs) left by it at the plinth level. Predominantly the horizontal

cracks developed in the walls in addition to some diagonal and vertical cracks (Photos 5.37 to 5.39). The shear wall 3-S got cracked more than the other one due to its larger stiffness. The cross-wall 3-W developed more cracks whereas wall 3-E cracked less.

It is obvious that the coefficient of friction between the different sliding surfaces of the model must have been non-uniform. As such this non-uniformity of the frictional coefficient might be more in wall 3-W and so greater resistance to sliding under wall 3-W might have resulted in more cracking due to its shear and diagonal tension. This cross-wall was thus divided into separate blocks held together by friction which could separate out in subsequent shocks.

(c) The shear-and cross-walls developed further horizontal cracks and less vertical and diagonal cracks after shock no. 8 (Photos 5.40 to 5.43). One significant vertical crack was observed near the south-west corner of the shear wall 3-S originating from the plinth level and extending upto the roof slab (Photo 5.41). West portion of the top spandrel shifted inward by about 5mm whereas at the west edge of the lintel, a gap of about 40mm was created (Photo 5.42). This damage may be due to the tendency of different blocks of the wall to move independently. The condition of the shear wall 3-N was better than that of the comparatively stiffer wall 3-S.

(d) In shock no. 9 (α_B = 1.24 g) the west pier of the shear wall 3-N was separated from rest of the wall and slide outward by about 70 mm (Photo 5.44). The piers remained uncracked. The other shear wall was further damaged under this shock by opening up of the old cracks very significantly. The cross-walls were in bad shape (Photo 5.45) as the previous cracks got very much widened. Thus, the structure was badly damaged during this shock.

(e) Major part of the top spandrel and left pier of the cross-wall 3-W (Photos 5.46 and 5.47) fell down under shock no. 10. A large chunk of masonry separated from the north-west corner (Photo 5.47). The east and west piers of the shear wall 3-N were pushed inward causing distortion of the window opening (Photo 5.47). The shear wall 3-S was very much damaged unlike 3-N. The lintel of the wall 3-S came down as the bottom of south-east corner moved eastward (Photo 5.46). After this shock, the model structure was nearing collapse. Therefore, its roof slab was lifted off and the portions of the wall were then demolished for placing the roof slab over it.

It is important to point out that the piers of the shear walls remained uncracked upto the state of collapse of the test structure. But, in contrast, their top and bottom spandrels continued to crack under subsequent shocks. Sliding of the superstructure was also

observed during every shock. The walls broke into large chunks and the portions near the plinth level shifted unequally under the shock. Although the alround crack at the plinth level of the model provided a sliding foundation for the superstructure so that it slide when the table base had shaken, yet on account of uneven friction along the crack surfaces, the base shear was concentrated at few points under subsequent impacts leading to local failures thereby dividing the walls into different separate blocks. From this observation of the behaviour of this model it could be inferred that a uniform and low coefficient of friction between the sliding surfaces may be useful for better performance under seismic loads.

Model 4 (Cement mortar, lintel band, vertical steel at corners and jambs)

In this model also, some initial cracks (marked in white paint) in the walls had developed before its testing started.

(a) No damage was observed in the model upto shock no. 6 (α_B = 1.05 g). During shock no.7 also, shear wall 4-N and the cross-wall 4-E did not show any cracks whereas the other shear and cross-walls developed few fine horizontal cracks (Photos 5.48 and 5.49). New cracks appeared in all the walls by shock no. 8. The cracks were mostly horizontal while a few were diagonal

also (Photos 5.48 through 5.51). Horizontal cracks appeared near the top and bottom of the corners. The possible reason for horizontal cracks near corners of the structure may be the overturning effect of the shock load. After rebound of the shake table with the second dead load wagon, the overturning effect would reverse and hence the opposite corners were also cracked. The vertical reinforcement provided at the corners seems to have been effective in restraining the opening of cracks since they were fine and of minor nature upto this shock.

(b) During shock no. 9 (α_B = 1.24 g), new cracks developed in all the walls which were mainly horizontal. A diagonal crack between the bottom west edge of the window and near the bottom of north-west corner developed in shear wall 4-N (Photo 5.51). Walls 4-S and 4-E did not show any distress under this shock also except a few horizontal crack of small length (Photos 5.52 and 5.53). Horizontal and vertical cracks developed in cross-wall 4-W (Photo 5.51). After shock no. 10, a few horizontal cracks were observed in cross-wall 4-W (Photo 5.51) while no crack was visible in wall 4-E (Photo 5.52). Significant horizontal and diagonal cracks were seen in the top spandrel of shear wall 4-S (Photos 5.53 and 5.54) whereas a few horizontal cracks appeared in the top and bottom spandrel of wall 4-N (Photo 5.55). Upto this shock, most of the cracks

remained horizontal having very small crack opening. The horizontal cracks were well distributed in all the walls. The effectiveness of the steel reinforcement provided at the vulnerable locations was clearly seen since the existing cracks did not widen under repeated and increasing shocks. This is in sharp contract to the behaviour observed in the unstrengthened model .3 discussed before.

(c) During shock nos. 11 and 12, additional fine horizontal cracks were seen well distributed on all the walls of the model as marked in Photos 5.53 to 5.57. Additional diagonal cracks were also observed in the left region of bottom spandrel of shear wall 4-N (Photo 5.55) under shock no. 11. This shear wall cracked more than the other walls due to its larger stiffness. Upto this shock, the crack widths were small and the overall condition of the model was not bad.

(d) After shock no. 13 (α_B = 1.26g) a few more minor cracks of small length were observed in both shear walls (Photos 5.58 and 5.59). It is significant to note that the piers of the shear walls remained practically uncracked (unlike the usual cross-pattern cracks) barring a few fine cracks of small length. This may be attributed to the presence of steel reinforcement at the critical locations. Comparatively, the cross-walls exhibited more cracks which were generally horizontal perhaps due to vertical bending of walls as plate

combined with overturning tension. The previous cracks were not widened much even under this shock.

(c) Under shock no. 14 (α_B = 1.30 g) the shear walls got greater damage than the cross-walls (Photos 5.56 and 5.57). The top spandrel, foundation and bottom region of the piers of shear wall 4-S exhibited many horizontal cracks and a few vertical and diagonal cracks (Photo 5.59). The other shear wall was also similarly damaged with even more cracks (Photo 5.64). The bottom of north-east and north-west corners were damaged more (Photos 5.58 and 5.60). This may be due to the fact that shear wall 4-N must have taken larger base shear, as it was stiffer than wall 4-S. At this stage of shock loading, the number of cracks had increased greatly in the test structure but width of the cracks was still small. It appears that under this shock, the flexural strength contributed by the vertical steel exceeded the shear strength of the shear walls.

(f) Shock no. 15 (α_B = 1.85g) was considerably larger than shock no. 14. Under this shock, the bottom of north-east and north-west corners (Photos 5.58 and 5.60) was shifted slightly outward as local failure occurred at these locations while very few cracks of small length were observed in shear wall 4-S (Photo 5.59). A diagonal crack (Photo 5.58) and few horizontal cracks

(Photo 5.64) developed in cross-wall 4-E. Many diagonal and vertical cracks appeared in the portion below the lintel-band of the cross-wall 4-W (Photo 5.65). The initial cracks (previously marked by white paint), which developed before testing of this test structure, had opened up in this shock (Photo 5.65).

The existing cracks widened further under this shock and new vertical and diagonal cracks also developed. The foundation masonry of the structure got damaged more than its other parts. It seems that perhaps the cold joints (as discussed earlier in the case of model 2) had reduced the foundation strength at the corners.

(g) Major damage of the structure occurred during the next shock no. 16, almost equal in intensity to no.15. The old cracks in the foundation region got widened very much. The bottom regions of the north-east and north-west corners were greatly damaged and shifted outward by about 20 mm (Photos 5.61 and 5.62) whereas shear wall 4-S exhibited some cracks in the bottom region of both its piers (Photo 5.63). The north-east corner portion of wall 4-E began to separate out from rest of the wall (Photo 5.61). The right portion of cross-wall 4-W between the plinth and window sill levels shifted outwards by about 15 mm (Photo 5.66). The walls 4-N and 4-W got cracked more than the other walls indicating presence of torsion due to unequal stiffness and earlier cracking of shear walls.

(h) Seeing the structure after the next shock no. 17, it appeared that it had lost its capacity to resist further shocks. The portions of the walls, which were heavily damaged before applying this shock, came in extremely bad shape after this shock. In particular, the north-east and north-west corners showed severe damage (Photos 5.64 and 5.67) almost to the state of collapse. The north-west corner portion developed into a wedge with its apex in this corner at the lintel band level (Photo 5.64). The north-east and north-west corners were pushed outward during this shock by about 80 mm and 40 mm respectively. Thus, the shear wall 4-N had almost lost its strength. The overall condition of the shear wall 4-S was however, not so bad. The bottom portion of south-west corner, which shifted outward, had very wide cracks (Photo 5.68). A portion between the plinth and window sill level of the cross-wall 4-W was shifted towards south (Photo 5.69). At this stage all the faces of the structure were full of wide cracks and some portions of the wall were nearing collapse. Yet the overall collapse or large scale falling of walls looked to be still far away.

Under the action of the last two shocks (α_B = 1.60gand 1.95g) shear wall 4-S got damaged further as more vertical and diagonal cracks developed (Photo 5.68). The bottom portions of south-east and south-west corners

slightly shifted outward. The cross-wall 4-E was in a better shape than the other in which different damaged portions shifted bodily creating wide gaps in between them (Photos 5.70 and 5.71). Under shock no. 19, the shear wall 4-N was at the verge of collapse. The north-east and north-west corners (Photos 5.70 and 5.71) shifted outwards diagonally by about 150 mm during the last shock.

It is significant to point out that upto the last shock, although the top spandrels of the walls were badly damaged yet they were not at the verge of collapse as was exhibited by the portion of the structure below the lintel band. From this model behaviour, it becomes quite clear that the portion of brick walls bounded by steel reinforcement, such as the top spandrels, tended to remain intact with only fine cracking. Flexural bending behavior of unreinforced model 3 was changed here to diagonal tension failure under much higher shocks.

5.5.2 Models of The Second Set

The second set also consisted of four model structures which were described in Section 5.3.2. As stated before, two of these were made with sliding arrangement at plinth level. Their behaviour as observed under the action of increasing shock loads is described below.

Model 5 (Mud mortar, sliding at plinth level, lintel and plinth bands and bond beam)

(a) The first shock was not too severe, the base acceleration α_B being 0.51g. Under this shock all the piers of the shear walls 5-N (Photos 5.72 and 5.73) and 5-S (Photo 5.74) showed fine diagonal cracks. The superstructure was observed to slide at the plinth level under the very first shock. The coefficient of friction at the surface was found by measurement later. Its value was 0.50. Since the acceleration was more than the coefficient of friction, the sliding motion should have occurred as it did. However, the actual movement was seen to be of unequal amount at the four corners. It was 6 mm towards west at the north east corner and 10 mm westward at the south-east corner. Photo 5.75 shows the movement by a black strip of small width at the plinth level as it was under wall 5-E. No sliding was observed at the south-west corner. It seems that due to faulty construction, the bond beam got bonded with the plinth band in this region thereby preventing sliding of the model there. The piers of the shear walls got cracked due to diagonal tension.

(b) The second shock inadvertently became too severe, the base acceleration becoming 2.15g. It changed the picture of all the models abruptly. In this model, the whole north-west corner between lintel band and bond beam shifted out westward by 15 mm whereas no sliding was noticed at the north-east corner. The old cracks opened

wide (5 to 20 mm) and many new diagonal and vertical cracks appeared in all the walls (Photos 5.77 to 5.80). A horizontal crack also developed alround the walls one-brick-course below the roof slab, that is in the mud bedding plane.

The shear wall 5-S was badly damaged under this severe shock. Both the piers of this wall were resting at the plinth band separately and connected only through the lintel band. These piers showed as if they slide independently under this shock behaving as cantilevers. The direction of the diagonal cracks was seen to be opposite in the two piers (Photo 5.77). Their sliding was towards each other by 10 mm and 65 mm and their jambs lifted up vertically by about 15 mm. This peculiar behaviour of the piers occurred since their strength in diagonal tension was less than the frictional resistance. Under the shock from west to east, the west pier lifted up and slide easily but the east pier was compressed at the corner, moved little and got cracked diagonally. In the rebound, the opposite happened. Thus finally they appear closed-in and cracked diagonally in opposite direction.

The north-east corner got badly damaged between the lintel band and bond beam (Photo 5.76). A portion of the right pier of wall 5-N between the lintel band and sill, separated out completely from rest of the wall

as seen in Photo 5.78 which also shows beautiful star cracks. The condition of the cross-walls was better than that of the shear walls.

(c) After the accidental severe shock no.2, the shocks were kept milder and increased gradually. Under shock no. 3 (α_B = 0.53 g) no new cracks appeared. In shock no. 4 (α_B = 0.66g), a fine crack of small length developed in the left corner of top spandrel of cross wall 5-W (Photo 5.80). The sliding of the superstructure occurred as seen in Photo 5.82. The cross-wall 5-E (Photo 5.82) developed a few new cracks while the existing cracks got opened up a lot. The north-east corner came to a very bad state. The north-west corner slid towards west by 18 mm. The old cracks of the shear wall 5-S (Photo 5.81) widened significantly together with new vertical cracks at the south-east corner which showed that separation of the wall 5-E had been initiated by this shock.

(d) In order to check further closing-in of the piers of wall 5-S a strut was inserted in the door opening close to the plinth band (Photo 5.83). After shock no. 5 was applied (α_B 0.58g) the bottom of the piers which were lifted up during the shaking, dropped flat over the plinth band (Photo 5.83). It appears therefore that the bonding member should go across door openings as well, so as to avoid separate cantilever

behaviour of the piers.

Photos 5.83 to 5.87 show the severe state of damage of the model after this shock , the shear wall 5-N collapsed and 5-S on the verge of falling down. The cross wall 5-W was in a better condition as the existing cracks did not widen much (Photo 5.84). This may be due to a relatively better sliding behaviour exhibited by this wall compared to the other one. The south-east corner portion between the lintel band and plinth band buldged out towards east (Photo 5.86) whereas the upper part of the north-east corner fell down completely (Photo 5.85). Major portion of the shear wall 5-N collapsed during this shock (Photo 5.87). The top spandrel and the north-west corner together with some part of the right pier fell down totally. As it was feared that the next shock would collapse the test structure, the roof slab was lifted off and the remaining walls were demolished and finally the roof slab was placed over the remains.

The purpose of observing the sliding behaviour, for which this model was constructed, could not be fulfilled fully on account of bonding which occurred in a particular region where sliding could not take place. Nevertheless, this test structure performed well under a recorded base acceleration of 2.15g.

Model 6 (Cement mortar, lintel band)

(a) No damage was observed in this structure under shock no. 1 (α_B = 0.51 g). However during shock no. 2 (α_B = 2.15 g) all the walls of the test structure got badly damaged, some cracks having quite significant width. The shear wall 6-N having door opening developed well distributed horizontal cracks (Photo 5.88). The bottom region of both its piers developed some vertical and diagonal cracks as well breaking them into separate blocks (Photo 5.89). The bottom few courses of the left pier had relative movements as well under this severe shock due to shear failure of the piers. The north-east and north-west bottom corners developed some wide cracks due to local diagonal tension failure. Extensive horizontal and diagonal cracks were observed in the cross-wall 6-E (Photo 5.90). Most of these cracks were extended from the adjoining walls. The cross wall 6-W was badly damaged during this shock. Its right pier was broken into two parts and shifted inside by about 18 mm (Photos 5.92 and 5.93). The bottom portion of the north-west corner together with some portion of the bottom spandrel of wall 6-N shifted inward by about 40 mm (Photo 5.91). The damage of the wall was predominantly due to shear failure. Mainly horizontal cracks and few vertical and diagonal cracks were exhibited by this shock in the shear-wall 6-S (Photo 5.93).

(b) Since shock no. 3 was much milder no new cracks developed. Under shock no. 4, the shear wall 6-N was further damaged by developing mainly horizontal cracks and a few vertical cracks as marked by 4 in the Photo 5.94 (this photograph was taken after shock no. 5 in which the badly damaged and broken parts of this wall are shown). The existing cracks opened during shock no.4. In wall 6-S, a vertical crack opening of about 50 mm was observed at the south-west corner, which ended into a wide horizontal crack about 150 mm below the lintel band (Photo 5.95).

A few diagonal cracks were observed in the cross-wall 6-E (Photo 5.98 which was taken after shock no.5) while in the wall 6-W, the north-west and south-west corner portions between the lintel band and plinth level were very badly damaged and bulged out to the state of collapse (Photo 5.96). Horizontal and a few vertical and diagonal cracks were also observed in the wall 6-W. Upto this shock, mainly the portions of the walls below the lintel band were badly damaged due to predominantly bond failure whereas the top spandrels were less damaged and were not in bad shape. This may be due to the effectiveness of providing lintel band as a strengthening measure.

(c) Under shock no. 5 ($\alpha_B > 0.58g$) the bottom portions of both the piers of shear wall 6-N were so much damaged that they reached the state of collapse

(Photo 5.94). The bottom portion of the left pier had fallen down and the wall had broken into many separate blocks. The wall 6-S was also divided into large chunks which moved from their position (Photo 5.97). The cross-wall 6-E was also separated into different blocks (Photo 5.98). The old cracks widened considerably and both the piers got deshaped by shifting of the different blocks. The wall 6-W exhibited worst damage. The different blocks were separated and displaced from their previous positions bringing the wall to dangerous position. The north-west and south-west corners were in a very critical state. The bottom spandrel of this wall bulged out under this shock (Photo 5.99).

After shock no. 5, since the model was severely damaged (more than the sliding base model no. 5), it was demolished as usual and the roof slab placed on the debris.

Model 7 (Cement mortal, sliding at plinth level, lintel and plinth bands and bond beam)

Two reference lines were marked by white paint on the vertical faces of the plinth band (Photo 5.101) at the four corners so as to measure the amount of sliding of the superstructure under various shocks as discussed in the following paragraphs.

(a) Under the very first shock (α_B = 0.51 g) the superstructure of the model slid towards west by 4.5 mm

but no damage occurred to the building. After the accidental severe shock no. 2, some did occur along with larger amount of sliding. A few fine horizontal cracks developed in shear wall 7-N (Photo 5.100) and two diagonal cracks occurred in the bottom spandrel of shear wall 7-S (Photo 5.101). The cracks in the cross-wall 7-E were diagonal (Photo 5.102) while in the wall 7-W, a fine horizontal crack developed in the top spandrel only (crack marked by 2 in Photo 5.103).

The superstructure slide towards west by 10 mm (a black strip of small width is seen in Photo 5.102 at the plinth band after sliding of the wall 7-E towards west). Thus the structure performed excellently due to its sliding behaviour even under the large table acceleration of 2.15g and stood it with only few minor cracks. Under the shock, the acceleration recorded at its roof top was only 0.19g. Therefore, it may be concluded that on account of sliding, the superstructure had attracted less lateral force due to the isolation. Also some input energy must have dissipated during the sliding movement.

(b) The shock no. 3 was much less intense and no damage or sliding were noticed. In the next shock (no.4) however some horizontal and diagonal cracks were observed in wall 7-E (see marking 4 on Photo 5.107). The superstructure shifted bodily towards east by 8mm. The overall condition of the model was good upto this shock but

started deteriorating under the subsequent shocks.

(c) After shock no. 5 a diagonal crack and a horizontal crack were observed in shear wall 7-N above as well as below the lintel band. The bottom edges of both its piers, lifted up behaved as cantilevers and closed in, resulting in the inner edges lifted off by an amount of about 5 mm (Photo 5.104). This behaviour is similar to that seen in mud mortar sliding structure. No damage was observed in shear wall 7-S (Photo 5.106) in this shock but many fresh horizontal and diagonal cracks appeared in both the cross-walls (Photo 5.103 and 5.107).

During this shock, the superstructure shifted significantly. This shift was 77 mm, 68 mm, 80 mm and 75 mm at north-east, north-west, south-east and south-west corners respectively. The small difference in the values of shift may be attributed partly to the closing in of the piers in shear wall 7-N and partly to the non-uniform distribution of stiffness in the two shear walls. The large shift resulted in overhanging of walls 7-W and 7-E beyond the plinth band by about 50 mm (Photos 5.104 and 5.105).

(d) Shock no. 6 (α_B = 1.08g) was applied from east to west in opposite direction to shock no. 5 and it resulted in two rebounds too from west to east and then from east to west. As a result of this shock and

the rebounds, many horizontal and a few vertical cracks of small length were caused in the south shear wall but both the piers remained free from cracks (Photo 5.106). More well distributed cracks developed in cross-wall 7-E most of which were horizontal and a few vertical or diagonal (Photo 5.107). A few fresh horizontal, vertical and diagonal cracks were also observed in wall 7-W and 7-N (Photos 5.108 and 5.109).

During this shock the superstructure shifted back to rest fully on the plinth. The amount of sliding measured was 40 mm, 30 mm, 50 mm and 55 mm at north-east, north-west, south-east and south-west corners respectively. It seems that due to overturning effect of the superstructure, the edge of the plinth band on the west side was seen to be crushed. This appears to be due to overturning compression.

(e) Shock no. 7 was again very severe with α_B = 2.36 g. An almost equal rebound was allowed in this case by keeping the opposite weighted-wagon close to the shake table. As a result the superstructure was seen to shift both ways and finally occupying approximately the same position as before the shock.

Additional vertical cracks of small length were caused in shear wall 7-N (Photo 5.109) under this shock whereas a vertical crack and many horizontal cracks were developed in the shear wall 7-S (Photo 5.110).

Still the condition of both the shear walls was not too bad after this shock. But the cross-walls got more worse cracked. Many new cracks appeared in this shock (Photo 5.111) and the old cracks widened. The left pier of the wall 7-E separated into two portions (Photo 5.112). The westward sliding of this wall is shown by Photo 5.112. There was significant damage of the westward plinth band in which an exposed steel bar could be seen (Photo 5.116). Under this shock, a few bricks, in the foundation of the west wall in the south end region were cracked and broken.

(f) Before the next shock was applied one wooden plank was inserted in the door opening as a strut near the plinth band. Shock no. 8 was the most severe with α_B = 2.45g. Many wide cracks appreared in the shear wall 7-N under this shock (Photo 5.113). The existing cracks widened thereby dividing the wall into different blocks. A few bricks were also broken in the left pier of this shear wall. Many cracks developed in the top and bottom spandrels whereas some cracks were seen in both the piers (Photo 5.114). The right pier was separated from the right portion of the bottom spandrel by a wide open crack. This upper portion had shifted outwards (Photo 5.114). The left pier of the wall 7-S was also separated from the bottom spandrel.

The cross-wall 7-E got very badly damaged as many new cracks developed and the existing ones opened

up, thus dividing the wall into separate blocks (Photo 5.119). The portions (1) and (2), as marked on Photo 5.119, shifted towards east by about 40 mm and 25 mm respectively. The upper portion of the left pier was thrown out during this shock (Photo 5.115). The cross-wall 7-W exhibited many new cracks (Photo 5.116) but was less damaged than the other cross-wall. Due to wide opening of the previous cracks, the wall below the lintel band was divided into several blocks. The upper part of the right pier was displaced outwards by about 20 mm (Photo 5.118). The foundation under the wall 7-W was also very badly damaged (Photo 5.117).

The superstructure got shifted towards west by this shock. The shift measured at the north-east, north-west, south-east and south-west corners was 75 mm, 52 mm, 58 mm and 60 mm respectively. It was felt that under next shock, the east and south walls would collapse completely and therefore testing was abandoned.

Model 8 (Cement mortar, lintel and plinth bands and vertical steel at corners and jambs)

(a) Under shock no. 1, no cracks appeared in any of the walls. Under the severe shock no. 2 (α_B = 2.15g) a horizontal crack occurred at the junction of the shear wall 8-S with the plinth band which extended into the adjoining walls (Photo 5.120). A horizontal turned diagonal crack was also seen in the top spandrel of this

wall. Horizontal cracks were observed near the junction of the wall 8-N (Photo 5.121) and 8-W (Photo 5.125) with the plinth band and also at the junction of the wall 8-E with the plinth band (Photo 5.124). In other words, the model got cracked alround at/near the junction of the walls with the plinth band.

(b) As the next shock had feeble intensity, no damage occurred. In shock no. 4 (α_B = 0.66g), wall 8-N (Photo 5.122) and 8-E (Photo 5.122) witnessed a few fine cracks while the other walls suffered no damage.

(c) In shock no. 5 ($\alpha_B \geq$ 0.58g) the lower spandrel of the shear wall 8-N (Photo 5.122) exhibited a few horizontal, vertical and diagonal cracks. Wider cracks developed in the bottom region of the north-west corner. Many cracks were seen in the top spandrel of wall 8-S (Photo 5.123) and bottom of its left pier was also damaged. The cross-wall 8-E remained almost undamaged except at the bottom of north-east corner (Photo 5.124). In the west wall, a significant vertical crack was observed near the north-west corner and a horizontal crack of small length occurred at the junction of the south-west corner with the plinth band (Photo 5.125).

(d) Under shock no. 6 (α_B = 1.08g) mainly horizontal cracks occurred in the top and bottom spandrels of the shear wall 8-N (Photo 5.122). The bottom portion of the north-west corner was further damaged. A vertical

crack was seen at the bottom region of south-west corner and a horizontal crack at the top of the left pier of the wall 8-S (Photo 5.123). Vertical and horizontal cracks developed in both the cross-walls (Photos 5.124 and 5.125).

The bottom regions of all the four corners were significantly damaged during this shock.

(e) Under the severe shock no. 7 (α_B = 2.36g) top spandrels of both the shear walls were heavily damaged in which most of the cracks were horizontal and a few diagonal (Photos 5.126 and 5.128). Strangely, the lintel band cracked in both the shear walls near the corner of the openings but the window piers were free from cracks. The bottom spandrel of wall 8-N developed many cracks. The bottom region of the north-east and north-west corners were badly damaged (Photo 5.127) and old cracks of the wall 8-N opened up by as much as 5 mm to 10 mm. The top spandrels of both the cross-walls got damaged in similar fashion. Also similar heavy damage was observed in the left pier of 8-W (Photo 5.129) and right pier of 8-E (Photo 5.130).

The region near the bottom of north-east and north-west corners was heavily damaged. This may be due to larger share of lateral force attracted by the stiffer shear wall 8-N during this shock. Lifting of the south-east corner was observed during this shock

which could be due to the failure of bond of vertical steel there. Some bricks also cracked in this shock.

(f) In the next severest shock (a_B = 2.45 g) the whole top spandrel and most part of the bottom spandrel of the shear wall 8-N were very heavily damaged (Photo 5.131). The bottom portion of the north-east corner shifted outwards by about 20 mm (Photo 5.132) whereas the north-west corner displaced outward by about 30 mm at the plinth band but it had not displaced at the lintel band level (Photo 5.133) due to minor cracks there. The top spandrel of the wall 8-S was also very badly damaged. The roof slab together with two courses of brickwork had separated from remaining portion of wall 8-S by a wide horizontal crack of maximum width of about 3 mm (Photo 5.134). A wide open crack developed just below the plinth band of the wall 8-S and the maximum width of this crack was about 3 mm in the portion below the door opening which had hogged up (Photo 5.134).

The top spandrel of wall 8-E as well as right pier together with the portion of bottom spandrel below it were very severely damaged (Photo 5.135). The central portion of the wall below the window was pushed inside by a maximum amount of 10 mm. In the north-east corner region, there were many open cracks having width of

about 10 mm which reduced towards lintel band. The roof slab got separated from the top of the wall. The cracks were widespread in all the portions of the wall 8-W under this shock. The left pier and the bottom spandrels were severaly damaged compared to the other portions (Photo 5.136). Although, this test structure had suffered severely, yet it was standing and could still sustain a few mild shocks further. But as the model was in bad shape, further testing was stopped at this stage.

5.5.3 Relative Competence of the Models to Withstand Dynamic Loads

The progressive damage to each test structure under dynamic loads has been discussed in the preceding section separately. Their relative competence to resist the shocks is examined here.

To have a quantitative measure of the damage resisting capability of any of the model structure, two parameters need to be identified: first, a parameter to define the extent of damage and the other, to define the input effort to cause damage. Moreover, the two parameters should be such that they could be summed from one shock to the other to obtain cumulative effects. The base acceleration could be taken as the parameter for defining input effort since this could be a good measure of the strength of a model against cracking. But since the

base acceleration has varied from shock to shock and summing of accelerations would be meaningless, it was discarded for the purpose of working out cumulative input effort. After great deal of thought, the following two measures are chosen for comparative study of the models:

(a) For defining dynamic action acting on the models, the 'input energy' is chosen. It has the merit that effect of all the shocks, rebounds, etc. can be taken into account by scalar addition. Since the base motion imparted to the table consisted of distinct half wave shocks, such as the one shown in Fig. 5.12, the motion almost dying completely before the other shock or rebound shock was given, the energy in each shock could be computed as

$$U_t = \frac{1}{2} m_t V_t^2 \qquad \ldots (5.1)$$

where,

U_t = total energy input in the shock

m_t = total mass of table including models

V_t = velocity of table attained at the end of the shock, equal to the area of the acceleration pulse

Thus the energy per unit mass is

$$U = \frac{1}{2} V_t^2 \qquad \ldots (5.2)$$

(b) For defining the damage level of the model, the parameter chosen is the ratio of the area of cracks in a wall to the total vertical area of the wall. The area of a crack is equal to its length multiplied by the wall thickness. In this definition, the width of crack which would have indicated the relative movement of masonry blocks and the energy absorption over and above the energy absorbed in cracking, has been neglected since the precise determination of the crack widths as well as masonry blocks posed an unsurmountable problem. To obtain idea of relative damage the adopted definition was considered adequate.

The two parameters as defined above have been computed for each shock and all the models. Where, in any shock, the exact information about acceleration or marking of cracks was not available, it was estimated by interpolation or comparison with other shocks. For example, for the first set of structures, the input energy for shock number 8, 10, 11 and 12, during which the base accelerations could not be recorded, has been assumed as it was under shock no. 13 because these shocks had the same positions of the shake table and dead load wagons for giving the impact. The cumulative extent of damage is plotted against cumulative input energy per unit mass for both the sets of test structures in Figs. 5.10 and 5.11.

The following significant observations are made from Figs. 5.10 and 5.11:

The extent of damage of all the models increases with the increase in input energy whether given in one big shock or a number of smaller shocks provided that each shock exceeded damage threshold. Increase in damage of the first set of test structures shows quite a regular trend (Fig. 5.10) whereas this is not so in case of the second set of test structures (Fig. 5.11). Accidental shock no. 2 (with input energy per unit mass = 2500 kgm.) was so severe that under this shock, a sudden jump in the extent of damage can be seen from Fig. 5.11, particularly in case of models 5 and 6.

From Fig. 5.10, it is observed that for a given amount of input energy, the percent of damage is least in case of strengthened structure built in cement sand mortar (model 4), then comes the strengthened structure in mud mortar (model 2) which is followed by the unstrengthened structure in cement mortar (model 3). The unstrengthened model in mud mortar (model 1) is the weakest structure among the first set of structures.

In the initial stages of shock applied to the second set of test structures, as the input energy per unit mass increases the sliding type (model 7) and strengthened structure in cement mortar (model 8) performed similarly (Fig. 5.11) whereas the sliding type

structure built in mud mortar (model 5) showed less damage compared to conventional structure in cement mortar with lintel band (model 6), But in the final stages of shocks, the models 5 and 6 have almost similar extent of damage while the model 7 has less damage compared to model 8.

Some specific comparisons are made in the following paragraphs. In these discussions reference to base accelerations as well as damage levels will also be made for an integrated picture. The shock numbers, corresponding base accelerations and damage levels of various models are listed in Tables 5.1 and 5.2 for the two sets of models. Six damage levels are identified on the basis of observed extent of cracks, their widening, separation of blocks of brickwork, fall of certain portions of walls etc. These are defined below:

0. No Damage-No cracks are seen in the walls at all.

I. Slight Damage - The damage is characterised by very fine cracks of small length and the extent of damage is estimated upto about 5 per cent.

II. Moderate Damage - Repairable cracks of small length and narrow width appear in the walls and the extent of damage is between 6 and 35 per cent.

III. Severe Damage - When a model exhibits wide and deep cracks of large length in the walls and the

extent of damage ranges from 36 to 65 per cent which would require costly repairs.

IV. Destruction Damage - Wide gaps are created in the walls thereby separating them into different blocks and in this condition the extent of damage is taken between 66 and 95 per cent rendering the model unserviceable but without collapse.

V. Total Damage - Beyond the stage of Destructions, some parts of the structure fall down or are on the verge of collapse. The extent of damage may be assumed between 96 and 100 per cent.

Base accelerations, roof accelerations where available,and the damage levels obtained in various shocks on the two sets of models are listed in Tables 5.1 and 5.2. For comparing their relative competence, Table 5.3 has been prepared which lists the base accelerations for damage threshold, maximum base acceleration reached in the life of the model, and the respective energy values. The comparative behaviour is discussed below:

(a) Unstrengthened, Strengthened and Sliding Base Structures in Mud Mortar:

From Fig. 5.10 and Table 5.3, it is seen that the unstrengthened structure in mud mortar (model 1) lost its full capability to withstand further shock and reached total damage level at 1500 kgm input energy and 0.83 g base acceleration. But in contrast, the

corresponding strengthened model (No.2) withstood many more shocks, such that total damage was observed at base acceleration of 1.30 g and total input energy of 5940 kgm. Thus, this model was not only stronger but could take repeated shocks much better, capable of absorbing four times as much energy as the unstrengthened model.

The sliding base structure in mud mortar (model 5) behaved better than the unstrengthened structure as it was capable of dissipating about two times as much energy as the unstrengthened model (Table 5.3) at total damage. But, in contrast, the threshold damage in the sliding base structure reached at input energy of about one-third of that required by the unstrengthened model. This peculiar behaviour of the sliding base model is believed to have occurred due to the fact that the sliding joint was rather imperfect under some parts of the superstructure base. As such, the much improved behaviour of this structure as observed in the sliding base model in cement mortar (model 7) could not be seen.

(b) Unstrengthened Structures in Mud and Cement Mortars:

It is observed from Table 5.3 that the unstrengthened structure in cement mortar (model 3) behaved much better than the structure in mud mortar (model 1) with respect to strength as well as energy absorbing capacity. The model in cement mortar shows

about 2.3 times as much energy absorbing capacity as that of the structure in mud mortar at total damage level. Also, it could resist base acceleration twice that of model 1 to attain total damage. The much better behaviour of the cement mortar model is mainly due to its larger tensile and shearing strengths as compared with mud mortar.

(c) Model Structures in Cement Mortar:

The unstrengthened model in cement mortar (model 3) showed its total damage at cumulative input energy of 3430 kgm and base acceleration of 1.26.g (Table 5.3). Comparing with strengthened model in mud mortar (model 2) its performance is seen to be poor as indicated by Fig. 5.11,although their cost of construction works out to be almost same as shown in Table 5.4.

Referring to Table 5.3, it looks puzzling that the values of base acceleration and cumulative input energy for damage of the unstrengthened model (No.3) are more than that of similar model except for lintel band (model 6). But, in fact these results should have been otherwise because the provision of lintel band ought to improve the strength and energy absorbing capacity of model 6. As explained earlier (see Subsection No. 5.5.1) after a few shocks, model 3 cracked at the junction of superstructure and plinth alround thereby a discontinuity was created at the plinth level.

Thus, under subsequent shocks, model 3 behaved as a sliding base structure and behaved better than model 6.

In the first set of test structures, performance of the strengthened model (No. 4) was excellent. For threshold damage, base acceleration was 0.83g and input energy 1500 kgm while its further damage levels were well distributed over the subsequent shocks (Fig. 5.10 and Table 5.1). Its potentiality to resist shocks is seen to be consistent with the increasing input energy. This structure absorbed about three times as much input energy as the corresponding unstrengthened structure (model 3) to reach their total damage while increase in its cost is only 4.5 per cent (Table 5.4). Base acceleration to cause total damage of this structure was as high as 1.94 g.

In the second set of test structures, it is observed from Fig. 5.11 that sliding base(model 7) and fully strengthened (model 8) structures did not reach their total damage level even upto the last shock. Before reaching an input energy of about 4,000 kgm (Fig. 5.11), both the structures performed similarly under shocks. The extent of damage of model 8 was about 15 per cent more than that of model 7 at input energy of 7,500 kgm which shows better performance of sliding base structure over strengthened one. Also, the cost of construction of the sliding type model was 0.5 per cent less (Table 5.4) than that of model 8.

Though models 7 and 8 did not reach their total damage upto the last shock, yet by referring to Table 5.3 it may be stated that ultimately both of these structures would definitely resist larger base acceleration for their total damage than model 4 and would also absorb more input energy. Thus, after carefully examining the test results of both the sets of test structures, it turns out that the sliding base model as well as strengthened structure (model 8) built in cement mortar are eminently suitable for good performance under repeated severe shocks.

5.5.4 General Conclusions

From damage study of the test structures, it is concluded that once a brick building cracks, its strength goes down, the value of damage threshold acceleration also goes on reducing as the extent of damage increases (Tables 5.1 and 5.2). Also the rate of damage tends to increase under subsequent shocks of even smaller intensity. This trend is particularly true of unstrengthened buildings whereas in strengthened buildings usually a higher base acceleration is needed to cause further damage. For unstrengthened buildings prevalent in the Koyna region of India, it was clearly observed that the buildings, which sustained hair cracks during the earthquake of 13th September 1967, collapsed, partly or completely during the earthquake of December 11, 1967. The latter was of course more intense than the former but the ones undamaged during

September shock did not collapse fully in December shock (Chandrasekaran, Srivastava and Arya, 1969).

It turns out from the relative competence study of the test structures that the sliding type and strengthened structures in cement sand mortar should prove equally dependable under similar situations with respect to level of damage and shock intensity. Also their cost of construction is almost same.

Unstrengthened brick structure built in mud mortar are found too weak under shock loads. But with strengthening measures, these should also be suitable for moderate seismic resistance and will be better than unstrengthened building in cement mortar which would cost about equal.

The accelerations recorded at the shake table and roof of the test structure during different shocks are shown in Tables 5.1 and 5.2. It is seen from Table 5.1 that in case of strengthened structure built in cement mortar (model 4), as the number of shock and damage level increases, its roof acceleration generally decreases compared to the table acceleration. This may be attributed to the increasing number and width of the cracks under subsequent shocks which reduce the stiffness of the structure and elongate its time period on the one hand and increase the internal damping on the other hand by dissipating the input energy through friction in these

cracks. Both these effects reduce the acceleration response of the structure. Similar trends are also generally observed in Table 5.2 for models 5 through 8.

In case of sliding type structure 7, the roof acceleration is seen to be remarkably less as compared to the table acceleration as well as the roof acceleration of the model 8. This feature as exhibited by the sliding type model clearly establishes that seismic force attracted by such structures would be significantly reduced in the event of earthquake type loads.

5.6 COST-BENEFIT STUDY OF THE MODELS

To assess the economic benefits that may be achieved from strengthening of brick buildings, the cost-ratio of the different structures of this test programme is presented in Table 5.4 along with the maximum base acceleration upto destruction damage (level IV) and also the corresponding cumulative energy input. For cost comparison, the unstrengthened test structure in 1:6 cement mortar is chosen as the base. The cost ratios are for the model structures. It is seen from this table that strengthening with steel or provision of sliding at plinth improve the dynamic behaviour of the structures much more than the added cost both in terms of resistance to base acceleration and the dissipation of input energy. The real measure of efficiency comes from the energy since an earthquake always involves repeated shocks requiring

not only strength against one shock but toughness also for deforming without failure under repeated shocks. From this angle, the models in cement mortar, with full strengthening measures and with sliding arrangement at the plinth show outstanding behaviour.

5.7 THEORETICAL RESPONSE ANALYSIS OF THE TEST STRUCTURES

Theoretical analysis of the uncracked test structures subjected to the table motion is made here to compare their response thus computed with that obtained experimentally. This would help in examining the efficiency of the mathematical model of conventional single storeyed brick building subjected to dynamic loads. For such study, only models 6 and 8 are selected as their roof accelerations were recorded before any cracks were observed in them.

Equivalent spring-mass-dashpot system is assumed for the dynamic analysis. Stiffness of the test structure is computed assuming box section in plan in view of the uncracked state as well as use of lintel bands to ensure integral action of walls in these models. Mass of the model is determined on the basis as discussed in Chapter 3. Its value is equal to 1.79 kg-sec^2/cm. Value of modulus of elasticity (E) is assumed as 14,100 kg/cm^2 for brickwork in 1:6 cement sand mortar (Chandra, 1963). The response computations are also made for the values of modulus of

elasticity as half and twice to that of the assumed value (14,100 kg/cm^2). Viscous damping is assumed to be 5 per cent of critical. The digitized acceleration pulse of the table motion which is used as an input for the models, is shown in Fig. 5.12. The spectral accelerations thus computed for the table motion are tabulated in Table 5.5.

It is observed from Table 5.5 that the spectral acceleration of the model 6 (for E = 14,100 kg/cm^2) is about 21 per cent less than the experimentally observed value whereas for model 8, this difference is about 10%. Therefore, it turns out that there is a reasonable agreement between the theoretically computed and experimentally observed values. It is also seen from Table 5.5 that the spectral acceleration values are rather insensitive to the time period of the structure hence little influenced by the assumption of the modulus of elasticity.

5.8 PREDICTION OF EARTHQUAKE SHOCK FOR PROTOTYPE BUILDINGS

An attempt is made here to predict the peak ground acceleration of an earthquake which would produce same threshold damage to prototype structure as was produced by the table motion to the model structures. For this purpose, it is assumed that the brickwork of the model has 10% higher tensile strength than the prototype (Sub-section 2.3.2 of Chapter 2). For this study model 8 is selected as its response acceleration values are available in undamaged condition under recorded

table motion. Thus the stage considered is that when the tensile strength of the brickwork is not exceeded in the shock. At this stage the period of prototype and model can be computed with reasonable accuracy as stated in Chapter 3 and damping can be assumed as about 5 per cent of critical value. For the elastic condition, the spectral acceleration values of the prototype earthquake motion will also be available. Prediction equations for seismic coefficient applicable to prototypes are derived below:

The pier method of analysis as described in Chapter 3 is employed here for computing tensile stresses in the building elements of the prototype and model structures. The net tensile stress in a pier is determined by superimposing axial stresses due to dead and live loads and the bending and overturning stresses due to earthquake load. Let a typical pier of model and the corresponding pier of the prototype be considered. The analysis will also be applicable to other piers.

Taking the unit weight of brickwork and reinforced concrete as 1920 and 2400 kg/m^3 respectively, and the structural properties of the piers computed as per Chapter 3, the different stresses computed for the model (Fig. 5.8) are found as given below:

$$\begin{aligned} p_{dm} &= + 0.25 \quad kg/cm^2 \\ p_{bm} &= \pm 2.45 \; C_m \quad kg/cm^2 \\ p_{om} &= \pm 0.69 \; C_m \quad kg/cm^2 \end{aligned} \qquad \ldots(5.3)$$

where p_{dm} = uniform stress in the pier of the model due to dead and live loads.

p_{bm} = bending stress in the pier of the model due to earthquake force

p_{om} = overturning stress in the pier of the model due to earthquake force

C_m = seismic coefficient for the model

Superimposing them, the net tensile stress, p_{tm}, in the pier of model 8 is

$$p_{tm} = (3.14\ C_m - 0.25)\ kg/cm^2 \qquad ...(5.4)$$

The corresponding stresses in the prototype pier will be as follows:

$$\begin{aligned} p_{dp} &= +\ 0.25\ \lambda \quad kg/cm^2 \\ p_{bp} &= \pm\ 2.45\ \lambda\ C_p \quad kg/cm^2 \\ p_{op} &= \pm\ 0.69\ \lambda\ C_p \quad kg/cm^2 \end{aligned} \qquad ...(5.5)$$

in which

p_{dp} = uniform dead and live loads stress in the prototype pier

p_{bp} = bending stress in the prototype pier due to earthquake load

p_{op} = overturning stress in the pier of the prototype due to earthquake load

λ = scale ratio, 2.0 in this case

C_p = seismic coefficient for the prototype

Thus, the net tensile stress, p_{tp}, in the prototype will be

$$p_{tp} = (3.14\ C_p - 0.25) \quad kg/cm^2 \qquad ...(5.6)$$

Since, the ratio of tensile strength in model and prototype is assumed as 1.1, by using Eqs. (5.5) and (5.6) the following equation is obtained for predicting the seismic coefficient of the prototype

$$C_p = 0.46\ C_m + 0.043 \qquad ...(5.7)$$

Thus for an effective seismic coefficient C_m causing threshold damage in a model structure, the corresponding value of the seismic coefficient C_p for prototype structure can now be evaluated by using Eq.(5.7).

Spectral acceleration of the model for the table motion, S_{am}, can be calculated as usual for the model period and damping. Therefore, the corresponding value of spectral acceleration, S_a', of the prototype for the table input may be computed by

$$S_a' = \frac{C_p}{C_m}\ S_{am} \qquad ...(5.8)$$

Now the period of the prototype structure will be λ times the period of the geometrically similar model. Knowing this time period and appropriate damping value the spectral acceleration of the prototype, S_{ap}, can be found for the prototype earthquake. Knowing S_{ap}, the ratio of S_a' to S_{ap} will indicate the scaling of the

peak ground acceleration of the prototype accelerogram to suit the threshold damage of the prototype. Thus the peak ground acceleration for prototype structure could be related to the maximum base acceleration of the model for threshold damage as follows:

$$a_p = \frac{C_p}{C_m} \cdot \frac{S_{am}}{S_{ap}} \cdot a \qquad \ldots(5.9)$$

in which

a_p = scaled peak ground acceleration of prototype earthquake accelerogram corresponding to threshold damage of prototype

a = actual peak ground acceleration of prototype earthquake motion

As an illustration, the Koyna earthquake is used here for predicting peak ground acceleration for threshold damage of the ptototype of model 8. The damping for both the structures is taken as 5 per cent of critical. The values of S_{am} (for E = 14100 kg/cm^2) and C_m for model 8 are listed in columns 5 and 7 of Table 5.5 respectively. For Koyna shock, the peak ground acceleration, a = 0.63 g. Using the prediction Eq. (5.7), the value of C_p for the prototype is evaluated as 0.312.

With the help of Eq. (5.9), the value of a_p is computed for the prototype. It works out to be 0.15 g.

From the result thus obtained, it is seen that about one-fourth of peak ground acceleration of Koyna earthquake would be required to produce none or slight damage to the prototype building corresponding to the model tested under table motion having peak acceleration equal to 0.51 g.

TABLE 5.1

ACCELERATION RECORDS FOR THE FIRST SET OF TEST STRUCTURES

SHOCK No.	DIRECTION OF SHOCK	ACCELERATION (g) AT THE TABLE BASE	ACCELERATION (g) AT ROOF TOP OF THE MODELS AND DAMAGE LEVEL (DL)								REMARKS
			MODEL 1		MODEL 2		MODEL 3		MODEL 4		
			DL	ACCELERATION (g)	DL	ACCELERATION (g)	DL	ACCELERATION (g)	DL	ACCELERATION (g)	
1	E to W++	0.22+	0		0		0		0		no rebound
2	E to W	0.22	0		0		0		0		one rebound
3	E to W	0.40	0		0		0		0		one rebound
4	W to E	0.51	0		0		0		0		one rebound
5	W to E	0.57	II		0		0		0		one rebound
6	E to W	1.05	IV		II	0.70	II	0.45	0		one rebound
7	E to W	0.83+	V			0.20	III	0.34	I		one rebound
8	W to E	1.24+							II		one rebound
9	W to E	1.24+			III		IV			1.16	one rebound
10	W to E	1.26+					V			1.42	one rebound
11	W to E	1.26+								0.84	one rebound
12	W to E	1.26+			IV				III	0.79	one rebound
13	W to E	1.26								0.90	one rebound
14	E to W	1.30			V					0.74	one rebound
15	E to W	1.85							IV	0.91	one rebound
16	E to W	1.84								0.91	one rebound
17	E to W	1.78								0.91	one rebound
18	E to W	1.60								0.80	one rebound
19	E to W	1.95							V	1.73	one rebound

+ Acceleration records could not be taken, values given by comparison

++ E and W stand for east and west directions respectively

TABLE 5.2

ACCELERATION RECORDS FOR THE SECOND SET OF TEST STRUCTURES

SHOCK No.	DIRECTION OF SHOCK	ACCELERATION (g) AT THE TABLE BASE	ACCELERATION (g) AT ROOF TOP OF THE MODELS AND DAMAGE LEVEL (DL)								REMARKS
			MODEL 5		MODEL 6		MODEL 7		MODEL 8		
			DL	ACCELERATION (g)	DL	ACCELERATION (g)	DL	ACCELERATION (g)	DL	ACCELERATION (g)	
1	E to W	0.51	II	0.64	0	0.67	0	0.55	0	0.59	one rebound
2	W to E	2.15	III	1.22	III	0.75	II	0.19	II	1.37	one rebound
3	E to W	0.53		0.31		0.26		0.12		0.55	no rebound
4	E to W	0.66	IV	>0.32	IV			0.12		0.53	no rebound
5	W to E	>0.58	V		V	0.40		0.12		0.45	no rebound
6	E to W	1.08					III	0.93	III	2.00	two rebounds
7	E to W	2.36						0.89		2.13	one rebound
8	W to E	2.45					IV	1.28	IV	1.79	one rebound

TABLE 5.3

RELATIVE COMPETENCE OF BRICK STRUCTURES FOR BASE MOTIONS

S.No.	Structures Compared		Model Nos.	Base Accelerations (g) for Damage		Cumulative Input Energy (kgm) for Damage	
				Threshold (a_{th})	Maximum	Threshold (E_{th})	Total
1	Mud Mortar	Unstrengthened	1	$0.51 < a_{th} < 0.57$	1.05	< 506	1,500
		Strengthened	2	$0.57 < a_{th} < 1.05$	1.30	< 810	5,940
		Sliding Base	5	$a_{th} < 0.51$	2.15	< 160	2,900
2	Unstrengthened	Mud Mortar	1	$0.51 < a_{th} < 0.57$	1.05	< 506	1,500
		Cement Mortar	3	$0.57 < a_{th} < 1.05$	1.26	< 2,260	3,430[+]
3	Cement Mortar	Unstrengthened	3	$0.57 < a_{th} < 1.05$	1.26	< 2,260	3,430[+]
		Unstrengthened With Lintel Band	6	$0.51 < a_{th} < 2.15$	2.15	< 160	2,900
		Strengthened	4	0.83	1.95	1,500	10,580
		Sliding Base	7	$0.51 < a_{th} < 2.15$	>2.45[++]	$160 < E_{th} < 2,520$	$>7,500$[++]
		Strengthened fully	8	$0.51 < a_{th} < 2.15$	>2.45	$160 < E_{th} < 2,520$	$>7,500$[++]

[+]This model showed lack of bond at plinth level and behaviour was similar to sliding base model

[++]Total damage level not reached.

TABLE 5.4

COST-BENEFIT RATIO OF THE TEST STRUCTURES

Model No.	Description of Model		Cost Ratio	Maximum Base Acceleration upto the stage of Destruction Damage (g)	Maximum Acceleration at Roof upto the stage of Destruction Damage (g)	Cumulative Input Energy upto Destruction Damage level (kgm)	REMARKS
	Mortar	Reinforcement					
1	Mud	No Steel	0.947	1.05	N.O	1,160	
2	Mud	LVJ+	0.992	1.26	0.70	4,600	
3	1:6 Cement Sand	No Steel	1.000	1.24	0.45	2,840	Showed Sliding Behaviour
4	1:6 Cement Sand	LVJ	1.045	1.85	1.42	6,870	
5	Mud	LPB	1.037	2.15	1.22	2,750	Sliding type, Non-Uniform Sliding, 18 mm
6 6	1:6 Cement Sand	L	1.025	2.15	0.75	2,750	
7	1:6 Cement Sand	LPB	1.073	2.45	1.28	7,500	Sliding type, sliding measured 35 mm
8	1:6 Cement Sand	LPVJ	1.078	2.45	1.79	7,500	

+Note - L = Lintel Band with 3 - 6 mm Ø
P = Plinth Band with 3 - 6 mm Ø
V = Vertical Steel at Corners, 1-6 mm Ø (0.016% of walls)
J = Jamb Steel, 1-6 mm Ø (0.032% of walls)
B = Bond Beam just above Plinth Band, 3-6 mm Ø
N.O = Not Observed

TABLE 5.5

RESULTS OF RESPONSE ANALYSIS

Column No.	1	2	3	4	5	6	7	8
Model No.	Time Period (sec.) for different values of Modulus of Elasticity (kg/cm^2)			Computed Maximum Roof Acceleration (g) for different values of Modulus of Elasticity (kg/cm^2)			Observed Roof Acceleration (g)	REMARKS
	7,050	14,100	28,200	7,050	14,100	28,200		
6	0.020	0.014	0.011	0.54	0.53	0.52	0.67	Unstrengthened with lintel band in cement sand mortar
8	0.019	0.013	0.010	0.51	0.52	0.54	0.59	Strengthened with plinth band in cement sand mortar

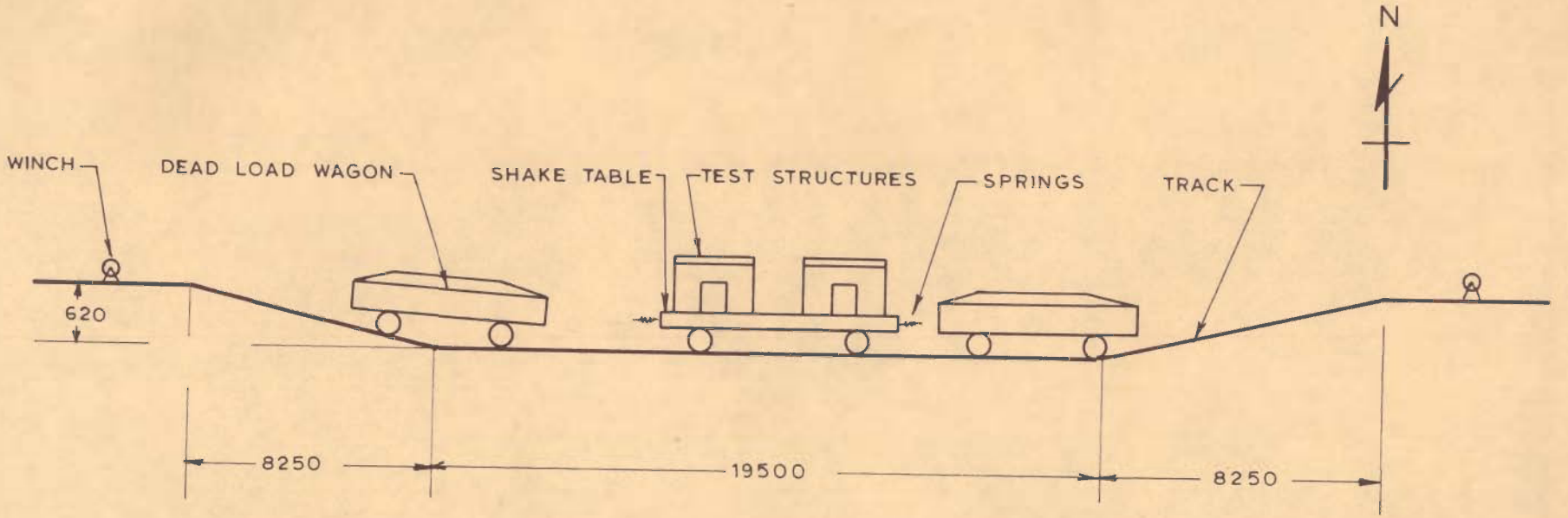

ALL DIMENSIONS IN mm

FIG. 5.1 – SCHEMATIC VIEW OF RAILWAY WAGON SHAKE TABLE TEST FACILITY

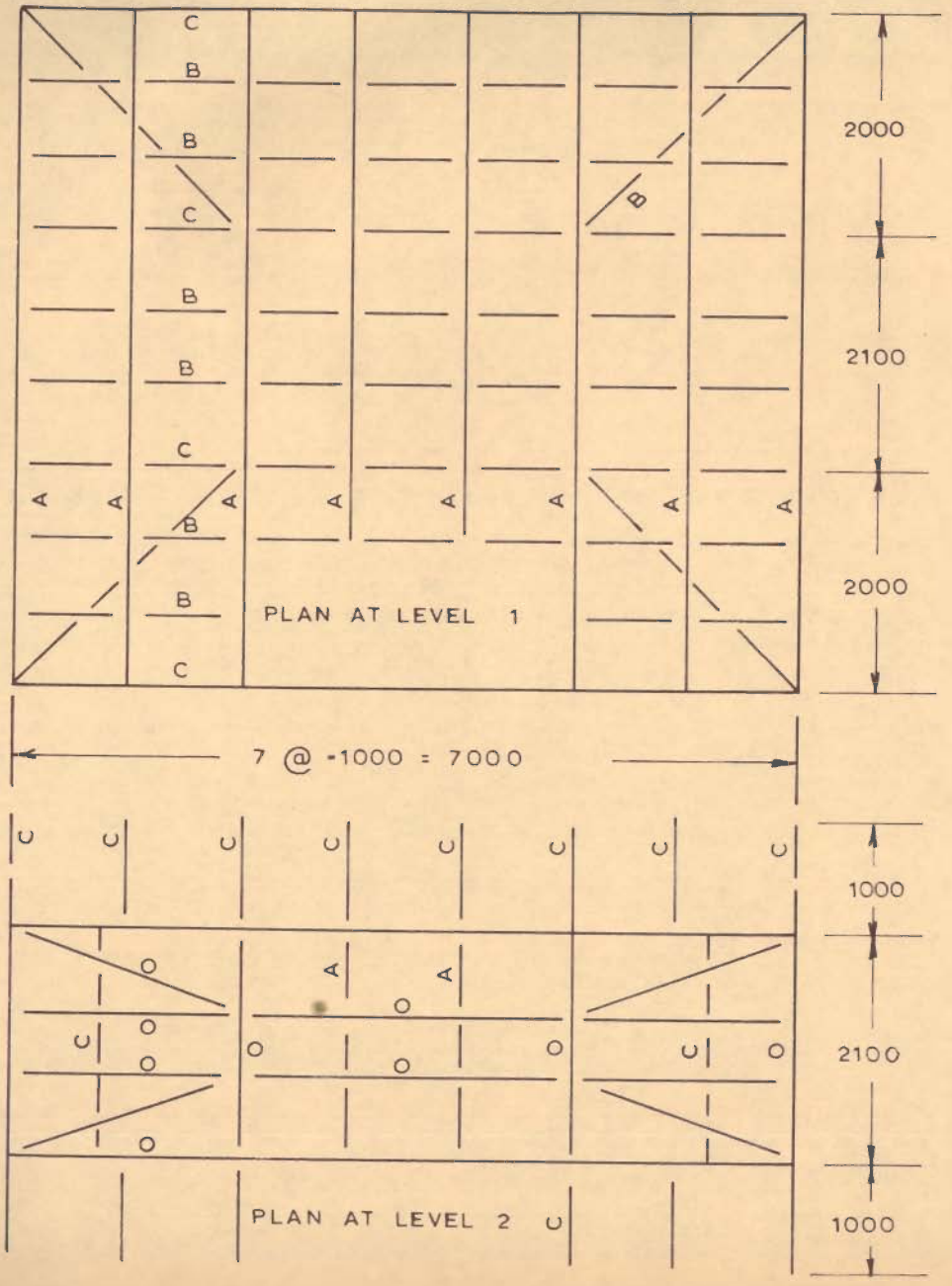

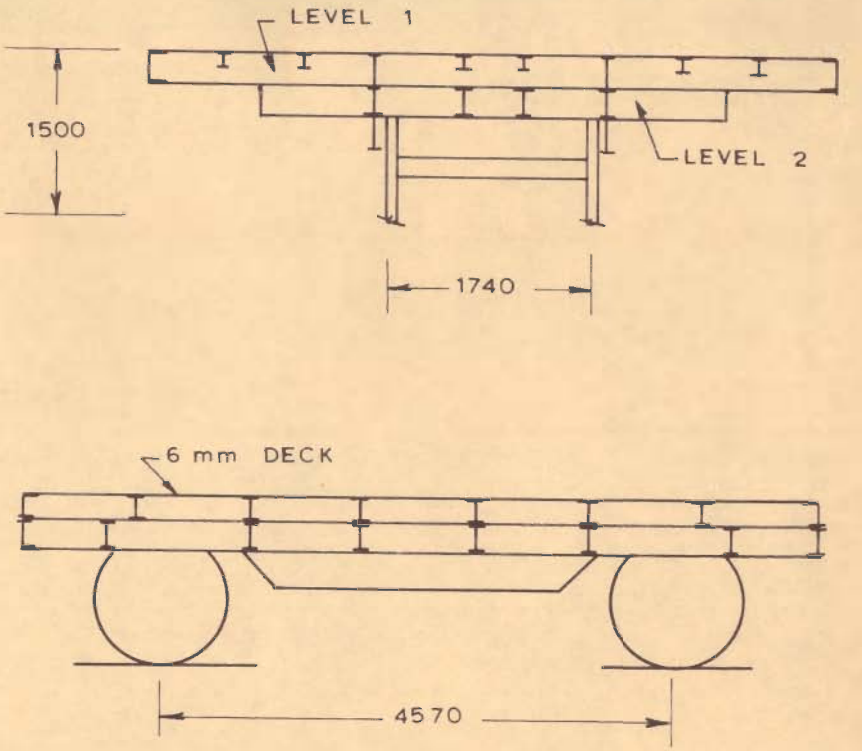

O - [250 x 75 , ORIGINAL FRAME

A - I 250 x 125 , 37.4 kg/m

B - I 100 x 50 , 8.0 kg/m

C - MADE FROM 6 mm PLATE

ALL DIMENSION IN mm

FIG. 5.2 - DETAILS OF STEEL ADDED TO WAGON CHASSIS FABRICATED SHAKE TABLE

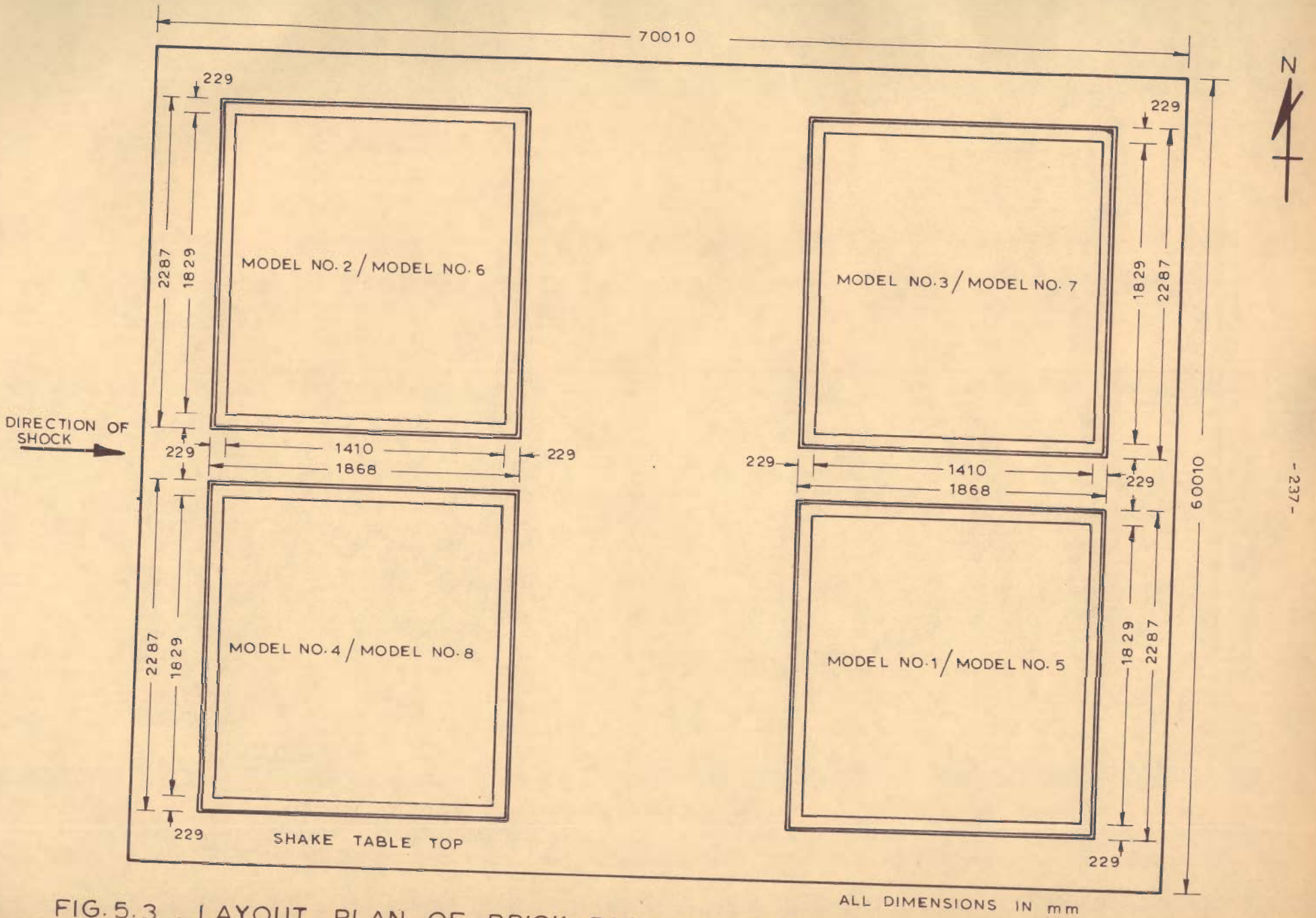

FIG. 5.3 - LAYOUT PLAN OF BRICK BUILDING MODELS CONSTRUCTED ON RAILWAY WAGON SHAKE TABLE

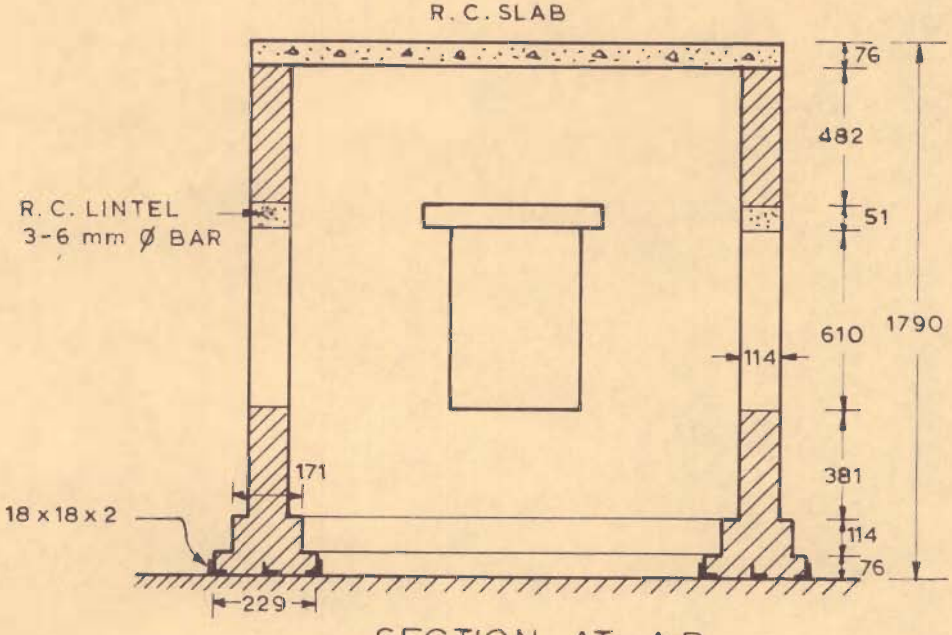

SECTION AT AB

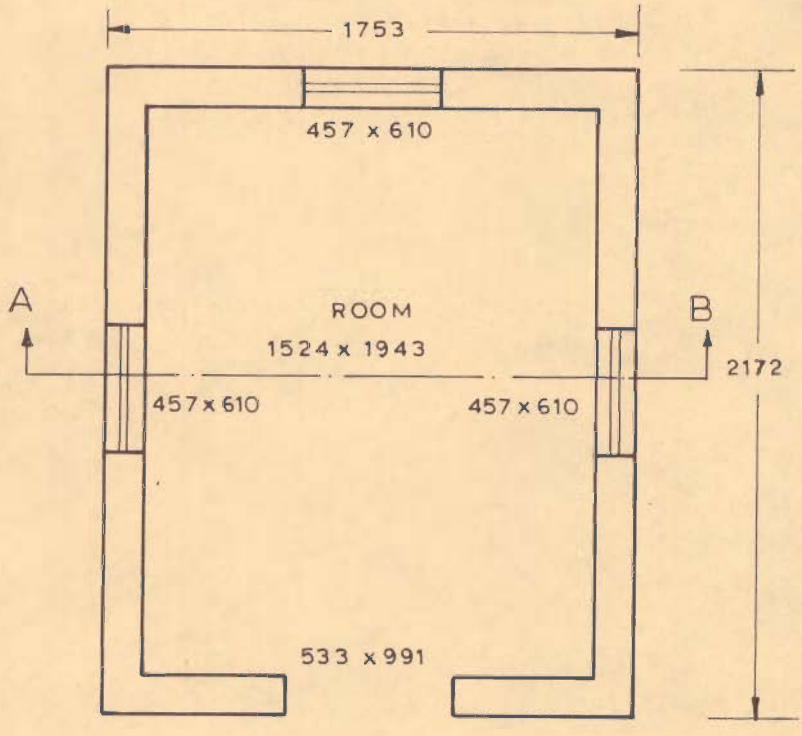

PLAN

ALL DIMENSIONS IN mm

FIG. 5.4 _ BRICK BUILDING MODEL IN CEMENT/MUD MORTAR

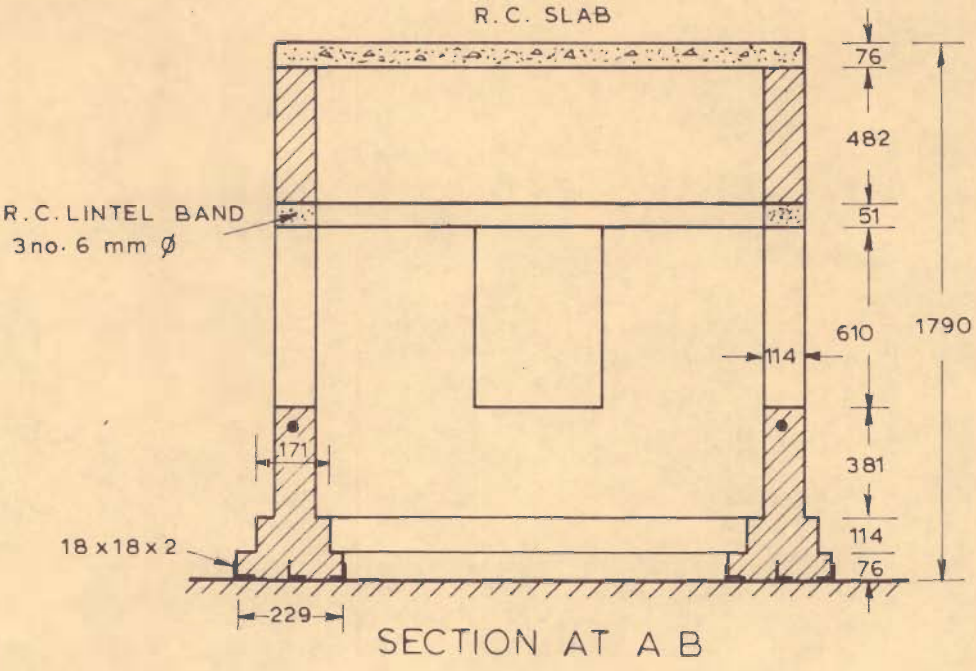

SECTION AT A B

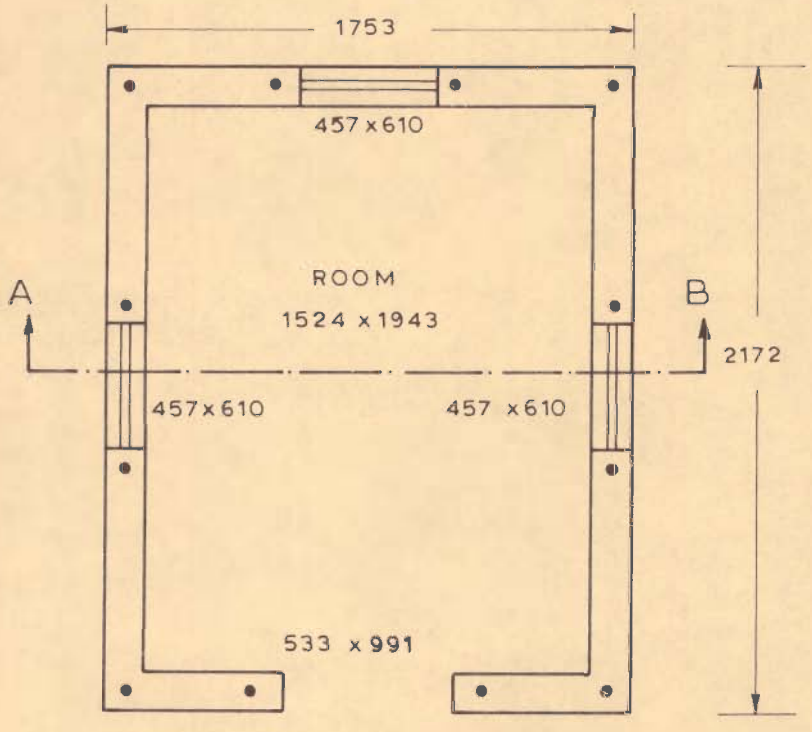

PLAN

● - 1 no. 6 mm ϕ

ALL DIMENSIONS IN mm

FIG. 5.5 - BRICK BUILDING MODEL IN CEMENT/MUD MORTAR WITH LINTEL BAND AND VERTICAL STEEL AT CORNERS AND JAMBS

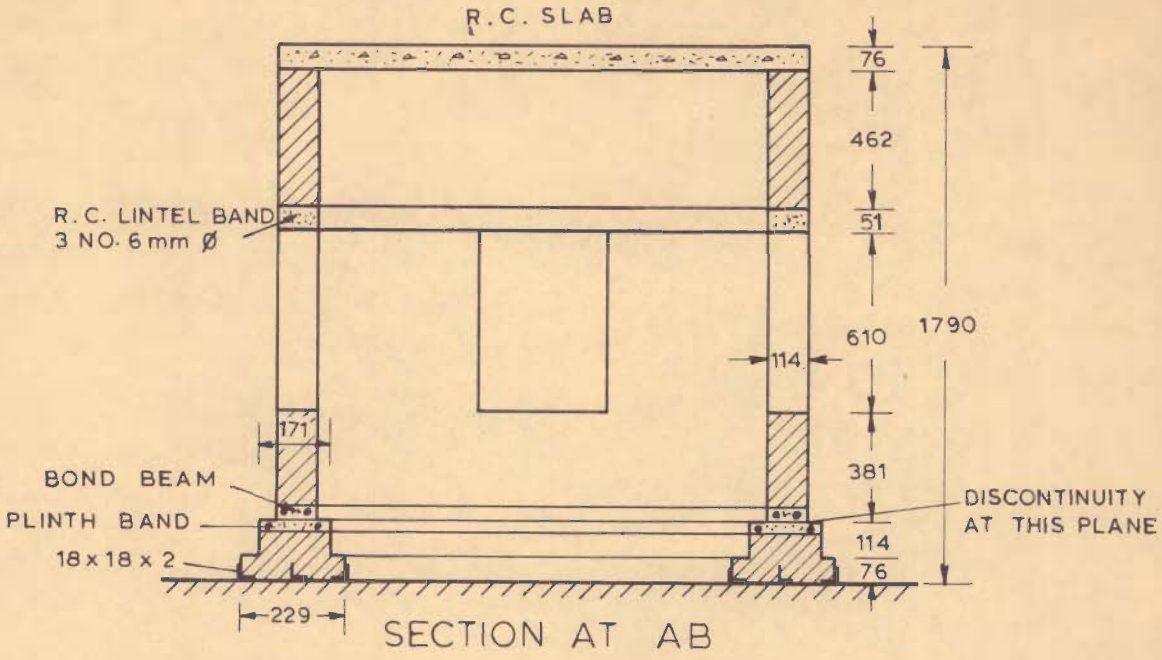

SECTION AT AB

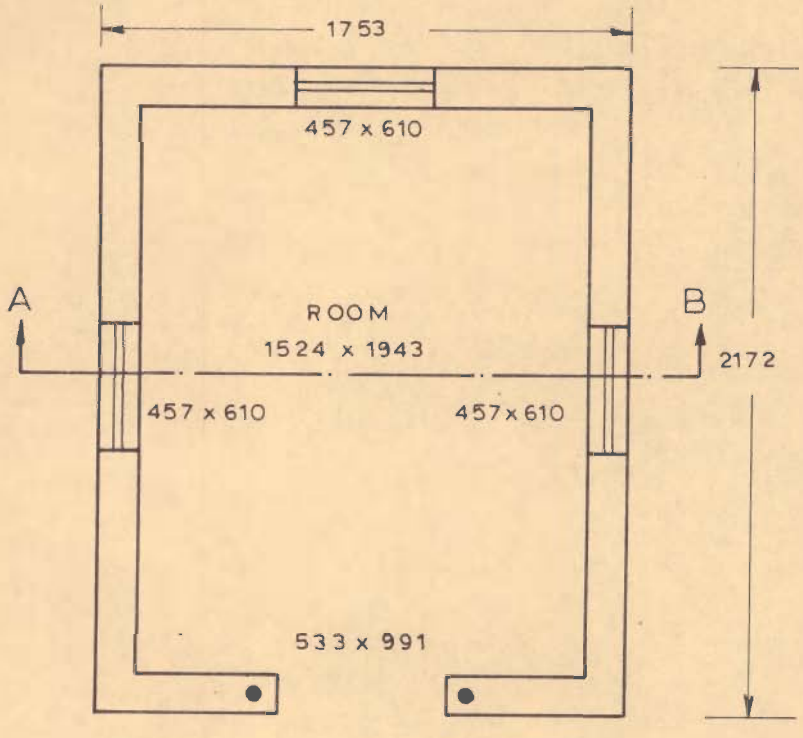

PLAN

● - 1 no. 6 mm Ø

ALL DIMENSIONS IN mm

FIG. 5.6 - SLIDING TYPE BRICK BUILDING MODEL IN CEMENT / MUD MORTAR

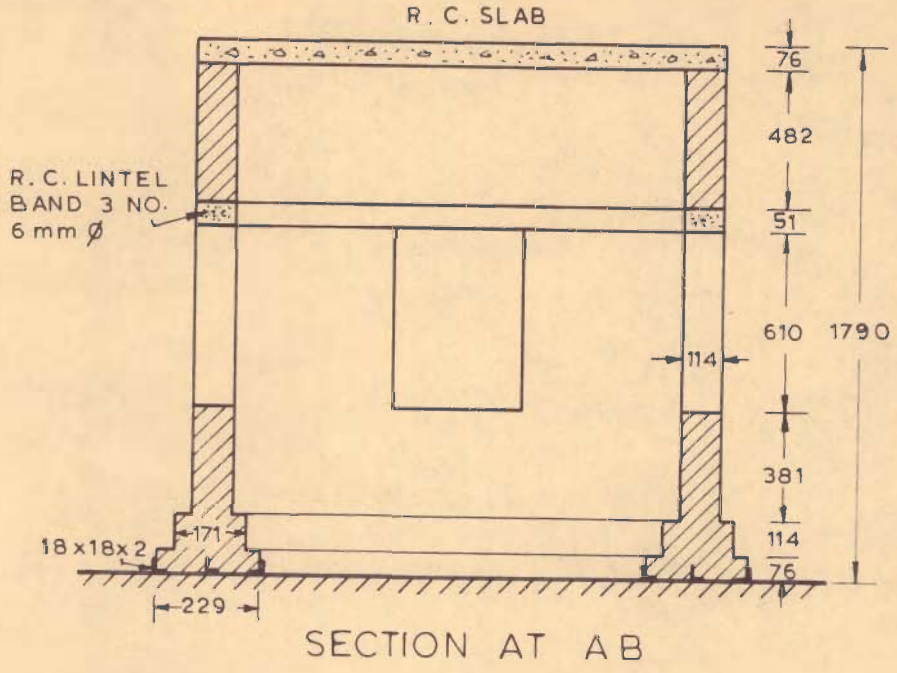

SECTION AT AB

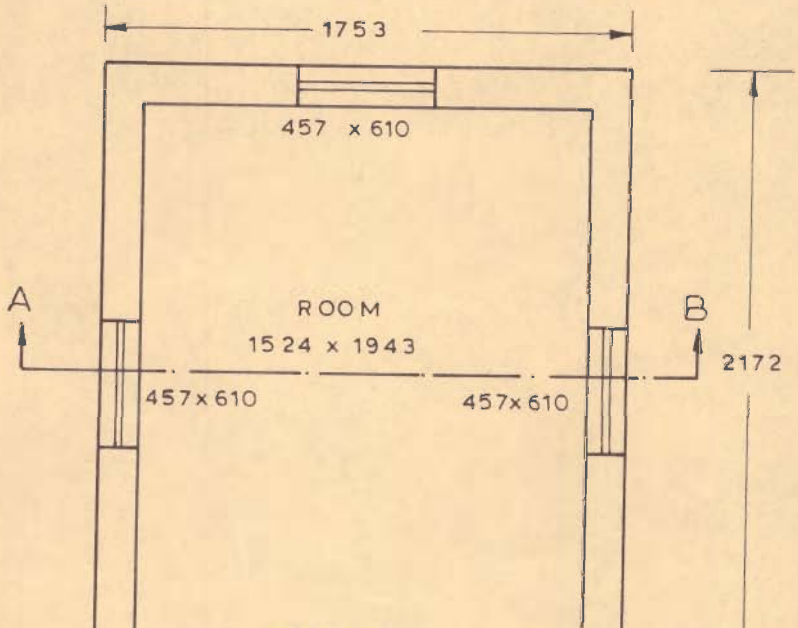

PLAN

ALL DIMENSIONS IN mm

FIG. 5.7 - BRICK BUILDING MODEL IN CEMENT MORTAR WITH LINTEL BAND

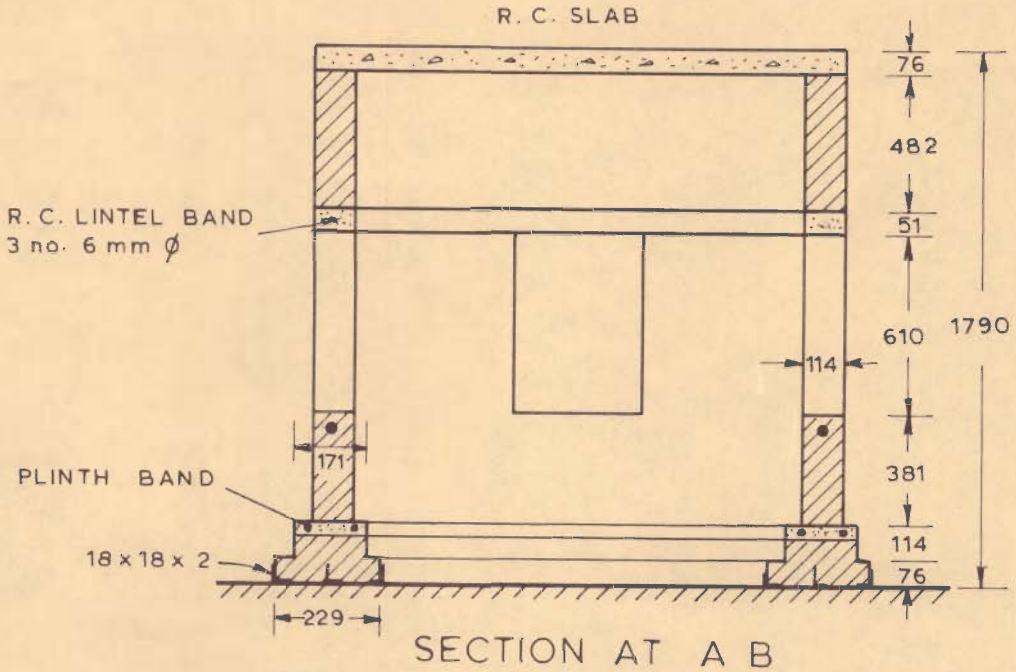

SECTION AT A B

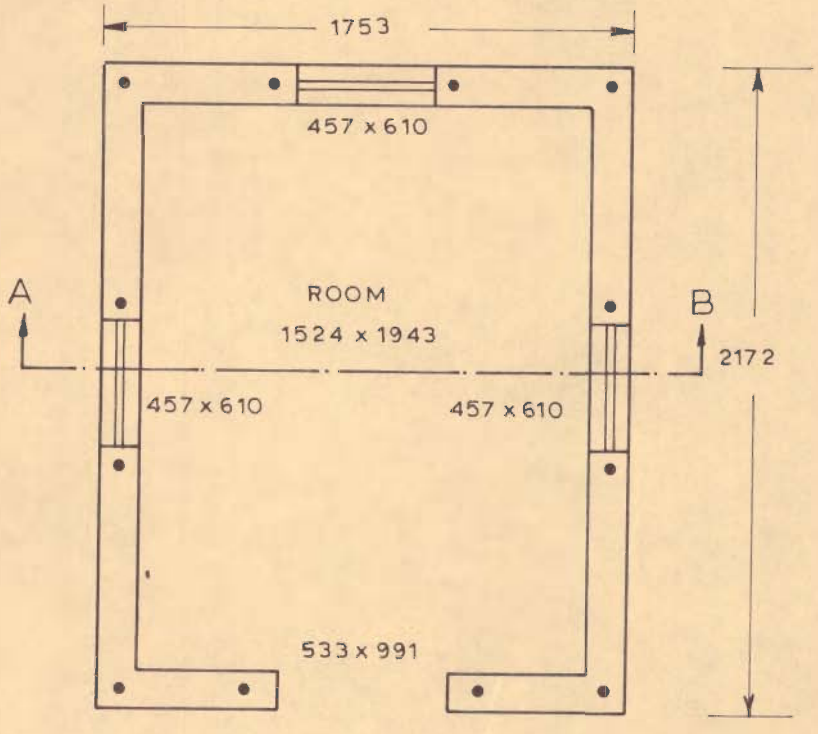

PLAN

● - 1 no. 6 mm ø

ALL DIMENSIONS IN mm

FIG. 5.8 - BRICK BUILDING MODEL IN CEMENT MORTAR WITH LINTEL AND PLINTH BANDS AND VERTICAL STEEL AT CORNERS AND JAMBS

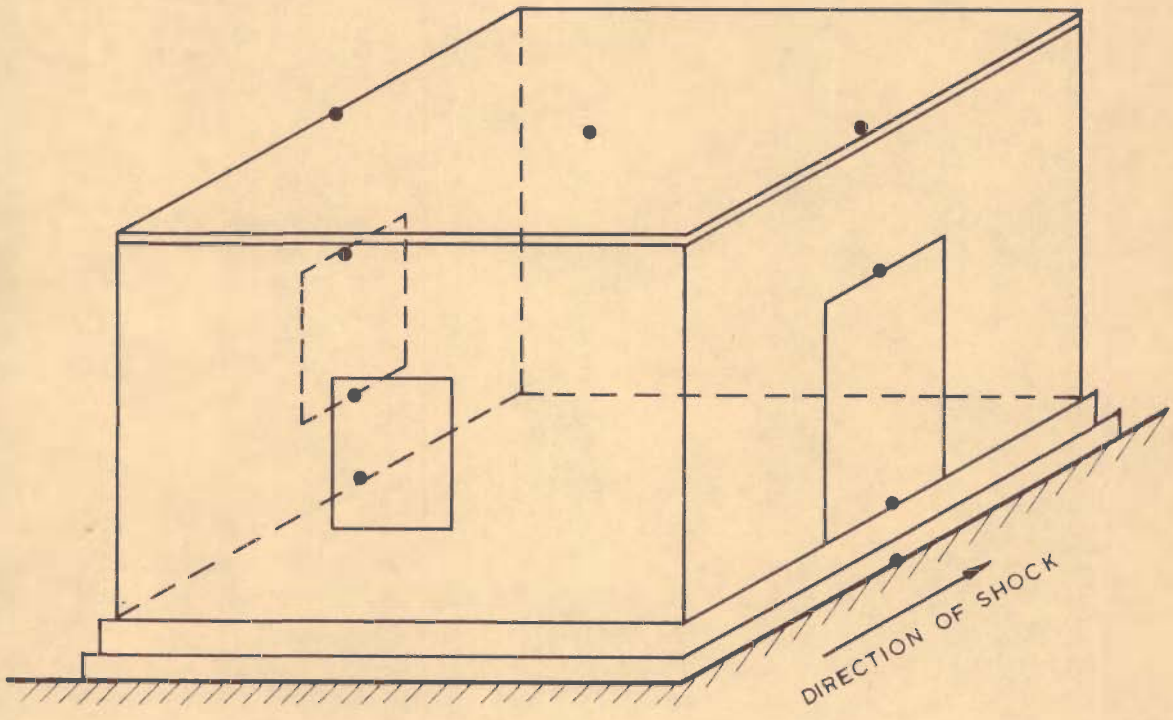

● - LOCATION OF ACCELEROMETERS

FIG. 5.9 - SCHEMATIC VIEW OF BRICK BUILDING MODEL SHOWING LOCATIONS OF ACCELEROMETERS

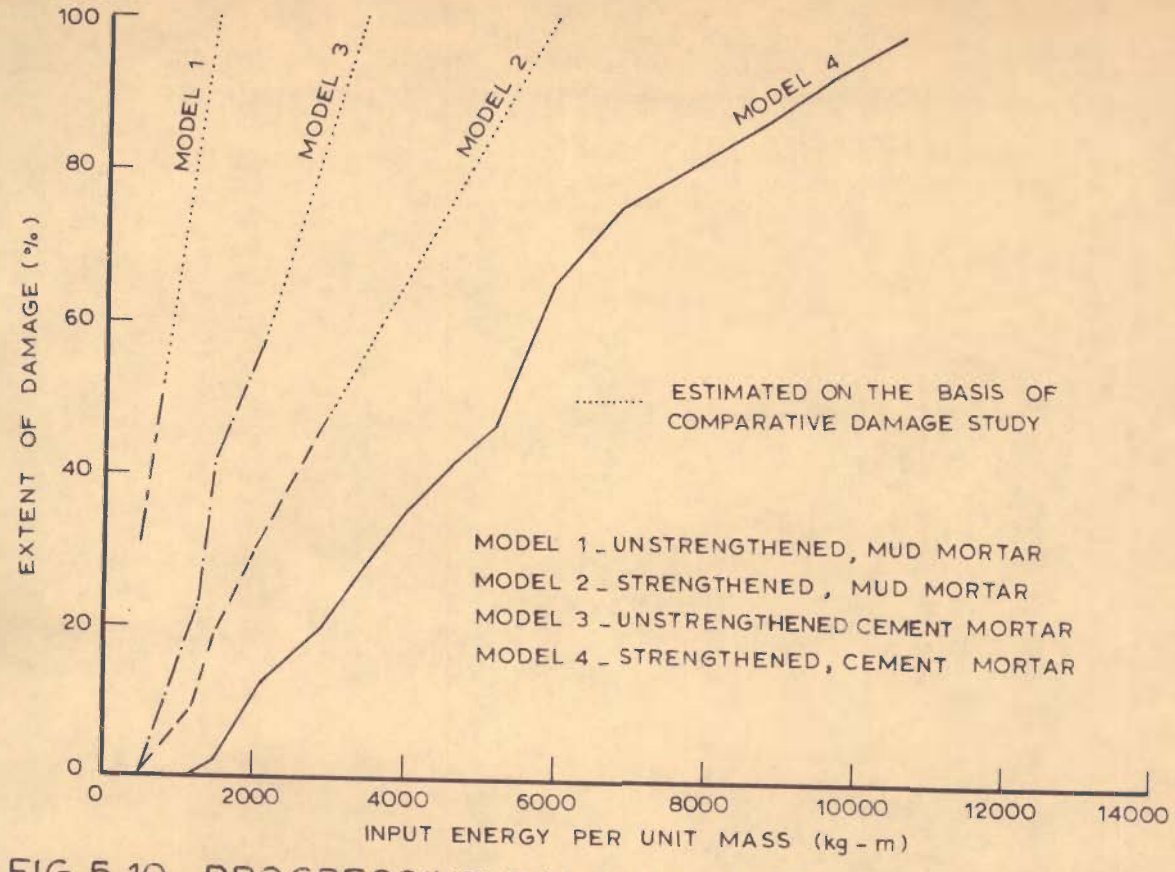

FIG. 5.10 - PROGRESSIVE DAMAGE & RELATIVE COMPETENCE OF FIRST SET OF BRICK TEST STRUCTURES SUBJECTED TO SHOCK LOADS

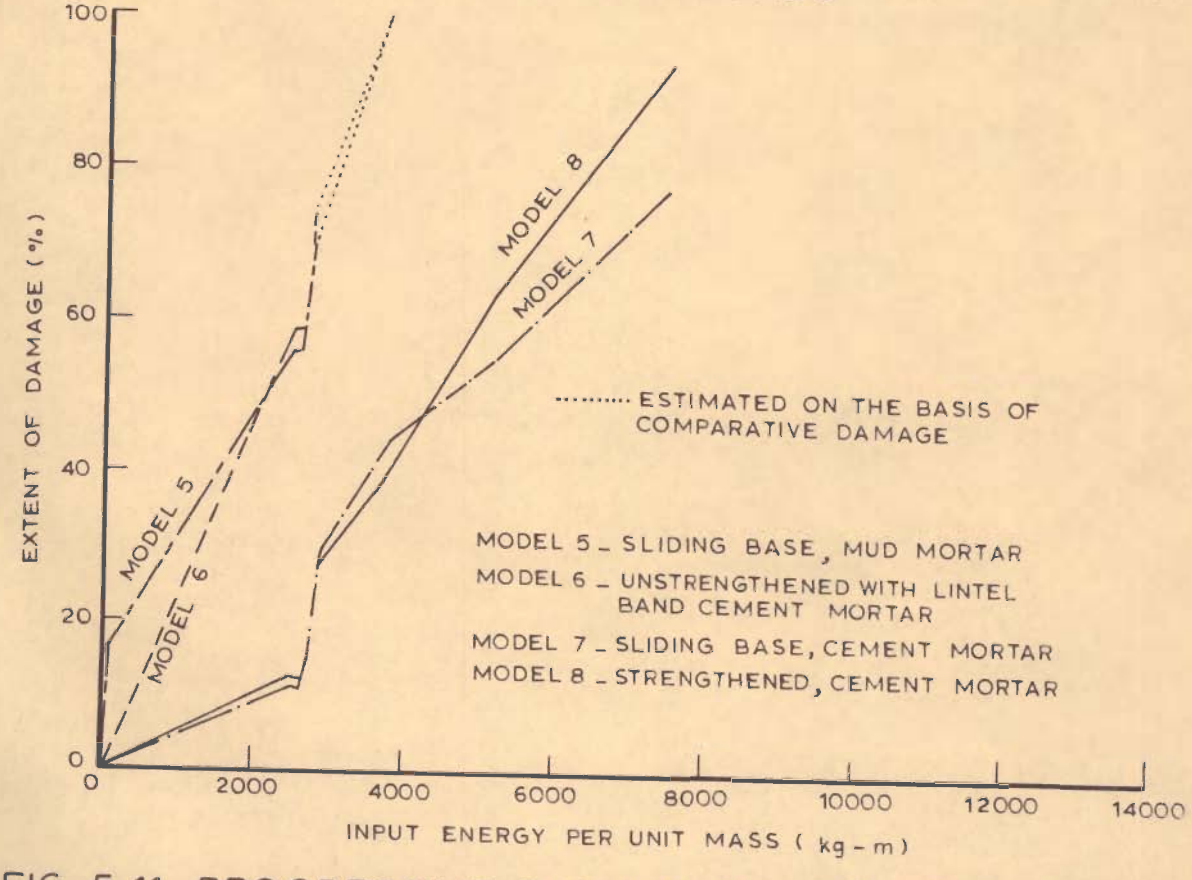

FIG. 5.11 - PROGRESSIVE DAMAGE AND RELATIVE COMPETENCE OF SECOND SET OF BRICK TEST STRUCTURES SUBJECTED TO SHOCK LOADS

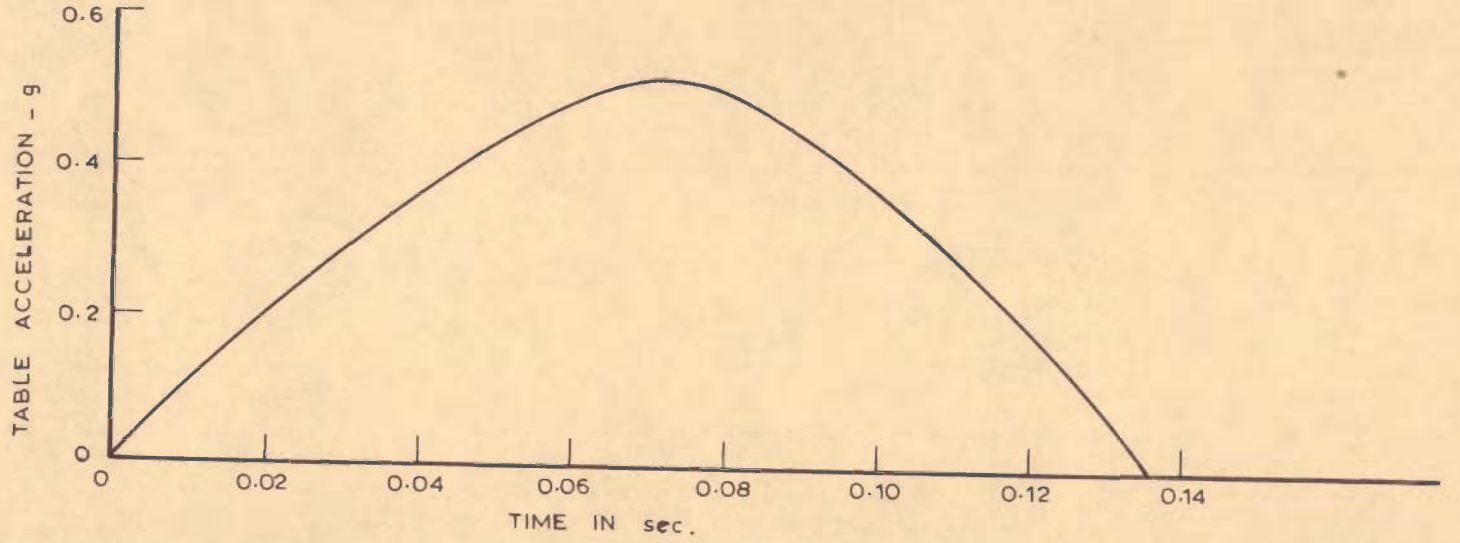

FIG. 5.12 - DIGITIZED PLOT OF THE SHAKE TABLE ACCELERATION PULSE (FOR SHOCK NO. 1 OF SECOND SERIES OF TESTING)

PHOTO 5.1 - AN ORIGINAL WAGON CHASSIS

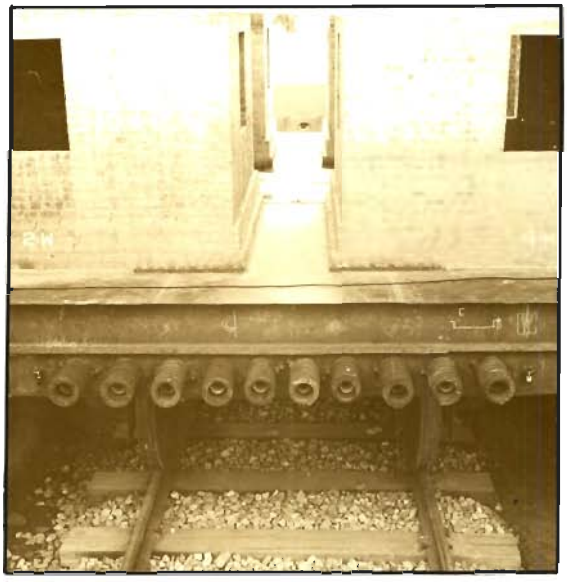

PHOTO 5.2 - TEN HELICAL COIL COMPRESSION SPRINGS

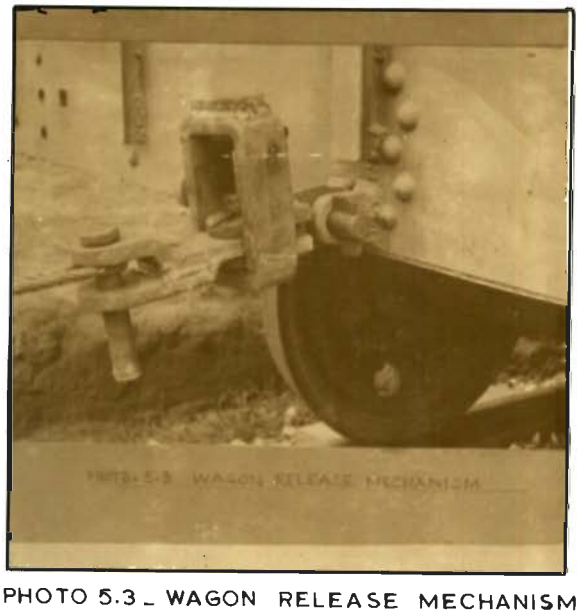

PHOTO 5.3 - WAGON RELEASE MECHANISM

PHOTO 5.4 - GENERAL VIEW OF RECORDING EQUIPMENTS ETC.

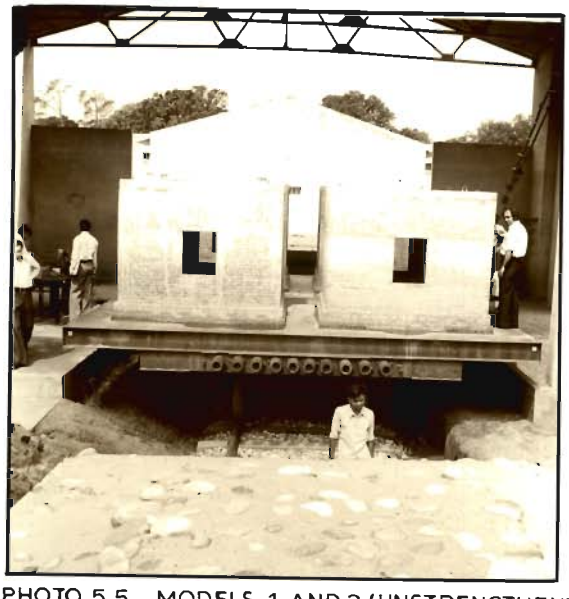

PHOTO 5.5 _ MODELS 1 AND 3 (UNSTRENGTHENED IN MUD AND CEMENT MORTAR) BEFORE SHOCK LOADS

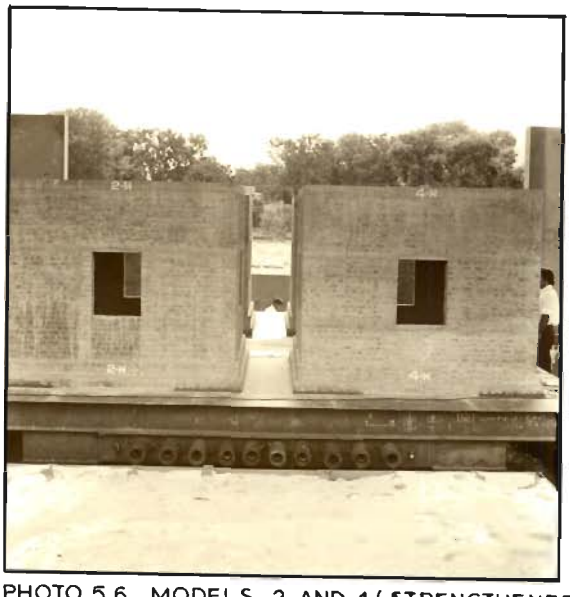

PHOTO 5.6 _ MODELS 2 AND 4 (STRENGTHENED IN MUD AND CEMENT MORTAR) BEFORE SHOCK LOADS

PHOTO 5.7 _ MODELS 5 AND 7 (SLIDING TYPE IN MUD AND CEMENT MORTAR) BEFORE SHOCK LOADS

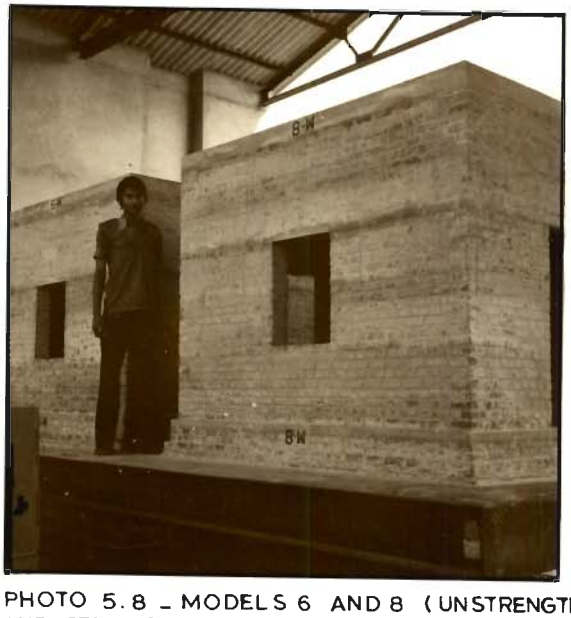

PHOTO 5.8 _ MODELS 6 AND 8 (UNSTRENGTHENED AND STRENGTHENED IN CEMENT MORTAR) BEFORE SHOCK LOADS

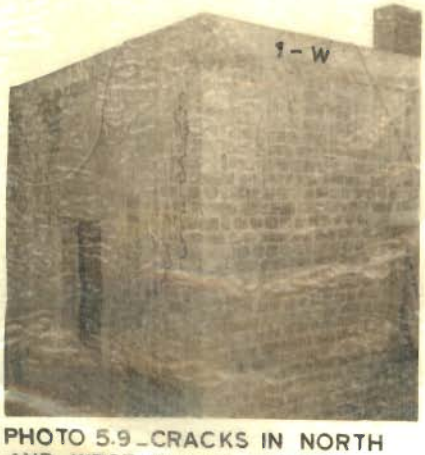

PHOTO 5.9_CRACKS IN NORTH AND WEST WALLS (MODEL 1)

PHOTO 5.10_VERTICAL CRACKS IN EAST CROSS WALL (MODEL 1)

PHOTO 5.11_VERTICAL AND DIAGONAL CRACKS IN SOUTH SHEAR WALL (MODEL 1)

PHOTO 5.12_EAST CROSS-WALL DEFLECTED INWARD AT TOP (MODEL 1)

PHOTO 5.13_EAST WALL TOP PORTION FELL DOWN (MODEL 1)

PHOTO 5.14_TOP PORTION OF WEST WALL FELL DOWN (MODEL 1)

PHOTO 5.15_ROOF SLAB FREELY SUPPORTED ON TOP OF SHEAR WALLS (MODEL 1)

PHOTO 5.16_MAJOR PORTION OF EAST CROSS-WALL FELL DOWN (MODEL 1)

PHOTO 5.17_ROOF SLAB LIFTED OFF (MODEL 1)

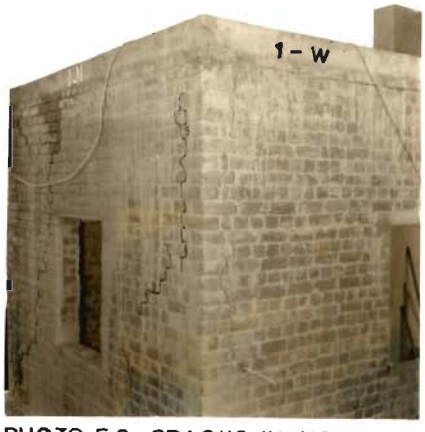

PHOTO 5.9_CRACKS IN NORTH AND WEST WALLS (MODEL 1)

PHOTO 5.10_VERTICAL CRACKS IN EAST CROSS WALL (MODEL 1)

PHOTO 5.11_VERTICAL AND DIAGONAL CRACKS IN SOUTH SHEAR WALL (MODEL 1)

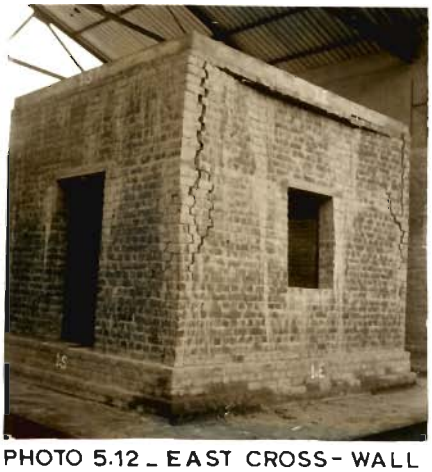

PHOTO 5.12_EAST CROSS-WALL DEFLECTED INWARD AT TOP (MODEL 1)

PHOTO 5.13_EAST WALL TOP PORTION FELL DOWN (MODEL 1)

PHOTO 5.14_TOP PORTION OF WEST WALL FELL DOWN (MODEL 1)

PHOTO 5.15_ROOF SLAB FREELY SUPPORTED ON TOP OF SHEAR WALLS(MODEL 1)

PHOTO 5.16_MAJOR PORTION OF EAST CROSS-WALL FELL DOWN (MODEL 1)

PHOTO 5.17_ROOF SLAB LIFTED OFF (MODEL 1)

PHOTO 5.18_ DIAGONAL CRACKS IN NORTH SHEAR WALL (MODEL 2)

PHOTO 5.19_VERTICAL AND DIAGONAL CRACKS IN SOUTH SHEAR WALL (MODEL 2)

PHOTO 5.20_MOSTLY DIAGONAL CRACKS IN NORTH WALL (MODEL 2)

PHOTO 5.21_ CRACKS IN WEST PIER OF SOUTH WALL AND WEST WALL (MODEL 2)

PHOTO 5.22_EAST PIER OF SOUTH WALL WITH FEW CRACKS (MODEL 2)

PHOTO 5.23_CRACKS IN TOP SPANDREL OF EAST WALL (MODEL 2)

PHOTO 5.24_ BOTTOM PORTION OF SOUTH-WEST CORNER PUSHED OUTWARDS (MODEL 2)

PHOTO 5.25_BOTTOM PORTION OF SOUTH-WEST AND SOUTH-EAST CORNERS PUSHED OUTWARDS (MODEL 2)

PHOTO 5.26_ SHIFTING OF NORTH-WEST CORNER BOTTOM (MODEL 2)

PHOTO 5.27_BIG GAP AT BOTTOM OF SOUTH-EAST AND SOUTH-WEST CORNERS (MODEL 2)

PHOTO 5.28_SOUTH-WEST CORNER PORTION ACTING AS A SEPARATE STRUCTURAL ELEMENT (MODEL 2)

PHOTO 5.29_SOUTH-WEST AND SOUTH-EAST CORNERS ACTING AS A SEPARATE STRUCTURAL ELEMENT (MODEL 2)

PHOTO 5.30_HALF TOP SPANDREL PORTION OF EAST CROSS-WALL

PHOTO 5.32_LOCALISED INITIAL CRACKS IN WEST WALL (MODEL3)

PHOTO 5.31_INITIAL CRACKS IN EAST CROSS-WALL (MODEL3)

PHOTO 5.33_INITIAL CRACKS BELOW ROOF SLAB OF SOUTH WALL (MODEL 3)

PHOTO 5.34_MANY INITIAL CRACKS IN NORTH SHEAR WALL (MODEL3)

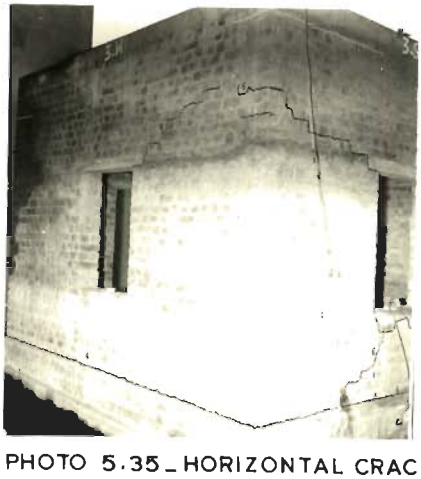

PHOTO 5.35_HORIZONTAL CRACKS IN SOUTH AND WEST WALLS AT PLINTH LEVEL (MODEL3)

PHOTO 5.36 _ MAINLY HORIZONTAL CRACKS IN EAST CROSS - WALL (MODEL 3)

PHOTO 5.37_ HORIZONTAL CRACKS IN NORTH SHEAR - WALL (MODEL 3)

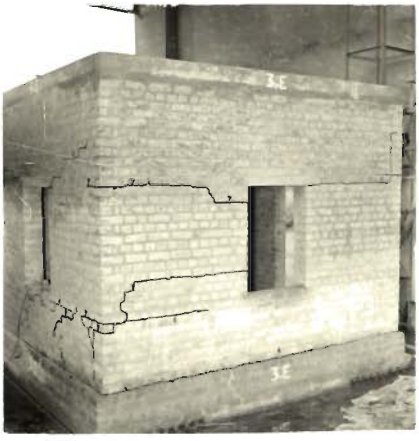

PHOTO 5.38_ CRACKS IN SOUTH AND EAST WALLS (MODEL 3)

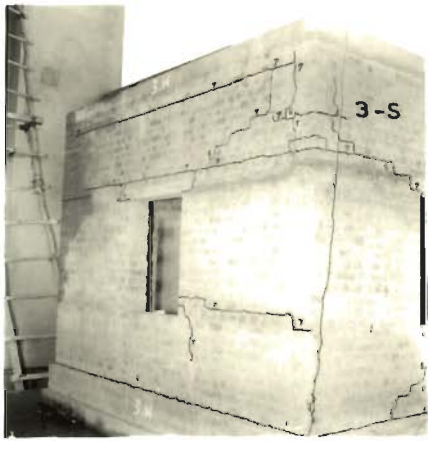

PHOTO 5.39_ CRACKS IN SOUTH AND WEST WALLS (MODEL 3)

PHOTO 5.40_ VERTICAL AND HORIZONTAL CRACKS IN NORTH AND WEST WALLS (MODEL 3)

PHOTO 5.41_ A SIGNIFICANT VERTICAL CRACK NEAR SOUTH-WEST CORNER (MODEL 3)

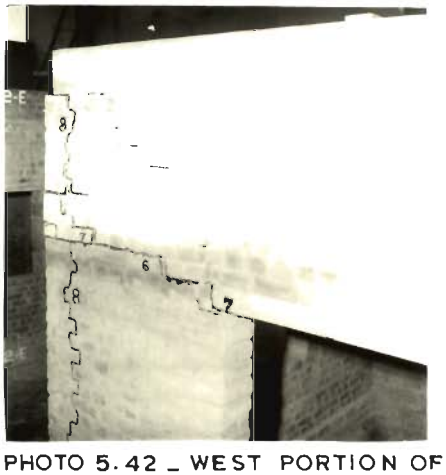

PHOTO 5.42 _ WEST PORTION OF TOP SPANDREL OF SOUTH WALL SHIFTED INWARD (MODEL 3)

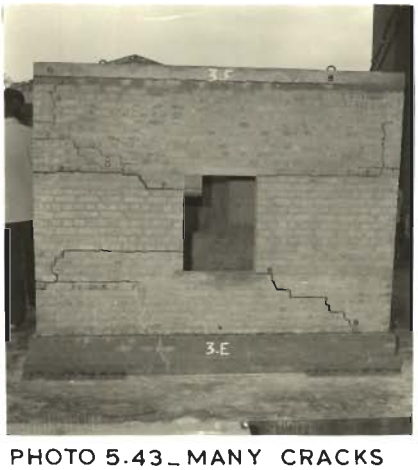

PHOTO 5.43_ MANY CRACKS DEVELOPED IN EAST WALL DURING SHOCK NO. 8 (MODEL 3)

PHOTO 5.44 _ WEST PIER OF NORTH WALL SLID OUTWARD (MODEL 3)

PHOTO 5.45_ WEST CROSS WALL BADLY DAMAGED (MODEL 3)

PHOTO 5.46_ SOUTH- SHEAR WALL IN BAD SHAPE (MODEL 3)

PHOTO 5.47_LARGE CHUNK OF MASONRY FROM WEST WALL FELL DOWN (MODEL 3)

PHOTO 5.48_ HORIZONTAL CRACKS IN SOUTH AND EAST WALLS (MODEL 4)

PHOTO 5.49_ FEW HORIZONTAL CRACKS IN WEST WALL (MODEL 4)

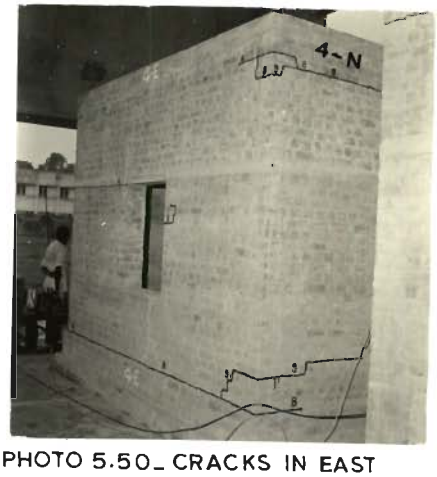

PHOTO 5.50_ CRACKS IN EAST CROSS-WALL (MODEL 4)

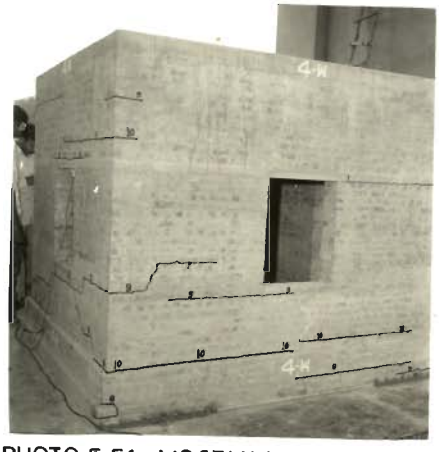

PHOTO 5.51_ MOSTLY HORIZONTAL CRACKS IN WEST CROSS-WALLS (MODEL 4)

PHOTO 5.53_ SIGNIFICANT HORIZONTAL AND DIAGONAL CRACKS IN TOP SPANDREL OF SOUTH WALL (MODEL4)

PHOTO 5.52_ DIAGONAL AND HORIZONTAL CRACKS IN SOUTH WALL (MODEL 4)

PHOTO 5.54_ FEW VERTICAL AND MOSTLY HORIZONTAL CRACKS IN WEST WALL (MODEL 4)

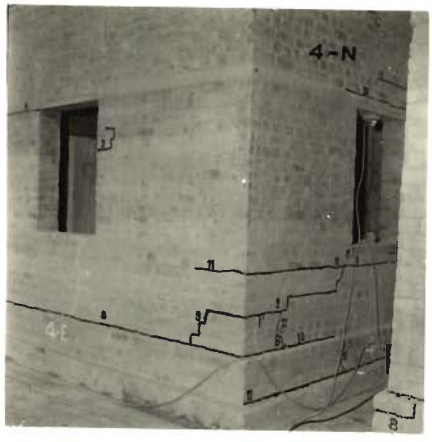

PHOTO 5.55_EAST PORTION OF BOTTOM SPANDREL OF NORTH WALL DEVELOPED MORE CRACKS (MODEL 4)

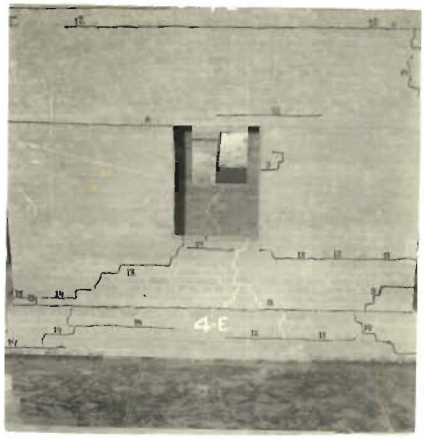

PHOTO 5.56 _ BOTTOM SPANDREL OF EAST WALL MORE CRACKED (MODEL4)

PHOTO 5.57_WELL DISTRIBUTED HORIZONTAL CRACKS IN WEST CROSS - WALL (MODEL 4)

PHOTO 5.58_BOTTOM PORTION OF NORTH-EAST CORNER DAMAGED (MODEL 4)

PHOTO 5.59_ TOP SPANDREL AND BOTTOM REGION OF SOUTH WALL MORE CRACKED (MODEL4)

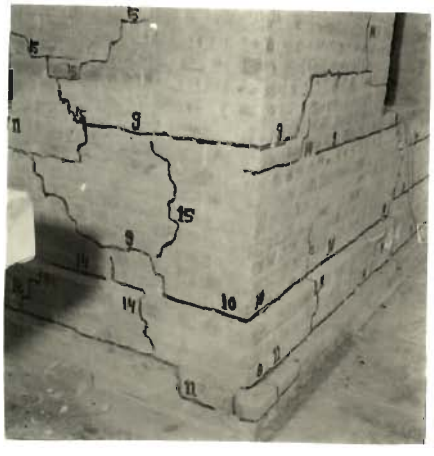

PHOTO 5.60_ NORTH - WEST CORNER BOTTOM REGION DAMAGED (MODEL4)

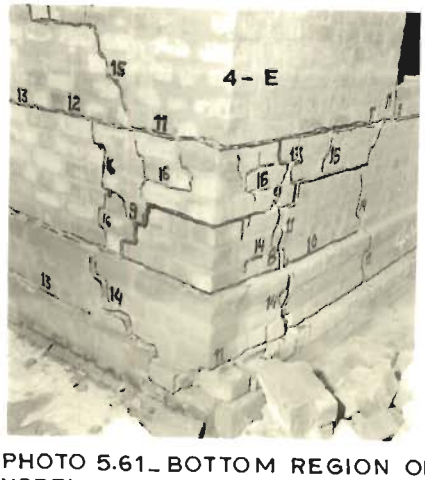

PHOTO 5.61_ BOTTOM REGION OF NORTH- WEST CORNER GREATLY DAMAGED AND SHIFTED OUTWARD (MODEL 4)

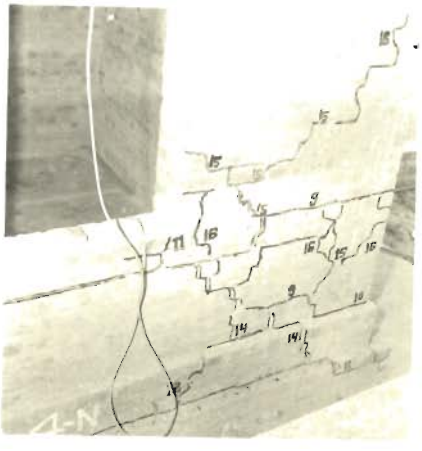

PHOTO 5.62_ BOTTOM PORTION OF NORTH- WEST CORNER SHIFTED OUTWARD (MODEL 4)

PHOTO 5·63_CRACKS IN BOTTOM REGION OF SOUTH WALL PIERS (MODEL 4)

PHOTO 5·64_NORTH-EAST AND NORTH WEST CORNERS PUSHED OUTWARD (MODEL 4)

PHOTO 5·65_INITIAL CRACKS (BELOW WINDOW) OPENED UP IN SHOCK NO.15 (MODEL4)

PHOTO 5·66_RIGHT PORTION OF WEST WALL BETWEEN PLINTH AND WINDOW SILL LEVELS SHIFTED OUTWARDS (MODEL 4)

PHOTO 5·67_SEVERE DAMAGE OF NORTH-EAST AND NORTH-WEST CORNERS (MODEL 4)

PHOTO 5·68_SOUTH-WEST CORNER SHIFTED OUTWARD (MODEL 4)

PHOTO 5·69_PORTION BETWEEN PLINTH AND WINDOW SILL LEVELS OF WEST WALL SHIFTED TOWARDS SOUTH (MODEL 4)

PHOTO 5·70_DIFFERENT DAMAGED PORTIONS OF WEST WALL SHIFTED BODILY CREATING WIDE GAPS BETWEEN THEM (MODEL4)

PHOTO 5.71_NORTH SHEAR-WALL AT THE VERGE OF COLLAPSE (MODEL 4)

PHOTO 5.72_FINE DIAGONAL CRACKS IN EAST PIER OF NORTH WALL (MODEL 5)

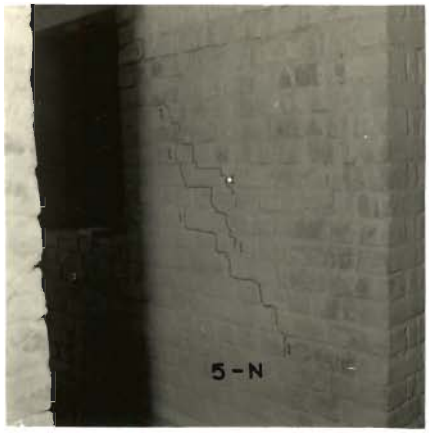

PHOTO 5.73_FINE DIAGONAL CRACKS IN WEST PIER OF NORTH WALL (MODEL 5)

PHOTO 5.74_DIAGONAL CRACKS IN BOTH PIERS OF SOUTH SHEAR WALL (MODEL 5)

PHOTO 5.75_EAST WALL MOVED TOWARDS WEST (MODEL 5)

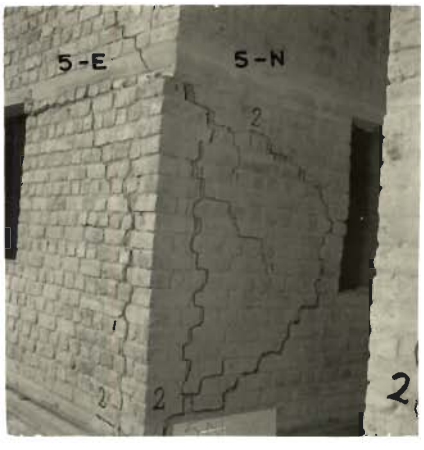

PHOTO 5.76_NORTH EAST CORNER BADLY DAMAGED BETWEEN LINTEL BAND AND BOND BEAM (MODEL 5)

PHOTO 5.77_WELL DISTRIBUTED WIDE CRACKS IN SOUTH SHEAR WALL (MODEL 5)

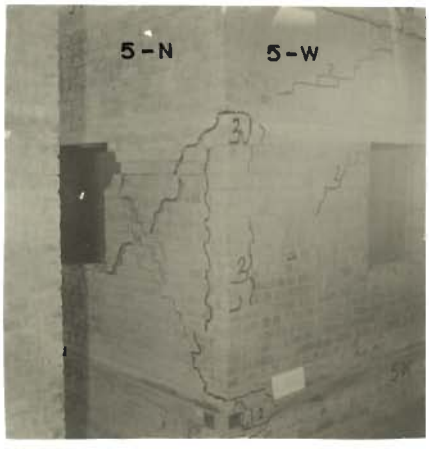

PHOTO 5.78_STAR CRACK PATTERN IN BADLY DAMAGED WEST PIER OF NORTH WALL (MODEL 5)

PHOTO 5.79 FEW HORIZONTAL AND DIAGONAL CRACKS IN EAST WALL (MODEL 5)

PHOTO 5.80 FEW HORIZONTAL AND DIAGONAL CRACKS IN WEST WALL (MODEL 5)

PHOTO 5·81_SEPARATION OF EAST WALL INITIATED AT SOUTH-EAST CORNER (MODEL 5)

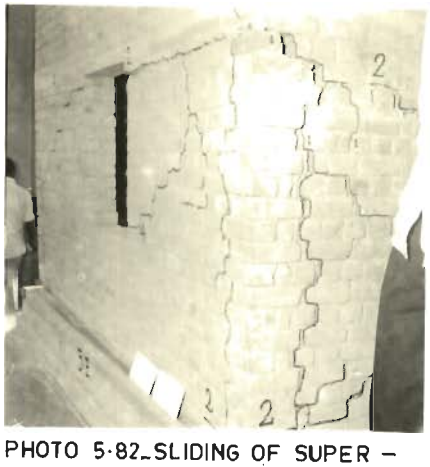

PHOTO 5·82_SLIDING OF SUPER - STRUCTURE SEEN AT PLINTH BAND OF EAST WALL (MODEL 5)

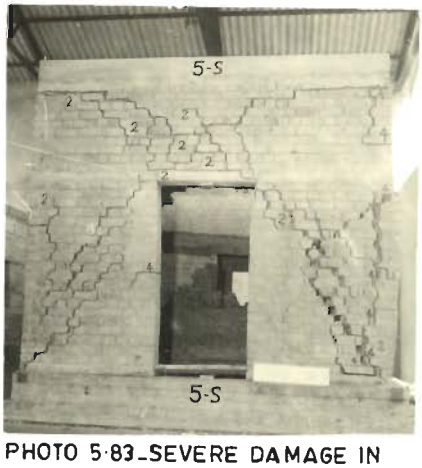

PHOTO 5·83_SEVERE DAMAGE IN SOUTH SHEAR WALL (MODEL 5)

PHOTO 5·84_NORTH SHEAR WALL AT THE VERGE OF FALLING DOWN WHILE WEST WALL IN A BETTER SHAPE (MODEL 5)

PHOTO 5·85_UPPER PART OF NORTH-EAST CORNER FELL DOWN COMPLETELY (MODEL 5)

PHOTO 5·86_EAST CROSS-WALL IN VERY BAD SHAPE (MODEL 5)

PHOTO 5·87_MAJOR PORTION OF NORTH SHEAR WALL COLLAPSED (MODEL 5)

PHOTO 5·88_WELL DISTRIBUTED HORIZONTAL CRACKS IN NORTH SHEAR WALL (MODEL 6)

PHOTO 5·89_NORTH SHEAR-WALL PIER BROKEN INTO SEPARATE BLOCKS (MODEL 6)

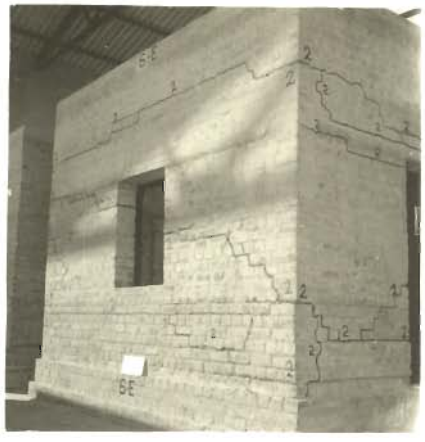

PHOTO 5.90 _ EXTENSIVE HORIZONTAL AND DIAGONAL CRACKS IN EAST WALL (MODEL 6)

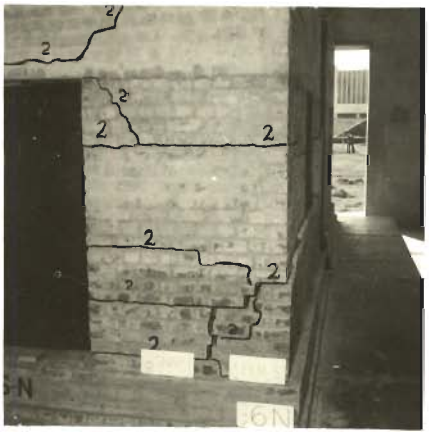

PHOTO 5.91_BOTTOM PORTION OF NORTH-WEST CORNER SHIFTED INWARD (MODEL 6)

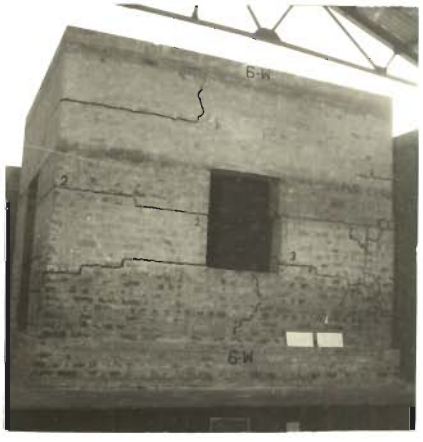

PHOTO 5.92 _ WEST CROSS-WALL BADLY DAMAGED, ITS RIGHT PIER BROKEN INTO TWO PARTS (MODEL 6)

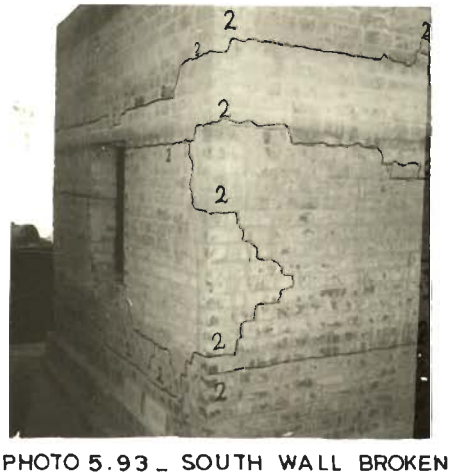

PHOTO 5.93 _ SOUTH WALL BROKEN INTO DIFFERENT BLOCK (MODEL 6)

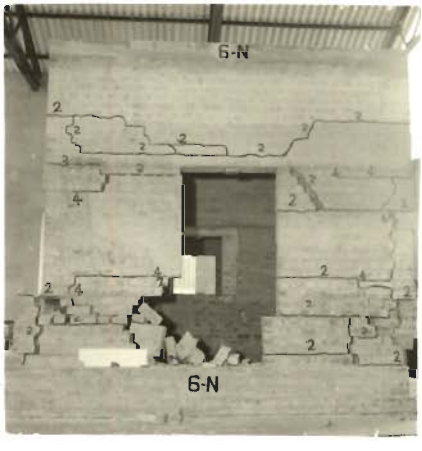

PHOTO 5.94_NORTH WALL BROKEN INTO SEPARATE BLOCKS, BOTTOM PORTION OF LEFT PIER FELL DOWN (MODEL 6)

PHOTO 5.95 _ A VERTICAL CRACK OPENING OF 50 mm AT SOUTH - WEST CORNER (MODEL 6)

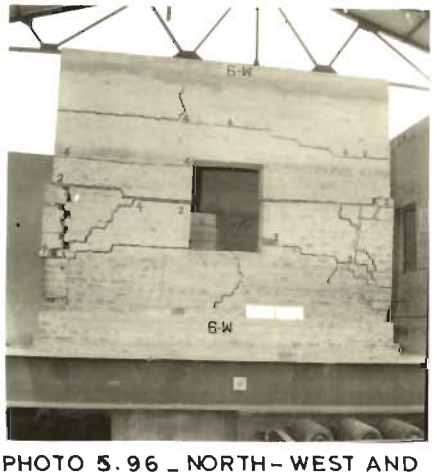

PHOTO 5.96 _ NORTH - WEST AND SOUTH - WEST CORNERS PORTIONS BADLY DAMAGED AND BULGED OUT (MODEL 6)

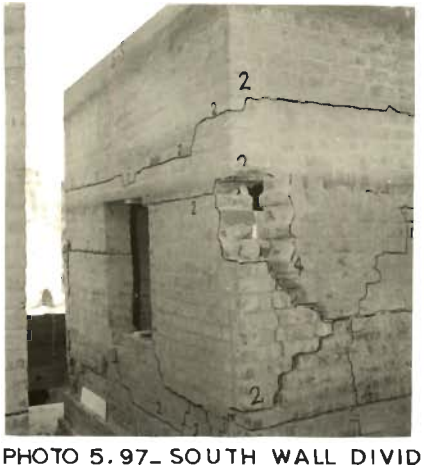

PHOTO 5.97_ SOUTH WALL DIVIDED INTO LARGE CHUNKS, MOVED FROM THEIR POSITION (MODEL 6)

PHOTO 5.98 _ PIERS OF EAST WALL DESHAPED BY SHIFTING OF DIFFERENT BLOCKS (MODEL 6)

PHOTO 5.99 _ WEST AND NORTH WALLS AT THE VERGE OF COLLAPSE (MODEL 6)

PHOTO 5.100 _ FEW FINE HORIZONTAL CRACKS IN NORTH SHEAR WALL (MODEL 7)

PHOTO 5.101_ TWO REFERENCE LINES IN WHITE PAINT ON VERTICAL FACES OF PLINTH BAND TO MEASURE AMOUNT OF SLIDING (MODEL7)

PHOTO 5.102_ A BLACK STRIP SEEN AT PLINTH BAND AFTER SLIDING OF EAST WALL TOWARDS WEST (MODEL 7)

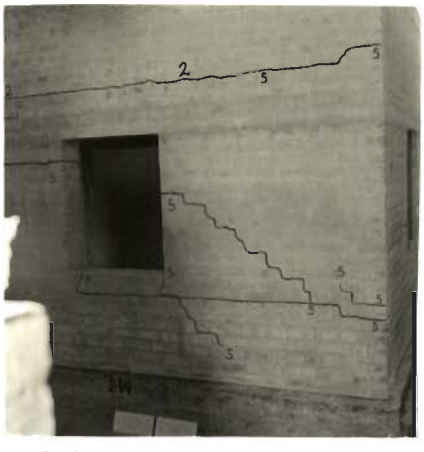

PHOTO 5.103 _ A FINE HORIZONTAL CRACK MARKED BY 2 IN WEST WALL (MODEL 7)

PHOTO 5.104 _ BOTTOM EDGES OF NORTH WALL PIERS LIFTED UP BY ABOUT 5mm, WEST WALL OVER-HANGING OVER PLINTH BAND (MODEL 7)

PHOTO 5.105 _ LARGE SHIFT OF EAST WALL AT PLINTH BAND (MODEL 7)

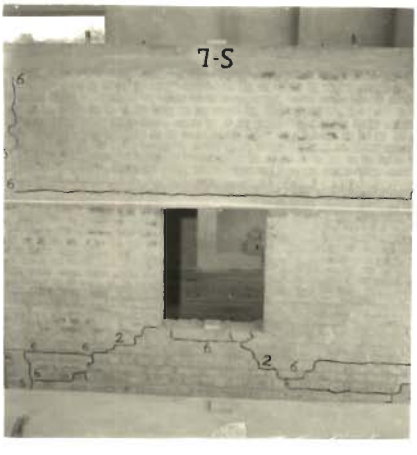

PHOTO 5.106 _ NO FRESH CRACKS IN SOUTH WALL DURING SHOCK NO. 5 (MODEL7)

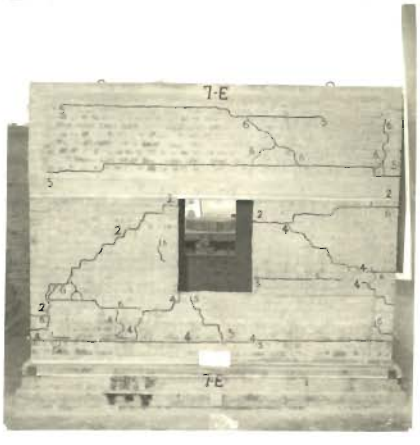

PHOTO 5.107 _ MANY HORIZONTAL AND DIAGONAL CRACKS IN EAST CROSS-WALL DURING SHOCK NO. 5 (MODEL 7)

PHOTO 5.108_ A FEW HORIZONTAL AND DIAGONAL CRACKS IN WEST CROSS-WALL DURING SHOCK NO.6 (MODEL 7)

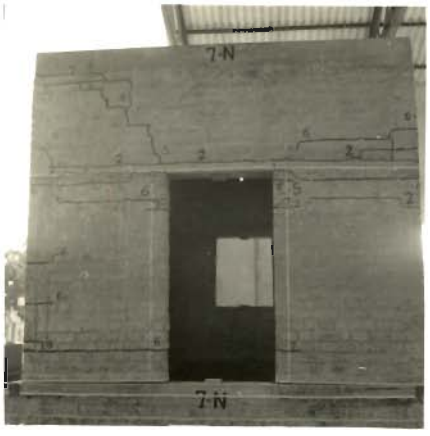

PHOTO 5.109_ MAINLY HORIZONTAL AND FEW DIAGONAL CRACKS IN NORTH SHEAR WALL DURING SHOCK NO.6 (MODEL 7)

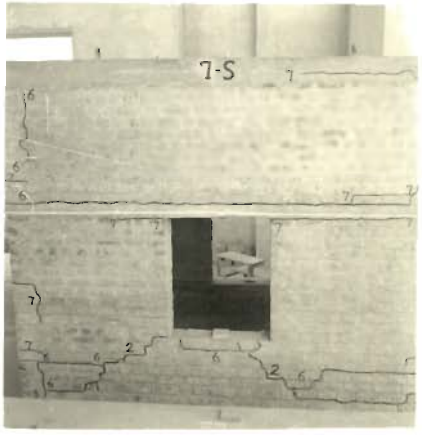

PHOTO 5.110_ MAINLY HORIZONTAL CRACKS DEVELOPED IN SOUTH WALL DURING SHOCK NO. 7 (MODEL 7)

PHOTO 5.111_ MANY NEW CRACKS APPEARED IN EAST CROSS WALL AFTER SHOCK NO. 7 (MODEL 7)

PHOTO 5.112_ LEFT PIER OF EAST WALL SEPARATED INTO TWO PORTIONS, WESTWARD SLIDING OF WALL (MODEL 7)

PHOTO 5.113 _ SEVERLY DAMAGED NORTH SHEAR WALL DURING SHOCK NO. 8 (MODEL 7)

PHOTO 5.114 _ RIGHT PIER SEPARATED FROM RIGHT PORTION OF BOTTOM SPANDREL OF SOUTH WALL (MODEL7)

PHOTO 5.115 _ UPPER PORTION OF LEFT PIER OF EAST WALL THROWN OUT DURING SHOCK NO.8 (MODEL 7)

PHOTO 5.116_ EXPOSED STEEL BAR IN WESTWARD PLINTH BAND DURING SHOCK NO.8 (MODEL 7)

PHOTO 5.117_FOUNDATION MASONRY UNDER WEST WALL VERY BADLY DAMAGED (MODEL 7)

PHOTO 5.118_UPPER PART OF WEST WALL RIGHT PIER DISPLACED OUTWARD TOWARD NORTH (MODEL 7)

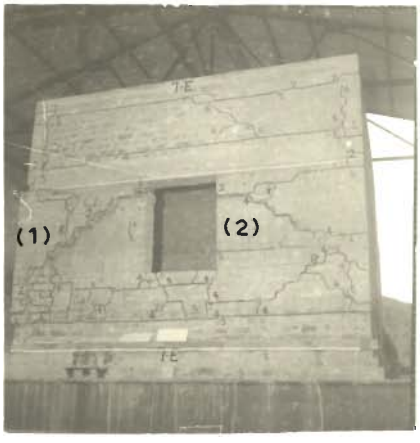

PHOTO 5.119_MAJOR MASONRY BLOCKS MARKED (1) AND (2) SHIFTED EASTWARD DURING SHOCK NO. 8 (MODEL 7)

PHOTO 5.120_A HORIZONTAL CRACK AT JUNCTION OF, SOUTH AND EAST WALL WITH PLINTH BAND (MODEL 8)

PHOTO 5.121_MANY CRACKS IN BOTTOM SPANDREL OF NORTH SHEAR WALL (MODEL 8)

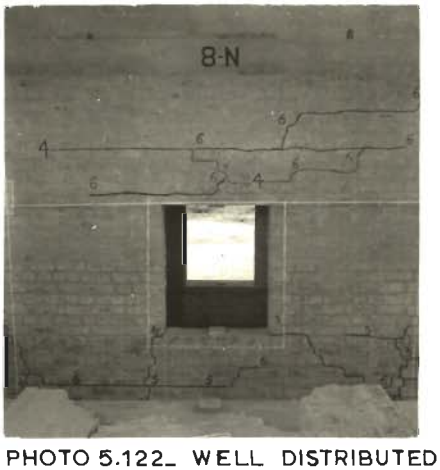

PHOTO 5.122_WELL DISTRIBUTED CRACKS IN TOP AND BOTTOM SPANDRELS OF NORTH WALL (MODEL 8)

PHOTO 5.123_MANY CRACKS IN TOP SPANDREL OF SOUTH WALL, ITS LEFT PIER BOTTOM DAMAGED (MODEL 8)

PHOTO 5.124_VERTICAL AND HORIZONTAL CRACKS IN EAST WALL (MODEL 8)

PHOTO 5.125_HORIZONTAL AND VERTICAL CRACKS IN WEST WALL (MODEL 8)

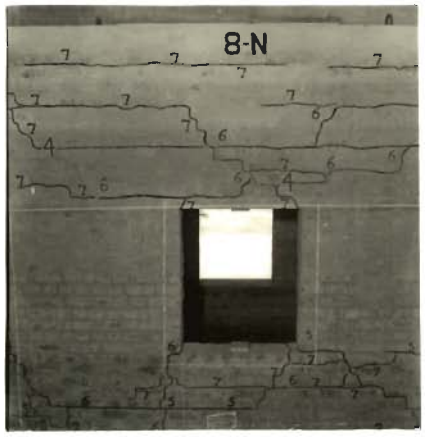

PHOTO 5.126 _ TOP SPANDREL OF NORTH WALL HEAVILY DAMAGED DURING SHOCK NO·7 (MODEL 8)

PHOTO 5.127_BOTTOM REGION OF NORTH-WEST CORNER BADLY DAMAGED (MODEL 8)

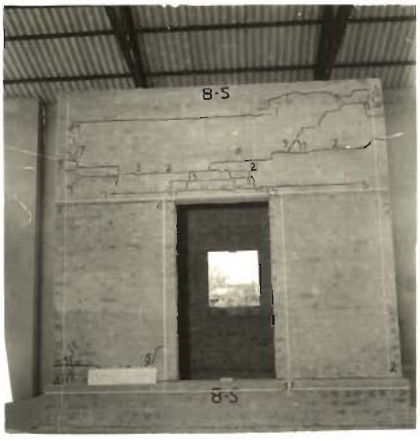

PHOTO 5.128_ SOUTH WALL TOP SPANDREL HEAVILY DAMAGED DURING SHOCK NO·7 (MODEL 8)

PHOTO 5.129 _ TOP SPANDREL OF LEFT PIER OF WEST WALL (MODEL 8)

PHOTO 5.130_ RIGHT PIER OF EAST CROSS WALL HEAVILY DAMAGED (MODEL 8)

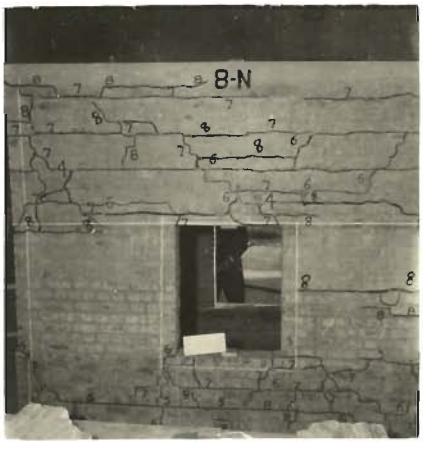

PHOTO 5.131_ SEVERLY DAMAGED NORTH WALL DURING SHOCK NO·8 (MODEL 8)

PHOTO 5.132 _ BOTTOM PORTION OF NORTH-EAST CORNER SHIFTED EASTWARD (MODEL 8)

PHOTO 5.133 _ NORTH WEST CORNER DISPLACED WESTWARD AT PLINTH BAND BY 30 mm (MODEL 8)

PHOTO 5.134_ WIDE OPEN CRACK BELOW PLINTH BAND OF SOUTH WALL DURING SHOCK NO. 8 (MODEL 8)

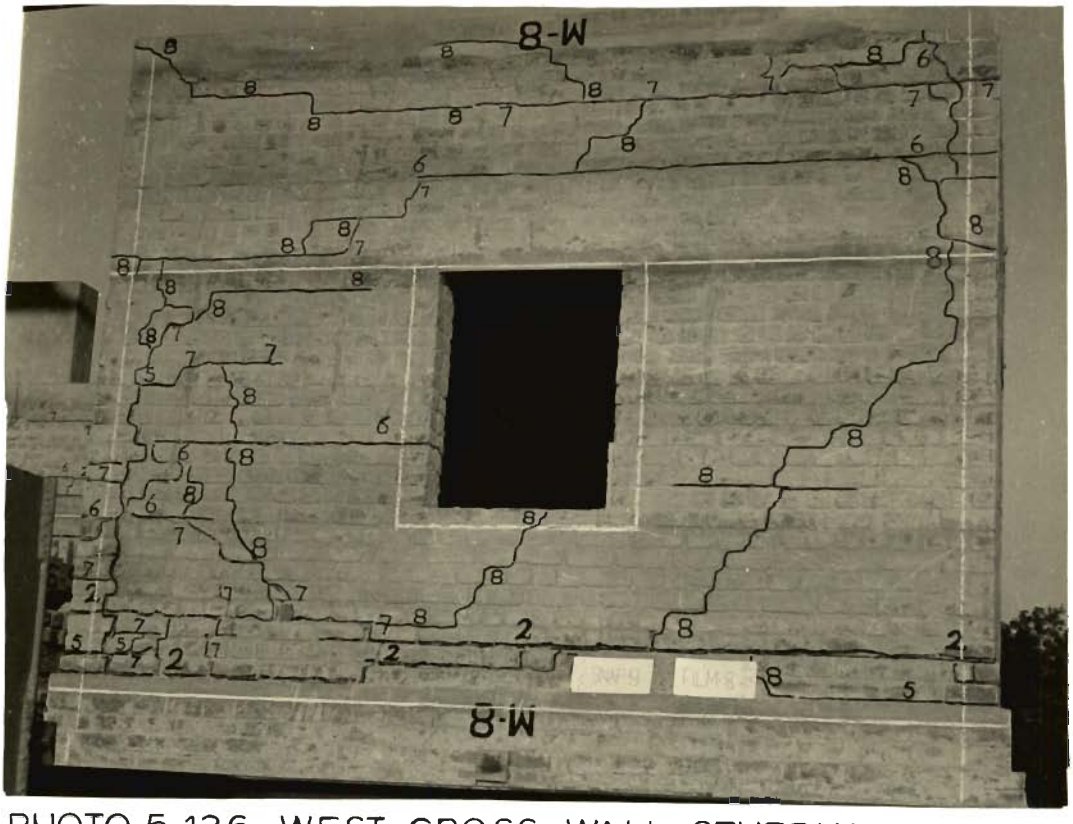

PHOTO 5.136_WEST CROSS WALL SEVERLY DAMAGED DURING SHOCK NO. 8 (MODEL 8)

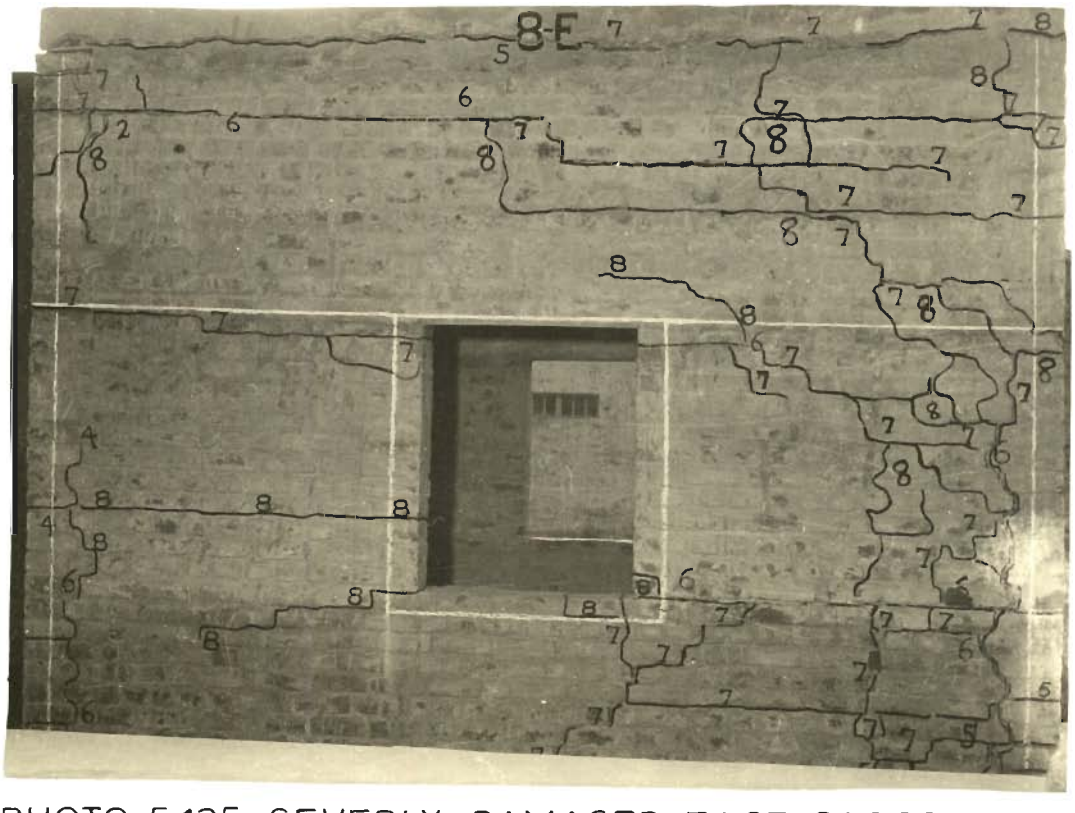

PHOTO 5.135_SEVERLY DAMAGED EAST CROSS WALL DURING SHOCK NO. 8 (MODEL 8)

CHAPTER 6

SUMMARY OF RESULTS AND CONCLUSIONS

6.1 GENERAL

A summary of the investigations carried out and results obtained is presented here under the following divisions:

(a) Dynamic response analysis of conventional brick building subjected to earthquake shocks.

(b) Pilot tests on sliding building models conducted to examine the feasibility of isolating the base motion or reducing its influence on the structure.

(c) Analysis of sliding type single-storeyed buildings subjected to earthquake excitations.

(d) Dynamic shock tests on half scale building models having different types of reinforcing arrangement as well as sliding at base.

Finally the main conclusions from these studies are presented and a few problems suggested for further research.

6.2 SEISMIC RESPONSE OF CONVENTIONAL BUILDINGS

The maximum tensile, shear and compressive stresses have been computed in the piers of single and multistoreyed brick buildings subjected to Koyna and El Centro earthquake accelerograms representing

two seismicity levels. Hence, the critical sections of the walls in the longitudinal and transverse directions of the buildings have been identified. The requirements of reinforcing steel have been estimated at the critical sections and thereby the reinforcing provisions of the Indian Standard Code IS:4326-1976 have been evaluated. A summary of the results is given below:

(1) It is found that under the action of severe shocks, tensile stresses exceeding the ultimate tensile strength of brick masonry may develop in all the piers. However, the compressive stresses are seen not to exceed the ultimate compressive strength and crushing of brick masonry does not seem to be a problem upto four storeys. But the shearing stresses exceed the shearing strength excessively. Thus tensile and shearing strengths turn out to be critical parameters in the safety of brick buildings during severe earthquakes.

(2) Vertical steel is necessarily required at the critical sections in view of deficiency of brick masonry to resist tensile stresses. The estimate of vertical steel shows that the quantity of reinforcement increases with the height of the building and with the severity of the earthquake.

(3) The estimated vertical steel has been compared with the reinforcing provisions of the Indian Standard Code. For this, the results obtained for

the buildings subjected to Koyna shock are compared with the provisions of steel as given in the Code for areas with design seismic coefficient equal to and more than 0.08. Similarly, the case of buildings subjected to El Centro shock is compared with the provisions for areas having design seismic coefficient of 0.06 or more but less than 0.08. This comparison shows that the reinforcing provisions of Indian Code are surprisingly close to the calculated requirements.

(4) Analysis shows that the brick buildings are quite deficient in shearing strength as well. Requirements of horizontal steel for taking shears in the piers have been estimated. No such provisions exist, however, in any of the seismic codes.

6.3 PILOT TESTS ON SLIDING BUILDING

Preliminary tests on sliding building models of one-fourth scale were performed to study the effect of different coefficients of friction on the response of the model by inserting graphite powder, dry sand and wet sand separately between the shake table top and base of the models. The model was first tested with base free to slide under steady-state horizontal table motion and then with fixed base. The following significant results are obtained:

(1) In all cases of sliding base, the roof acceleration is less than the corresponding table acceleration.

(2) The ratio of roof to base acceleration increases as the coefficient of friction increases.

(3) In the case of model with fixed base, roof acceleration is much more than the table acceleration.

(4) No damage was observed in the models with sliding base whereas cracks developed in them when tested with fixed base under the same base accelerations.

6.4 SEISMIC RESPONSE OF THE SLIDING BUILDINGS

Seismic response of the sliding buildings has been computed and compared with the seismic response of conventional type building having the same dimensions. The important results achieved in this study are as follows:

(1) Unlike the conventional systems, the friction spectral values do not change much with the period of the system for any value of mass ratio, critical damping or coefficient of friction for Koyna as well as El Centro shocks. Only slight variation in spectral acceleration has been observed, that too for coefficients of friction more than 0.25.

(2) Significant variation in the residual and maximum displacements is noticed with the change in time period while other parameters are kept constant. The variation of displacement with time period is of a typical pattern except in a few cases of parameter combinations.

(3) The increase in damping coefficient decreases the spectral acceleration value in all cases for sliding as well as conventional systems.

(4) For low values of coefficient of friction, the variation of relative displacement with viscous damping is rather inconsistent and does not follow the usual trend where the response decreases with increase in damping. However as μ increases, the pattern of the spectal displacement becomes more regular with respect to viscous damping. That is, for most of the period range and for almost all value of mass ratio, the displacement response decreases as viscous damping increases.

(5) The spectral acceleration generally decreases as coefficient of friction decreases in practically all cases of different parameter combinations of the system for both the earthquakes considered.

(6) As coefficient of friction decreases, the spectral dipplacement increases for various values of mass ratio as well as damping.

(7) The spectral acceleration decreases as the mass ratio increases, in all cases for both the shocks.

(8) In most cases, the spectral displacement decreases as the mass ratio increases keeping the other parameters constant.

(9) Comparison of acceleration response for the conventional system having the same period and damping as the sliding system indicates that the spectral acceleration of the latter is much less than that of the former for both El Centro and Koyna earthquakes and for all combinations of the parameters but with an exception.

The only exception is the sliding systems having period less than 0.05 second and coefficient of friction nearer to the peak ground acceleration of the El Centro shock where the response of the conventional system is less. Use of sliding in such a case is to be avoided.

6.5 EXPERIMENTAL BEHAVIOUR OF BUILDING MODELS

Experimental behaviour of conventional and sliding type buildings has been studied by dynamic shock tests on single-storeyed half scale models upto ultimate stage. Also, the relative competence of different brick building systems have been examined. Description of models 1 through 8 are given below for ready reference:

Model No.	Description
1	Unstrengthened in mud mortar
2	Strengthened with lintel band and vertical steel at corners and jambs, built in mud mortar
3	Unstrengthened in cement mortar
4	Similar to model 2 but built in cement mortar
5	Sliding type in mud mortar
6	Unstrengthened with lintel band and built in cement mortar
7	Sliding type in cement mortar
8	Similar to model 4 but plinth band in addition

The significant results of this part of the investigations are briefly enumerated in the following paragraphs,

(1) The extent of damage of all the models increases with the increase in input energy whether given in one big shock, or a number of small shocks. This happens only if intensity of each shock exceeded the damge threshold.

(2) The percentage damage in strengthened structure in cement mortar (model 4) is much less compared to that in a similarly strengthened model in mud mortar (model 2) for the same amount of input energy.

(3) The unstrengthened structure in cement mortar (model 3) performed much better than the

structure in mud mortar (model 1) with respect to strength as well as input energy. Model 3 resisted about 2.3 times as much input energy as model 1 at total damage level. Also, model 3 could resist base acceleration two times that of model 1 to reach total damage level.

(4) The sliding type structure (model 7) and the fully strengthened structure in cement mortar (model 8) behaved similarly in regard to damage as the input energy supplied by the shocks was increased in the initial stages. But later the sliding models showed better behaviour. For example, the sliding type model built in mud mortar (model 5) showed less damage compared to the conventional structure in cement mortar even when having the lintel band (model 6). In the final stages of shocks, almost similar extent of damage was observed in the models 5 and 6 while model 7 showed less damage than model 8.

(5) The strengthened structure in mud mortar (model 2) was not only stronger than the corresponding unstrengthened model but was also capable of withstanding four times as much input energy as the unstrengthened structure.

(6) The strengthened model in mud mortar (model 2) performed better than the unstrengthened structure in cement mortar (model 3) although their

cost of construction works out to be almost same.

(7) The extent of damage of the strengthened structure in cement mortar (model 4) increases more or less uniformly with the increasing input energy. This structure withstood about thrice as much input energy as the corresponding unstrengthened structure (model 3) to reach its total damage condition while increase in its cost was only about 4.5 percent.

(8) The sliding base (model 7) and fully strengthened (model 8) structures did not reach their total damage level even upto the last shock imparted during the tests.

(9) As the number of shocks and damage level increased, the amplification of acceleration in model 4 generally decreased indicating decreasing stiffness and elongation of period. Similar trends were also observed in models 5 to 8. The roof acceleration of sliding type structure (model 7) was remarkably less compared to the base motion and the roof acceleration of other models.

(10) The dynamic behaviour of the structures, strengthened with steel or with provision of sliding at plinth was considerably improved both in terms of resistance to base acceleration and capacity to dissipate input energy. This improved behaviour was achieved at little increase in cost of their construction.

(11) There is a reasonable agreement between the theoretical acceleration response at roof level computed for the observed table motion and the experimentally observed values of roof accelerations in test structures 6 and 8.

(12) Attempt made for predicting the damage threshold acceleration of prototype buildings from the observed damage threshold of models indicates that a Koyna type accelerogram with the maximum peak scaled down to 0.16 g would be needed to just cause cracking in brick buildings of good quality construction in 1:6 cement-sand mortar.

6.6 CONCLUSIONS

The following general conclusions are arrived at from the present study:

(1) Material Strength. Analytical response study of one to four storeyed brick buildings and dynamic tests of one storey half scale models confirm that the usually low tensile and shearing strengths of brickwork are the main cause of cracking, displacements and collapse during severe earthquakes.

(2) Unstrengthened Conventional Buildings. Unstrengthened brick buildings of conventional construction show varied strength and energy capacity depending on the mortar bond strength. Also the damage threshold

acceleration is seen to be quite low as predicted for the prototype buildings from the model tests. Hence they could be used without strengthening measures only in areas of low to medium seismicity and in low height construction. Rational limits are yet to be determined.

(3) Buildings with Strengthening Measures. Calculations of required steel reinforcement in one to four storeyed brick buildings and shock-table tests of one storey half scale models to destruction show that the provisions of lintel band as horizontal steel and vertical steel at corners and junctions of walls as well as at jambs of openings as per IS:4326 is generally adequate in imparting the desired strength and energy absorbing capacity even for the probable maximum earthquakes. The only deficiency is in the shearing strength of piers for which specifications for providing hoeizontal steel reinforcement are called for.

(4) Buildings with Sliding Joint at Plinth Level. From the analytical response study of one storey brick buildings resulting into "frictional response spectra" and the shock-table tests on one storey half scale models it is clearly seen that there is significant reduction in the effective seismic force acting on the superstructure to the extent that the cracking and damage are much reduced and the behaviour was as good as the buildings with strengthening measures. The

relative displacement at the plinth level depends on the coefficient of friction but is not so large as to throw away the building off its plinth altogether.

(5) Behaviour of Damaged Building. It is seen from the damage study of the model tests that once a brick building cracks, its strength and threshold acceleration for further damage go on reducing as the extent of damage increases. Also the rate of damage tends to increase under subsequent shocks of equal intensity. Therefore minor looking cracks in such buildings caused during an earthquake shock should not be ignored or simply plastered over but should be grouted fully so as to restore original strength.

6.7 PROBLEMS FOR FUTURE INVESTIGATION

A number of problems which could not be investigated in this thesis and are considered important are stated below for further research:

(a) Cross Walls. To study the behaviour of cross-walls to work out requirements of their strengthening for realistic earthquake motions and their contribution to the seismic resistance of brick building through 'flange' action with shear walls or box action of whole building. Both analytical and experimental investigations will be necessary.

(b) Strengthened Conventional Building. To analyse the dynamic response and behaviour of strengthened single and multistoreyed brick buildings of conventional construction subjected to real earthquake shocks taking into account the flange effect of cross-walls and cracked sections of brick piers and verify the same through suitable large scale or prototype tests.

(c) Sliding Buildings. To extend the study carried out in this thesis to cover multistoreyed buildings both analytically and experimentally.

(d) Restoration of Damaged Buildings. To perform dynamic tests on damaged large scale brick building models after their proper repairing so as to evaluate their strength under shock loads and to predict the behaviour of prototype building damaged and then repaired under similar situations.

REFERENCES

1. Agnihotri, V.K., "Strength of Single Storeyed Brick Shear Walls Against Earthquake Forces", M.E. Thesis, Civil Engineering Department, University of Roorkee, Roorkee, 1962.

2. Arya, A.S., "Design and Construction of Masonry Buildings in Seismic Areas", Bull. Indian Society of Earthquake Technology, Vol. 4, No. 2, 1967.

3. Arya, A.S., "Construction of Small Buildings in Seismic Areas", Bull. Indian Society of Earthquake Technology, Vol. 5, Nos. 3 and 4, 1968.

4. Arya, A.S., Chandra, B. and Gupta, P.R., "Influence of Natural Disasters (Earthquakes) on Educational Facilities", Annotated Bibliography - Annexure to Part I, Final Report submitted to Educational Facilities Division, UNESCO, Paris, School of Research and Training in Earthquake Engineering, University of Roorkee, Roorkee, Dec. 1977.

5. Arya, A.S., Chandra, B., and Gupta, P.R., "Influence of Natural Disasters (Earthquakes) on Educational Facilities, Part I, Final Report submitted to Educational Facilities Division, UNESCO, Paris, School of Research and Training in Earthquake Engineering, University of Roorkee, Roorkee, Dec. 1977.

6. Arya, A.S. and Pal, S., "Analysis of Shear Walls With Opening", Cement and Concrete, October-December 1969, pp. 217-230.

7. Arya, A.S. and Swaminathan, V., "Multistorey Brick Shear Walls under Lateral Earthquake Forces", Earthquake Engineering Studies, School of Research and Training in Earthquake Engineering, University of Roorkee, 1969.

8. Arya, A.S., Chandra, Brijesh and Thakkar, S.K., "Influence of Natural Disasters (Earthquakes) on Educational Facilities, Part II, Final Report Submitted to Educational Facilities Division, UNESCO, Paris, School of Research and Training in Earthquake Engineering, University of Roorkee, Dec. 1977.

9. Benjamin, J.R., "Statically Indeterminate Structure", McGraw Hill, 1959.

10. Benjamin, J.R. and Williams, H.A., "The Behaviour of One Storey Brick Shear Walls", Proc. of ASCE, Journal of Structural Division, Vol. 84, No. ST4,1958.

11. Benett, A.A., Milne and Bateman, H., "Numerical Integration of Differential Equations", Chapter III, Dover Publications, Inc., New York, 1956.

12. Blume, J.A., Newmark, N.M. and Corning, L.H.,"Design of Multistorey Reinforced Concrete Buildings for Earthquake Motions, Portland Cement Association, Illinois, 1961.

13. Chandra, B., "Strength of Single Storeyed Unreinforced Brick Buildings Against Earthquake Forces", M.E. Thesis, Civil Engineering Department, University of Roorkee, Roorkee, 1963.

14. Chandra, Brijesh, "Study of Inelastic Response of Multistorey Frames During Earthquakes", Ph.D. Thesis, University of Roorkee, Roorkee, 1971.

15. Chandra, Brijesh and Kumar, Krishen, "Earthquake Resistant Construction of Brick Buildings", Earthquake Engineering, Sarita Prakashan, Meerut, India, 1974.

16. Chandrasekaran, A.R., "Earthquake Response of Friction Mounted Masses", Bull. of Indian Society of Earthquake Technology, Vol. VII, No. 1, March,1970. pp. 47-53.

17. Chandrasekaran, A.R., Srivastava, L.S. and Arya, A.S., "Behaviour of Structures in the Koyna Earthquake of December 11, 1967, "The Indian Concrete Journal, December 1969.

18. Haller, P., "Load Capacity of Brick Masonry", Designing, Engineering and Constructing with Masonry Products, edited by F.B. Johnson, 1969.

19. Hilsdorf, H.J., "Investigations into the Failure Mechanism of Brick Masonry Loaded in Axial Compression", Designing, Engineering and Constructing with Masonry Products, edited by F.B. Johnson, Gulf Publishing Company, Houston, Tex., 1969.

20. Housner, G.W., "Behaviour of Structures during Earthquakes", Journal of Engineering Mechanics Division, ASCE, Vol. 85, No. EM-4, pp. 109-129, 1959.

21. IS:1893-1975, "Indian Standards Code of Practice for Earthquake Resistant Design of Structures", Indian Standards Institution, New Delhi.

22. IS: 4326-1976, "Indian Standards Code of Practice for Earthquake Resistant Construction of Buildings", Indian Standards Institution, New Delhi.

23. Joshi, R.N., "Striking Behaviour of Structures in Assam Earthquakes", Proc. of Second World Conference on Earthquake Engineering, Japan 1960, Vol. III, pp. 2143-2158.

24. Kalita, U.C. and Hendry, A.W., "An Experimental and Theoretical Investigation of the Stresses and Deflections in Model Cross-Wall Structures", Proc. of Second International Brick Masonry Conference, Stoke-on-Trent, April, 1970.

25. Keightley, W.O., "Report of Indo-U.S. Subcommission on Education and Culture", School of Research and Training in Earthquake Engineering, University of Roorkee, Roorkee, 1977.

26. Krishna, J., and Arya, A.S., "Earthquake Resistant Design of Buildings", Journal of the Institution of Engineers (India), Vol. XLV, No. 7, 1965.

27. Krishna, J., Arya, A.S. and Kumar, K., "Distribution of Maximum Intensity of Force in the Koyna Earthquake of Dec. 11, 1967", Earthquake Engineering Studies, School of Research and Training in Earthquake Engineering, University of Roorkee, Aug. 1969.

28. Krishna, J.,Arya, A.S. and Kumar, K., "Distribution of Maximum Ground Accelerations in the Broach Earthquake of March 23, 1970", Earthquake Engineering Studies, School of Research and Training in Earthquake Engineering, University of Roorkee, Roorkee, October, 1971.

29. Krishna, Jai, Arya, A.S., and Kumar, Krishen, "Determination of Isoacceleration Lines by Sliding and Overturning of Objects", Proc. of Fifth World Conference on Earthquake Engineering, Rome,1973, Vol. I, pp. 1270-1279.

30. Krishna, J. and Chandra, B., "Strengthening of Brick Buildings Against Earthquake Forces", Proceedings of the Third World Conference on Earthquake Engineering, New Zealand, 1965.

31. Krishna, J., and Chandra, B., "Strengthening of Brick Buildings in Seismic Zones", Proceedings of the Fourth World Conference on Earthquake Engineering, Chile, 1969.

32. Krishna, J., Chandra, B., and Kanungo, S.B., "Behaviour of Load Bearing Brick Walls during Earthquakes", Proceedings of the Third Symposium on Earthquake Engineering, University of Roorkee, Roorkee, 1966.

33. Lal, Murari, "Analysis of Brick Shear Walls with Openings", M.E. Thesis, Department of Civil Engineering, University of Roorkee, Roorkee, 1968.

34. Mallick, D.V., "Damping Characteristics of Brick Masonry in Different Mortars", M.E. Thesis, Department of Civil Engineering, University of Roorkee, Roorkee, 1961.

35. Mayes, R.L. and Clough, R.W., "A Literature Survey-Compressive, Tensile, Bond and Shear Strength of Masonry", Report No. EERC 75-15, June 1975, Earthquake Engineering Research Centre, University of California, Berkeley, California.

36. Mital, S.K., "Dynamic Study of Stacklike Structures", M.E. Thesis, University of Roorkee, Roorkee, 1969.

37. Mittal, K.C., "Sliding and Overturning of Objects during Earthquakes", M.E. Thesis, Earthquake Engineering Department, University of Roorkee, Roorkee, 1971.

38. Moinfar, A.A., "Earthquake Resistant Design of Brick Masonry Buildings", European Symposium on Earthquake Engineering, Imperial College, London, 1972.

39. Monge, J.E. "Seismic Behaviour and Design of Small Buildings in Chile", Proceedings of the Fourth World Conference on Earthquake Engineering, Chile, 1969, pp. B-6-1 to B-6-10.

40. Newmark, N.M., "Effects of Earthquakes on Dams and Embankments", Geotechnique, Institution of Civil Engineers, London, England, Vol. XV, No. 2, June 1965.

41. Plummer, H.C., and Blume, J.A., "Reinforced Brick Masonry —— Lateral Force Design", Structural Clay Products Institute, Washington, 1953.

42. Priestley, M.J.N. and Bridgeman, D.O., "Seismic Resistance of Brick Masonry Walls", Bull. of the New Zealand National Society for Earthquake Engineering, Vol. 7, No. 4, December, 1974, pp. 167-187.

43. Scrivener, J.C. and Williams, D., "Behaviour of Reinforced Masonry Shear Walls under Cyclic Loading", Bull. of New Zealand Society for Earthquake Engineering, Vol. 4, No. 2, April, 1971.

44. Sinha, B.P. and Hendry, A.W., "Further Investigations of Bond Tension, Bond Shear and the Effect of Precompression on the Shear Strength of Model Brick Masonry Couplets", British Ceramic Research Association, Technical Note No. 80, 196C.

45. Sinha, B.P. and Hendry, A.W., "Racking Tests on Storey Height Shear-Wall Structures with Openings, subjected to Precompression", Designing, Engineering and Constructing with Masonry Products, edited by F.B. Johnson, 1969.

46. Sinha, B.P., Maurenbrechar, A.H.P. and Hendry, A.W., "Model and Full Scale Tests on a Five-Storey Cross-Wall Structure under Lateral Loading", Proc. of Second International Brick Masonry Conference, Stoke-on-Trent, April, 1970.

47. Steinbrugge, K.V. and Flores, R., "The Chilean Earthquake of May 1960, A Structural Engineering View Point", Bull. Seismological Society of America, Vol. 53, No. 2, 1963.

48. Stafford-Smith, B., Carter, C. and Choudhury, J.R., "The Diagonal Tensile Strength of Brickwork", The Structural Engineer, No. 4, Vol. 48, June 1970.

49. Williams, D. and Scrivener, J.C., "Response of Masonry Shear Walls under Static and Dynamic Cyclic Loading, Proc. of Fifth World Conference on Earthquake Engineering, Vol. II, Rome, 1972. pp 1491-1494.

50. Yorkdale, Alan. H.,"Masonry Building Systems", State of Art Report No. 9, Technical Committee No. 3, International Conference on Planning and Design of Tall Buildings, Lehigh University, 1970.

51. _____, "Analysis of Small Reinforced Concrete Buildings for Earthquake Forces", Portland Cement Association, Chicago, 1955.

APPENDIX - A

FLOW DIAGRAM FOR EARTHQUAKE ANALYSIS OF MULTISTOREYED BRICK BUILDING

The flow diagram giving the computational scheme for seismic response and stress analysis of multistoreyed brick building is shown by Fig. A.1. The important steps indicated by the various blocks of the flow diagram are briefly explained in the following paragraphs:

(1) Input Parameters. The dimensions of a multistoreyed unstrengthened conventional brick building, its number of storeys and properties of the building materials are given as input data.

(2) Computation of Mass and Geometrical Properties. Mass subroutine computes mass of the walls and floor lumped at the storey levels of the building. Another subroutine computes the geometrical properties and stiffness of the piers such as, cross-sectional area, moment of inertia, location of principal axes of the piers etc.

(3) Torsional Properties. Firstly, a check is applied to see whether torsional problem exists and if it does then the torsional properties of the piers are computed with the help of a subroutine for computing additional shear due to torsion at a later stage.

(4) Stiffness Matrix. Stiffness of the different piers computed earlier is used to generate stiffness matrix for the building to find out its eigen values and eigen vectors.

(5) Eigen Value and Eigen Vector. Using the mass and stiffness matrices of the building, eigen values and eigen vectors are computed using a subroutine. Frequencies in all the modes of vibration are determined.

(6) Participation Factors. A subroutine computes participation factor of all the modes of vibration as response of the building is to be calculated making use of all the modal response of the building.

(7) Ground Motion Data. Digitized accelerogram is given as earthquake shock data. The proper time-interval for numerical integration of equation of motion is also defined.

(8) Modal Response Computation. Time-wise response (e.g relative displacement, relative velocity and absolute acceleration) is computed through a separate subroutine.

(9) Computation of Time-wise Response. Time-wise response of the building is computed at the storey levels by using mode superposition method (all the modal responses are considered). Print-outs of time-wise response may be taken if desired.

(10) Shear due to Torsional Moment. By a separate subroutine, additional shear is computed on account of torsional moment. The net shear in the piers is also determined.

(11) Seismic Stress Computation. Time-wise bending, overturning, shear and net (compressive or tensile) stress are determined through a subroutine. Printouts for time-wise stresses may also be obtained.

(12) Maximum Stresses. Maximum values of the time-wise stresses in various piers of the walls are obtained as final printouts.

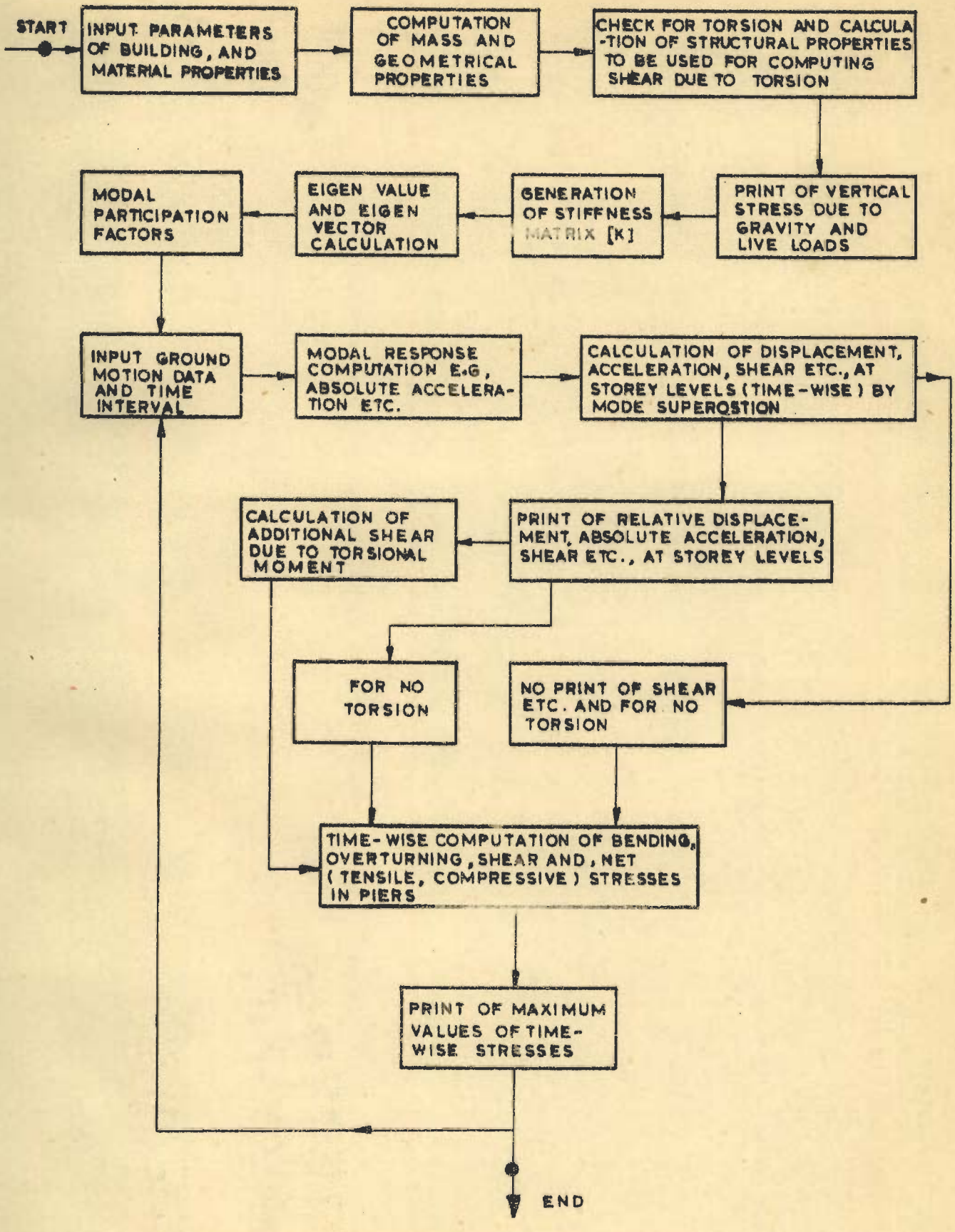

FIG. A-1 _FLOW DIAGRAM FOR EARTHQUAKE RESPONSE ANALYSIS OF MULTISTOREYED UNSTRENGTHENED CONVENTIONAL BRICK BUILDING

APPENDIX - B

FLOW DIAGRAM FOR EARTHQUAKE RESPONSE OF SLIDING TYPE BUILDING

Computational scheme for finding out seismic response of sliding single-storeyed building is presented through a flow diagram as shown in Fig. B.1. The important steps involved in this process are briefly described as follows:

(1) Ground Motion Data. Digitized accelerogram of actual earthquake shock is used as data. The time-step for numerical integration of equation of motion is also defined.

(2) Structural Properties. Parameters, such as period of the system, damping and ratio of masses lumped at roof and plinth levels (mass-ratio) are given as input data to represent structural properties of the sliding system.

(3) Response Computation Treating the System as S.D.F. Initially and also when sliding of bottom mass stops, seismic response of the system is computed treating it as a single degree of freedom.

(4) Check for Sliding. A check is applied to see whether sliding of bottom mass begins. For this, force to cause sliding should be greater than the frictional resistance of the system.

(5) Response Calculation after Sliding Starts. Response computation of the system is made treating it as two degrees of freedom system if sliding of the bottom mass begins.

(6) Check for No Sliding. If sign of relative velocity of bottom mass changes, then it is again checked whether the force to cause sliding still exceeds the frictional resistance. If not, then the control for computational work is shifted to (3) otherwise to (5).

(7) Response Computation Print Outs. After each of the process (3) and (5), if print outs of time-wise response is required, it could be taken. After end of the ground motion data, print outs of the spectral values of relative displacement, relative velocity and absolute acceleration of top and bottom masses are obtained.

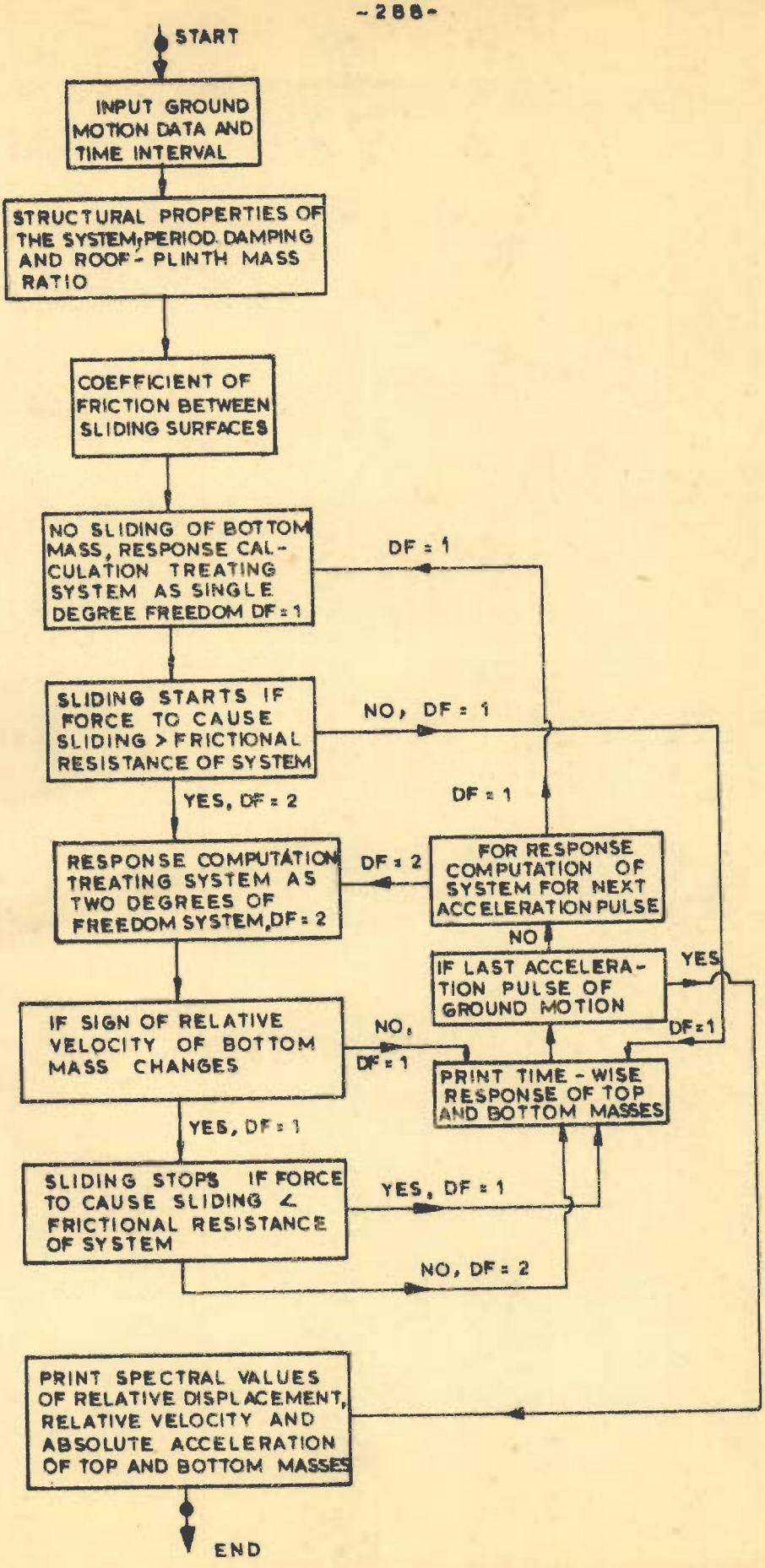

FIG. B-1 - FLOW DIAGRAM FOR EARTHQUAKE RESPONSE OF SLIDING TYPE SINGLE-STOREYED BUILDING